INVESTIGATING CONTROLLED RELEASE PULMONARY DRUG DELIVERY SYSTEMS

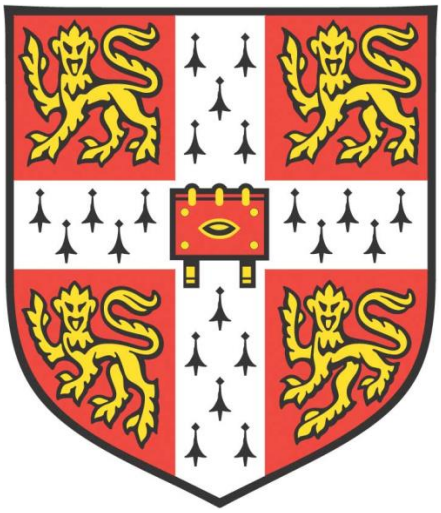

Leonard Sze Onn Chia

Queens' College

Structured Materials Group

Department of Chemical Engineering and Biotechnology

University of Cambridge

This dissertation is submitted for the degree of Doctor of Philosophy

February 2018

TITLE: INVESTIGATING CONTROLLED RELEASE PULMONARY DRUG DELIVERY SYSTEMS

NAME: LEONARD SZE ONN CHIA

ABSTRACT

The therapeutic effect of pulmonary drug delivery systems is limited by its rapid clearance from the lungs by robust clearance mechanisms. By controlling the release of drugs, the therapeutic effect of pulmonary drug delivery systems, as well as patient convenience and compliance could be improved by reducing the number of times drugs need to be administered.

In this study, two controlled pulmonary drug delivery systems for drugs of different solubilities were investigated and they were characterised for their viability as effective controlled release pulmonary drug delivery systems, particularly in areas of aerosol performance and dissolution profile.

A hybrid protein-polymer controlled release pulmonary drug delivery system was developed to sustain the release of a water-soluble anti-asthma drug, cromolyn sodium (CS). Two excipients with complementary characteristics – a protein, bovine serum albumin, and a polymer, polyvinyl alcohol – were formulated together with CS *via* co-spray drying, with varying protein-polymer ratios and drug loadings. The hybrid particles showed promise in combining the positive attributes of each excipient, with respirable particles shown to sustain the release of CS with a fine particle fraction of 30%. Combining the two excipients was complex, with further optimisation of the hybrid formulations possible.

A commercially available polymer, Soluplus® was spray-dried with a poorly-water soluble corticosteroid, beclomethasone dipropionate (BDP). The resultant respirable powders were shown to have potential for use as a controlled release pulmonary drug delivery system with up to 7-fold improvement in the amount of BDP released compared to spray-dried BDP. The spray-dried BDP-Soluplus® powders were found to be amorphous, and physically stable against re-crystallisation for up to 9 months at accelerated stress test conditions with drug loadings of up to 15 % (w/w). Although it provided a platform to compare between formulations, the USP 4 flow-through cell

dissolution apparatus was found to be inadequate to accurately study the dissolution profiles of the pulmonary drug delivery systems due to the formation of a gel in the apparatus.

Preliminary work on the use of a novel technique to predict the crystallisation of amorphous formulations with terahertz time-domain spectroscopy was also conducted. The system confirmed the re-crystallisation tendencies of several hybrid CS/BSA/PVA formulations. Modification to the experimental setup to probe the formulations at different relative humidities instead of temperatures could yield improved results.

For my family

DECLARATION

This dissertation is the result of my own work and includes nothing which is the outcome of work done in collaboration except as declared in the Preface and specified in the text. It is not substantially the same as any that I have submitted, or, is being concurrently submitted for a degree or diploma or other qualification at the University of Cambridge or any other University or similar institution except as declared in the Preface and specified in the text. I further state that no substantial part of my dissertation has already been submitted, or, is being concurrently submitted for any such degree, diploma or other qualification at the University of Cambridge or any other University or similar institution except as declared in the Preface and specified in the text

This disseration contains fewer than 65,000 words including appendices, bibliography, footnotes, tables and equations, and has fewer than 150 figures.

Leonard Sze Onn Chia

SUMMARY

Pulmonary delivery has several advantages such as the localised treatment of respiratory diseases, reduction of systemic effects, avoidance of hepatic first-pass metabolism, a large absorptive surface with a thin diffusion barrier, as well as a non-invasive route of drug delivery. However, the therapeutic effect of inhaled drugs is limited by its rapid clearance from the lungs by robust clearance mechanisms such as mucociliary clearance in the upper airways, and phaygocytosis in the lower airways. By controlling the release of drugs at a rate where there are no initial concentration spikes (which could prompt an adverse response) followed by a sharp decline in concentration levels, patient convenience and compliance could be improved by reducing the number of times drugs need to be administered. Developing cost-effective controlled release pulmonary drug delivery systems for the unmet needs of developing countries where the majority of deaths from the most common respiratory ailments such as asthma and chronic obstrutive pulmonary disease (COPD) occur is also of great importance. Controlled pulmonary drug delivery systems could have an outsized effect in those countries, as treatments could be administered by non-medically trained professionals, without the use of sterile injections and cold chain supply lines.

In this study, two controlled pulmonary drug delivery systems were investigated, each for a different class of drug: a highly water-soluble drug, and a poorly water-soluble drug. The controlled release pulmonary drug delivery systems were characterised for their viability as effective controlled pulmonary drug delivery systems, particularly in areas of aerosol performance and dissolution profile.

A hybrid protein-polymer controlled release pulmonary drug delivery system was developed to sustain the release of a water-soluble anti-asthma drug, cromolyn sodium (CS). Two excipients with complementary characteristics – bovine serum albumin (BSA), a protein, and polyvinyl alcohol (PVA), a polymer – were formulated together with CS *via* co-spray drying, an industrially scalable formulation process, with different protein-polymer ratios and drug loadings. While PVA was effective in sustaining the release of CS, it tended to form large, hollow and dense particles, which had poor aerosolisation ability. BSA was shown to produce small, respirable particles and to improve the fine particle fraction (FPF). The hybrid particles showed some promise in combining the positive attributes of each excipient, with respirable particles shown to sustain the release of CS with a FPF of 30%. The complex process of combining two excipients was

highlighted, with further optimisation of the hybrid particles possible.

For the second controlled pulmonary drug delivery system, a commercially available amphiphilic graft co-polymer, Soluplus® was spray-dried with a poorly-water soluble corticosteroid, beclomethasone dipropionate (BDP). The resultant powders were shown to have potential for use as a controlled release pulmonary drug delivery system with up to 7-fold improvement in the amount of BDP released compared to spray-dried BDP. The spray-dried BDP-Soluplus® powders were found to be amorphous in nature, while spray-dried BDP was initially microcrystalline, and BDP had to be cryo-milled for many cycles before amorphous powders were produced. The amorphous state, and the dissolution rate and solubility enhancement it brings, were maintained over accelerated stress tests for up to nine months at drug loadings of up to 15% (w/w). Although it provided a platform to compare between formulations, the USP dissolution apparatus 4 (flow-through cell) was found to be inadequate to accurately study the dissolution profiles of the pulmonary drug delivery systems due to the formation of a gel-phase in the flow-through cell.

Preliminary work on the use of a novel technique to predict the crystallisation of amorphous formulations with terahertz time-domain spectroscopy (THz-TDS) was also conducted. The system confirmed the re-crystallisation tendencies of several hybrid pulmonary drug delivery systems of CS/BSA/PVA. Modification to the experimental setup to probe the drug delivery systems at different relative humidities instead of temperatures could yield improved results.

ACKNOWLEDGEMENTS

I would like to thank the Agency for Science, Technology and Research (A*STAR, Singapore) for granting me an A*STAR Graduate Scholarship (Overseas) to undertake my PhD jointly at the University of Cambridge and the Institute of Chemical and Engineering Sciences (ICES). It was an immense opportunity helped by their generous sponsorship.

My supervisors Prof. Geoff Moggridge and Prof. Reginald Tan have always made themselves available for me whenever I needed advice. Their patience through the ups and downs of this PhD was very helpful. Thanks to Prof. Axel Zeitler for opening the world of terahertz spectroscopy to me, and tirelessly trying to help with the analysis of the results.

I owe a debt of gratitude to all the lab officers of the Department of Crystallisation and Particle Science, ICES, A*STAR, both past and present, for all the tests you have helped me to conduct: Mr Frederick Toh, Ms Li Teng Tan, Ms Agnes Phua, Mr Bao Ren Tan (all of whom have gone on to other endeavours); and to Mr Xavier Chin, Ms Li Ling Lim, Ms Inez Kwek, Ms Lei Bing Tan still ably assisting in research at ICES. Mr Junwei Ng has always put others before himself, and never said no to any help I asked of him, busy as he is, given his wealth of knowledge on equipment and processes.

I am immensely thankful for the advice and guidance of Dr Desmond Heng and Dr Sie Huey Lee for always being available to offer advice on the then unknown (to me) field of pulmonary delivery and for allowing me to mentor Mr Wee Kong Ong from the Division of Chemistry and Biological Chemistry, Nanyang Technological University, Singapore, for his research attachment. Wee Kong's contribution to the conduct of the *in vitro* dissolution tests was very welcome. Many thanks too to Drs Martin Schreyer and Sendhil Poornachary for their time, advice and help with the conduct of some preliminary experiments into the study of the gel formation which occured during the dissolution tests involving Soluplus®.

Many thanks for all the researchers who have willingly offered me advice, materials and equipment at various stages of my study. To Dr Shoucang Shen who has always been a constant source of experienced advice, to Dr Alexander Jackson for patiently explaining polymers to me, and to Dr Wai Kiong Ng, who has been watching out for my growth as a person and researcher for the past 10 years.

I also wish to extend grateful thanks to Mr Zlatko Saračević of the Department of Chemical Engineering and Biotechnology, University of Cambridge and Ms Wei Leu Seet of the Singapore Institute for Manufacturing Technology (SIMTech) for their kind assistance with the density measurements, as well as Mr Cambridge Kon from WinTech Nano-Technology Services for his expertise in operating the FIB-SEM. A special shout out to Drs Juraj Sibik and Nicholas Tan for all their patient help with the terahertz measurements.

Thanks to the M1 office in the old Chemical Engineering Building at the New Museums Site, for all the hugely enjoyable tea times and making me feel welcome. I always looked forward to the weekly football sessions both in Cambridge and Singapore, as a welcome respite from the lab and computer, and to also developing great friendships with Petar Besevic and Mohammad Ainte.

Thank you to Kayla Friedman and Malcolm Morgan of the Centre for Sustainable Development, University of Cambridge, UK for producing the Microsoft Word thesis template used to produce this document.

Thank you to God for sustaining me through this period, for giving me strength to persevere and for watching over, and guiding me.

Last, but not least, to my wonderful family, who have always supported me throughout this period. To my loving wife, Charmaine, for always being there, and being a terrific mother to our twins, Rachel and Hannah. To my mum and parents-in-law for making extended stays in Cambridge to help look after the girls, and also to Aunty Stella for flying up to help. To my sister, Charlene and to my dad, who I am sure would have been extremely proud of me. I could not have done this without all your support.

To God be the glory.

PUBLICATIONS

Journal Articles

1. Chia, L.S.O., Heng, D., Lee, S.H., Ng, W.K., Zeitler, J.A., Moggridge, G.D. & Tan, R.B.H. Hybrid protein-polymer particles for the release modulation of inhaled powders. *Powder Technology*, in preparation.
2. Chia, L.S.O., Ng, W.K., Moggridge, G.D. & Tan, R.B.H. Physicochemical evaluation of a beclomethasone dipropionate-Soluplus® amorphous solid dispersion for pulmonary drug delivery. *Drug Development and Industrial Pharmacy*, in preparation.

Conference Posters

1. Chia. L.S.O., Heng, D.W.C., Shen, S.C., Ng, W.K., Zeitler, J.A., Tan, R.B.H. & Moggridge, G.D. Physicochemical characterization of a co-spray dried controlled release drug (protein-polymer) pulmonary delivery system. *Respiratory Drug Delivery 2014*, Farjardo, Puerto Rico, USA. 4-8th May 2014.
2. Chia. L.S.O., Zeitler, J.A., Ng, W.K., Tan, R.B.H. & Moggridge, G.D., Investigating the physical stability of a spray-dried pulmonary drug delivery system. *The 43rd Annual Meeting & Exposition of the Controlled Release Society*, Seattle, Washington, USA. 17-20th July 2016.

CONTENTS

LIST OF TABLES

LIST OF FIGURES

NOMENCLATURE

Acronyms and abbreviations

Symbol	Description
API	Active pharmaceutical ingredient
BDP	Beclomethasone dipropionate
BSA	Bovine serum albumin
CFC	Chlorofluorocarbon
CM	Cryo-milled
CMC	Critical micelle concentration
COPD	Chronic obstructive pulmonary disease
CS	Cromolyn sodium
DPI	Dry powder inhaler
DPPC	Dipalmitoylphosphatidylcholine
DSC	Differential scanning calorimetry
DVS	Dynamic vapour sorption
ESCA	Electron spectroscopy for chemical analysis
FESEM	Field emission scanning electron microscopy
FIB	Focused ion beam
FPF	Fine particle fraction
HA	Hyaluronic acid
HFA	Hydrofluoroalkane
HPLC	High-performance liquid chromatography
HPMC	Hydroxypropyl methylcellulose
ICH	International Conference on Harmonisation of Technical Requirements of Pharmaceuticals for Human Use
JG	Johari-Goldstein
MDSC	Modulated differential scanning calorimetry
MMAD	Mass median aerodynamic diameter
M_r	Relative molecular mass
MSLI	Multi-stage liquid impinger
P_2O_5	Phosphorous pentoxide
PLGA	Poly(lactic-co-glycolic acid)
pMDI	Pressurised metered dose inhaler

Symbol	Description
PTFE	Polytetrafluoroethylene
PVA	Poly(vinyl alcohol)
PVP K130	Polyvinylpyrrolidone (M_r 130,000)
RH	Relative humidity
SAXS	Small angle X-ray scattering
SD	Spray-dried
SEM	Scanning electron microscopy
SFD	Spray freeze-drying
SFL	Spray-freezing into liquid
SLN	Solid lipid nanoparticles
THz-TDS	Terahertz time-domain spectroscopy
UK	United Kingdom
US FDA	United States Food and Drug Administration
USP	United States Pharmacopoeia
UV-vis	Ultraviolet-visible
VDOS	Vibrational density of states
WHO	World Health Organisation
XPS	X-ray photoelectron spectroscopy
XRD	X-ray diffraction

Symbols – Greek

Symbol	Description	Units
γ	Relative coverage of the different components in controlled release pulmonary drug delivery systems	
η	Viscosity of air	mPa·s
κ_p	Shape factor for aerosol particle	
κ_o	Shape factor for equivalent sphere aerosol	
ρ_p	Density of aerosol particle	g/cm^3
ρ_0	Density of unit density sphere	g/cm^3
τ_{JG}	Johari-Goldstein relaxation time	s

Symbols – Latin

Symbol	Description	Units
A	Surface area of solid	cm^2
a	Constant incorporating structural and geometrical aspects of the drug particles	
$C(d_v)$	Slip correction factors for an equivalent volume sphere	
$C(d_{ae})$	Slip correction factors for an aerodynamically equivalent sphere	
C_b	Concentration of drug in the bulk phase	mg/mL
C_s	Concentration of drug in the stagnant phase	mg/mL
C_0	Initial concentration of drug in the matrix	mg/mL
C_{ms}	Drug solubility in the matrix	mg/mL
d_{ae}	Aerodynamic diameter	cm
d_v	Geometric diameter	cm
dC/dt	Dissolution rate of the drug	mg/s
D	Diffusion coefficient	cm^2/s
D_m	Diffusion coefficient	cm^2/s
f	Vector containing the elemental composition of a formulation's surface	
f_t	Fraction of drug dissolved at time t	
h	Thickness of the stagnant layer	cm
I	Matrix of the elemental composition of the pure components	
g	Acceleration due to gravity	cm/s^2
K_0	Rate constant for zero order release	mol/L·s
K_1	Rate constant for first order release	s^{-1}
K_β	Rate constant for the Hixson-Crowell model	mol/L·s
K_H	Rate constant for the Higuchi model	mol/L·s
$K_{w/o}$	Water/oil partition coefficient of the drug	
M_t	Amount of drug released at time t	mol
M_∞	Amount of drug released at infinite time	mol
n	Release exponent related to the drug release mechanism	
Q_0	Initial amount of drug in solution	mol
Q_t	Amount of drug dissolved at time t	mol

Symbol	Description	Units

r_0	Radius of the spherical particle matrix	cm
T_g	Glass transition temperature	°C
V	Volume of the dissolution medium	L
V_T	Terminal settling velocity of the particle	cm/s

1 INTRODUCTION

1.1 Pulmonary drug delivery

Pulmonary delivery is primarily employed to treat respiratory conditions such as asthma, cystic fibrosis and obstruction of the lung, but the large surface area of the lungs and good epithelial permeability (Patton, (1996)) has also opened up huge potential for the systemic delivery of therapeutic agents through the lungs (Patton and Byron, (2007)). The first known recording of treatment *via* inhalation was in ancient Egypt, more than 3,500 years ago (Bryan, (1930)). However, the advent of modern inhaled therapy in a form that we are familiar with can be linked back to the introduction of the pressured metered dose inhaler (pMDI) in 1956 by Riker Laboratories for the delivery of epinephrine and isoproterenol (Porush and Maison, (1959); Thiel, (1996)), although the first inhaler was thought to have been invented around 1778 by John Mudge (Mudge, (1778)). In the 1980s, a ban chlorofluorocarbons (CFCs) led to a renewed interest in inhaled drug delivery formulation as manufacturers sought out alternative propellants that were safe for the environment, and this interest was bolstered by the boom in biotechnology-based products. These large macromolecules have been difficult to administer through the parenteral and oral routes of administration, leading some researchers to turn to the pulmonary delivery route (Kunda *et al.*, (2015)).

The global impact of lung disease is high. Asthma and chronic obstructive pulmonary disease (COPD) are the two most common lung diseases which plague the population worldwide. Especially in lower-income countries, access to cost-effective solutions to respiratory diseases can reduce its human burden and societal impact (*The Global Impact of Respiratory Disease - Second Edition*, (2017)). An estimated 235 million people in the world suffer from asthma and it is the most common chronic ailment plaguing children, with 14% of children affected by it. Of the 383,000 asthma-related deaths worldwide in 2015, most occurred in low or lower-middle income countries ("WHO | Asthma," (2017)). Three million die from another lung disease, COPD, as well each year, making it the third leading cause of death worldwide, although more than 90% of the deaths are from lower and middle-income countries ("WHO | Chronic obstructive pulmonary disease (COPD)," (2016)). These diseases can be controlled effectively using local treatment using inhaled devices. Advancements in dry powder inhaler technology have produced cheap, disposable dry powder inhalers (Berkenfeld *et al.*, (2015)) which could be used as part of a strategy to deliver vaccines and other typically parenterally delivered formulations such as oxytocin in the form of heat-stable dry powders using dry powder inhalers (Prankerd *et al.*, (2013)), negating the need for cold-chain storage, and bringing easier access to greatly needed vaccines for the developing world (*Technology Solutions for Global Health - Intranasal and Pulmonary Delivery Devices*, (2013)). Clearly, cost-effective strategies for respiratory diseases are necessary but currently still lacking.

There are several advantages to the use of pulmonary drug delivery, not least for the localised action of lung related disorders, avoiding side effects from the systemic delivery of therapeutic agents as well the potential to use a lower dose compared to the oral delivery route. Drugs delivered through the pulmonary route are also able to circumvent hepatic first pass metabolism and have a more rapid onset of action for locally acting drugs (Olsson *et al.*, (2011); Pilcer and Amighi, (2010)). For the delivery of systemic drugs, pulmonary delivery also offers several advantages such as a large alveolar surface area for drugs to be absorbed across a thin epithelial barrier ($\leq$ 0.3-1 μm) into the blood stream (Courrier *et al.*, (2002)). Such a delivery route is less invasive than parenteral delivery and once again a faster release of drugs can be achieved.

There are, however, a number of limitations for the delivery of drugs through the pulmonary route. Most drugs available in the market are immediate release products. A rapid, excessive, initial release of drugs can lead to adverse effects. This is then followed by drug release levels that may be too low to be therapeutic (Loira-Pastoriza *et al.*,

(2014)). With a successfully designed controlled pulmonary drug delivery system, the reduced need to dose frequently can improve patient compliance and convenience, which is already greater than that required for oral delivery due to the relatively more complex process of administration.

However, the lung airways offer particular challenges for any pulmonary drug delivery system because the airways are highly sensitive to inflammation and they are highly efficient at clearing deposited materials. Achieving sustained therapeutic effects requires the carrier to pass through the mucus after deposition in the airways, avoid mucociliary clearance and rapid absorption. This challenge has yet to be overcome in a clinical setting and as a result, there are no commercial systems that offer controlled pulmonary drug delivery.

In the lab, there has been a whole range of different excipients used for pulmonary formulations. However, only a handful have been tested and approved for use in humans as a result of the difficulty in selecting a suitable excipient that is non-immunogenic, does not compromise aerosol performance, and is suitable for controlling the drug release all at the same time (Sheth and Myrdal, (2011a)).

There have been several types of excipients mooted for potential controlled pulmonary delivery systems. Liposomes have been known to be biologically inert and thus are a promising candidate for the choice of excipient for controlled pulmonary delivery, although they are costly, and drug loading into (Beloqui *et al.*, (2013)) and release out of these carriers (Lamprecht *et al.*, (2004)) has been found to be tricky. Polymeric systems are amongst the most investigated for controlling the release of drugs. They offer a cost-effective and well-studied route to form particles with suitable properties for controlling drug release. However, there are some concerns about their effect on cell viability and bioaccumulation (Sheth and Myrdal, (2011b)).

It is clear that controlled pulmonary delivery to the lung, while desirable, has many complex challenges. Different formulation strategies can be adopted to control the release of drug in the lung and the characteristics of the drug will also dictate the strategy taken. An appropriate strategy can only be decided after considering the fate of the inhaled drug in the lung after administration, with knowledge of the physicochemical factors affecting deposition in the lung, and the physiology of the lung (Cryan *et al.*, (2007)).

1.1.1 Physiology of the lung

The human respiratory tract, as seen in Figure 1.1, can be considered to be simply divided

into three compartments of the upper or extrathoracic airways (nasal cavity, nasopharynx, mouth oropharynx and larynx), conducting or tracheobronchial airways (trachea, carina, hilum, left and right main bronchi) and the alveolated or respiratory airways (bronchi, bronchioles, alveoli). Put simply, the lung can be described as a series of bifurcating tubes, starting at the trachea and dividing into the bronchi, conducting bronchioles and ending in the terminal bronchioles and alveoli. The upper airways help to bring inhaled air up to 99% relative humidity (RH) and body temperature. The upper airways also act as efficient filters for inhaled particles.

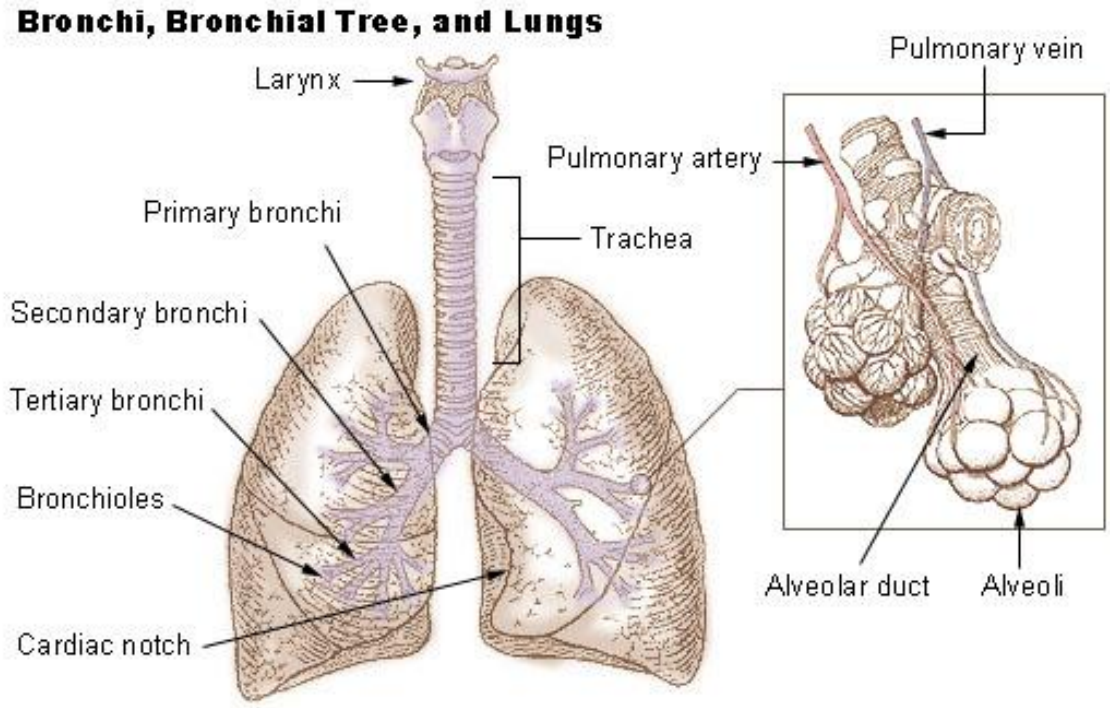

Figure 1.1. Detail of human respiratory system ("Respiratory System," n.d.)

A simple, symmetrical model of the lung was proposed by Weibel (Weibel, (1963)) in 1963 which is still useful today. As seen in Figure 1.2, the modified (2005) model of the lung is divided into 23 generations, which split into two branches at each generation. Generations 0 to 14-16 are known as the conducting airways, where airflow is by convection. The next eight generations are known as the acinar airways, where gas exchange with blood occurs. The airway bifurcates an average of 23 times from the trachea to the alveolar sacs, representing a circuitous route for any inhaled matter. The surface area of the alveolar region is greater than 100 m^2 (Stocks and Hislop, (2001)) while the rest of the airways only have a surface area of a few square metres. As such, the velocity of air declines to very low values in the deep lung. Oxygen is able to diffuse through the alveolar epithelium and capillary epithelium. This forms the basis of the ability to utilise the lung as an alternative systemic delivery route compared to the

traditional routes of gastrointestinal, buccal, transdermal, or nasal delivery (Patton, (1996)).

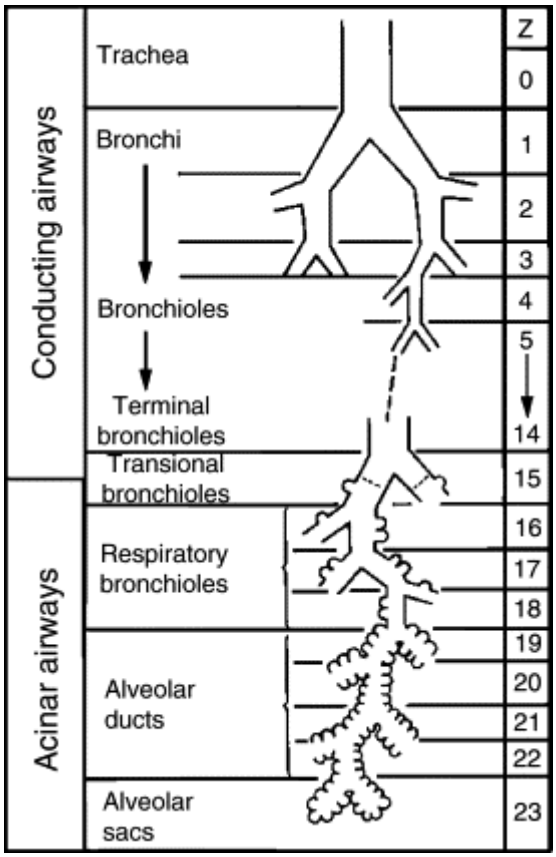

Figure 1.2. Weibel symmetrical lung model of human airway system (Used with permission from Weibel *et al.*, 2005)

The epithelium lining the lungs, bronchi, and bronchioles (airways), and the cells lining the alveoli are distinctly different (Figure 1.3). The airways possess a pseudostratified epithelium which is lined with three major cell types: goblet (mucus-producing), basal (stem or progenitor cells), and ciliated (responsible for mucociliary clearance) (Widmaier *et al.*, (2008)). The alveolar epithelium has two different types of cells called pneumocytes: type 1, which cover most of the surface and act as a barrier; and type 2 cells, which produce pulmonary surfactant. The pulmonary surfactant consists largely of phospholipids (~85-90%) with the remainder formed by proteins, and is responsible for decreasing surface tension in the alveoli (Pérez-Gil, (2008)). Macrophages are also present in the alveoli. They are a defence mechanism against foreign matter in the alveoli and will engulf and attempt to digest any insoluble particle that deposits in the lung.

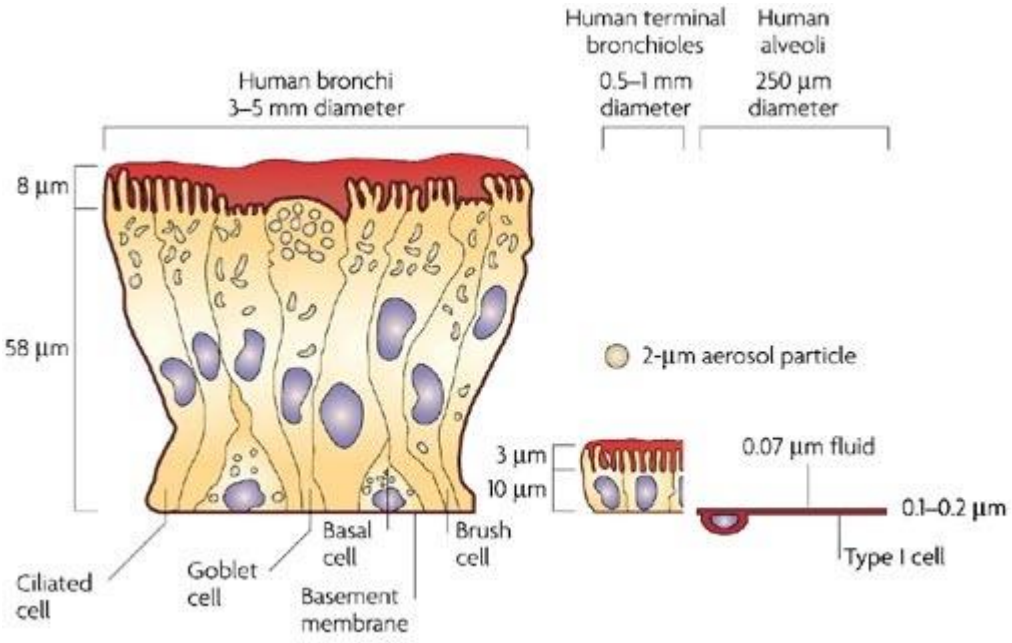

Figure 1.3. Comparison of lung epithelium at different sites in the lung (Used with permission from Patton & Byron, 2007)

1.1.2 Physicochemical factors affecting deposition in the lung

One of the key physicochemical parameters affecting inhalation drug delivery is the particle size of the aerosols (defined as a colloidal suspension of particles dispersed in air or gas). Particles have to be small enough to get to the deep lung *via* the mouth, throat, and airways, yet not too small that they are exhaled (Byron, (1986); Labiris and Dolovich, (2003)). The optimum size range for therapeutic inhaled particles vary but is approximately in the range of 2.5-6 µm (Patton, (1996)). The inhaled aerosols are usually characterised by an aerodynamic diameter parameter. For a particular aerosol particle, the aerodynamic size can be described in terms of a sphere of unit density with the same terminal settling velocity as the aerosol particle. This can be described by the following equation (Raabe, (1976)):

$$V_T = \frac{\rho_p g d^2 C(d_v)}{\kappa_p 18\eta} = \frac{\rho_0 g d_{ae}^2 C(d_{ae})}{\kappa_0 18\eta} \quad (1)$$

Where V_T is the terminal settling velocity of the particle; κ_p and κ_o are the shape factors for the aerosol particle (>1) and an equivalent sphere (=1) respectively; η is the viscosity of air; ρ_p and ρ_0 are the densities of the particle and a unit density (1 g/cm^3) sphere respectively; d_v and d_{ae} are the geometric and aerodynamic diameter of the particle respectively; $C(d_v)$ and $C(d_{ae})$ are the slip correction factors for an equivalent volume and

an aerodynamically equivalent sphere respectively; and g is the acceleration due to gravity.

From Equation 1, we can infer that the particle diameter, density and shape are key parameters. The slip correction factors become important for particles smaller than 1 μm, which is not common for pharmaceutical aerosols. Hence, since the shape factors are important only when the aerosols deviate from sphericity, the equation can be simplified as follows for spherical particles:

$$d_{ae} = d_v\sqrt{\rho_p} \tag{2}$$

1.2 Deposition and fate of inhaled particles in the lung

The deposition of aerosol particles in the respiratory tract is governed principally by three mechanisms – inertial impaction, gravitational sedimentation and Brownian diffusion. Inertial impaction occurs when a stream of air containing particles changes direction at a bifurcation or airway branch. Particles carrying too much momentum may then impact on the walls of the airway. This typically happens for particles with mass median aerodynamic diameters (MMAD) – the particle diameter that has 50% of the aerosol mass above and below it, greater than 10 μm (Carvalho *et al.*, (2011); Heyder, (2004)) – in the upper airways (nose, mouth, larynx and pharynx). Gravitational sedimentation may take place when particles between 1 to 8 μm fall by gravity onto the smaller airway walls and respiratory bronchioles. Brownian diffusion occurs when particles <0.5 μm are bombarded by gas molecules which may direct them towards an airway wall and can take place in the alveoli where the air is more stationary. For particles to reach the deep lung, aerodynamic diameters between 1-5 μm and below 0.1 μm are preferable (Heyder *et al.*, (1986); Schiller *et al.*, (1988)).

It is important to note the parameters that affect deposition. An increased airflow velocity will result in a higher deposition by impaction but decreases sedimentation and diffusion. An individual's breathing pattern also influences deposition. Total respiratory deposition increases with tidal volume and residence time of particles in the respiratory tract (Kim and Jaques, (2004)).

Upon deposition in the airways, the fate of the inhaled particle depends on its solubility and position in the respiratory tract. Deposition in the lung is a complex combination of absorption and the various clearance mechanisms in the lung (Sakagami, (2006)).

1.3 Lung clearance mechanisms

The lung has developed robust clearance mechanisms to rid itself of foreign objects which may enter. Any form of inhalation therapy has to consider these mechanisms and ways to elude them.

1.3.1 Mucociliary clearance

Insoluble particles that deposit in the conducting airways get trapped in the mucus layer lining it and are then removed by mucociliary clearance (Lansley, (1993)). The ciliated cells in the epithelium will be in harmony with neighbouring cilia to drive the insoluble or slowly dissolving particle towards the larynx to be expectorated or swallowed (Sleigh *et al.*, (1988)). Most particles with geometric diameters above 6 µm will be cleared *via* mucociliary clearance in about 24 hours (Kreyling *et al.*, (2006); Stahlhofen *et al.*, (1990)).

1.3.2 Clearance *via* alveolar macrophages

In the alveolar region, slow dissolving and insoluble particles will be cleared by alveolar macrophage phagocytosis. Once phagocytosed, the particles are disposed of by translocation to the tracheobronchial lymph, digested internally or transported along the alveolar surface for clearance *via* the mucociliary escalator (Labiris and Dolovich, (2003); Lombry, (2003)). The process is rapid and almost all particles in the alveoli are phagocytosed within 6-12 h of deposition, although there are size-dependent factors for this process (He *et al.*, (2010); Lehnert, (1992)). The optimal size for phagocytosis appears to be between 1-3 µm (Oberdörster, (1988); Oberdörster *et al.*, (1994)).

1.4 Controlled drug delivery

While pulmonary delivery has many advantages, as highlighted earlier, it has to navigate the well-adapted lung clearance mechanisms, thus leading to significant drawbacks such as the short duration of action and the need to deliver drugs several times a day (Byron, (1986)). Techniques to control the release of active ingredients have been in existence for many decades in the form of oral sustained release products, fertilisers, and anti-fouling agents. Controlled pulmonary drug delivery could offer possibilities for product line

extensions, better clinical response and product development opportunities. However, to date, there are no controlled release products for inhalation that are commercially available despite significant academic research on the subject (R. Salama *et al.*, (2009); Smyth and Hickey, (2011); Uhrich *et al.*, (1999); Zeng *et al.*, (1995)). Some of the main challenges behind this are the lack of regulatory approval for excipients that can be inhaled to the lung and efficient lung clearance mechanisms (Martonen *et al.*, (2005); Patton *et al.*, (2010)).

As current inhalation therapies require dosages up to four times a day due to short drug residence times in the lung (Byron, (1986)), sustaining the release of drugs in the lungs will require less frequent dose administration, which can lead to increased patient compliance and convenience (Koushik and Kompella, (2004)). Furthermore, a fast dissolving drug has low pulmonary selectivity (the amount of drug present in the lung compared to systemic circulation) as it will be absorbed into the systemic circulation quickly. If the dissolution rate of the drugs can be slowed down, this would increase the drug concentration in the lung over a longer period of time compared to that in systemic circulation (Issar *et al.*, (2003)). Immediate release also gives rise to an initially high rate of release and absorption, followed by a rapid decline, often to below therapeutic levels (Ravi Kumar, (2000)).

Another poignant consideration is that of poor, developing countries. There, access to medical supplies that one takes for granted such as sterile needles and clean syringes are often difficult, and inhalation therapy offers an opportunity for patients to treat themselves safely in a cost-effective manner (Park, (1997)). However, due to reasons mentioned above, controlled release in the lung remains one of the biggest challenges for inhaled drug delivery (El-Sherbiny *et al.*, (2011)).

1.4.1 Formulation strategies

In order for particles to be respirable, they need to be under 5 µm. However, the small size of these particles is problematic for sustaining the release of water-soluble drugs as there is a significant increase in the surface area-to-mass ratio when the particle size is reduced. Consequently, by the Noyes-Whitney Equations (Nernst, (1904); Noyes and Whitney, (1897)) (Equations 3 & 4), an increase in surface area entails an increase in the dissolution rate.

Noyes-Whitney Equation $$\frac{dC}{dt} = DA(C_s - C_b) \quad (3)$$

Modified Noyes-Whitney Equation $$\frac{dC}{dt} = \frac{DAK_{w/o}(C_s - C_b)}{Vh} \quad (4)$$

Where *dC/dt* is the dissolution rate of the drug; *D* is the diffusion coefficient; *A* is the surface area of the solid; C_s the concentration of drug in the stagnant phase; C_b is the concentration of drug in the bulk phase; $K_{w/o}$ is the water/oil partition coefficient of the drug; *V* is the volume of the dissolution medium; and *h* is the thickness of the stagnant layer.

One of the most established techniques for controlling the release of drugs is to formulate them with excipients to prolong the release of drugs in the lungs. The choice of excipients depends on several factors such as the physicochemical properties of the drug, type of inhaler device used, and carrier properties.

1.4.1.1 Microparticles

Polymers have been widely studied for controlled release purposes in all forms of drug delivery (Park, (2014)). These carriers typically slow down the rate of release of an active ingredient by forming a barrier between the drug and the dissolution fluid (Pilcer and Amighi, (2010)). Both natural and synthetic polymers have been investigated for use as carriers for pulmonary drug delivery.

Chitosan is a polysaccharide derived from deacetylation of the naturally occurring polymer chitin. It has mucoadhesive properties which lead to its potential for controlling drug release. Learoyd *et al.*, (2008) studied the ability for chitosan with different molecular weights to sustain the release of terbutaline sulphate and found that high molecular weight chitosan was able to display a substantially longer dissolution profile compared to low and medium molecular weight chitosan. However, chitosan is prone to aggregation and solubility at physiological pH is low. It may not be the most suitable for pulmonary delivery as it opens up tight epithelia junctions and may cause pulmonary oedema, an abnormal buildup of fluid in the lungs (Yeh *et al.*, (2011)).

Hyaluronic acid (HA) is another natural polymer which has attracted attention as an excipient for controlled pulmonary delivery. It is endogenous to the lung, plays a role in inflammatory mediation and is bioadhesive (Rouse *et al.*, (2007)), making in an attractive excipient for pulmonary delivery. Surendrakumar *et al.*, (2003), spray-dried hyaluronic acid with insulin and found that HA was able to increase both the mean residence time and half-life of insulin in beagle dogs.

For oral drug delivery, poly(lactic-co-glycolic acid) (PLGA) has emerged as one of the foremost polymers in use today, due to its biocompatibility and biodegradability (Brannon-Peppas and Vert, (2000); Uhrich *et al.*, (1999)). Naturally, controlled release systems for pulmonary drug delivery have also featured PLGA prominently (Beck-Broichsitter *et al.*, (2012); El-Sherbiny and Smyth, (2012); Hamishehkar *et al.*, (2010); Kang *et al.*, (2004); Kim *et al.*, (2012); Lee *et al.*, (2010); Moghaddam *et al.*, (2013); Sun *et al.*, (2009)) and it is the most investigated of all polymers for controlled release microparticles for pulmonary delivery (Ungaro *et al.*, (2012b)). Doan *et al.*, (2011) used a solvent evaporation method to prepare rifampicin-loaded PLGA microparticles and were able to release 80% of drug from 12 hours to 4 days. An *in vivo* study of heparin-loaded PLGA microparticles prepared by spray drying showed that it was more effective to inhibit airway hyper-reactivity than an equivalent dose of heparin solution (Yildiz *et al.*, (2012)).

However, PLGA may not be the most appropriate polymer for use in drug delivery to the lung, not least because the degradation period for PLGA microspheres varies between weeks to months although it only delivers drugs for a much shorter period of time (Batycky *et al.*, (1997)). This could lead to a large, undesired build-up of polymer in the lungs (Cook *et al.*, (2005)).

1.4.1.2 Large porous particles

Exploiting Equation 2, Edwards *et al.*, (1997) developed large porous PLGA particles to deliver insulin to rats. The large porous particles had a large geometric size to minimise phagocytosis (engulfment followed by digestion) by alveolar macrophages but had a low density which resulted in a small aerodynamic size, allowing it to avoid deposition in the upper airways and be delivered deep into the lungs. Since then, a wealth of research has been conducted on large porous particles using a wide range of porogen (Kim *et al.*, (2012); Pham *et al.*, (2013); Vanbever *et al.*, (1999); Yang *et al.*, (2009)). The most utilised method to manufacture large porous particles is a double-emulsion process (w/o/w), with ammonium bicarbonate and cyclodextrins as popular choices for porogen. However, almost all research done on large porous particles for delivery to the lung have utilised PLGA as the polymer (Liang *et al.*, (2015)) and as such, the same questions about polymer build up is raised.

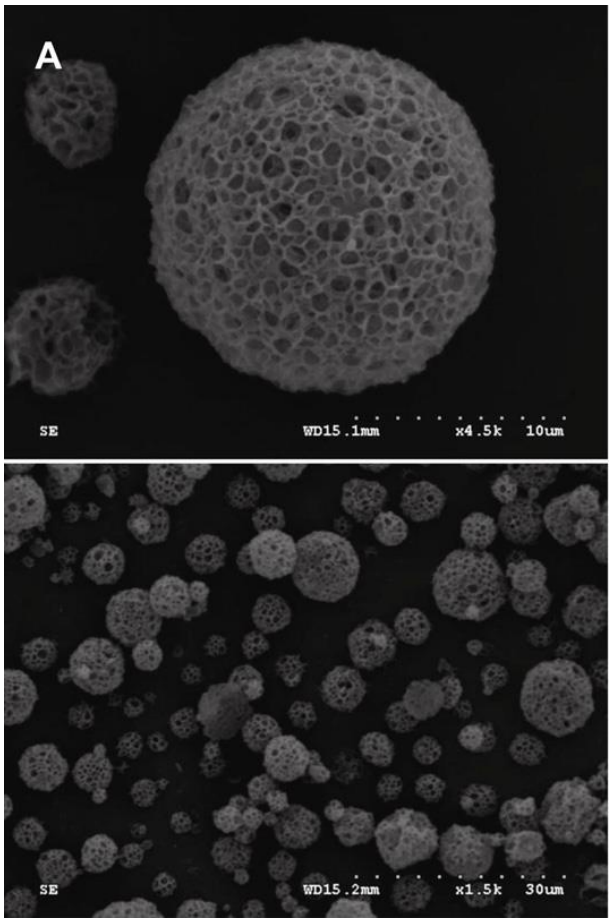

Figure 1.4. Scanning electron microscope images of doxorubicin-loaded highly porous large PLGA microparticles (Used with permission from Kim et al., (2012))

Although they present an attractive proposition for controlled release in the lung, large porous particles face some barriers to use. Their porosity, which is their defining feature, makes their structures more friable and manufacturing difficult to scale.

1.4.1.3 Swellable microparticles

With a similar concept to large porous particles, swellable microparticles were developed to minimise alveolar macrophage phagocytosis, while still possessing a suitable size for delivery into the deep lung (Ibrahim M El-Sherbiny and Smyth, (2010); Selvam *et al.*, (2011)). These microparticles have a respirable particle size when dry but swell upon contact with the wet lung surfaces. The swollen microparticles are then able to reduce macrophage clearance. Swellable microparticles also offer a more controlled architecture for drug release than large porous particles (Möbus *et al.*, (2012)). El-Sherbiny *et al.*, (2010) prepared freeze-dried microparticles with PEG-grafted chitosan with Pluronic® F-108 to deliver a model drug, sodium fluorescein. They reported sustained release of up to 10 or 20 days, in the presence and absence of lysozyme, respectively. Ni *et al.*, (2017)

embedded hydrophobic drug nanocrystals into swellable chitosan-based microparticles, showing that the technology is also suitable for delivering hydrophobic drugs.

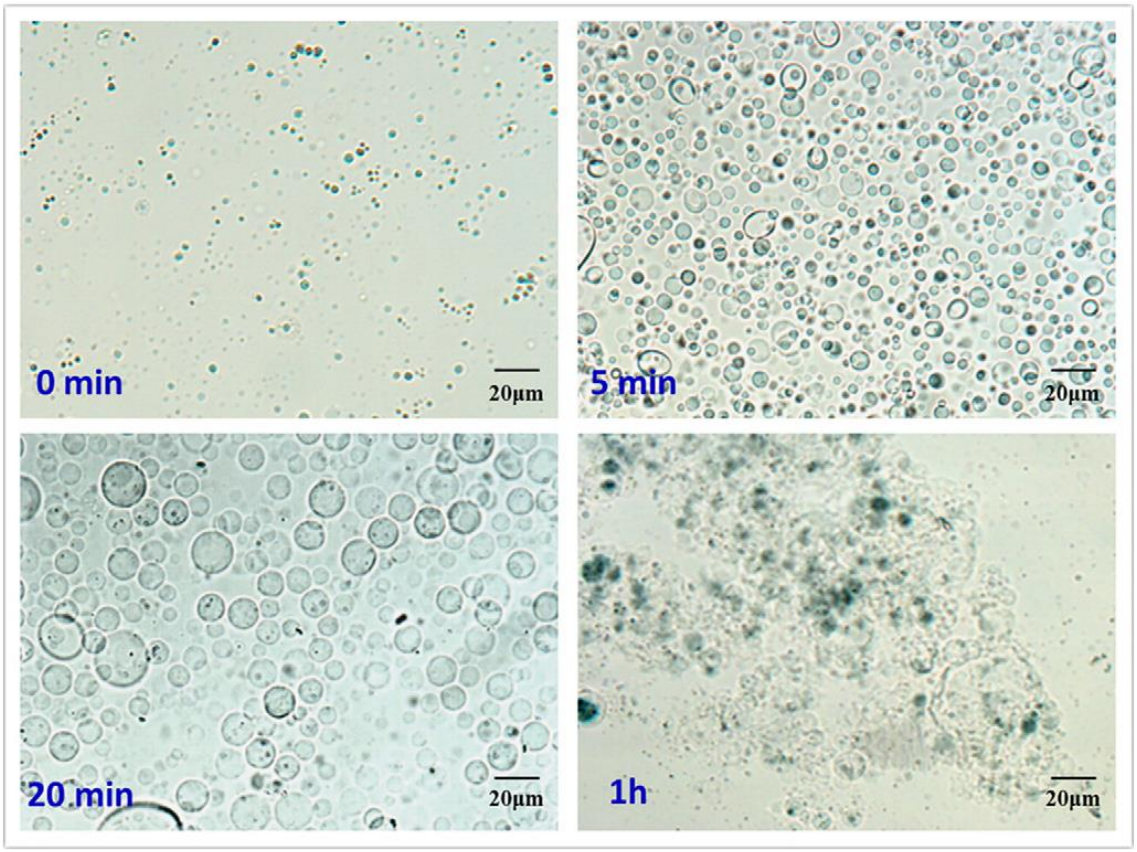

Figure 1.5. SEM micrographs of chitosan-based swellable microparticles over time (Used with permission from Ni et al., (2017))

Combining two formulation strategies, drug-loaded nanoparticles were embedded in swellable microparticles (El-Sherbiny and Smyth, (2012)). They offer a method to deliver nanoparticles *via* dry powder inhalers (DPIs) as DPIs are not able to disperse nanoparticles on their own. El-Sherbiny & Smyth, (2010) encapsulated PEG-grafted N-phthaloyl chitosan nanoparticles into sodium alginate microspheres. The formulation showed an initial burst release for the first two hours, followed by a more gradual release over four days.

Swellable microparticles, however, suffer the same drawbacks at traditional microparticles in terms of less than ideal fluidisation and dispersibility, and that it may be challenging to tune the release of drugs through the swollen microparticles.

1.4.1.4 Liposomes

Liposomes are vesicles formed by lipid bilayers and can encapsulate hydrophilic drugs in the core and hydrophobic drugs in the lipid bilayers. By the use of rigid phospholipids or

cholesterol, a less permeable membrane can be created for drugs to diffuse through (Beck-Broichsitter *et al.*, (2013)). Liposomes can be prepared using lipids endogenous to the lung, such as dipalmitoylphosphatidylcholine (DPPC), the major phospholipid in lung surfactant, allowing such liposomes to be very well tolerated by the lung. Liposomal formulations are the only sustained release pulmonary delivery products which have reached clinical trials (Swaminathan and Ehrhardt, (2011)).

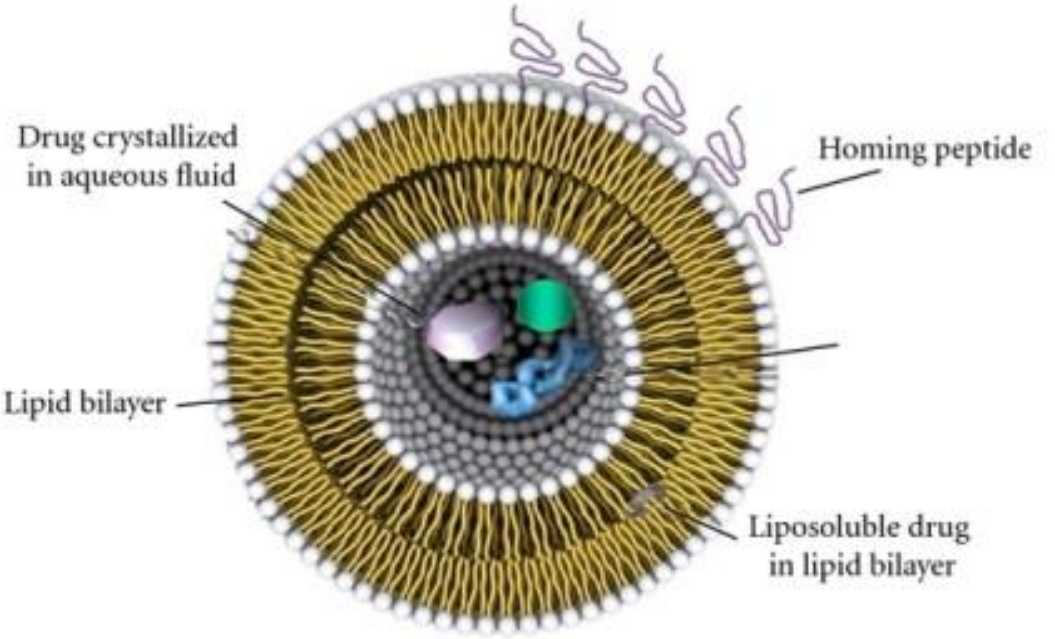

Figure 1.6. Schematic of a typical liposome developed for drug delivery. Peptides can be conjugated with the lipids to direct it to a particular location (Used with permission from (Bitounis et al., (2012)).

Arikayce®, liposomal amikacin formulations developed by Insmed are in phase III clinical studies for the treatment of nontuberculous mycobacterial lung infection and phase II clinical studies for chronic *Pseudomonas aeruginosa* in non-cystic fibrosis bronchiectasis (Ehsan and Clancy, (2015); "Pipeline," n.d.). Liposomal amikacin was able to provide slow sustained release in unaffected rat lungs. It is attracted to the negatively charged mucus and biofilms, and are able to deliver high levels of amikacin to the infection site, allowing once daily dosing in comparison to free aminoglycoside therapy of twice daily dosing of tobramycin.

Liposomes are widely delivered by nebuliser from a suspension, but long-term instability is a concern. Nebulisation can also disrupt the structure of the liposome, causing premature release of drug. As such, liposomes have also been formulated into dry powders by lyophilisation, spray-drying or spray freeze-drying (Bi *et al.*, (2008); Gibbons

et al., (2010); Misra *et al.*, (2009); Tang *et al.*, (2015); Willis *et al.*, (2012)). Another important factor to consider for the use of lipids in formulations is the high cost associated with the raw materials for the lipid excipients and the high production cost because of third party manufacturing (Jeong *et al.*, (2006)).

1.4.1.5 Solid lipid nanoparticles

Solid lipid nanoparticles (SLNs) were introduced in 1991 as an alternative carrier system to systems such as liposomes, emulsions and polymeric particles (Müller *et al.*, (2000)). A solid lipid core is stabilised by a surfactant with the active ingredient dissolved or dispersed. SLNs are well tolerated by the lungs and are more stable under nebulisation compared to liposomes.

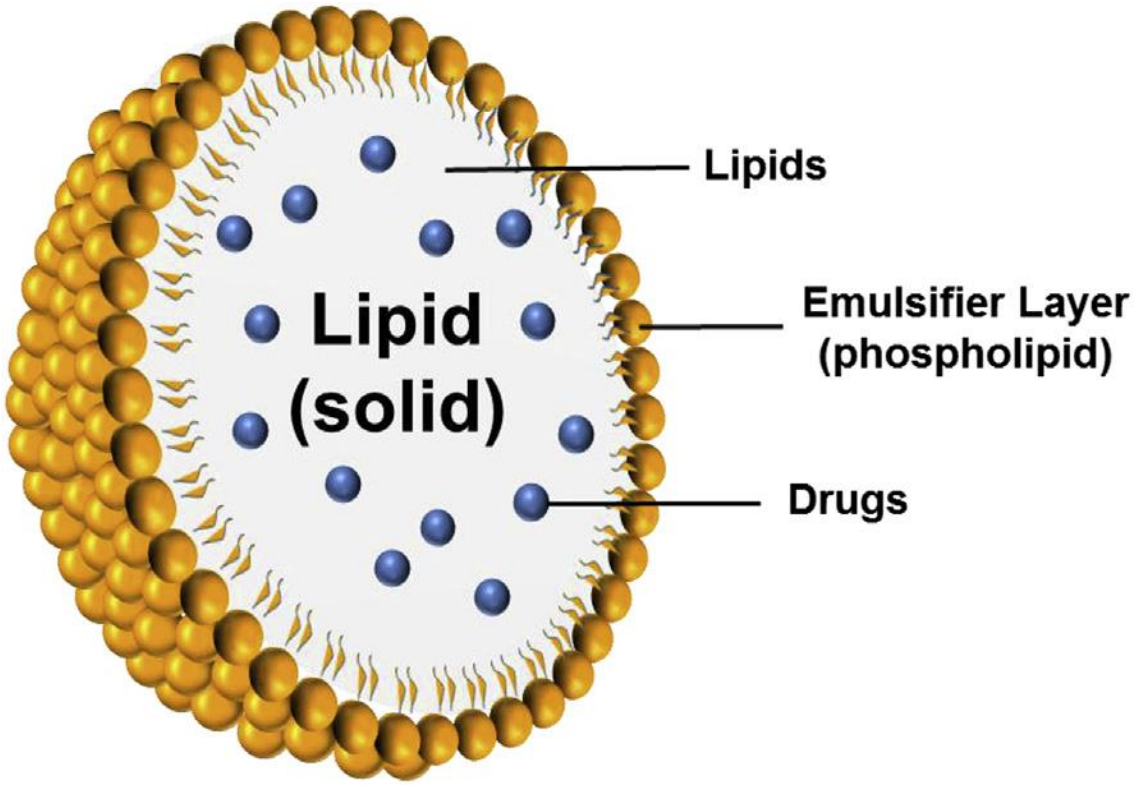

Figure 1.7. Structure of a solid lipid nanoparticle (SLN) (Used with permission from (Lin et al., (2017)).

C. Wu *et al.*, (2016) prepared SLNs loaded with a flavonoid compound, naringenin, by emulsification and were able to release 80% of the drug over 48 hours with a sustained profile. The lyophilised powders were stable at both refrigerated and ambient temperatures for three months, and the bioavailability of the drug in Sprague-Dawley rats was shown to be 2.5 times greater than that of naringenin suspensions. Zhao *et al.*, (2017) prepared essential oil-loaded SLNs by homogenisation and demonstrated extended

pulmonary retention of up to 24 h *in vivo*, with up to 7.7 fold increase of bioavailability compared to the essential oil solution.

However, SLNs are still a relatively immature technology with many advancements still to be made in the field. It also suffers from poor drug loading and potential gelation from polymorphism of the solid lipids.

1.4.1.6 Nanoparticle-embedded microparticles

As mentioned earlier, nanoparticles are not able to be dispersed by dry powder inhalers. As with the earlier examples of embedding nanoparticles within swellable microparticles, nanoparticles can also be embedded into microcarriers. Tsapis *et al.*, (2002) proposed combining the drug release advantage of nanoparticles with the flowability, aerosolisation and processing ease of microparticles by spray-drying nanoparticles with large porous particles. The large porous particles dissolve to release the nanoparticles, who bear the drug release load.

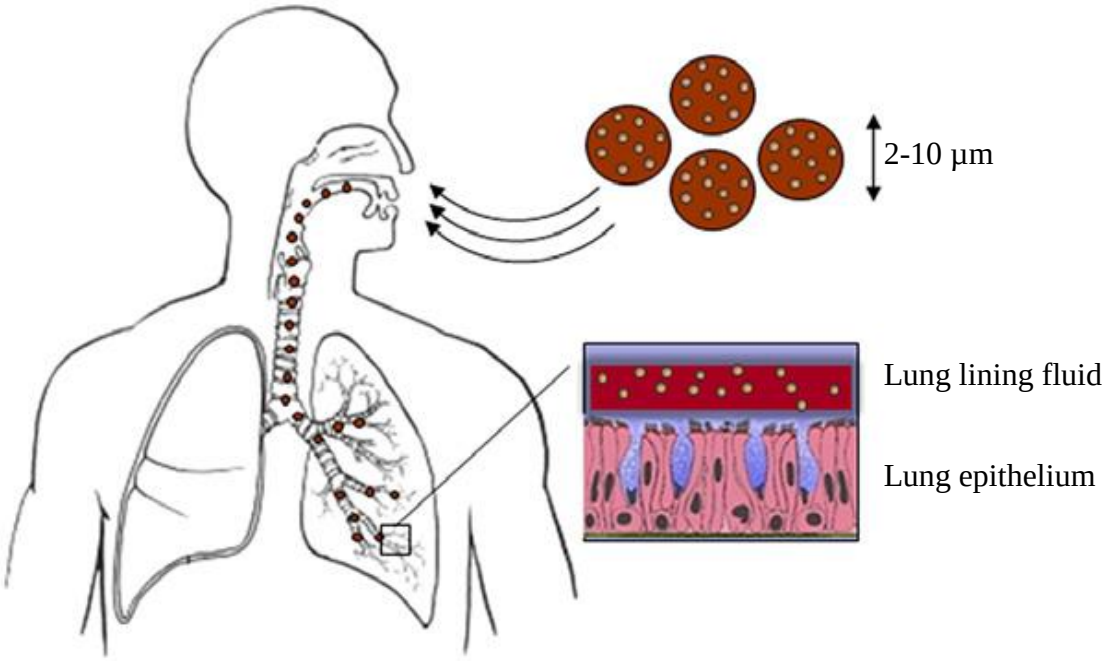

Figure 1.8. Mechanism for release of nanoparticles from nanoparticle-embedded microparticles in the lung.

2-10 µm

Ungaro, D'Angelo, *et al.*, (2012) developed a pulmonary delivery system of tobramycin-loaded PLGA nanoparticles embedded in lactose microparticles. The nanoparticles were optimised for size and surface properties by the addition of hydrophilic polymers such as polyvinyl alcohol (PVA) and chitosan, while alginate enabled the efficient entrapment of

Lung lining fluid

Lung epithelium

tobramycin and its release for up to one month *in vitro*.

Gold nano-in-micro dry powder formulations were investigated for the treatment of lung cancer (Silva *et al.*, (2017)). These gold nanoparticle-embedded microparticles were functionalised for disease targeting as well as theragnosis and were prepared by supercritical CO_2-assisted spray-drying. The nanoparticles displayed a sustained and controlled release of the gold nanoparticles, with enhanced cellular uptake.

While nanoparticle-embedded microparticles offer promise as a formulation strategy for controlling the release of active ingredients in the lung, redispersal of nanoparticles from the microparticles are not well controlled yet, with room for further improvement.

Table 1.1. Comparison of Different Formulation Strategies for Controlled Pulmonary

Delivery.

Formulation strategy	Advantages	Disadvantages
Microparticles	• Straightforward manufacturing • Mature process	• Non-ideal fluidisation and dispersibility • Phagocytosis by alveolar macrophages
Large porous particles	• Reduced phagocytosis by alveolar macrophages • Better aerosolisation properties	• Poor control of encapsulation and release • Difficult to scale up manufacturing process
Swellable microparticles	• Reduced phagocytosis by alveolar macrophages	• Non-ideal fluidisation and dispersibility • Tricky to tune drug release
Liposomes	• Biocompatible • Reduced phagocytosis by alveolar macrophages • Able to solubilise poorly soluble drugs	• Expensive • Drug leakage due to instability
Solid lipid nanoparticles	• Biocompatible • More stable than liposomes	• Poor drug loading • Possibility of gelation
Nanoparticle-embedded microparticles	• Reduced phagocytosis by alveolar macrophages	• Redispersal of nanoparticles not well controlled

1.5 Pulmonary delivery devices

There are three main types of inhaler devices for pulmonary delivery: Nebulisers, pressurised metered dose inhalers (pMDIs) and dry powder inhalers. When considering which type of inhaler device to use, several studies have concluded that there is little difference between them and that factors to consider in choosing an appropriate device depend not only on physicochemical properties such as drug particle size but also on an individual patient's inspiratory airflow, skill and choice (Bonini and Usmani, (2015); Brocklebank *et al.*, (2001); Haughney *et al.*, (2010)). However, dry powder inhalers are

touted as having the greatest research and development potential for improved pulmonary therapy as the newest technology of the three (de Boer *et al.*, (2017)).

1.5.1 Nebulisers

Nebulisers are amongst the oldest devices used for delivering therapeutic agents. They are used to deliver a single dose of therapeutic agent in an aqueous medium, usually over multiple breaths *via* tidal breathing. They are typically used for the delivery of bronchodilators for those afflicted with asthma or COPD who cannot use other devices effectively, such as the elderly and young, as they do not require coordination between inhalation and actuation.

Nebulisers utilise different technologies to deliver drug aerosols and there are three commonly used types: jet nebulisers which use compressed air to deliver the drug formulation through a spray nozzle; ultrasonic nebulisers which form aerosols from a vibrating piezoelectric crystal; and vibrating membrane/mesh nebulisers where the drug is extruded through a vibrating membrane or mesh. Jet nebulisers operate by the Bernoulli principle (Venturi effect). High pressure compressed gas is passed through a nozzle called a venturi. This creates a low-pressure region at the nozzle where a liquid (or suspension) drug formulation will be drawn up into the air into droplets. Larger droplets are blocked from entering the mouthpiece or facemask by a baffle, which in turn recycles these larger droplets to be re-nebulised.

Nebulisers are easy to use and are able to deliver most drugs in any given dose. However, they are bulky to handle and can only deliver single doses and are thus usually limited to a hospital or home setting.

1.5.2 Pressurised metered dose inhalers

As previously mentioned, modern drug delivery to the lungs was started by the commercial availability of pressurised metered dose inhalers (pMDIs) for the treatment of asthma by Riker Laboratories in 1956 (Crompton, (2006)). However, the effect of CFCs used as propellants in pMDIs on the depletion of the ozone layer hypothesised by Molina & Rowland in 1974 prompted their substitution by the relatively more environmentally friendly hydrofluoroalkane (HFA) gases as directed by the Montreal protocol in 1987 (*Handbook for the Montreal Protocol on Substances that Deplete the Ozone Layer*, (2017)). Since the transition to the new propellants, pMDIs have remained

a widely used and accepted form of inhalation therapy worldwide (Myrdal *et al.*, (2014)). A schematic of a pMDI is shown in Figure 1.9. A canister holds the propellant formulation (either a solution or suspension) with a metering valve crimped to its lid. Upon actuation, the metering valve releases a known quantity of the formulation. The propellant expands when it exits the nozzle, resulting in a fine mist, which is quickly evaporated off to leave micron-sized drugs for inhalation.

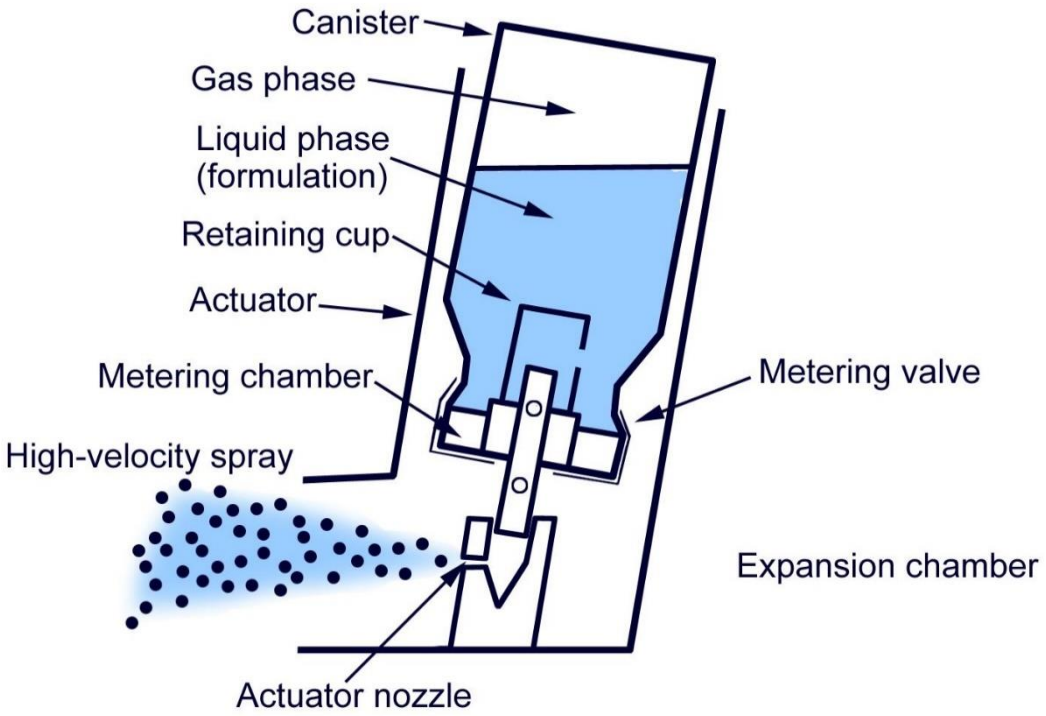

Figure 1.9. Schematic of the major components of a pMDI (Reproduced from Buddiga, (2015))

The advantages of pMDIs are that they are portable, easy to handle, capable of delivering multiple doses of drug, have better protection against moisture, and have a lower risk of bacterial contamination (Newman, (2005)). However, they have a lower capacity than dry powder inhalers and are thus able to deliver fewer doses (Traini and Young, (2013)). In some instances, patients have had adverse reactions to the Freon propellants used in the inhalers (Oenbrink, (1993)) and some complain of the cooling effect that the rapid evaporation of propellant causes (Purewal and Grant, (1997)). However, the greatest patient related drawback to pMDIs is that it requires the patient to make a coordinated effort to actuate the device and inhale simultaneously, compared to the breath actuated DPIs and the tidal breathing regime of nebulisers. The delivery of drugs are highly dependent on the inhalation technique and it is possible to get very little drug in the lung with poor technique; if the patient inhales before or after actuations, most of the drug will

be caught in the throat and swallowed, instead of depositing in the lung (Traini and Young, (2013)).

In order to address these issues, two modifications to classical pMDIs have been adopted: the use of spacers and breath-actuated pMDIs.

A spacer is a device which is attached to the mouthpiece of the inhaler. The aerosol is actuated into the spacer first, for the patient to inhale using tidal breathing (normal, automatic breathing). Since spacers are add-on devices, they do not require modification to an existing pMDI. Being able to inhale the dose *via* tidal breathing brings benefits to certain subpopulations such as children and the elderly. However, whilst still portable, spacers can add some bulk to the inhaler device, so convenience is compromised. As spacers are another "space" between the inhaler and the patient, it is another item to consider when handling the inhaler. Variations in the aerosol cloud and dose could occur due to this intermediate "space" (Chew and Chan, (2000)) and these spacers have to be maintained in a proper manner to minimise static charge on the inner surfaces of the spacers, which could attract particles to it and thus reduce the delivered dose (Anhøj *et al.*, (1999)).

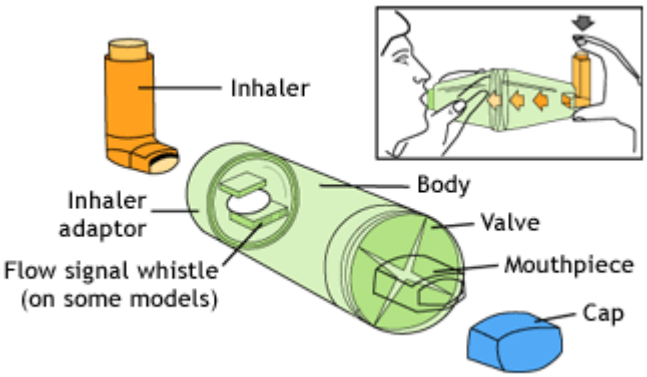

Figure 1.10. Schematic of a spacer attachment for a pMDI ("How to Use Your Inhaler," n.d.)

Breath-actuated pMDIs require modifications to the device, where the canister is held in a post-actuated state to be released when the patient inhales. This does away with the need to coordinate actuation and breathing but still requires forced inspiration as opposed to tidal breathing with the use of spacers. Although fewer patients display improper inhaler technique with these devices compared to pMDIs (Lenney *et al.*, (2000)), they require greater inspiratory flow compared to pMDIs and also do not solve the issue of the cooling effect mentioned above (Lavorini, (2013)).

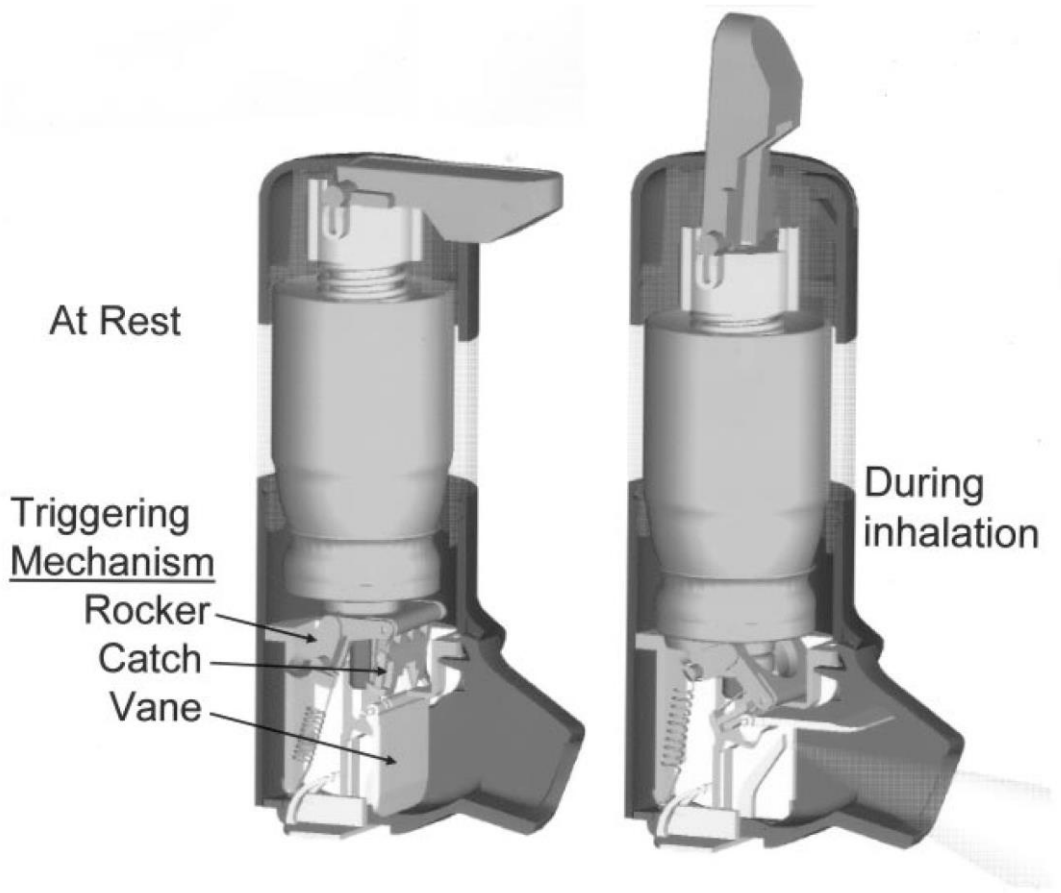

Figure 1.11. Schematic of a breath-actuated pMDI (Autohaler, 3M Pharmaceuticals, St Paul, MN, USA) (Used with permission from Newman, 2005).

1.5.3 Dry powder inhalers

Dry powder inhalers were developed to address some of the limitations of pMDIs. Some issues arising from the use of pMDIs include low solubility (Smyth, (2003)), crystal growth (Phillips and Byron, (1994)), chemical instability (Wu *et al.*, (2012)) of active ingredients. DPIs are propellant-free [negating the discussion on the potency of HFAs as greenhouse gases, notwithstanding their minuscule contribution to overall greenhouse gas emissions (McDonald and Martin, (2000))] and do not require patients to simultaneously actuate the device with inspiratory airflow, which could prove difficult for certain patients (O'Connor, (2004); Stein *et al.*, (2014)). However, the patient convenience that actuation through a patient's inspiratory airflow brings, also means that the deposition efficiency is dependent on individual patients' inspiratory airflow. Dry powder inhalers can be classified as 'passive' devices, where DPIs utilise the patient's inspiratory airflow to deliver the medication to the lungs; or 'active' devices, where the energy needed to

aerosolise the powder comes from an external source such as compressed air or a battery. There are more than 20 different commercially available DPIs which are used for local and systemic delivery (Valdes *et al.*, (2014)) of active ingredients (Berkenfeld *et al.*, (2015)). Recently, low-cost, single-use disposable DPIs have been developed, which opens up avenues to the cheap and reliable delivery of vaccines as well as medication for rescue operations (Berkenfeld *et al.*, (2015)).

As mentioned earlier, an aerodynamic diameter of 1-5 μm is required for particles to deposit in the small airways and the alveolar regions (Labiris and Dolovich, (2003)). However, at these sizes, the micronised powders tend to be cohesive/adhesive and form agglomerates due to interparticulate forces such as van der Waals, mechanical interlocking, capillary, and electrostatic forces (Telko and Hickey, (2005)). These agglomerates have to be deagglomerated before they enter the respiratory system as they affect the respirable dose. Traditionally, the micronised powders have been blended with a coarse carrier (30-90 μm) such as lactose, to improve flow properties and enhance dispersion. However, problems may arise if the carrier is not blended uniformly and if there is poor detachment from of the drug from the carrier, while the aforementioned interparticulate forces are only reduced and not eliminated (Thalberg *et al.*, (2012)). As such, some studies are focused employing particle engineering techniques, such as spray-drying and wrinkled surfaces, to develop carrier-free formulations for dry powder inhalers which reduce the cohesion forces of the particles, while maximising redispersion of the powders (Healy *et al.*, (2014)).

Dry powder inhaler devices can be categorised into three groups: single dose, multi-unit dose and multi-dose reservoir systems. Single-unit dose inhalers are the most commonly used type of DPI. The patient loads a capsule filled with the micronised powder into the DPI and ruptures it before the inhalation manoeuvre. The punctured capsule shell must be removed before administrating the next dose. Multi-dose devices come with pre-metered doses stored in individually sealed packaging such as blister packs or discs, while multi-dose reservoir systems contain a reservoir of dry powder which is dispensed by a built-in mechanism.

Single-unit dose inhalers have also been developed as disposable single use devices (Friebel and Steckel, (2010)). TwinCaps® inhaler (Hovione, Loures, Portugal) is a disposable DPI which has been approved for use in Japan. It is used in the postexposure prophylactic treatment of influenza A and B infections. Disposable DPIs also open up the potential for the delivery of vaccines in developing countries, where access to sterile

medical supplies and uninterrupted cold chain storage conditions may be less than ideal. DPIs present a non-invasive delivery route which may be administered by a non-medically trained person. Disposable DPIs could also be used in the delivery of medication in rescue situations.

1.6 Particle production technologies for pulmonary delivery

As highlighted, the physicochemical properties of aerosol particles play an important role in its deposition in the lung. Despite its relatively long history in treating diseases and ailments in the lung, there is still much room for improvement for the delivery of active agents to the lungs including in the areas of deposition efficiency, targeting and sustained or controlled release (Koushik and Kompella, (2004); Smyth and Hickey, (2011)). Inhaled drug powders were traditionally produced by crystallising the drug, then milling it down to a suitable size. These days, a number of engineering strategies can be employed to produce inhalation products, especially in particle engineering where methods such as spray freeze-drying and spray-drying could be used to find solutions to the delivery of therapeutic agents in the treatments of the pulmonary ailments. Particle engineering advancements have enabled the development of pulmonary delivery systems that are carrier-free, have biodegradable fine carriers and offer combinational therapy amongst others. Particle engineering technology has also been adopted to modify the physicochemical properties of the particles, such as density, morphology, surface characteristics, and the formation of amorphous and polymorphic forms of active ingredients, to achieve improvements in aerosol performance, lung deposition and dissolution (Chow *et al.*, (2007)).

1.6.1 Spray freeze-drying

Spray freeze-drying (SFD) is a technology combining spray drying and freeze drying, as its name suggests. In SFD, a drug solution is sprayed into the cold vapour above a freezing medium (usually liquid nitrogen) to form droplets. The droplets are subsequently lyophilised to remove ice and generate powders (Figure 1.12). The process is able to produce light particles with virtually 100% product yield. However, it was found that the time required for the droplets to freeze and the air-liquid interface formed on the surface of the droplets may result in a broad particle size distribution and aggregation (Webb *et al.*, (2002); Yu *et al.*, (2006)). Spray freezing into liquid (SFL) was developed to

overcome this problem (Hu *et al.*, (2002)). In SFL, the drug solution is sprayed directly into the liquid cryogen instead of its vapour, at a faster speed compared to SFD. This process produces amorphous powders with a narrow size distribution, high surface area and low bulk density exhibiting good flowability (Hu *et al.*, (2003); Rogers *et al.*, (2002)). However, the use of cryogens makes it an expensive process, justifiable only for an expensive drug.

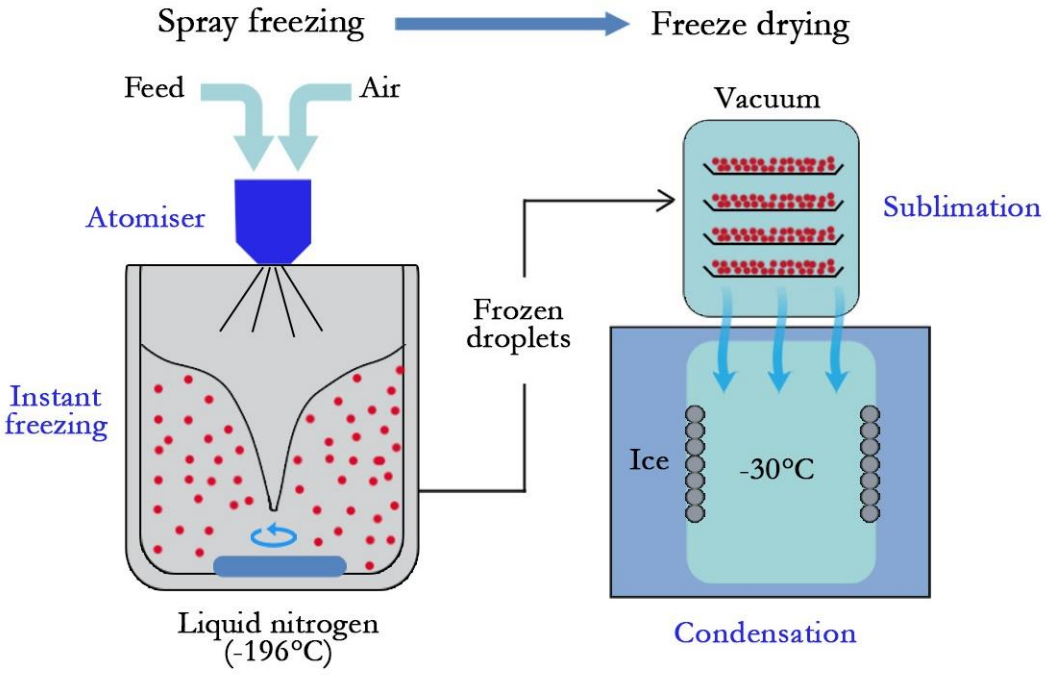

Figure 1.12. Schematic of spray freeze-drying process.

1.6.2 Spray drying

In the spray drying process, a drug solution or suspension is passed through an atomising nozzle to form fine droplets. These droplets are then rapidly dried by a hot air current to form dry powders, which are separated from the air flow by a cyclone into a collection vessel (Figure 1.13a). The spray dryer can also be set up to run in a 'closed loop' for poorly water-soluble drugs, with an inert loop to condense organic solvent vapours (Figure 1.13b).

There is a range of different nozzles which can be used for spray drying: rotary atomisers, ultrasonic nozzles, and two-fluid nozzles. Son & McConville, (2012) utilised a three-fluid nozzle to simultaneously encapsulate and coat rifampicin particles in a single, continuous process for sustained release in the lung. This presents an interesting prospect of combining a particle engineering process together with a coating process to minimise

both time and loss of material into a single operation.

Spray drying has become a standard technique to produce powders for inhalation. It is an important tool in the particle engineering field as it offers a facile, one-step process which is scalable for larger production while giving one control over the particle size, particle size distribution, particle morphology, moisture content of particles and surface properties such as particle surface area, which are all important characteristics in any DPI system, by tuning the aspirator flow rate, inlet temperature, spray gas flow and feed solution rate (Seville *et al.*, (2007); Vehring, (2008)). Spray drying has been employed to produce commercially available inhaler products (Carvalho *et al.*, (2015)).

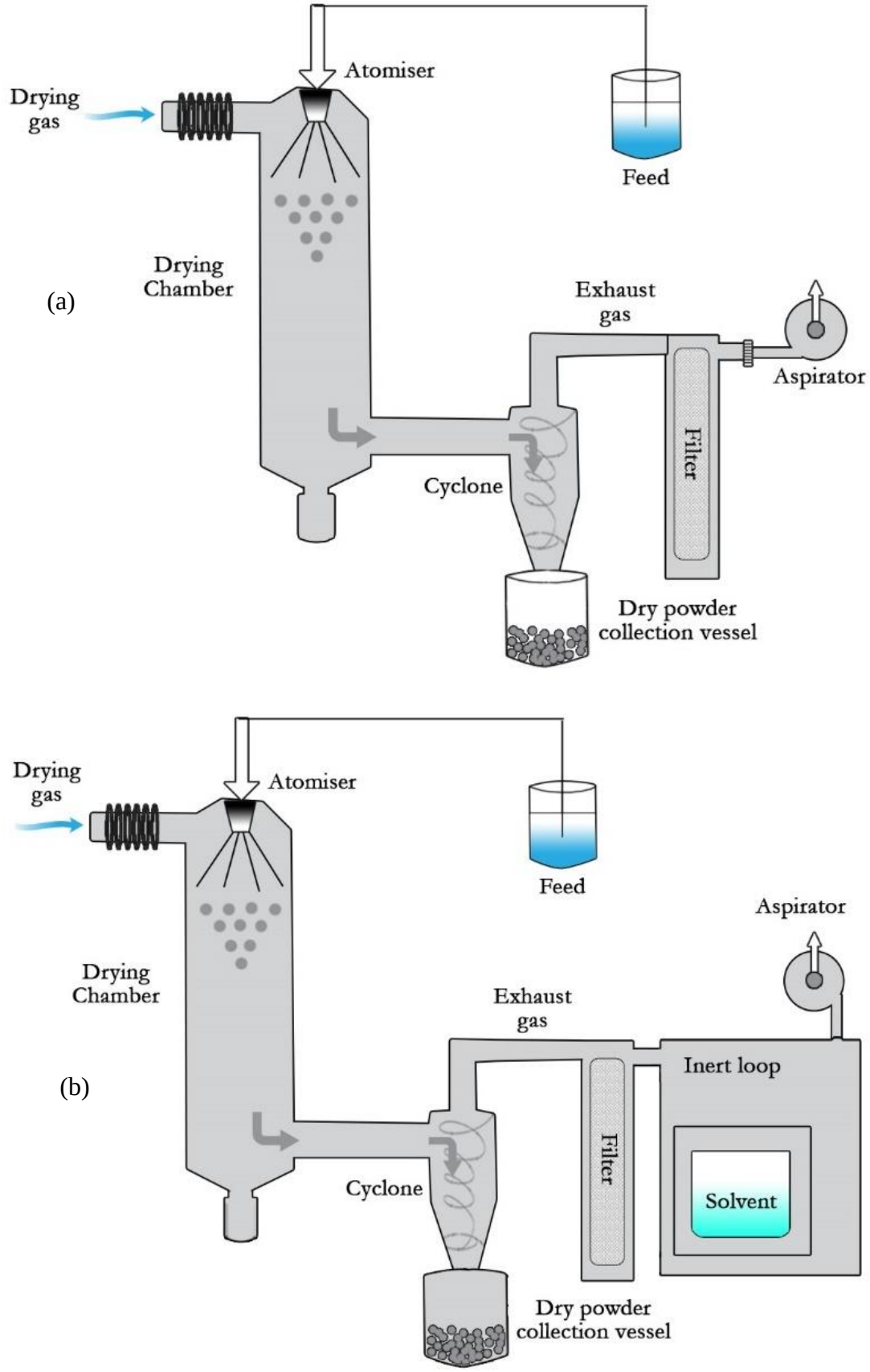

Figure 1.13. Schematic of spray dryer in (a) 'open loop' and (b) 'closed loop' configuration.

1.6.2.1 Nano spray-drying

While spray drying can be used to effectively prepare microparticles, it is unable to do so for nanoparticles because of separation and collection limitations (Heng *et al.*, (2011)). The nano spray dryer from BÜCHI (Flawil, Switzerland) was developed specifically to generate particles with sizes ranging from 300 nm to 5 µm, which is a size range which has great potential for the pulmonary field as nanoparticles are able to reduce phagocytosis by alveolar macrophages (Todoroff and Vanbever, (2011)). However, it is limited by a low throughput and long processing times. The technology is still in its early stages and is characterised by high cost (which may go down as the technology matures) that may limit its current use to high-value products.

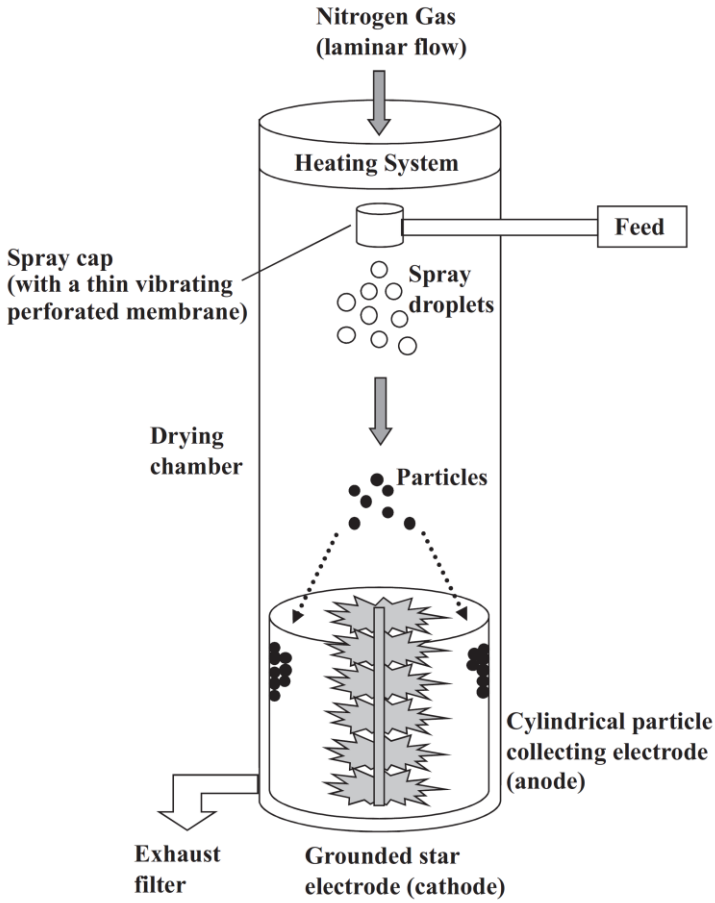

Figure 1.14. Schematic of the laboratory scale Nano Spray Dryer B-90 (Used with permission from S.H. Lee *et al.*, 2011).

1.7 Aims and objectives

The aim of this thesis is to investigate controlled pulmonary drug delivery systems. Two systems have been formulated for drugs of different natures: water-soluble and poorly water-soluble. The fast release of drugs results in high absorption with high concentrations but a short duration of action while overly slow release may result in non-therapeutic drug levels (Loira-Pastoriza *et al.*, (2014)).

These systems were designed to be cost-effective for greater access to inhaled therapy worldwide, where there is a high incidence of mortality from respiratory diseases and where there is an unmet demand for cheap and effective inhaled therapy. Pulmonary delivery offers a safe and convenient means of administering medicine without the need of a trained medical professional, and controlling the release of the drugs from pulmonary delivery systems may enhance patient convenience and compliance.

To that end, administration of drugs using dry powder inhalers was selected for this study as they offer greater physicochemical stability of drugs, the possibility to deliver drugs in a cheap, disposable form, and the greatest potential for new, improved therapies (de Boer *et al.*, (2017)).

Spray drying is a mature manufacturing technology which has been applied to produce powders for inhalation commercially. It offers a facile, continuous and scalable process from feed to dry powder, and hence is ideal for producing inhalable powders.

More specifically, the objectives can be described as:

1. Develop controlled pulmonary drug delivery systems with a suitable release rate and necessary characteristics for effective pulmonary delivery.
2. Evaluate the feasibility of using a hybrid drug delivery system to modulate the release of a water-soluble drug with the use of two excipients with complementary features.
3. Explore the use of a commercially available amphiphilic excipient, with the ability to solubilise poorly water-soluble drugs and form solid solutions, as a strategy to formulate poorly water-soluble corticosteroids and increase its dissolution rate in the lung.
4. Study the physical stability of the spray-dried powders.

2 SCIENTIFIC METHODS

2.1 Yield, drug loading, and entrapment efficiency

The formulations were evaluated for their spray-drying yield using the following equation:

$$\text{Yield (\%)} = \left(\frac{\text{Weight of solids collected from spray dryer}}{\text{Weight of solids added to spray-drying feed solution}}\right) \times 100 \quad (5)$$

Weighed amounts of spray-dried powder were dissolved in dissolution medium and left to stir for three days. The drug content in the dissolution was analysed either by ultraviolet-visible (UV-vis) spectroscopy or high-performance liquid chromatography (HPLC) and calculated using the following equations:

$$\text{Drug loading (\%)} = \left(\frac{\text{Weight of drug in spray-dried powder}}{\text{Weight of spray-dried powder}}\right) \times 100 \quad (6)$$

$$\text{Entrapment efficiency (\%)} = \left(\frac{\text{Weight of drug in spray-dried powder}}{\text{Weight of drug added to spray-drying feed solution}}\right) \times 100 \quad (7)$$

2.2 Powder crystallinity

Powder X-ray diffractograms were obtained for the co-spray dried particles using an X-ray diffractometer (D8 ADVANCE, Bruker Corporation, Madison, WI, USA) in steps of 0.02° using Cu Kα radiation as the X-ray source. The measurement conditions were as follows: target, Cu; filter, Ni; voltage, 35 kV; current, 40 mA; scanning speed, 10°/min

2.3 Moisture sorption

The moisture sorption properties of the formulated powders were investigated using dynamic vapour sorption (DVS) (DVS-Advantage, Surface Measurement Systems, London, UK). About 30 mg of powder was used per measurement, subjected to two cycles of 0-90% RH with 10% RH steps. The system was considered to have attained equilibrium when the rate of change of mass per time (*dm/dt*) was less than 0.001% per step.

2.4 Surface composition

The surface of the formulations was probed by X-ray photoelectron spectroscopy (XPS) (also known as electron spectroscopy for chemical analysis [ESCA]) using an ESCALAB 250 Xi X-ray photoelectron spectrometer microphobe (Thermo Scientific, Waltham, MA, USA). The measurements were carried out using an XR6 monochromated Al Kα (1486.68 eV) X-ray source with a circular analysis spot size of 200 µm at an analysis depth of less than 110 Å. The powders were mounted onto adhesive copper tape.

The surface composition of the powders can be estimated by studying the relative atomic concentrations of different elements in the pure spray-dried components and the spray-dried formulations (Elversson and Millqvist-Fureby, (2005); Fäldt *et al.*, (1993)).

For CS:

$$\begin{bmatrix} \boldsymbol{I}^{\mathrm{C}}_{\mathrm{CS}} & \boldsymbol{I}^{\mathrm{C}}_{\mathrm{BSA}} & \boldsymbol{I}^{\mathrm{C}}_{\mathrm{PVA}} \\ \boldsymbol{I}^{\mathrm{O}}_{\mathrm{CS}} & \boldsymbol{I}^{\mathrm{O}}_{\mathrm{BSA}} & \boldsymbol{I}^{\mathrm{O}}_{\mathrm{PVA}} \\ \boldsymbol{I}^{\mathrm{N}}_{\mathrm{CS}} & \boldsymbol{I}^{\mathrm{N}}_{\mathrm{BSA}} & \boldsymbol{I}^{\mathrm{N}}_{\mathrm{PVA}} \\ \boldsymbol{I}^{\mathrm{Na}}_{\mathrm{CS}} & \boldsymbol{I}^{\mathrm{Na}}_{\mathrm{BSA}} & \boldsymbol{I}^{\mathrm{Na}}_{\mathrm{PVA}} \end{bmatrix} \cdot \begin{pmatrix} \boldsymbol{\gamma}_{\mathrm{CS}} \\ \boldsymbol{\gamma}_{\mathrm{BSA}} \\ \boldsymbol{\gamma}_{\mathrm{PVA}} \end{pmatrix} = \begin{pmatrix} \boldsymbol{I}^{\mathrm{C}}_{\mathrm{formulation}} \\ \boldsymbol{I}^{\boldsymbol{O}}_{\mathrm{formulation}} \\ \boldsymbol{I}^{\mathrm{N}}_{\mathrm{formulation}} \\ \boldsymbol{I}^{\mathrm{Na}}_{\mathrm{formulation}} \end{pmatrix} \quad (8)$$

For BDP:

$$\begin{bmatrix} I^{\mathrm{C}}_{\mathrm{BDP}} & I^{\mathrm{C}}_{\mathrm{Soluplus®/PVP\ K130}} \\ I^{\mathrm{O}}_{\mathrm{BDP}} & I^{\mathrm{O}}_{\mathrm{Soluplus®/PVP\ K130}} \\ I^{\mathrm{N}}_{\mathrm{BDP}} & I^{\mathrm{N}}_{\mathrm{Soluplus®/PVP\ K130}} \\ I^{\mathrm{Cl}}_{\mathrm{BDP}} & I^{\mathrm{Cl}}_{\mathrm{Soluplus®/PVP\ K130}} \end{bmatrix} \cdot \begin{pmatrix} \gamma_{\mathrm{BDP}} \\ \gamma_{\mathrm{Soluplus®/PVP\ K130}} \end{pmatrix} = \begin{pmatrix} I^{\mathrm{C}}_{\mathrm{formulation}} \\ I^{\boldsymbol{O}}_{\mathrm{formulation}} \\ I^{\mathrm{N}}_{\mathrm{formulation}} \\ I^{\mathrm{Cl}}_{\mathrm{formulation}} \end{pmatrix} \quad (9)$$

Or

$$I\gamma = f \quad (10)$$

where I is the matrix of the elemental composition of the pure components, f is the vector containing the elemental composition of a formulation's surface, and γ the relative coverage of the different components. The equation can be solved to find out which

components are on the surface of the formulations using a linear least squares method which gives:

$$\gamma = (I^{\mathrm{T}}I)^{-1}I^{\mathrm{T}}f \quad (11)$$

To compare the estimated surface coverage results with that of the bulk composition of the spray-dried formulations, the estimated molar percentages were converted to mass percentages.

2.5 Powder morphology

Particle size morphology was examined using a high-resolution field emission scanning electron microscope (FESEM, JSM-6700F, Jeol Ltd, Tokyo, Japan). Each sample was mounted onto a SEM stub using double-sided copper tape then sputter coated with gold for one min under vacuum at 0.05 mbar by a sputter coater (High Resolution Sputter Coater 208HR, Cressington Scientific, Watford, UK). The SEM was operated at an accelerating voltage of 2-5 kV.

2.6 Particle size analysis

Particle size distributions and mean particle diameters were measured by static light scattering on a Malvern Mastersizer 2000 with the Scirocco dry dispersion unit (Malvern Instruments Ltd, Malvern, UK). Analysis was conducted based on the refractive index of CS (1.681) and BDP (1.564). Samples were added at a feed pressure of 3.5 bar for cromolyn sodium (CS) formulations and 2.0 bar for beclomethasone dipropionate (BDP) formulations. Each experiment was conducted in triplicate at ambient temperature.

2.7 *In vitro* aerosol performance

The aerosol performance of the spray-dried powders was assessed using a multi-stage liquid impinger (MSLI, Copley Scientific, Nottingham, UK) coupled with a United States Pharmacopoeia (USP) stainless steel throat in a walk-in environmental chamber (Synersys, Singapore) maintained at 25 °C and 40% RH. Prior to testing, 20 mL of deionised water (for CS formulations) or methanol-water (3:1 v/v) (for BDP formulations) was added across all four stages of the MSLI. Powder from each formulation was filled into a hydroxypropyl methylcellulose (HPMC) capsule (size 3, Capsugel®, Morristown, NJ, USA), loaded into the high-efficiency Aerolizer® inhaler (Novartis Pharmaceuticals, Basel, Switzerland) and pierced. The powder was then

dispersed for 4 s at 60 L/min. The flow through the MSLI was measured with a calibrated flow meter (TSI Model 4040C, TSI Instrument Ltd., Buckinghamshire, UK), controlled by a critical flow controller (TPK 2000, Copley Scientific, Nottingham, UK) and a dry-running rotary vane vacuum pump (Seco SV 1040 C, Busch LLC, Virginia Beach, VA, USA). The test was performed in triplicate to obtain mean values.

After dispersion, the device, capsule, throat and each stage of the MSLI were washed separately and thoroughly using deionised water (for CS formulations) or methanol-water (3:1 v/v) (for BDP formulations). Drug deposited at different locations was assayed by UV spectrophotometry (Cary 50 Conc UV-visible spectrophotometer, Varian Inc., Palo Alto, CA, USA) or HPLC (1100 series; Agilent Technologies, Santa Clara, CA, USA). In this study, fine particle fraction (FPF) represents the mass fraction of drug particles smaller than 5 μm in the aerosol cloud relative to the total mass recovered and was obtained by interpolation to the cumulative percent undersize at 5 μm. FPF (emitted) was obtained when the fine particle dose was expressed relative to the emitted dose. At a flow rate of 60 L/min, the aerodynamic cut-off diameters of stages 1, 2, 3 and 4 are 13.0, 6.8, 3.1 and 1.7 μm. Particles with diameters less than 1.7 μm were captured on an integral glass fibre filter paper.

2.8 Mathematical models of dissolution profiles

There are several models which can describe drug dissolution from pharmaceutical dosage forms. The type of drug, its crystallinity, particle size distribution, solubility, polymorphic form of drug, and drug loading can all affect the release kinetics (Ei-Arini and Leuenberger, (1995)). The dissolution profiles of the formulations were analysed by various established mathematical kinetic models in literature (Costa and Sousa Lobo, (2001)) and described further below.

2.8.1 Zero order kinetics

Pharaceutical dosage forms that do not disaggregate and release the drug slowly can be described the zero order kinetics. It has the ideal profile of the same quantity of drug release per unit time.

Zero order kinetics:

$$f_t = K_0 t \tag{12}$$

where f_t represents the fraction of drug dissolved at time and K_0 the rate constant for zero order release

2.8.2 First order kinetics

First order kinetics describe pharmaceutical dosage forms whereby the drug release is proportional to the amount of drug remaining. The amount of drug release per unit time decreases over time. This model assumes that the matrix is insoluble, does not swell, and is inert to the drug. The release of water-soluble drugs from a porous matrix will follow such a dissolution profile.

First order kinetics:

$$\ln Q_t = -K_1 t + \ln Q_0 \quad (13)$$

where Q_t is the amount of drug dissolved at time t, Q_0 is the initial amount of drug in solution, and K_1 is the rate constant for first order release.

2.8.3 Hixson-Crowell model

The Hixson-Crowell model (Hixson and Crowell, (1931)) describe the situation where the dosage form's geometric shape diminish proportionately over time. In this case, the assumption is that the rate-limiting step is the drug particle's dissolution rate, rather than diffusion rate through a polymeric matrix.

Hixon-Crowell model:

$$(1 - f_t)^{1/3} = 1 - K_\beta t \quad (14)$$

where f_t represents the fraction of drug dissolved at time, and K_β is the rate constant for the Hixson-Crowell model.

2.8.4 Higuchi model

The Higuchi model bases itself on Fick's first law (Higuchi, (1963), (1961)), and describes drug release as a diffusion process which is square root time dependent. In contrast to the Hixson-Crowell model, the rate-limiting step for the Higcuhi model is the

diffusion rate, rather than a drug particle's dissolution rate. It can be used to describe systems such as water-soluble drugs in a tablet matrix.

Higuchi model:

$$f_t = K_H t^{1/2} \tag{15}$$

where f_t represents the fraction of drug dissolved at time, and K_H is the rate constant for the Higuchi model.

2.8.5 Baker-Lonsdale model

The Baker-Lonsdale model was derived from the Higuchi model for drug release from a spherical matrix (Baker and Lonsdale, (1974)). Drug particles are assumed to be small relative to matrix radius, and the matrix is assumed to be non-swelling and non-erodible.

Baker-Lonsdale model:

$$f_t = \frac{3}{2}\left[1 - \left(1 - \frac{M_t}{M_\infty}\right)^{2/3}\right] - \frac{M_t}{M_\infty} = \frac{3D_m C_{ms}}{r_0^2 C_0} t = kt \tag{16}$$

where f_t represents the fraction of drug dissolved at time, M_t is the amount of drug released at time t, M_∞ is the amount of drug released at infinite time, D_m is the diffusion coefficient, C_{ms} is the drug solubility in the matrix, r_0 is the radius of the spherical particle matrix, C_0 is the initial concentration of drug in the matrix, and k is the slope of the linear Baker-Lonsdale model plot.

2.8.6 Korsmeyer-Peppas model

The Korsmeyer-Peppas model (Korsmeyer et al., (1983)) is a semi-empirical model where drug release is related to the time exponentially. The release exponent accounts for different types of drug transport mechanisms (Fickian, anomalous, Case-II, Super Case-II), and can be used to describe pharmaceutical dosage forms where the release mechanism is not well known or complex (more than a single type of release mechanism involved).

Korsmeyer-Peppas model:

$$\log M_t = n \cdot \log t + \log(a \cdot M_\infty) \quad (17)$$

where M_t is the amount of drug released at time t, M_∞ is the amount of drug released at infinite time, n is the release exponent related to the drug release mechanism, a is a constant incorporating structural and geometrical aspects of the drug particles.

3 HYBRID PROTEIN-POLYMER PARTICLES FOR RELEASE MODULATION OF INHALED POWDERS

3.1 Introduction

The potential advantages of administering medication by inhalation are well known to us (Bryan, (1930)); for respiratory related diseases, therapeutics can be delivered with a rapid onset of action directly to the ailment site in the lung and has the advantage of avoiding hepatic first pass metabolism in the process. The required amount of dose can be decreased with localised delivery to the lung and side effects usually associated with systemic delivery may be minimised (McCalden, (1990); Olsson *et al.*, (2011)). Recently, delivery through the lungs has also been mooted as an attractive non-invasive route for delivery of drugs into systemic circulation (Patton and Byron, (2007)) as the lung presents a large surface area for absorption with only a thin barrier to absorption.

However, pulmonary drug delivery systems are limited by the effective clearance systems in the lung. Water-soluble drugs are often quickly absorbed upon administration and may

experience uncomfortable peaks in local concentrations, followed by lower than therapeutic level concentrations (Loira-Pastoriza *et al.*, (2014)). Sustaining the release of drugs may reduce the need for frequent dosing, leading to greater patient convenience and compliance.

Particle engineering plays an important part in the development of controlled inhalation therapy strategies, particularly for dry powder inhalers (DPIs) (Chow *et al.*, (2007); Hickey and Mansour, (2008)). Particles in the nanometre range are predominantly exhaled from the lungs, while large particles will be trapped in the oropharynx for clearance *via* the mucociliary escalator (Grenha *et al.*, (2007)). Hence, to be viable, any controlled release system should efficiently produce particles with a mass median aerodynamic particle (MMAD) size of 1-5 μm (Labiris and Dolovich, (2003); Patton and Byron, (2007)). Controlling the release of water-soluble drugs in the lungs has an additional conundrum in that small particles are required for delivery to the lower airways, but a high surface area-to-mass ratio simultaneously favours a more rapid release. DPIs are also governed largely by particle properties such as particle size (Chew and Chan, (1999); Zeng *et al.*, (2000)), particle size distribution (Chew and Chan, (2002)), density (D'Addio *et al.*, (2012)), morphology (Adi *et al.*, (2008); Berkenfeld *et al.*, (2015); Chan, (2008); Chew *et al.*, (2005); Dunbar *et al.*, (1998)), and electrostatic forces (Chow *et al.*, (2008); Kwek *et al.*, (2013); Zhu *et al.*, (2008), (2007)).

Polymeric microparticles have been widely adopted to control the release of drugs for oral delivery and can easily be prepared by established manufacturing techniques. Much research on the ability of polymeric particles to control the release of drugs in the lung has been conducted (Learoyd *et al.*, (2008); Möbus *et al.*, (2012); Saigal *et al.*, (2013); R. O. Salama *et al.*, (2009b)).

However, there is an inherent difficulty in controlling the release of water-soluble drugs due to the size constraints required to deliver particles to the lower airways, given that increasing the size of the particles is one of the most commonly adopted strategies for controlling the release of a drug.

Poly(vinyl alcohol) (PVA) is a well-established polymer for biomedical applications as a drug carrier (Gul *et al.*, (2009); Mallapragada and McCarthy-Schroeder, (2000)). PVA has been used for controlling the release of therapeutic agents in the lung (Haghi *et al.*, (2012); Saigal *et al.*, (2013); R. Salama *et al.*, (2008); R. O. Salama *et al.*, (2009a), (2009b), (2008)) after it was found that 1% (w/w) of PVA could affect the pulmonary absorption significantly (Yamamoto *et al.*, (2004)). In 2009, Salama *et al.* studied the

controlled release of BSA from PVA microparticles. They found that they were able to delay the release of BSA by up to 12 times with the addition of 90% (w/w) PVA. Furthermore, the authors were able to display that PVA was not toxic to human alveolar basal epithelium cells, A549, *in vitro*. However, as effective as PVA is in delaying the release of therapeutic agents, its long-term effects are still largely unknown (Nakamura *et al.*, (2001); Sheth and Myrdal, (2011b)).

Albumin is the most abundant blood protein in humans. Albumins have been used as a natural polymer for drug delivery since first described by Kramer in 1974, but have been receiving increased attention in recent years as a versatile drug carrier (Elsadek and Kratz, (2012); Kratz, (2008); Park, (2012)). Certain properties that make albumins such an attractive drug carrier include its biodegradability, non-toxicity and non-immunogenicity (Kratz, (2008)). Intravenous albumin-bound paclitaxel (Abraxane) has been approved by the United States Food and Drug Administration (US FDA) for use in the treatment of non-small-cell lung cancer (Green *et al.*, (2006)), although the use of albumin for pulmonary drug delivery has seen far less research and development. As serum albumins are present in pulmonary surfactant (Whitsett and Weaver, (1991)) and are also found in large quantities in lung epithelial fluid, coupled with the aforementioned qualities, they have potential for use in pulmonary delivery systems. Li *et al.* have developed bovine serum albumin (BSA) microspheres to deliver ciprofloxacin as a dry powder to the lung and cross-linked BSA has been found to be beneficial in controlling the release of terbutaline sulphate (Sahin *et al.*, (2002)). The use of albumin nanoparticles for drug delivery to the lung has recently been explored by (Woods *et al.*, (2015), (2014), (2013)) where albumin nanoparticles were shown to be an attractive candidate for controlling the release of drugs in the lung *in vivo* and were also demonstrated to be largely degraded by 48 hours. The addition of proteins (e.g. albumins like BSA) to pulmonary delivery systems has also been suggested to be beneficial in enhancing the aerosol performance of such systems by inducing corrugation (Bosquillon *et al.*, (2001); Chew and Chan, (2001)).

Cromolyn sodium (CS), also known as sodium cromoglycate or cromoglicic acid, is an anti-allergic drug used in the treatment of asthma. However, it requires administration four times daily by metered dose inhaler or nebuliser, making it inconvenient for the patient (Fanta, (2009)). Vidgren *et al.*, 1987 first attempted to spray-dry CS for inhalation therapy in 1987, producing particles that were smaller in size and had a better impaction test performance than their micronised counterparts. CS is a highly water-soluble drug, so producing and retaining it in its amorphous form is not necessary, but control of

particle size and surface properties, as well as its release rate, are desirable.

In this work, we describe a spray-dried hybrid protein/polymer microparticle pulmonary drug delivery carrier system comprising two excipients with complementary attributes - a protein which has been found to improve aerosol performance, BSA; and a polymer known to control the release of therapeutic agents in the lung, PVA - to deliver an anti-asthma drug, CS. The unique drug delivery system seeks to complement the sustained release characteristics of PVA with the aerosol dispersibility of BSA. A factorial design approach was adopted to study the behaviour of this hybrid system, investigating the influence of drug loading and protein/polymer ratio to the physicochemical properties of the formulation, in particular, the drug release profiles and the deposition studies. It is hoped that with the detailed study of the physicochemical characteristics of the hybrid formulation, the feasibility of employing two excipients, each with a specific purpose, to obtain an optimised formulation combining the advantages of both excipients, can be investigated.

3.2 Materials and Methods

3.2.1 Materials

CS was supplied by Sanofi-Aventis (Paris, France) while PVA (MW 88,000) was supplied by Tokyo Chemical Industry Co. Ltd (Tokyo, Japan). BSA was procured from Sigma-Aldrich (St. Louis, MO, USA). Potassium dihydrogen phosphate (Alfa-Aesar, Ward Hill, MA, USA) and sodium hydroxide (Merck KGaA, Darmstadt, Germany) were used to make pH 7.4 phosphate buffer solution (PBS). All water used throughout was purified *via* reverse osmosis by an ELGA PURELAB Option-Q (Veolia Water, Paris, France) purification system.

3.2.2 Methods

3.2.2.1 Microparticle preparation *via* co-spray drying

Using a 3 x 2 factorial design where two variables (drug loading and protein/polymer ratio) have three levels each, a range of microparticles with 20, 50 and 80% (w/w) CS loadings, and protein/polymer ratios of 1:1, 4:1 and 1:4 (by weight) were prepared from aqueous solutions as detailed in Table 3.1.

Typically, varying amounts of the active ingredient were measured out and dissolved in

deionised water before the dispersion of corresponding amounts of carrier materials. The spray drying was performed on a laboratory scale spray dryer equipped with a high performance separating cyclone and 0.7 mm nozzle (B-290 Mini Spray Dryer, BÜCHI Labortechnik AG, Flawil, Switzerland). The mini spray dryer was operated in an 'open loop' configuration for aqueous solutions with the following conditions: Inlet temperature 140 °C, outlet temperature ~70 °C, aspirator gas flow rate 35 m^3/h, atomising spray air flow rate 601 L/h and solution feed rate at 5 mL/min. All spray-dried powders were dried overnight in a vacuum oven (Heraeus Vacutherm VT 6060M, Thermo Electron Corporation, Waltham, MA, USA) set at 25 °C after collection.

3.2.2.2 Thermal analysis

The thermal profiles of the powders were determined by differential scanning calorimetry (DSC) and modulated differential scanning calorimetry (MDSC). Experiments were conducted on a TA Instruments Q2000 Differential Scanning Calorimeter (New Castle, DE, USA). Approximately 3-5 mg of powder was placed into a Tzero® aluminium pan and a lid was crimped on. An empty pan was used as reference. Measurements were taken in DSC mode with a heating rate of 10 °C/min, and in modulation mode with a heating rate of 5 °C/min, and modulation of ± 0.5 °C every 100s. Glass transition temperatures (T_g) were determined by analysing the reversing heat flow signal.

3.2.2.3 Particle microstructure

The microparticles' microstructure was probed by focused ion beam (FIB) milling using a focused ion beam/scanning electron microscope dual beam system (FEI Nova NanoLab 200, FEI Company, Hillsboro, OR, USA & Zeiss CrossBeam 1540, Carl Zeiss Microscopy GmbH, Jena, Germany). The accelerating voltage and beam current were adjusted to accommodate the fragility of each formulation and were approximately 30 kV and 100-500 pA respectively. The powders were mounted onto double-sided adhesive copper tape and coated with platinum. The samples were examined under high-resolution FESEM at 2-5 kV.

3.2.2.4 Density and aerodynamic diameter

Pycnometry on the samples was performed using a helium pycnometer (AccuPyc 1330, Micromeritics Instrument Corporation, Norcross, GA, USA) equipped with a 3.5 cm^3 insert. The typical mass used was between 0.5 g to 1 g, with the values quoted being the mean and standard deviation from a cycle of 10 measurements.
The aerodynamic diameter was calculated using Equation 2 in Section 1.1.2.

3.2.2.5 *In vitro* dissolution studies

The release studies of the prepared microparticles were assessed by two different methodologies – United States Pharmacopoeia (USP) dissolution apparatus 1 (basket apparatus) and the USP dissolution apparatus 4 (flow-through cell). Prior to the dissolution studies, assays of each prepared formulation were conducted whereby a measured quantity of powder was dissolved in pH 7.4 PBS for 24 hours before a spectrophotometric analysis of the dissolved drug concentration was conducted to determine the amount of drug loading.

3.2.2.5.1 USP dissolution apparatus 1 (basket apparatus)

The dissolution profile of CS was measured using a United States Pharmacopoeia (USP) dissolution apparatus 1 (basket apparatus) (Varian VK 7010 Dissolution Apparatus, Varian Inc., Palo Alto, CA, USA) with online flow cell (Cary 50 Conc UV-visible spectrophotometer, Varian Inc., Palo Alto, CA, USA). The basket rotation speed was set at 50 RPM and the vessel temperature at 37 °C. Typically, 40 mg of spray-dried aerosol powders and 20 mg of spray-dried pure CS was used for dissolution studies in 900 mL of pH 7.4 PBS. Samples were taken by the auto sampling system at five-minute intervals, after which the samples were returned to the dissolution vessel by a peristaltic pump. UV readings were taken at 326 nm.

3.2.2.5.2 USP dissolution apparatus 4 (flow-through cell)

A USP dissolution apparatus 4 (flow-through cell) (DFZ 720 flow-through-cell dissolution tester, Erweka GmbH, Heusenstamm, Germany) was used in the 'closed-loop' configuration to conduct release studies of CS. The temperature of the water baths surrounding the cells were maintained at 37 °C. 900 mL of dissolution media was maintained at 37 °C before being pumped through the system using a peristaltic pump (IPC 8 microprocessor-controlled dispensing pump, Ismatec SA, IDEX Health & Science

GmbH, Wertheim, Germany) at a constant flow rate of 0.5 mL/min. 25-100 mg of spray-dried aerosol powders or 20 mg of spray-dried pure CS were used for dissolution studies. As seen in Figure 3.1, the powders were sandwiched between 1 mm glass beads (to promote laminar flow), which were bounded by 0.45 µm PTFE filters. The area exposed to vertical flow was 1.25 cm in diameter and dissolution medium exiting the flow-through cell was returned to the 900 mL dissolution medium. At pre-determined time intervals, 3 mL aliquots were collected from the dissolution medium for analysis with the UV-vis spectrophotometer.

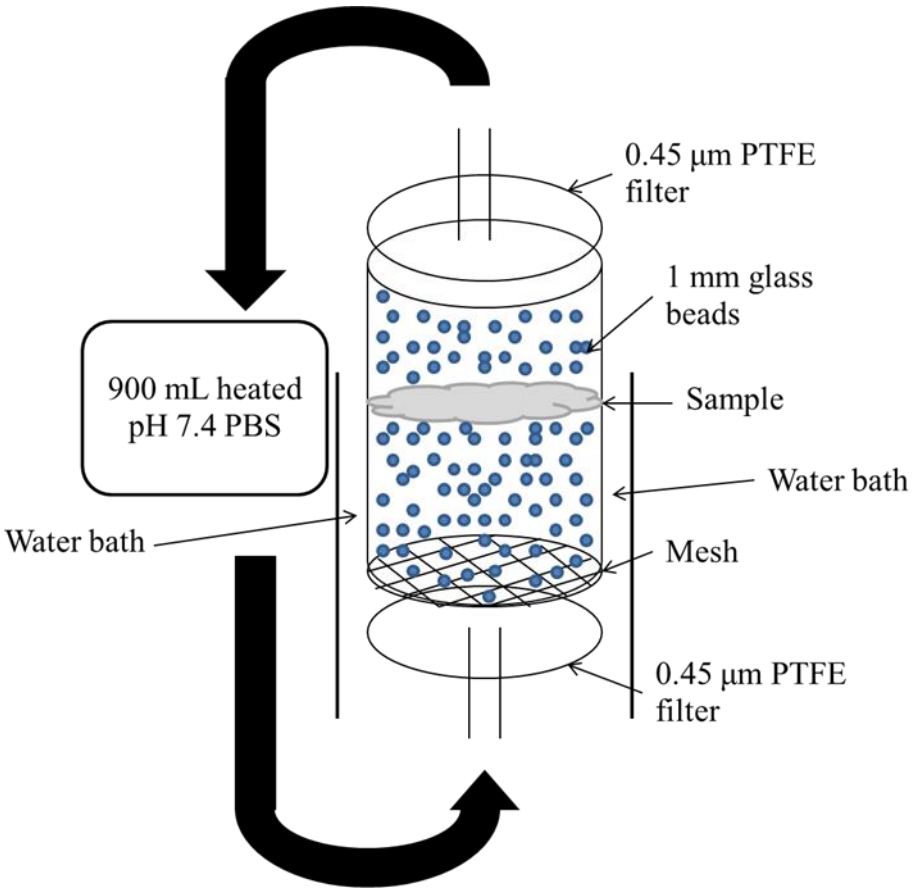

Figure 3.1. Schematic of Erweka DFZ 720 USP dissolution apparatus 4 (flow-through cell) in 'closed loop' configuration.

3.2.2.6 Spectrophotometric study of CS

The concentrations of CS in the prepared powders were analysed spectrophotometrically (Cary 50 Conc UV-visible spectrophotometer, Varian Inc., Palo Alto, CA, USA) at a wavelength of 326 nm. All samples and standards were prepared in pH 7.4 PBS. The standards showed a good linear fit by least squares linear regression (Figure 3.2.). The addition of BSA (wavelength 280 nm) and PVA to CS did not interfere with the UV

spectrum.

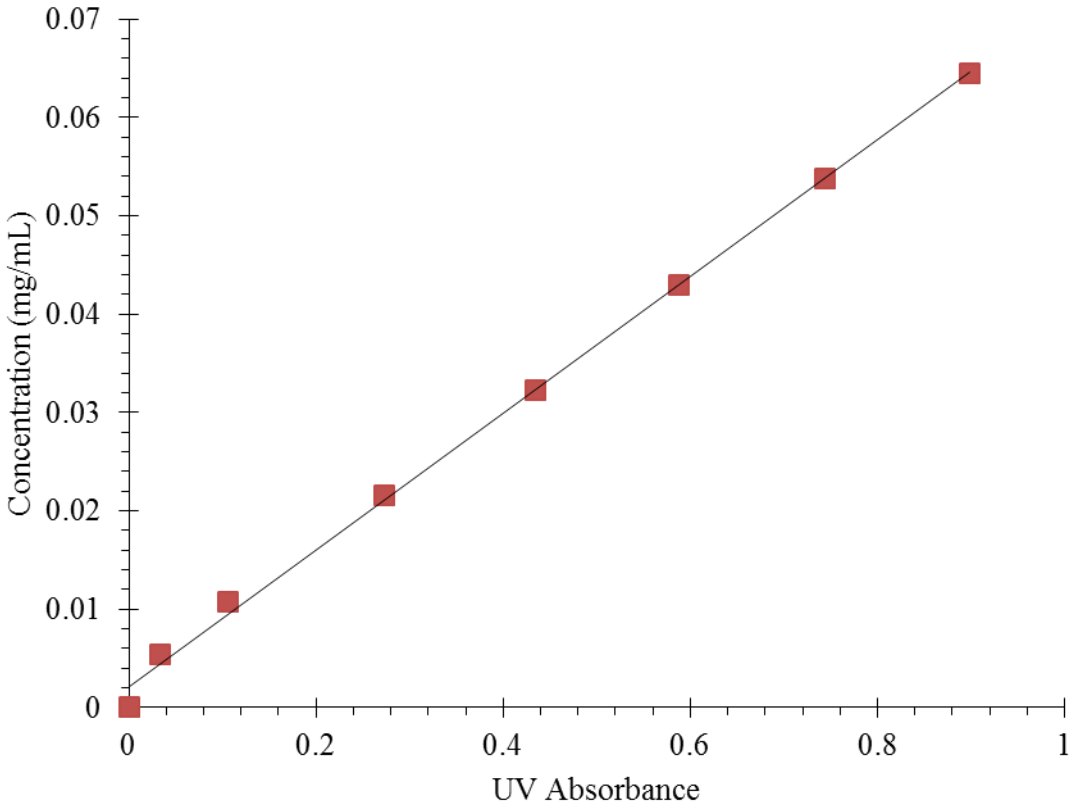

Figure 3.2. Relationship between CS concentration and UV absorbance.

3.3 Results and discussion

Analysis was performed to investigate the effect of drug loading and protein/polymer ratio on the physicochemical characteristics of the formulations. The design of experiments was based on a 3 x 2 factorial design, with three levels for the two variables (Table 3.1).

3.3.1 Yield, drug loading, and entrapment efficiency

The spray-drying yield, experimental drug loading and entrapment efficiency of each spray-dried formulation is shown in Table 3.1. Spray-dried CS and CS/BSA-50/50- SD both achieved high yields of > 80% (w/w) compared to the typical yield of 50-70% for spray-dried inhalable particles ("Laboratory scale spray drying Of inhalable drugs: A review," (2010)). The yield dropped drastically to 27% for CS/PVA-50/50-SD. For the hybrid formulations, a clear trend can be seen where the formulations with a greater BSA/PVA ratio had higher yields. A possible reason for the low yields for the

formulations with PVA is that the outlet temperature of ~70 °C was too close to the 'sticky point' of PVA (Maury *et al.*, (2005)), which is estimated to be approximately ~10-20 °C above a substance's T_g, which for PVA would be ~95 °C, given its T_g of 85 °C (Mallapragada *et al.*, (1996)), causing the spray particles to stick to the walls of the drying chamber and separating cyclone.

The experimental drug loadings of all the formulations were close to their theoretical values and the minimum entrapment efficiency was ~90%, which showed that spray-drying was indeed a viable process to form drug-loaded hybrid particles.

Table 3.1. Spray-drying Yield, Drug Loadings, Entrapment Efficiency and Protein/Polymer Ratios of CS/BSA/PVA Microparticle Formulations. SD Denotes Spray-

dried.

No.	Name	Spray-drying Yield (%)	Theoretical Drug Loading (% w/w)	Experimental Drug Loading (% w/w)	Entrapment Efficiency (%)	BSA/PVA
0	CS-raw	-	-	-	-	
1	CS-SD	81.28	-	-	-	1:0
2	CS/BSA-50/50-SD	88.35	50	47.27	94.53	0:1
3	CS/PVA-50/50-SD	27.05	50	45.06	90.12	4:1
4	CS/BSA/PVA-20/64/16-SD	67.80	20	19.78	98.89	4:1
5	CS/BSA/PVA-50/40/10-SD	67.75	50	44.80	89.61	4:1
6	CS/BSA/PVA-80/16/4-SD	57.92	80	73.55	91.94	4:1
7	CS/BSA/PVA-20/10/10-SD	46.62	20	18.81	94.04	1:1
8	CS/BSA/PVA-50/25/25-SD	52.60	50	45.31	90.62	1:1
9	CS/BSA/PVA-80/10/10-SD	52.45	80	71.87	89.83	1:1
10	CS/BSA/PVA-20/4/16-SD	37.03	20	19.50	97.48	1:4
11	CS/BSA/PVA-50/10/40-SD	35.90	50	46.89	93.78	1:4
12	CS/BSA/PVA-80/4/16-SD	36.04	80	81.31	101.63	1:4

3.3.2 Powder crystallinity

Figure 3.3 displays the X-ray diffractograms of the raw CS drug and the spray-dried

formulations with varying amounts of BSA and PVA. The results indicate that the spray-dried formulations were all in the amorphous state after spray drying.

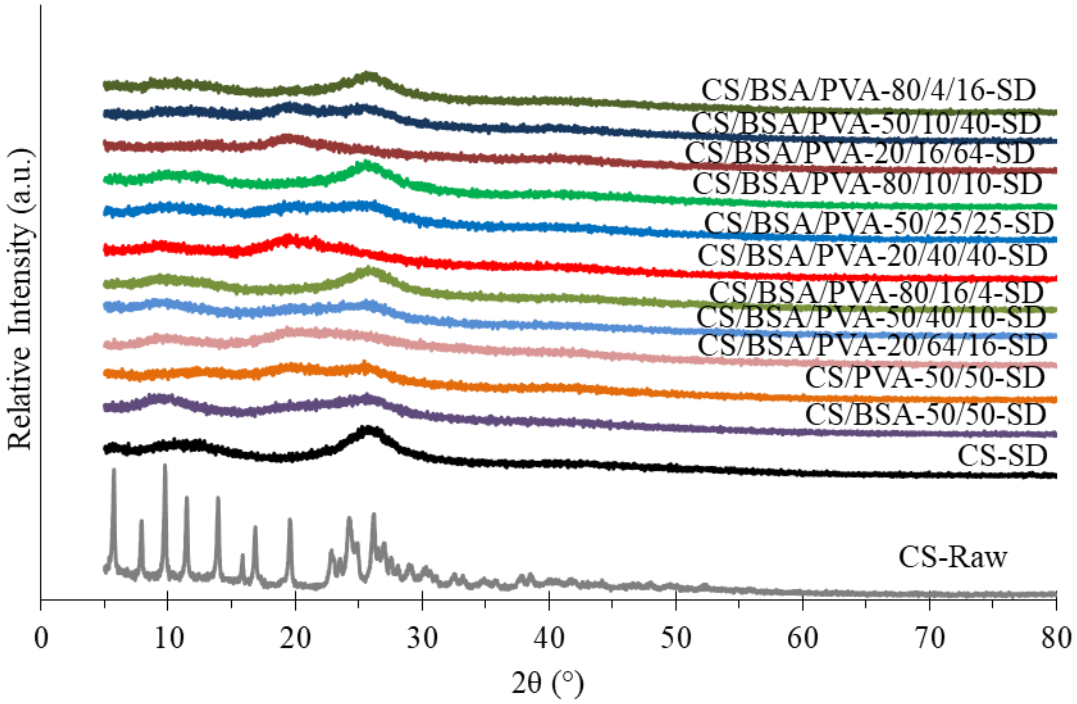

Figure 3.3. X-ray diffractograms of crystalline raw CS and amorphous co-spray dried formulations based on a 3 x 2 factorial design.

3.3.3 Thermal analysis

The T_g of CS has hitherto not been reported as it overlaps with the large solvent evaporation endotherm (Najafabadi *et al.*, (2004); Nolan *et al.*, (2011)). Using MDSC, we were able to separate the heat flow into its heat capacity (reversing heat flow) and kinetic (non-reversing heat flow) components. Upon investigation of the reversing heat flow component of the MDSC thermogram of spray-dried CS in Table 3.3, the T_g of CS was determined to onset at approximately 58 °C.

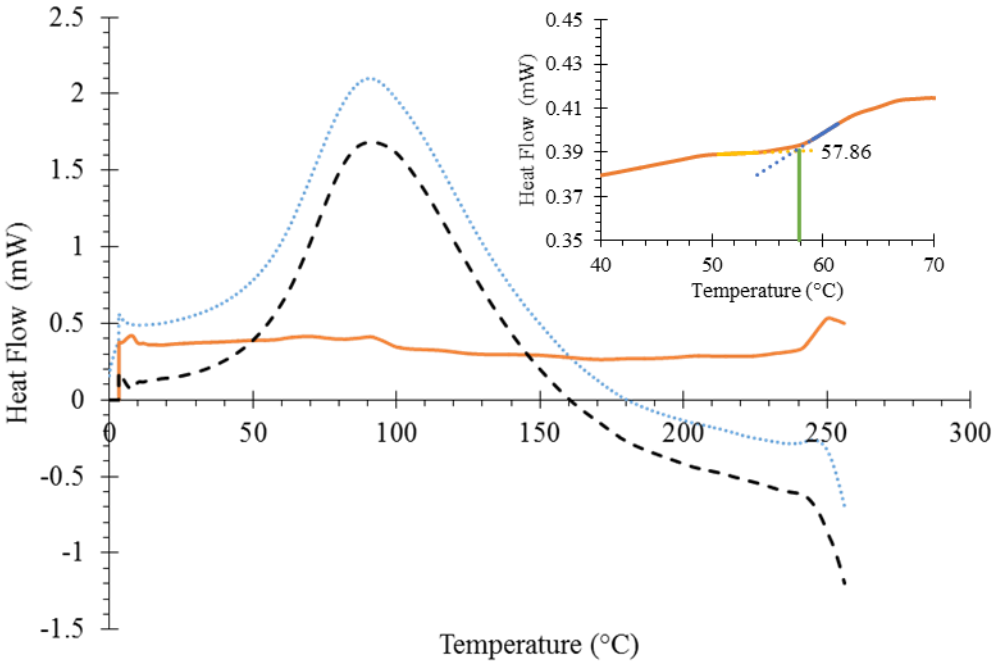

Figure 3.4. MDSC thermogram of CS-SD with inset of the glass transition. Total heat flow represented with (• • • •), non-reversing heat flow with (— —), and reversing heat flow with (——).

Analysis of the MDSC thermograms of the spray-dried formulations revealed that at least two disparate thermal transitions were observed. The first of which typically occurs at approximately 40 °C for all formulations. This transition has the appearance of a glass transition but has been postulated by Mizuno and Pikal, (2013) to be a protein internal transition related to α-mobility. The second transition occurs at approximately that of PVA at 85 °C.

3.3.4 Moisture sorption

The equilibrium moisture sorption isotherms of the spray-dried formulations are shown in Figure 3.5. Spray-dried CS had the highest moisture sorption with 48.81% mass change at 90% RH, while CS/BSA-50/50-SD and CS/PVA-50/50-SD had 42.41% mass change and 38.53% mass change at 90% RH, respectively. Formulations with 20% drug loading are shown with ● markers, in shades of red; formulations with 50% drug loading are shown with ▲ markers, in shades of blue; and formulations with 80% drug loading are shown with ■ markers, in shades of green. There was no evidence of moisture-induced crystallisation. As can clearly be seen in Figure 3.5, the formulations had similar sorption isotherms when they had the same drug loading, with the moisture sorption decreasing slightly when the protein/polymer ratio went from 4:1 to 1:1 to 1:4 (w/w). Drug loading,

however, appeared to have the larger influence on the amount of moisture sorption with formulations of 20% drug loading having the lowest equilibrium moisture sorption, while formulations with 80% drug loading had sorption isotherms similar to that of spray-dried CS.

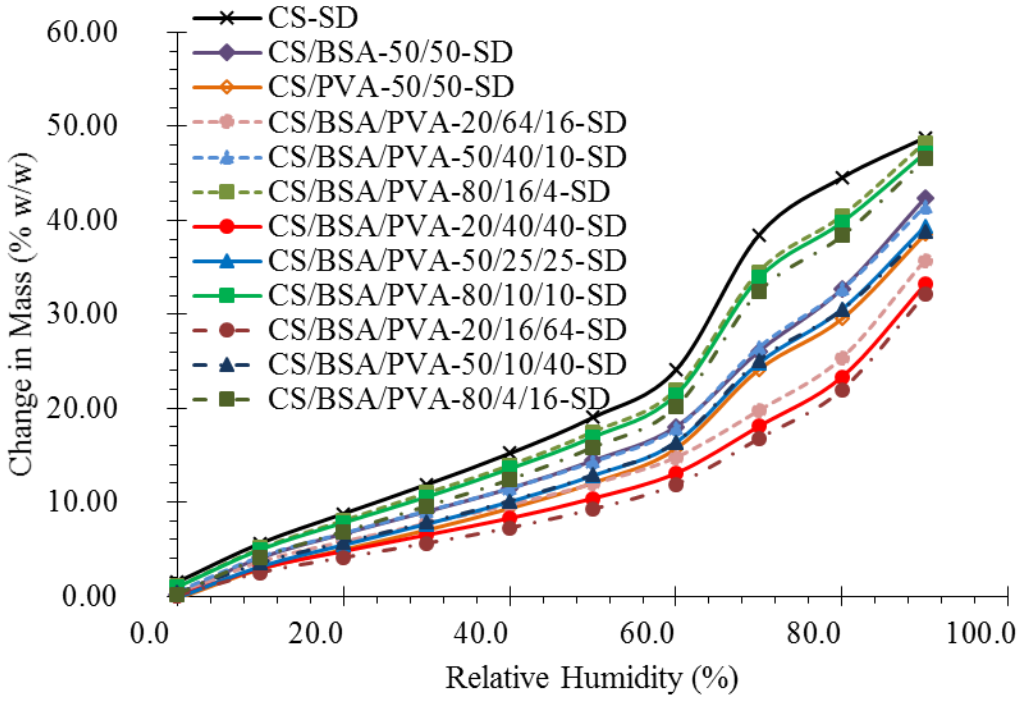

Figure 3.5. DVS sorption isotherms of spray-dried formulations.

As water is a very powerful plasticiser, the amount of moisture absorbed is important in deciding the storage conditions of the drug formulations. However, from the perspective of dissolution performance, as CS is a highly water-soluble compound, its crystallisation from an amorphous, spray-dried state is arguably of less importance than that of a poorly water-soluble drug compound which would benefit greatly from the dissolution rate enhancement of its amorphous form. On the other hand, moisture absorption was found to have a deleterious effect on the aerosol performance of CS powders (Li *et al.*, (2016)) which could be due to re-crystallisation increasing the size of the particles to beyond that of the respirable range, so appropriate packaging, such as sealed blister packs, should be considered when packaging these powders.

3.3.5 Surface composition estimation

The surface composition of the raw and spray-dried drug, protein, polymer and hybrid formulations were estimated from XPS peaks and shown in Table 3.2. The raw and spray-dried forms of CS and BSA did not differ much in their experimentally derived surface

composition while there was a slight change in the composition of spray-dried PVA compared to its raw counterpart.

Table 3.2. Surface Composition (Atomic %) of Raw and Spray-dried CS, BSA, PVA.

Sample	Carbon (%)	Oxygen (%)	Nitrogen (%)	Sodium (%)
CS-raw	72.28	24.3	-	2.92
CS-SD	73.18	24.13	-	2.68
BSA-raw	71.64	15.52	12.84	-
BSA-SD	70.55	15.53	13.92	-
PVA-raw	76.79	23.21	-	-
PVA-SD	72.7	27.3	-	-

In Table 3.3, the estimated surface coverage of the spray-dried hybrid formulations can be seen. It is clear that there is little to no CS on the surface of the particles and that the surface coverage of the hybrid particles was dominated by the excipients, BSA and PVA. This relationship can be seen more clearly in Figure 3.6. In concentrations greater than 25% (w/w) in the feed solution, PVA completely dominated the surface. This did not appear to have a beneficial or detrimental effect based on the characterisation tests performed, but this effect could possibly be harnessed in coating the drug in with a protective (e.g. moisture-protective) compound.

Table 3.3. Estimated Surface Coverage (Wt %) of Spray-dried Hybrid Formulations.

Formulation	CS-SD (%)	BSA-SD (%)	PVA-SD (%)
2	0.03	99.97	-
3	-0.14	-	100.14
4	0.03	2.26	97.71
5	0.11	7.54	92.35
6	0.24	32.08	67.68
7	0.04	0.64	99.32
8	-0.06	-0.94	101.00
9	0.79	12.51	86.70
10	0.11	1.76	98.13
11	-0.06	-0.95	101.02
12	0.40	6.25	93.35

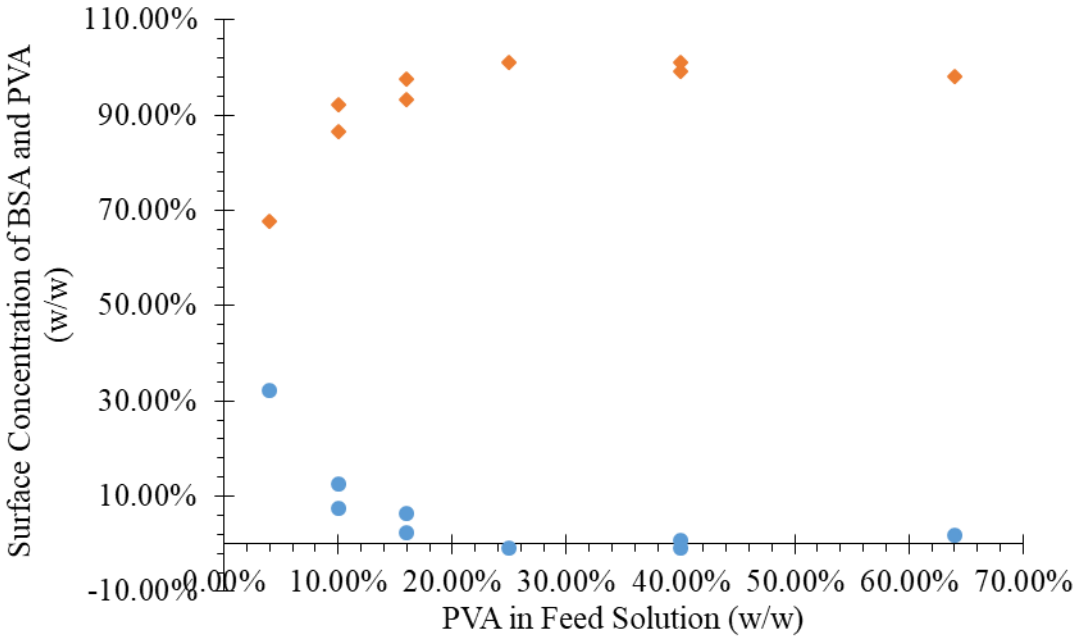

Figure 3.6. Relationship between surface coverage of BSA (●) and PVA (◆) and the concentration of PVA in the feed solution.

3.3.6 Particle morphology

Figure 3.7 shows spherical particles of CS/BSA/PVA formed after spray-drying as well as the plate-shaped particles of raw CS [Figure 3.7-(0)]. The images are broadly in agreement with particle size distribution data shown later in Table 3.4. Spray-dried

CS/BSA-50/50-SD [Figure 3.7-(2)] was seen to comprise of small particles with corrugated surfaces while spray-dried CS/PVA-50/50-SD [Figure 3.7-(3)] displayed larger particles with smooth surfaces.

The effect of drug loading on the particles can be seen for different protein/polymer ratios. Figure 3.7-(4), Figure 3.7-(5) and Figure 3.7-(6) show particles with a protein/polymer ratio of 4:1; Figure 3.7-(7), Figure 3.7-(8) and Figure 3.7-(9) show particles with a protein/polymer ratio of 1:1; Figure 3.7-(10), Figure 3.7-(11) and Figure 3.7-(12) show particles with a protein/polymer ratio of 1:4. At all three protein/polymer ratios, it can be seen that for increasing drug loading, the particles' surface corrugation appeared to progressively increase toward that seen for spray-dried CS in Figure 3.7-(1). The surface corrugation has been suggested to improve the aerosol dispersibility of the formulations (Bosquillon *et al.*, (2001); Chew and Chan, (2001)).

Similarly, when observing the particles for the effect of protein/polymer ratio; Figure 3.7-(4), Figure 3.7-(7) and Figure 3.7-(10) for 20% (w/w) drug-loaded particles; Figure 3.7-(5), Figure 3.7-(8) and Figure 3.7-(11) for 50% (w/w) drug-loaded particles; Figure 3.7-(6), Figure 3.7-(9) and Figure 3.7-(12) for 80% (w/w) drug-loaded particles, the surface roughness of the particles appeared to increase with increasing protein/polymer ratio, towards that of CS/BSA-50/50-SD [Figure 3.7-(2)] although not to the same extent as seen for increasing drug loading. It can also be observed that increasing the protein/polymer ratio yielded a greater amount of small particles, with Formulation 4, CS/BSA/PVA-20/64/16-SD in Figure 3.7-(4), in particular, displaying a high amount of small particles.

The particle size distribution of the microparticles observed in the SEM micrographs was in good agreement with the laser diffraction data seen later in Section 3.3.8. Smaller particles were produced when the drug loading was low, with a high protein/polymer ratio. It was also noted that when more polymer was included in the carrier composition (1:4 (w/w) protein/polymer ratio: [Figure 3.7-(10), Figure 3.7-(11) and Figure 3.7-(12)]), the surfaces appeared smoother and there was an increased aggregation tendency.

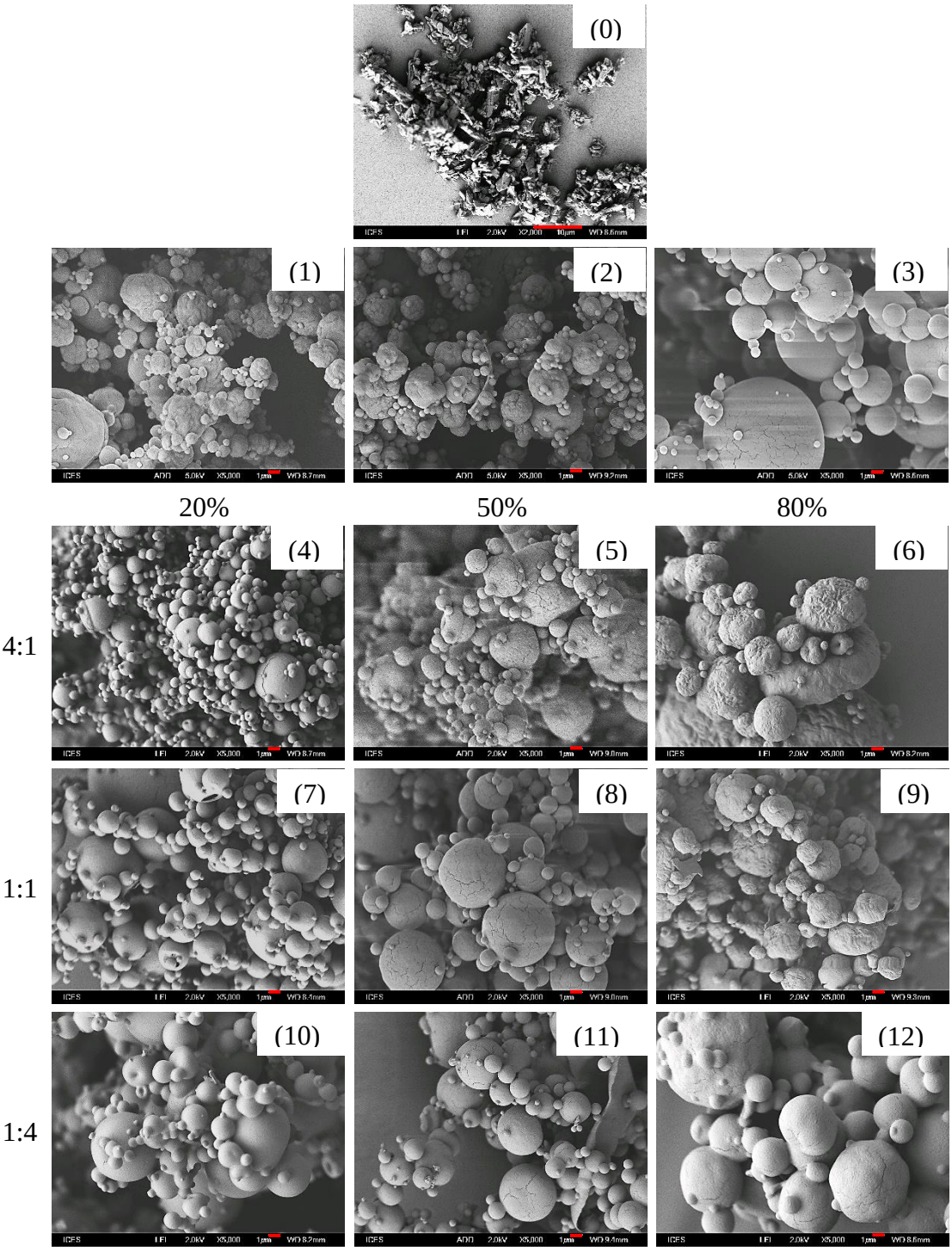

Figure 3.7. Scanning electron micrographs of formulations 0-12. Scale bars (in red) are 1 µm for all images except for (0) CS-raw, for which it is 10 µm.

3.3.7 Microparticle microstructure

Images of FIB-milled microparticles can be seen in Figure 3.8. Both CS-SD [agreeing with data from (Heng *et al.*, (2007))] and CS/BSA-50/50-SD comprised of solid particles,

while CS/PVA-50/50-SD exhibited a slightly hollow interior. Most of the hybrid formulations, however, were hollow with only CS/BSA/PVA-20/64/16-SD and CS/BSA/PVA-20/40/40-SD having solid interiors, suggesting that a low percentage of CS and a high percentage of BSA created conditions for the formation of solid particles. Interestingly, when two formulations with a similar median particle size, Formulation 6 – CS/BSA/PVA-80/16/4-SD and Formulation 7 – CS/BSA/PVA-20/40/40-SD, but with a different microstructure – Formulation 6 had hollow particles whilst Formulation 7 had solid particles – were studied, the FPF of Formulation 6 with the hollow particles was less than that of Formulation 7 with solid particles. As will be investigated further later, while the formulations may have a similar geometric median particle size (4.68 µm vs 4.77 µm), their aerodynamic diameters were quite different (9.99 µm vs 5.15 µm) with corresponding FPFs of 22.1% and 30.5%, due to the difference in their densities, implying that although the particle microstructure directly affects its density, solid particles with inherently lower densities may have a greater effect on the aerosol performance of the powders.

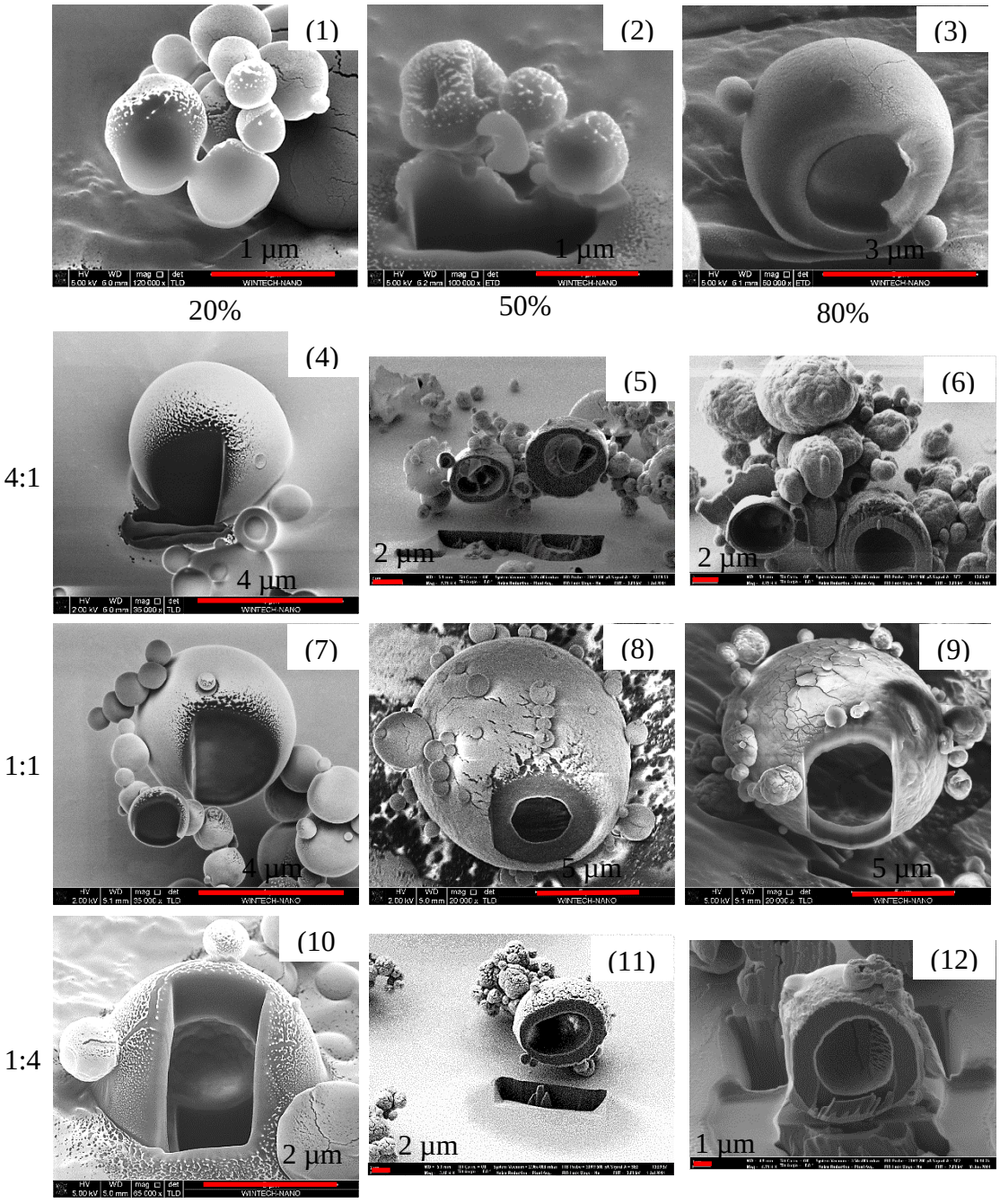

Figure 3.8. Secondary electron images of the FIB cross-sections of the spray-dried formulations.

3.3.8 Particle size analysis

As mentioned earlier, the particle size distribution of a formulation is an important factor in the viability of any pulmonary delivery system in order to circumvent the clearance mechanisms of the respiratory system. The particle size of the formulations affect most of the other physicochemical characteristics of the formulations and are integral to the performance of the formulations. The particle size distributions of the formulations are

shown in Table 3.4. From Table 3.4, we can observe that the bulk of the formulations had median particle sizes within the respirable range.

Table 3.4. Volume Particle Size Distributions of Spray-dried Formulations.

Formulation	d_{10} (μm)	d_{50} (μm)	d_{90} (μm)	Span (μm)
0	1.11 ± 0.03	2.24 ± 0.05	4.61 ± 0.18	1.56
1	1.15 ± 0.06	2.68 ± 0.03	5.71 ± 0.18	1.70
2	1.27 ± 0.02	2.69 ± 0.04	5.41 ± 0.21	1.54
3	2.99 ± 0.03	10.51 ± 0.18	32.06 ± 3.12	2.76
4	1.06 ± 0.03	2.99 ± 0.06	8.18 ± 0.11	2.38
5	1.40 ± 0.01	4.24 ± 0.07	12.40 ± 1.25	2.59
6	1.59 ± 0.08	4.68 ± 0.26	11.31 ± 0.30	2.08
7	1.48 ± 0.00	4.77 ± 0.10	13.29 ± 0.15	2.48
8	1.61 ± 0.05	5.83 ± 0.03	18.10 ± 1.52	2.83
9	1.94 ± 0.15	5.71 ± 0.34	14.56 ± 1.57	2.21
10	2.34 ± 0.04	8.13 ± 0.15	20.80 ± 0.32	2.27
11	2.42 ± 0.03	8.24 ± 0.31	24.33 ± 3.07	2.66
12	2.45 ± 0.19	8.00 ± 0.33	21.08 ± 0.43	2.33

In Figure 3.9, the effect of drug loading on the particle size distribution of the formulations was studied. It was observed that the effect of drug loading on the median particle size of the formulations decreased as the protein/polymer ratio went from 4:1 to 1:1 to 1:4 (w/w). Although spray-dried CS had a small particle size (2.68 μm), it did not appear to have had a great influence on reducing the particle size of the formulation and the protein/polymer ratio seemed to have had a far greater effect.

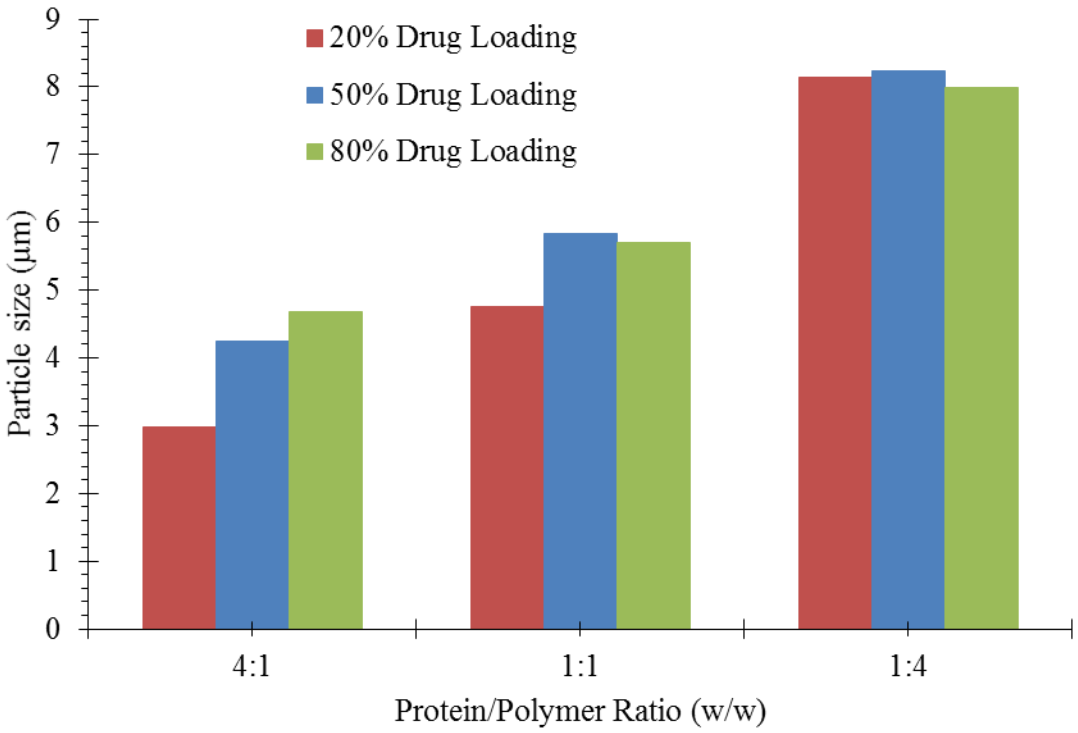

Figure 3.9. Effect of drug loading on median particle size.

The effect of protein/polymer ratio of the formulations was compared in Figure 3.10. At all drug loadings, it can clearly be seen that the median particle size of the hybrid formulations fell as the protein/polymer ratio was increased. Spray-dried PVA has been found to be hollow, thereby increasing its particle size (Ting *et al.*, (1992)). When the particles were split using FIB (Figure 3.8), it was observed that while CS-SD and CS/BSA-50/50-SD were small solid particles, there existed hollow particles in most of the other formulations, possibly contributing to the larger particle sizes.

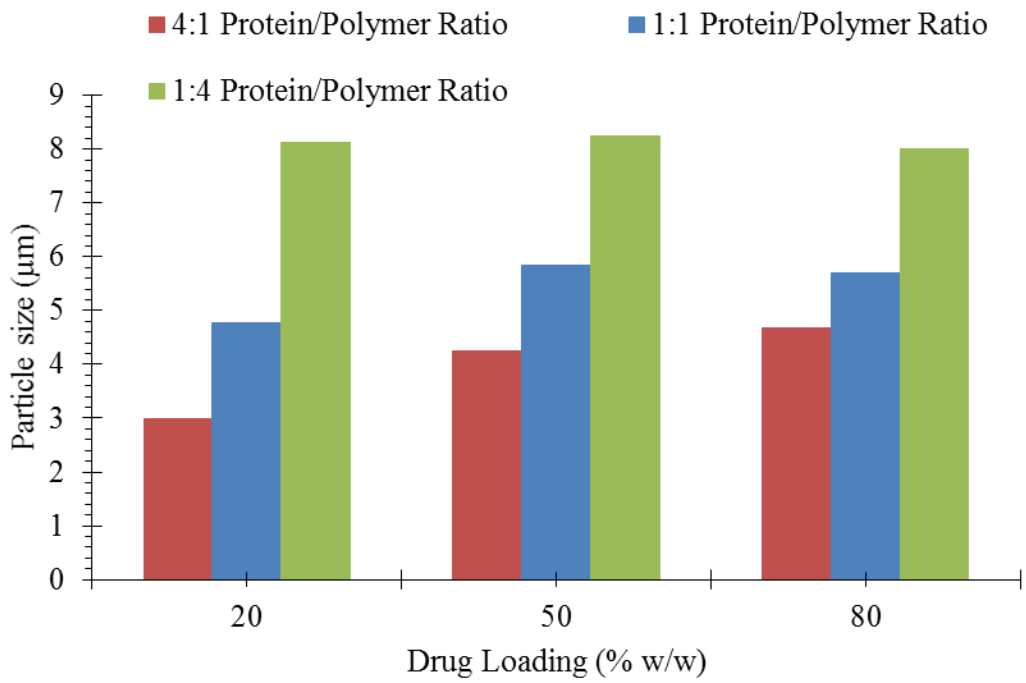

Figure 3.10. Effect of protein/polymer ratio on median particle size.

3.3.9 Density and aerodynamic diameter

The densities of spray-dried CS and the hybrid formulations were measured by helium pcynometry and are shown in Table 3.5 alongside the estimated proportional density, median particle size, calculated aerodynamic diameter (d_{ae}), the percentage of $d_{ae} < 5$ µm, and the FPF (discussed in Section 3.3.10). The density of spray-dried CS was approximately 1.58 g/cm^3 and agreed with data previously reported (Cox *et al.*, (1971)). From Figure 3.11, it can be seen that the specific density of the formulations rose when drug loading was increased for all protein/polymer ratios while the specific density decreased when the protein/polymer ratio was increased (Figure 3.12). It is worthwhile to note that at 80% (w/w) drug loading, the specific density only decreased to approximately that of spray-dried CS, while at lower drug loadings, increasing the protein/polymer ratio was able to reduce the specific density to approach that of spray-dried CS/BSA-50/50-SD (1.43 g/cm^3).

Table 3.5. Specific Density Measurements and Estimations, Aerodynamic Diameter Calculations, and Deposition Parameters (Mean ± SD, n=3) of Formulations Measured by MSLI.

Formulation	Density (g/cm^3)	Standard Dev. (g/cm^3)	Estimated Proportional Density (g/ cm^3)	d_{50} (µm)	d_{ae} (µm)	d_{ae} < 5 µm (%)	FPF (%)	FPF (emitted) (%)
0	1.65	0.0019	-	2.24	-	-	5.6 ± 0.2	5.9 ± 0.2
BSA-SD	1.32	0.0008	-		-	-	-	-
PVA-SD	1.66	0.0036	-		-	-	-	-
1	1.58	0.0018	-	2.68	3.37	74.0	28.0 ± 2.1	37.4 ± 3.3
2	1.43	0.0010	1.45	2.69	3.21	78.0	50.2 ± 2.9	57.3 ± 2.7
3	1.56	0.0030	1.62	10.51	13.15	10.0	11.4 ± 1.8	12.4 ± 1.9
4	1.40	0.0015	1.43	2.99	3.54	67.0	30.8 ± 2.5	37.2 ± 2.8
5	1.47	0.0011	1.48	4.24	5.80	44.0	25.9 ± 3.3	30.9 ± 1.6
6	1.57	0.0010	1.54	4.68	9.99	23.0	22.1 ± 1.7	24.4 ± 1.7
7	1.48	0.0017	1.51	4.77	5.15	49.0	30.5 ± 3.0	37.8 ± 3.9

Table 3.5. Specific Density Measurements and Estimations, Aerodynamic Diameter Calculations, and Deposition Parameters (Mean ± SD, n=3) of Formulations Measured by MSLI.

Formulation	Density (g/cm^3)	Standard Dev. (g/cm^3)	Estimated Proportional Density (g/ cm^3)	d_{50} (µm)	d_{ae} (µm)	d_{ae} < 5 µm (%)	FPF (%)	FPF (emitted) (%)
8	1.49	0.0013	1.53	5.83	7.11	36.0	19.7 ± 2.1	22.1 ± 2.0
9	1.64	0.0014	1.56	5.71	10.25	22.0	17.9 ± 1.6	19.7 ± 1.4
10	1.51	0.0025	1.59	8.13	5.86	43.0	20.5 ± 2.5	23.3 ± 3.1
11	1.55	0.0018	1.58	8.24	7.31	33.0	13.9 ± 0.8	15.3 ± 1.0
12	1.72	0.0048	1.58	8.00	10.48	21.0	12.9 ± 1.2	14.1 ± 1.2

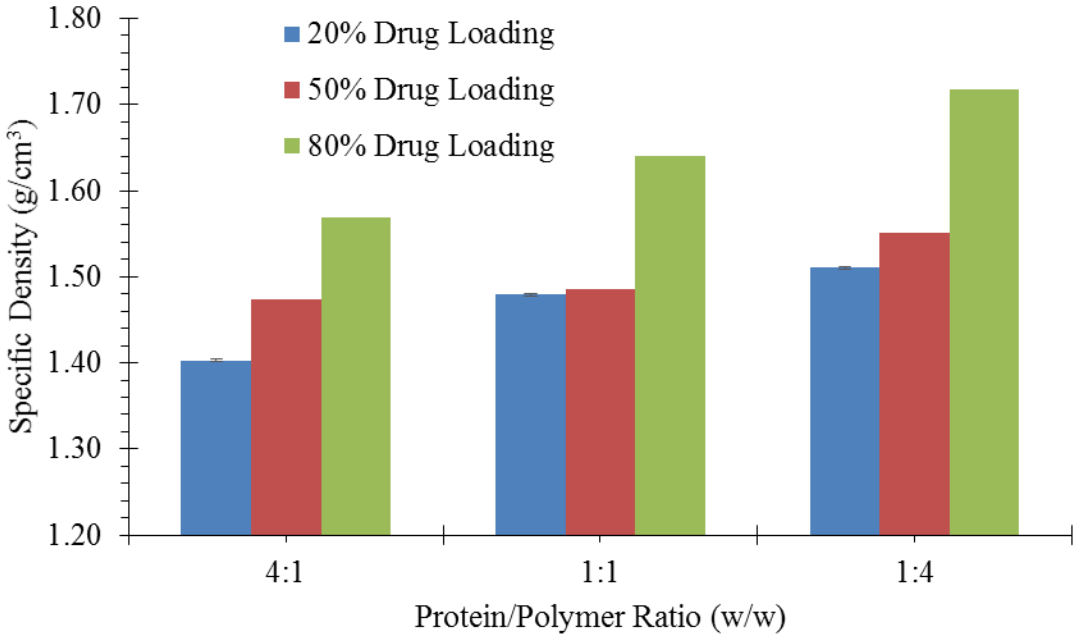

Figure 3.11. Effect of drug loading on specific density.

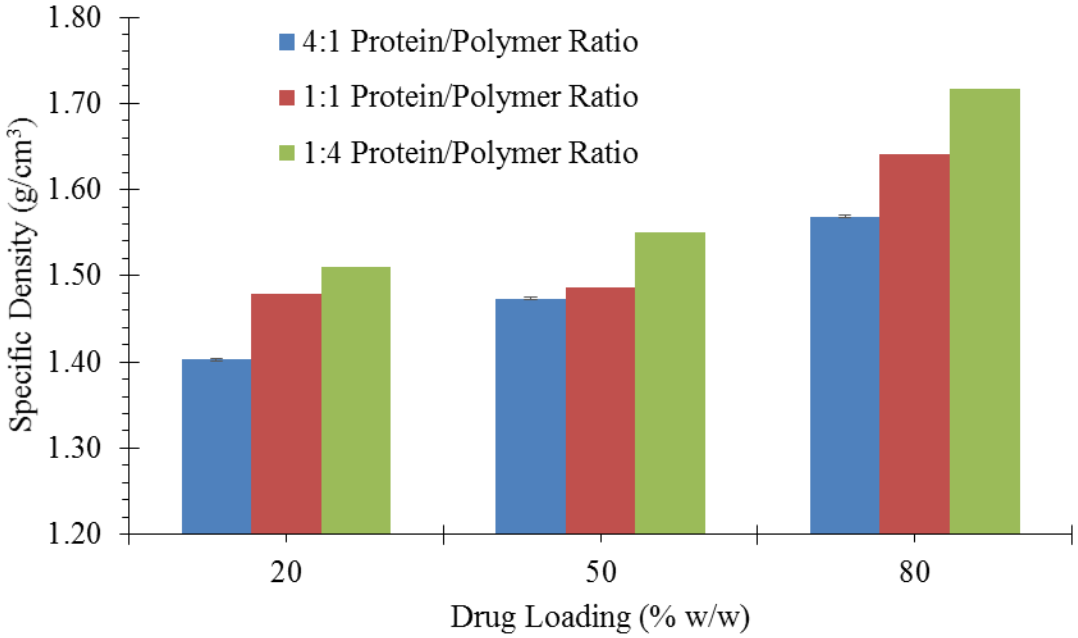

Figure 3.12. Effect of protein/polymer ratio on specific density.

The specific densities of the hybrid formulations were calculated from the proportional densities of their individual components and shown in Table 3.5 and Figure 3.13. As can be seen, the calculated specific densities were very similar to the measured specific densities, indicating that there was no interaction when the components were mixed together and spray-dried. As seen earlier in the FIB-milled particles, the addition of PVA to the formulations seemed to induce the formation of large, hollow particles. Although

hollow particles are generally less dense than solid particles, the inherent specific density of PVA was greater than that of BSA, resulting in large, hollow particles with a large aerodynamic diameter.

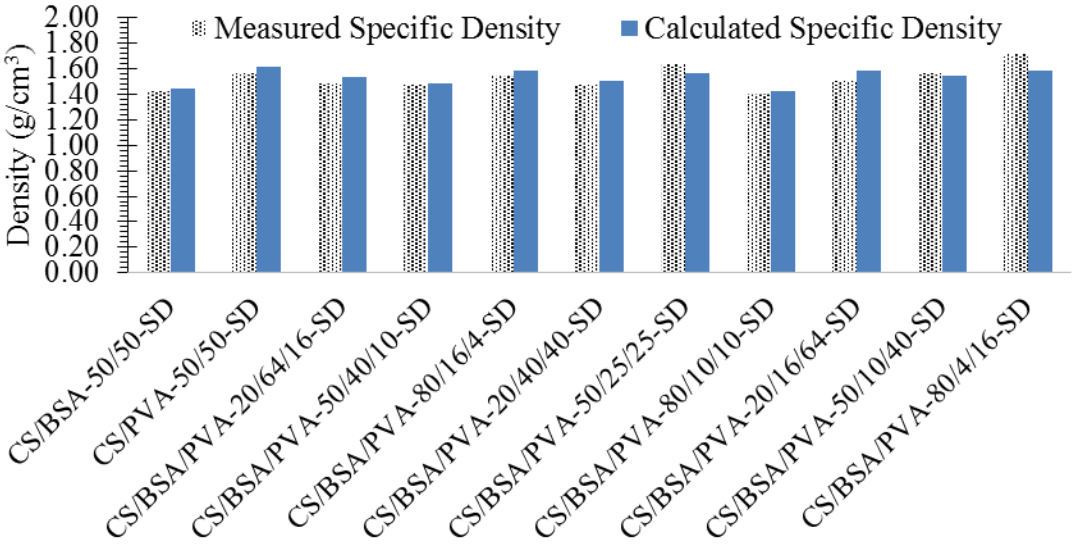

Figure 3.13. Specific density of spray-dried formulations compared with calculated density of formulations from the proportional density of individual components.

The effect of drug loading and protein/polymer ratio on the aerodynamic diameter of the particles can be seen in Figure 3.14 and Figure 3.15. Increasing the drug loading resulted in a larger aerodynamic diameter although that effect was largely diminished at high polymer concentrations at 1:4 protein/polymer ratios. The effect of protein/polymer ratio was more amplified by comparison, as was the case for the geometric particle size distribution of the particles. The aerodynamic diameter increased greatly when more polymer was present due to the higher specific density of PVA-SD compared to CS-SD and PVA-SD

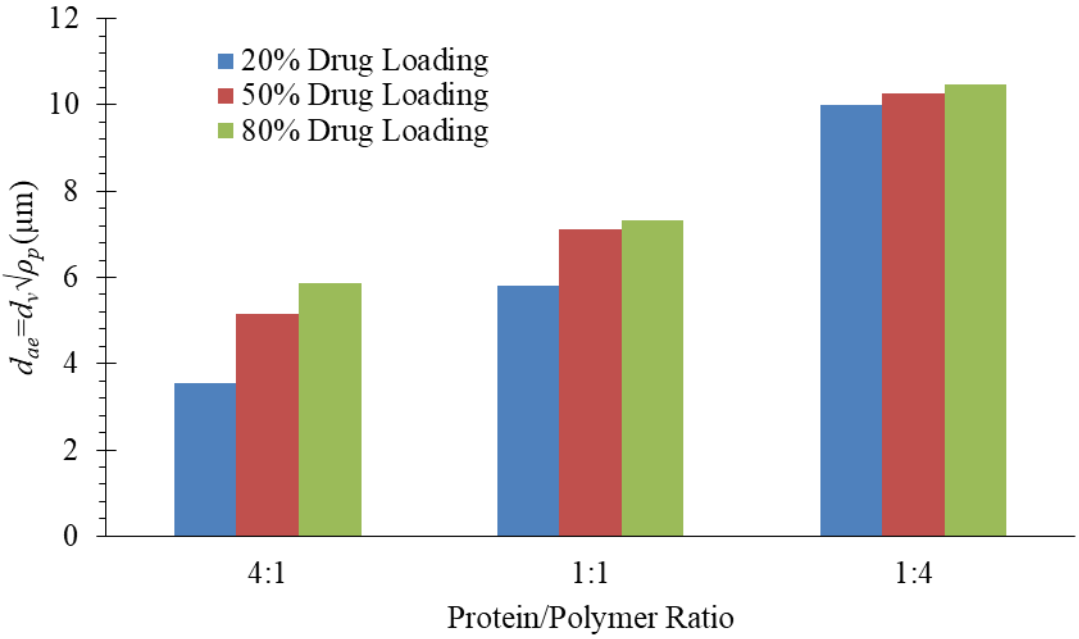

Figure 3.14. Effect of drug loading on the aerodynamic diameter of the formulations.

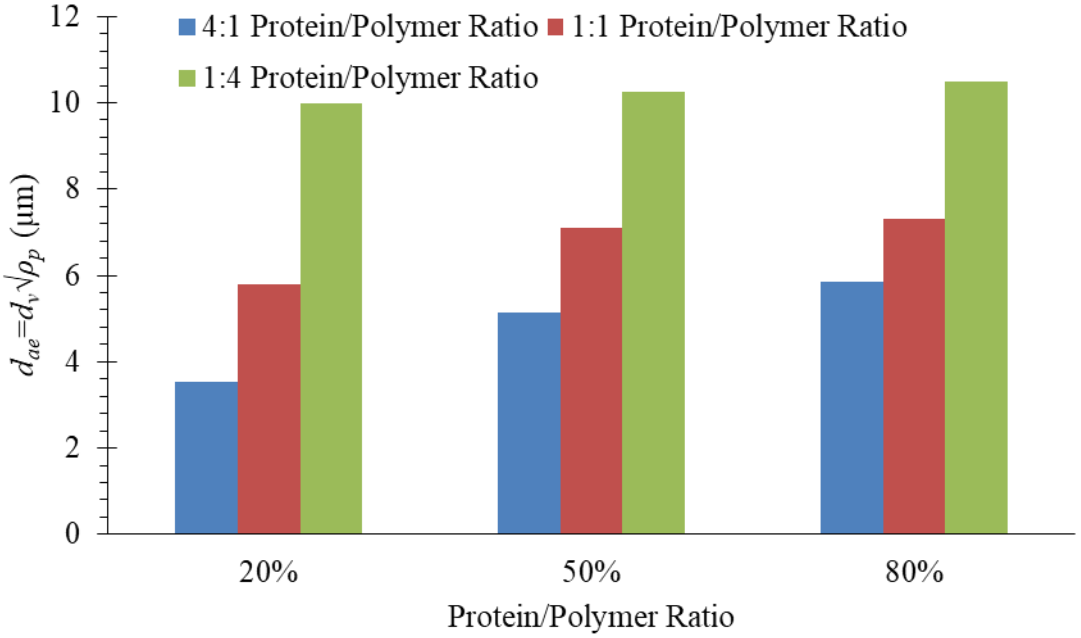

Figure 3.15. Effect of protein/polymer ratio on the aerodynamic diameter of the formulations.

In Figure 3.16, we can see the relationship between the FPF and the percentage of particles with aerodynamic diameters less than 5 µm. There was a fair fit to the data points by least squares linear regression with a coefficient of determination (R^2) of 0.76. Of note is the high FPF of CS/BSA-50/50-SD. The figure shows that its exceptional FPF was not due solely to its low aerodynamic diameter. CS-SD had a similarly low median particle

size (2.68 µm) and percentage of particles with aerodynamic diameter under 5 µm, but had an FPF of nearly half that of CS/BSA-50/50-SD, confirming the work by (Bosquillon *et al.*, (2001); Chew and Chan, (2001)) mentioned earlier that the addition of albumin enhances the aerosolisation performance of inhaled powders. Formulation 4, CS/BSA/PVA-20/64/16-SD had a low median geometric diameter with a relatively high amount of particles with aerodynamic diameter < 5 µm (67%) but had an FPF nearly 20% lower than that of CS/BSA-50/50-SD (30.76% vs 50.22%). Clearly, the addition of PVA also had dramatic effects on the physicochemical properties of the formulation and will have to be studied in greater depth.

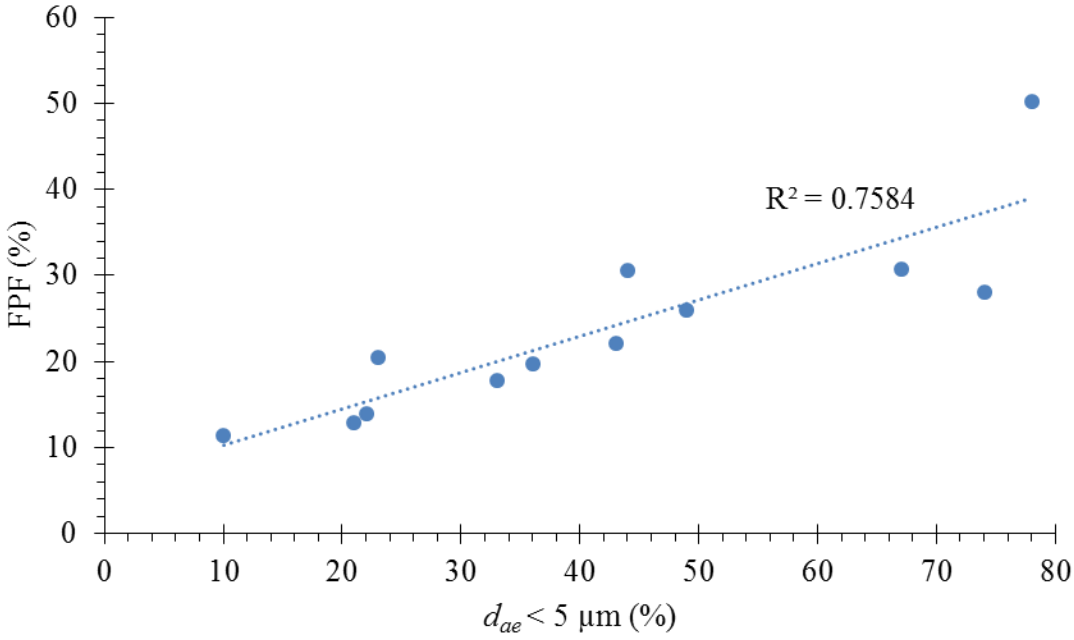

Figure 3.16. The relationship between FPF and percentage of particles under 5 µm.

3.3.10 *In vitro* aerosol performance

The *in vitro* aerosol performance of the formulations was examined using an MSLI. A table of the FPF and FPF (emitted) of each formulation as well as the raw drug is shown in Table 3.5. Figure 3.17 shows the *in vitro* deposition of spray-dried powders at different protein/polymer ratios while Figure 3.18 shows the effect of drug loading on the FPF. It was found that for all protein/polymer ratios, increasing the drug loading resulted in a decreased FPF. As discussed in the previous sections, the particle size increased when the protein/polymer ratio went from 4:1 to 1:1 to 1:4 (w/w). Although the addition of PVA to the formulations tended to form hollow particles, the shells were still rather thick and there was no resultant reduction in the density of the particles. It is pertinent to study

Figure 3.17 (c) in greater detail as the average particle diameters of the microparticles were approximately equal, negating any size related changes to the *in vitro* aerosolisation of the formulations. Here, it is very clear that an increase in drug loading reduces the FPF of the formulations.

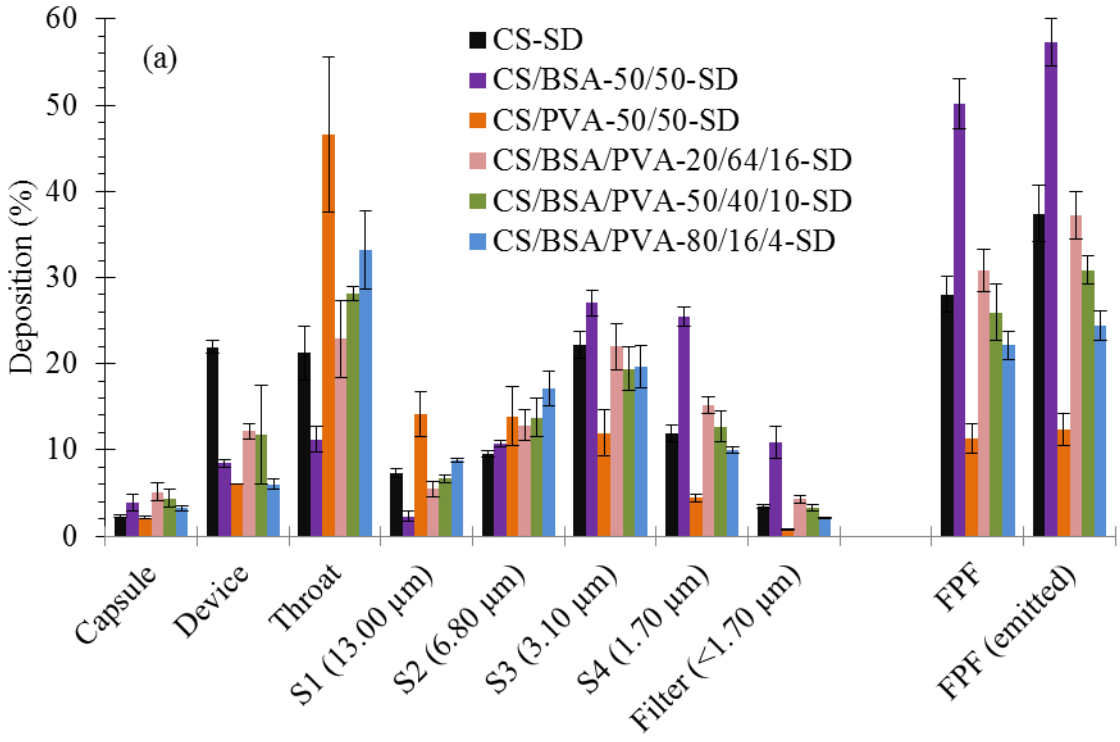

Figure 3.17. *In vitro* deposition (mean ± standard deviation [n=3]) of spray-dried powders at 60 L/min of 20%, 50%, 80% (w/w) CS-loaded microparticles with (a) 4:1, (b) 1:1 and (c) 1:4 (w/w) protein/polymer ratios. S1-S4 denote impactor stages, followed by their corresponding lower aerodynamic cutoff diameter in parentheses.

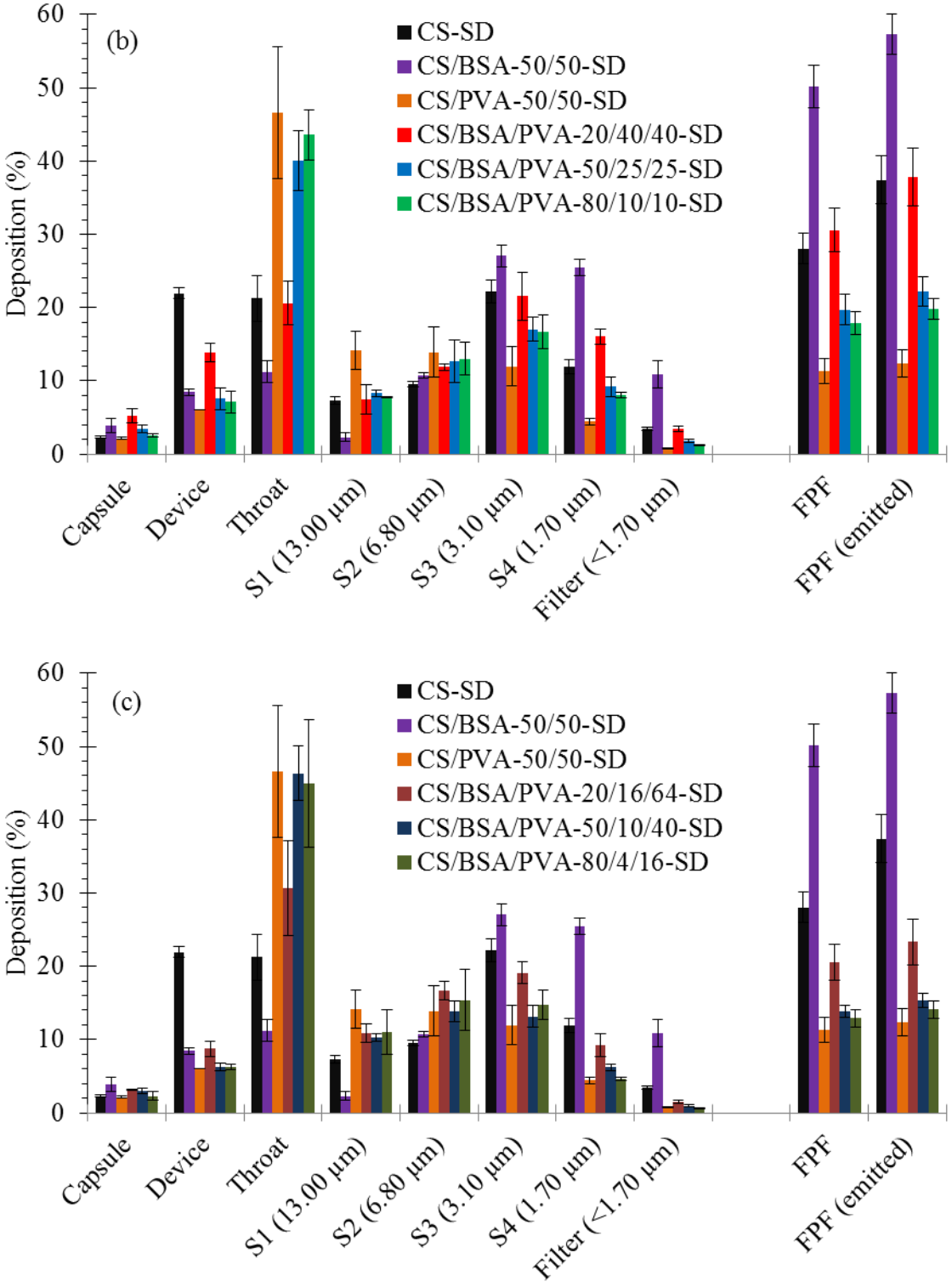

Figure 3.17. *In vitro* deposition (mean ± standard deviation [n=3]) of spray-dried powders at 60 L/min of 20%, 50%, 80% (w/w) CS-loaded microparticles with (a) 4:1, (b) 1:1 and (c) 1:4 (w/w) protein/polymer ratios. S1-S4 denote impactor stages, followed by their corresponding lower aerodynamic cutoff diameter in parentheses.

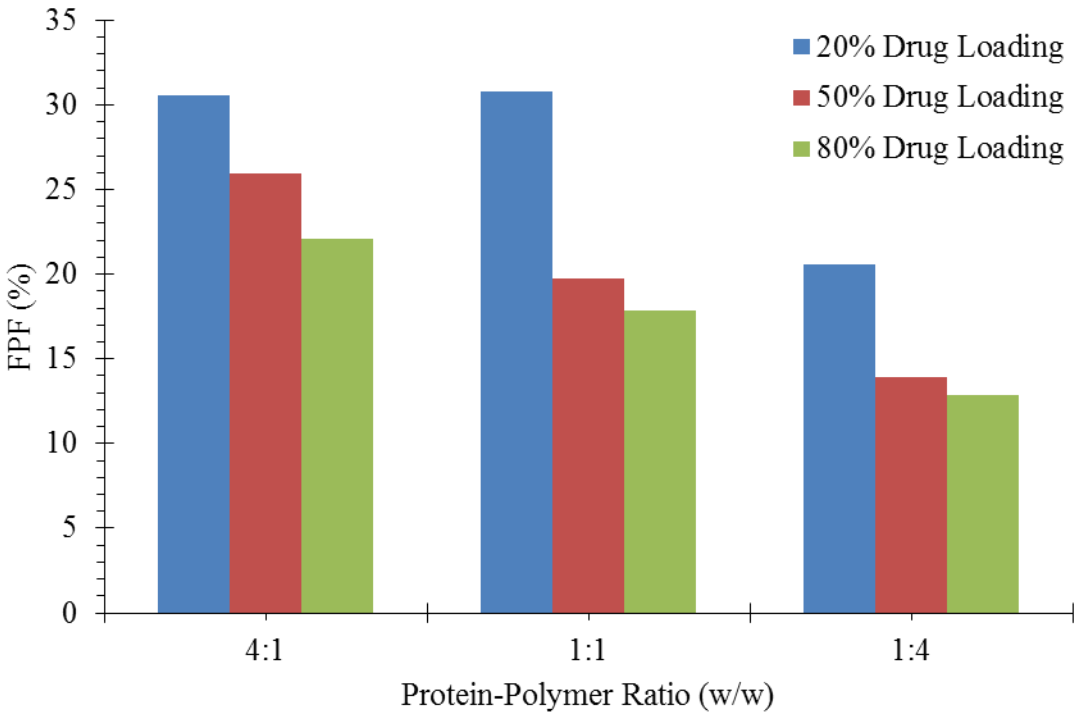

Figure 3.18. Effect of drug loading on FPF.

As previously suggested, the addition of BSA to the formulation did indeed confer it increased aerosolisation ability as seen by the two-fold increase in FPF of spray-dried CS/BSA-50/50-SD (Formulation 2) to CS-SD (Formulation 1). Interestingly, in Figure 3.19 (a), the deposition profile of 4:1 and 1:1 protein/polymer ratios for 20% CS drug loading were very similar, which may suggest that there may be a limit to the effect of BSA on the aerosolisation properties of the formulations at certain drug loadings even though the average particle size of the 1:1 formulation (4.77 μm) was larger than that of the 4:1 formulation (2.99 μm). In Figure 3.19 (b), we note that even a small addition of PVA to the formulation reduced the FPF of the formulation by about half, which was almost exactly how much the average particle size diameter increased by (2.67 μm to 5.13 μm). However, one can safely conclude that the addition of BSA to a hybrid pulmonary drug delivery carrier had a positive effect on its aerosol performance while helping to reduce the amount of polymer in the delivery system.

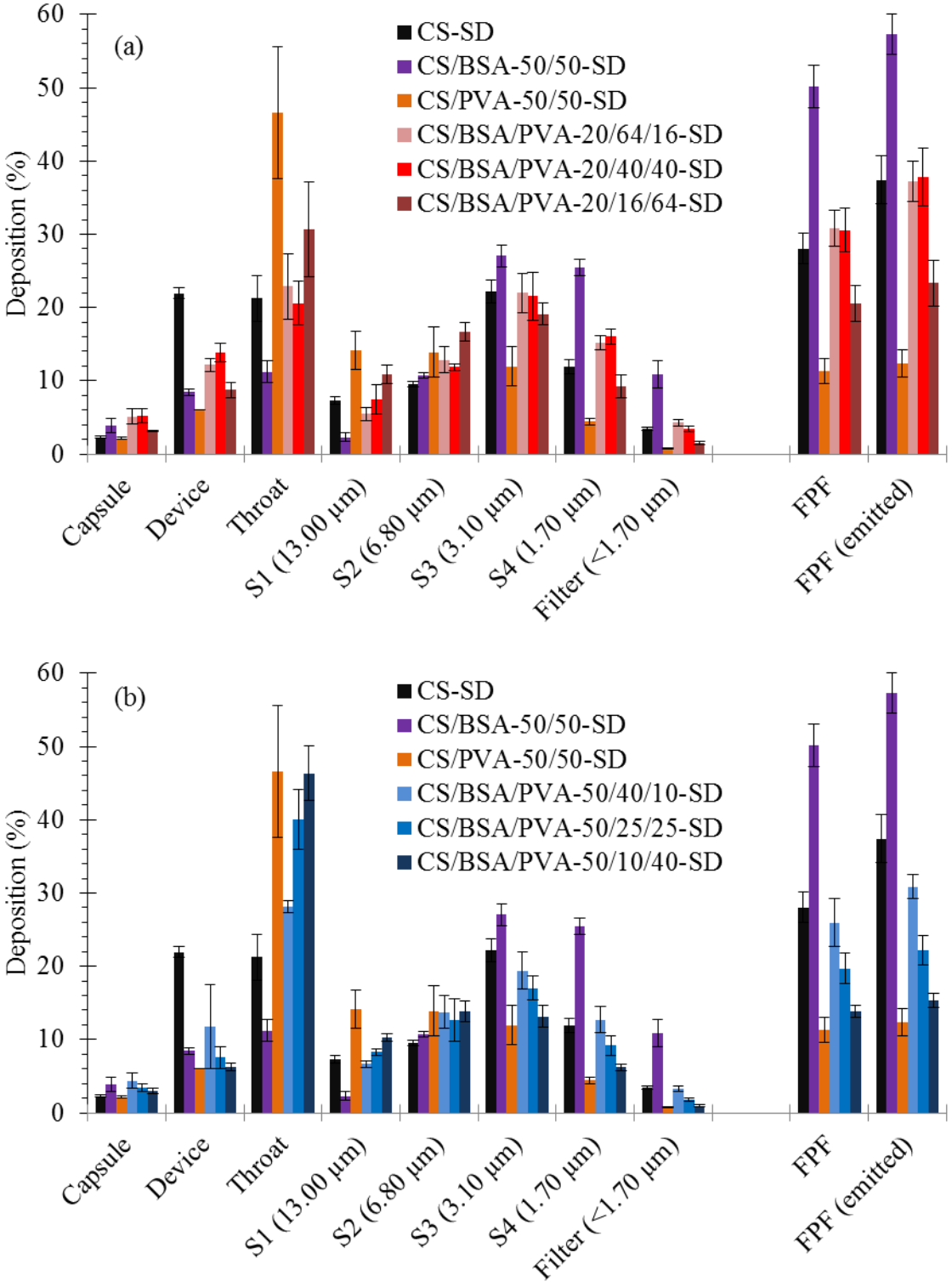

Figure 3.19. *In vitro* deposition (mean ± standard deviation [n=3]) of spray-dried powders at 60 L/min of (a) 20%, (b) 50%, (c) 80% (w/w) CS-loaded microparticles with 4:1, 1:1 and 1:4 (w/w) protein/polymer ratios. S1-S4 denote impactor stages, followed by their corresponding lower aerodynamic cutoff diameter in parentheses.

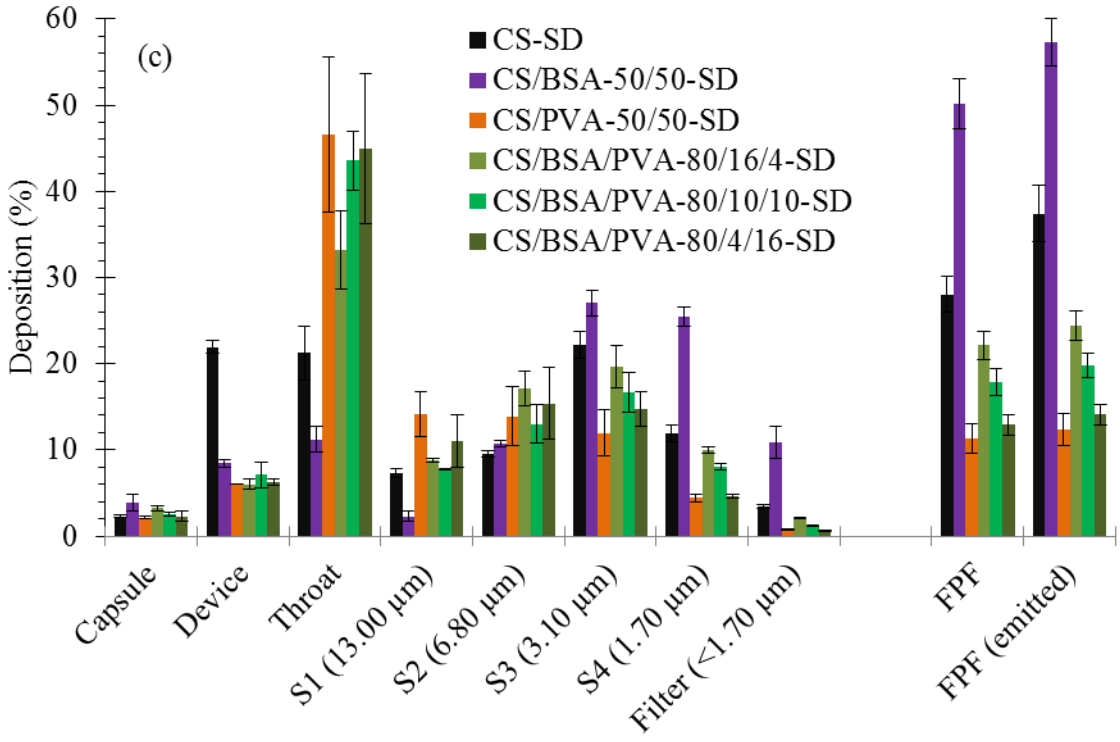

Figure 3.19. *In vitro* deposition (mean ± standard deviation [n=3]) of spray-dried powders at 60 L/min of (a) 20%, (b) 50%, (c) 80% (w/w) CS-loaded microparticles with 4:1, 1:1 and 1:4 (w/w) protein/polymer ratios. S1-S4 denote impactor stages, followed by their corresponding lower aerodynamic cutoff diameter in parentheses.

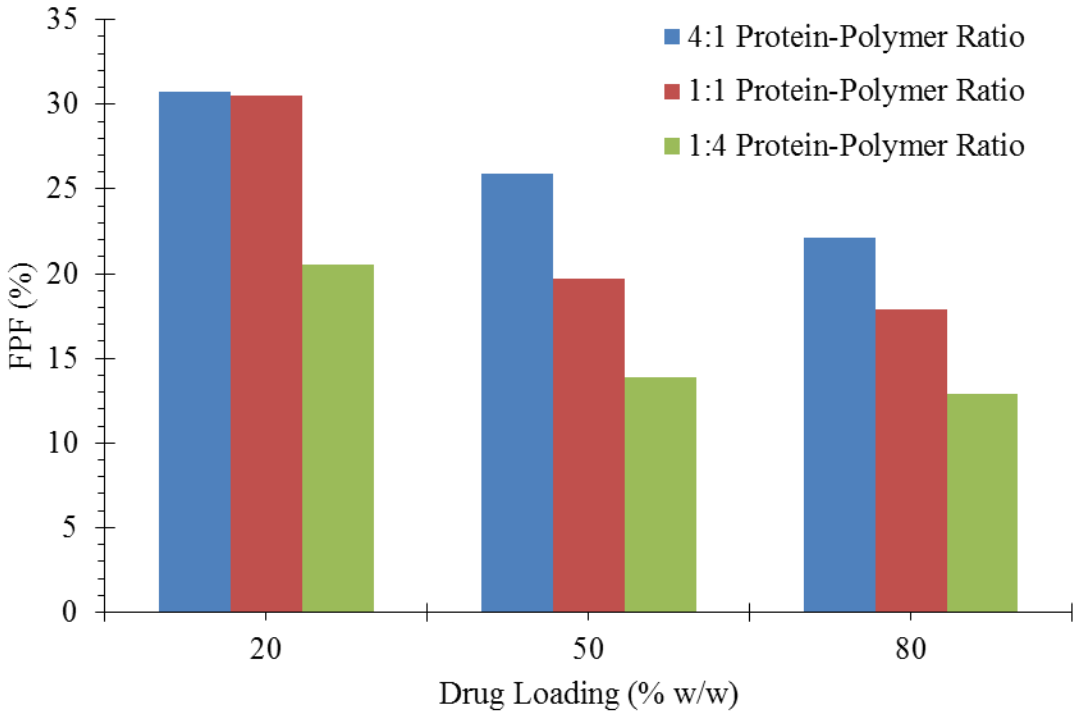

Figure 3.20. Effect of protein/polymer ratio on FPF.

It is interesting to note the *in vitro* deposition performance of spray-dried CS/BSA-50/50-SD. It had, by far, the highest FPF compared to all the other formulations and that the addition of just 10% (w/w) of PVA to the formulation decreased the FPF from ~50% to 30% and even though the amount of BSA in the formulation increased to 64% (w/w) in Formulation 4, the FPF was still only about 30%. The increased adhesion that small particles have may be the reason why more CS/BSA-50/50-SD was deposited in the capsule and device than CS/PVA-50/50-SD. However, upon leaving the device, CS/BSA-50/50-SD had a low deposition in the throat and stages 1 and 2.

3.3.11 *In vitro* dissolution studies

Dissolution profiles of each formulation are shown for different protein/polymer ratios in Figure 3.21 and different drug loadings in Figure 3.22. As there is currently still no pharmacopoeia methodology for the evaluation of release rate of pulmonary drug delivery systems (Riley *et al.*, (2012)), the dissolution tests were conducted using two commonly used types of dissolution apparatus, the USP dissolution apparatus 1 (basket apparatus), and the USP dissolution apparatus 4 (flow-through cell) to establish the merits and suitability of using each method to analyse the release behaviour of aerosols.

From both Figure 3.21 and Figure 3.22, it is clear to see that CS was released more quickly with the USP dissolution apparatus 1 (basket apparatus) than it was with the USP dissolution apparatus 4 (flow-through cell). Given the large volume of dissolution medium (900 mL) and a hydrophilic drug, it was unsurprising that this was the case. This made distinguishing between the release profiles of different formulations tricky, especially when there was a high drug loading [Figure 3.22(c-1)]. Although the USP dissolution apparatus 1 (basket apparatus) presented a far more convenient method to perform dissolution tests, its large dissolution medium volume and stirring rate did not represent physiological conditions in the lung accurately. It could have utility as a quick method to determine a formulation's approximate dissolution profile, but a far more nuanced analysis can be had with the USP dissolution apparatus 4 (flow-through cell).

It is important to note the spread of particle size distributions for the different formulations as particle size affects dissolution rate directly. However, one is still able to glean certain insights into the characteristics of each excipient in the hybrid formulations. It can be seen that for Formulation 2 (CS/BSA-50/50-SD), the addition of BSA did not impact the dissolution rate in any way from the spray-dried drug, displaying a similarly rapid release within minutes. Paying closer attention to Figure 3.21c, for formulations

with 1:4 protein/polymer ratio, we were able to decouple the size effect from the dissolution rate and deduce the influence that drug loading has on the dissolution rate as all three formulations had a similar particle size distribution. It is clear that the dissolution rate increased dramatically when the drug loading was increased to 50% (w/w) and beyond as the CS is highly hydrophilic.

As mentioned earlier, increasing protein/polymer ratio decreased the particle size, which also meant we were unable to look at any drug loading amounts where the particle size distribution was similar, as was for Figure 3.21c. In general, the dissolution rate increased with increasing protein/polymer ratio (although some of that effect has to be attributed to the decrease in particle size previously observed). However, it has to be noted that the 20% drug-loaded formulations were unable to obtain 100% dissolution as the CS may be trapped within the PVA matrix with an insufficient pore network for release. A similar effect was seen in previous work on antibiotic-loaded bone cement, where a critical amount of mesoporous silica was required to form an efficient network for the antibiotic to diffuse from the poly(methyl methacrylate)-based bone cement's polymer matrix (Shen *et al.*, (2011)). This effect was less exaggerated for Formulation 4 (●) in Figure 3.22a where there was an increased amount of BSA in the carrier, which being highly water-soluble, may aid in the creation of a network for release.

For the hybrid protein/polymer carriers we studied, the slowing of the dissolution rate was less pronounced at higher drug loadings (Figure 3.21) or greater protein/polymer ratios (Figure 3.22), probably because both CS and BSA are highly water-soluble and may create pores within the PVA matrix during dissolution. This observation could be exploitable, as it would give the formulator the opportunity to regulate the dissolution rate of the drug. It must be noted that too much polymer can slow the release to undesirable levels and a balance between a slower release rate and efficient release must be reached for an optimal release profile.

As serum albumins are endogenous to the lung, the addition of BSA may also serve to reduce the toxicity and increase the biocompatibility of formulations compared to those containing a higher proportion of PVA. Although the short-term toxicity of PVA has been investigated (R. O. Salama *et al.*, (2009b)), longer-term testing will be needed to support chronic use of carrier systems containing it (similar to those described by (Nakamura *et al.*, (2001))).

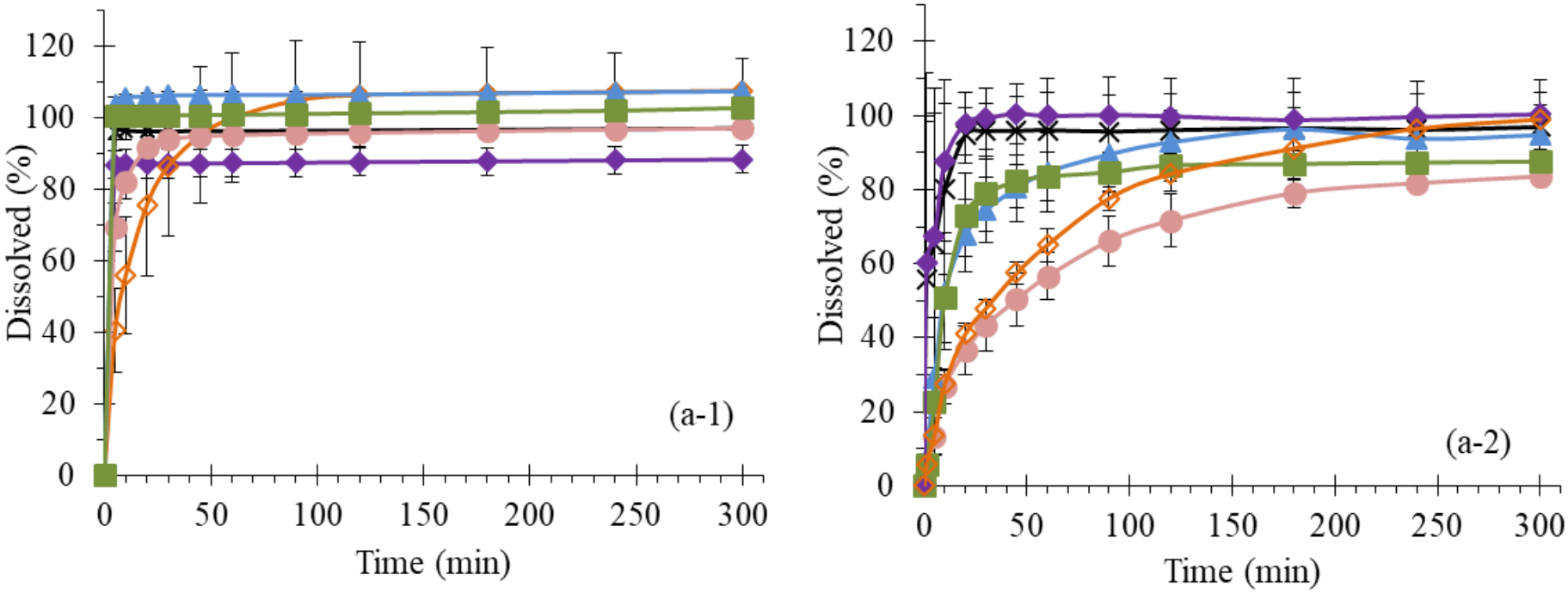

Figure 3.21. Effect of drug loading on dissolution profiles for USP dissolution apparatus 1 (basket apparatus) (a-1, b-1, c-1) and USP dissolution apparatus 4 (flow-through cell) (a-2, b-2, and c-2). Dissolution profiles (presented as mean ± standard deviation [n=3]) of 20% (●), 50% (▲), 80% (■) (w/w) CS-loaded microparticles with (a) 4:1, (b) 1:1 and (c) 1:4 (w/w) protein/polymer ratios. Dissolution profiles of spray-dried CS (✕), 50% CS-loaded microparticles with 50% BSA (◆) and 50% PVA (◇) are also shown.

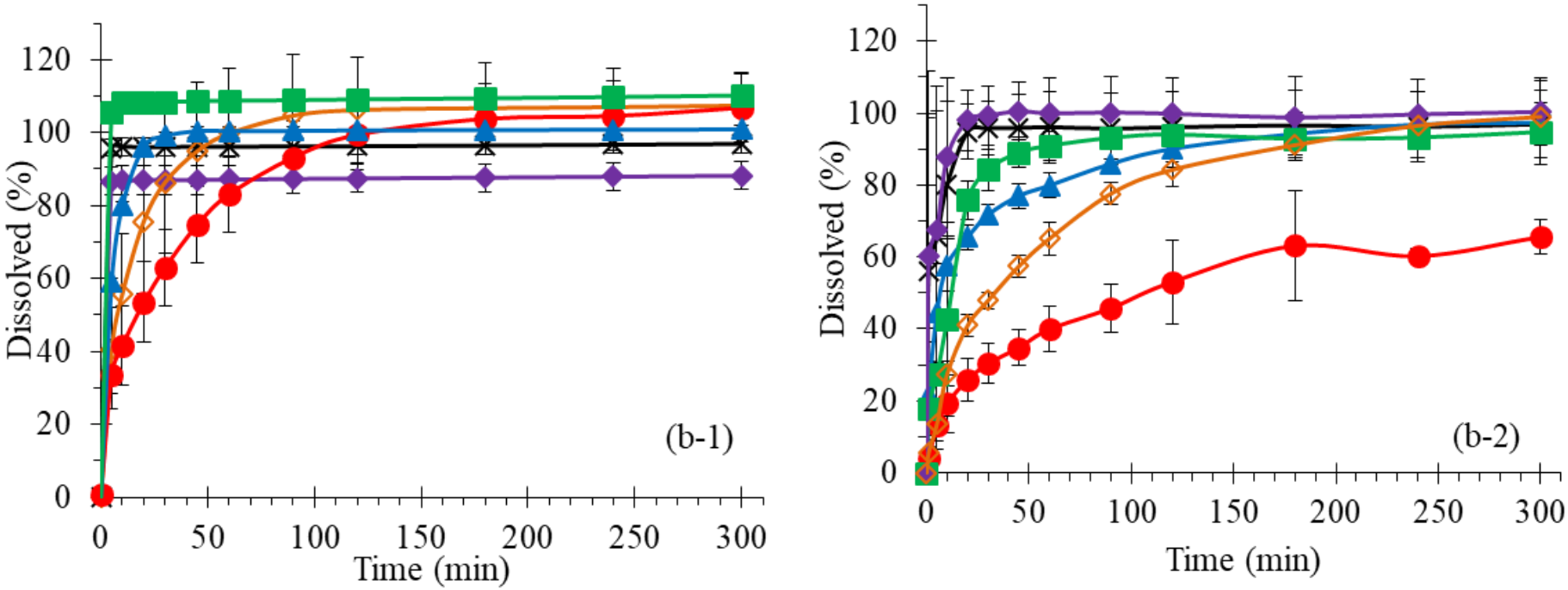

Figure 3.21. Effect of drug loading on dissolution profiles for USP dissolution apparatus 1 (basket apparatus) (a-1, b-1, c-1) and USP dissolution apparatus 4 (flow-through cell) (a-2, b-2, and c-2). Dissolution profiles (presented as mean ± standard deviation [n=3]) of 20% (●), 50% (▲), 80% (■) (w/w) CS-loaded microparticles with (a) 4:1, (b) 1:1 and (c) 1:4 (w/w) protein/polymer ratios. Dissolution profiles of spray-dried CS (✕), 50% CS-loaded microparticles with 50% BSA (◆) and 50% PVA (◇) are also shown.

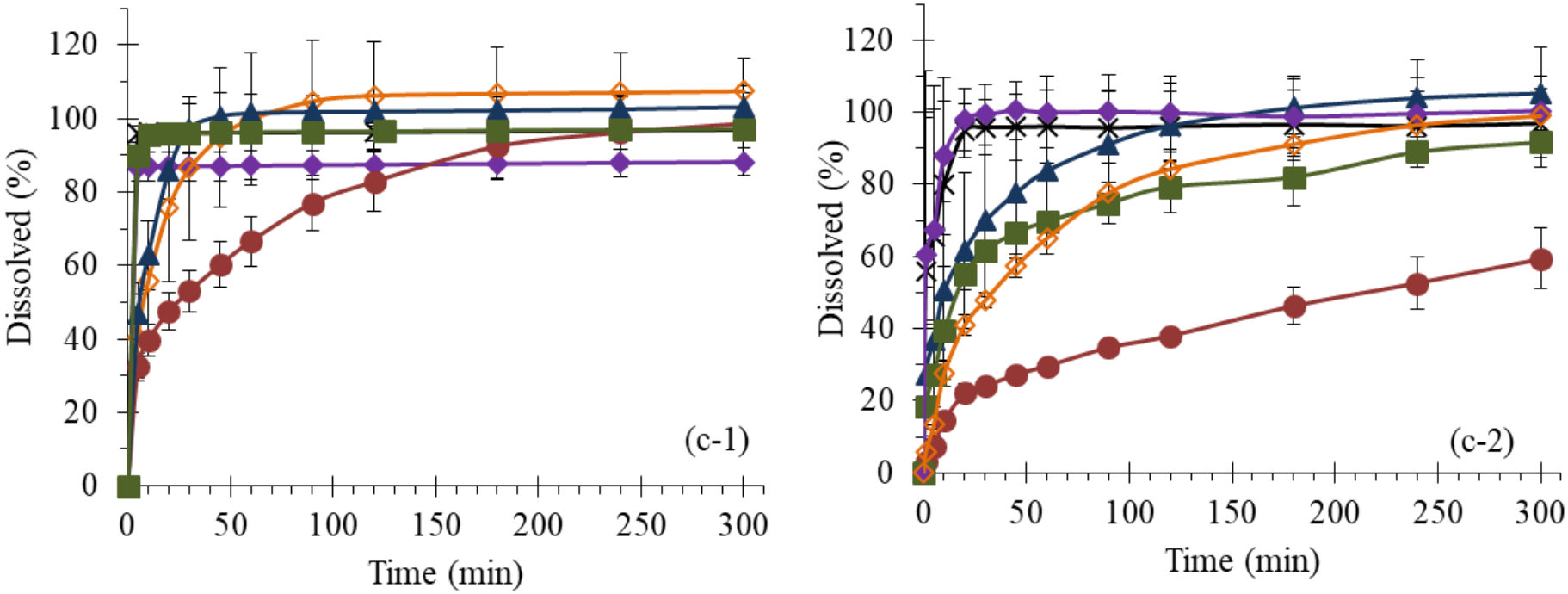

Figure 3.21. Effect of drug loading on dissolution profiles for USP dissolution apparatus 1 (basket apparatus) (a-1, b-1, c-1) and USP dissolution apparatus 4 (flow-through cell) (a-2, b-2, and c-2). Dissolution profiles (presented as mean ± standard deviation [n=3]) of 20% (●), 50% (▲), 80% (■) (w/w) CS-loaded microparticles with (a) 4:1, (b) 1:1 and (c) 1:4 (w/w) protein/polymer ratios. Dissolution profiles of spray-dried CS (✕), 50% CS-loaded microparticles with 50% BSA (◆) and 50% PVA (◇) are also shown.

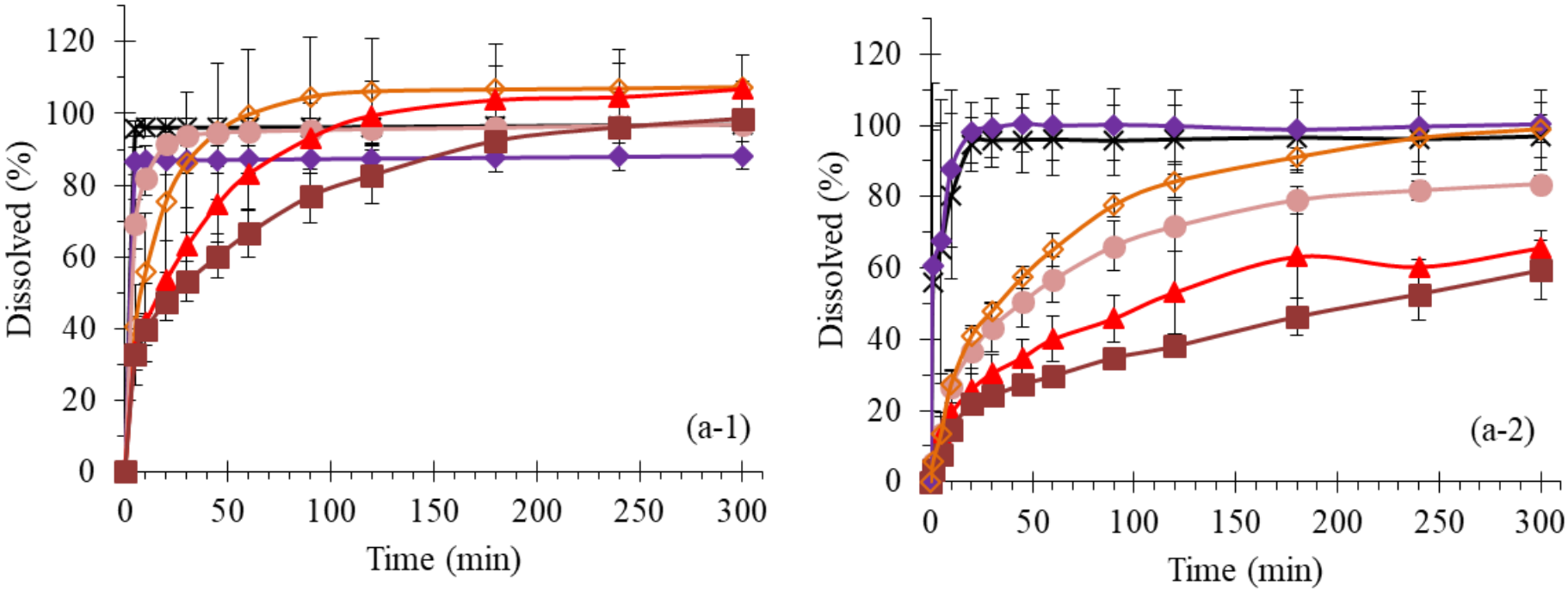

Figure 3.22. Effect of protein/polymer ratio on dissolution profiles for USP dissolution apparatus 1 (basket apparatus) (a-1, b-1, c-1) and USP dissolution apparatus 4 (flow-through cell) (a-2, b-2, and c-2). Dissolution profiles (presented as mean ± standard deviation [n=3]) of (a) 20%, (b) 50%, (c) 80% (w/w) CS-loaded microparticles with 4:1 (●), 1:1 (▲) and 1:4 (■) (w/w) protein/polymer ratios. Dissolution profiles of spray-dried CS (✕), 50% CS-loaded microparticles with 50% BSA (◆) and 50% PVA (◇) are also shown.

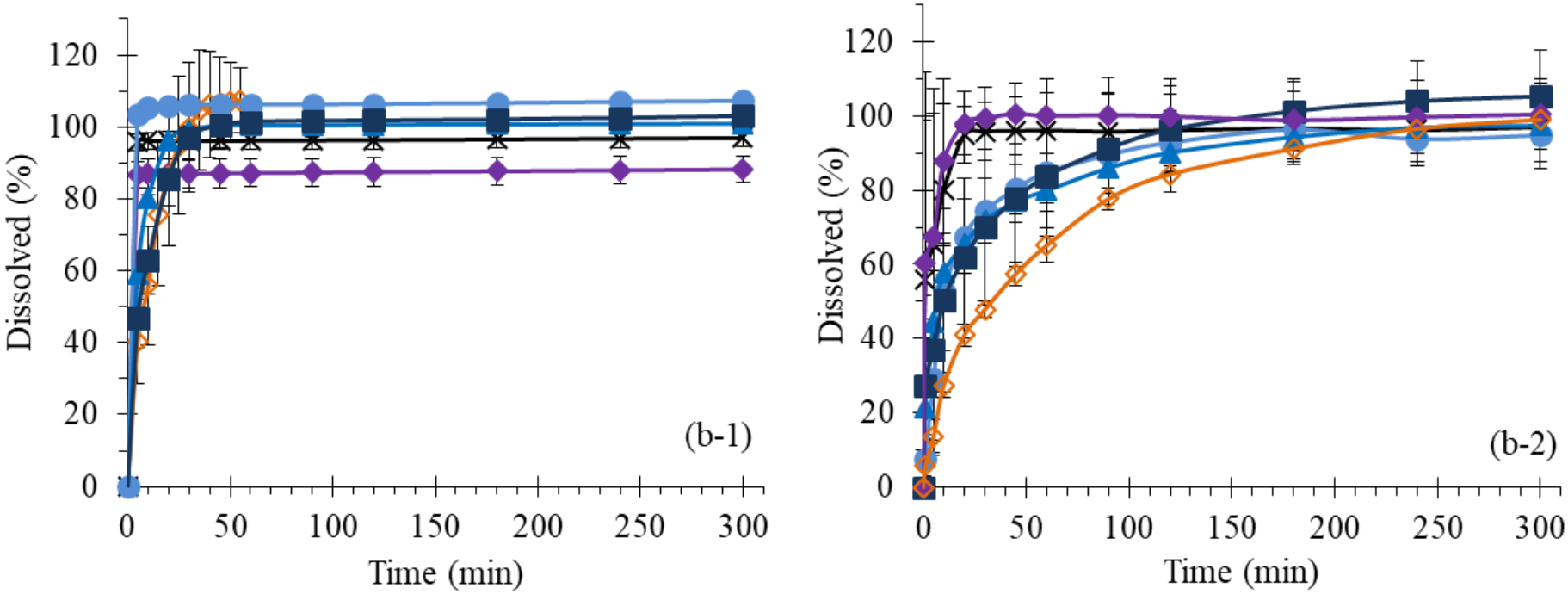

Figure 3.22. Effect of protein/polymer ratio on dissolution profiles for USP dissolution apparatus 1 (basket apparatus) (a-1, b-1, c-1) and USP dissolution apparatus 4 (flow-through cell) (a-2, b-2, and c-2). Dissolution profiles (presented as mean ± standard deviation [n=3]) of (a) 20%, (b) 50%, (c) 80% (w/w) CS-loaded microparticles with 4:1 (●), 1:1 (▲) and 1:4 (■) (w/w) protein/polymer ratios. Dissolution profiles of spray-dried CS (✕), 50% CS-loaded microparticles with 50% BSA (◆) and 50% PVA (◇) are also shown.

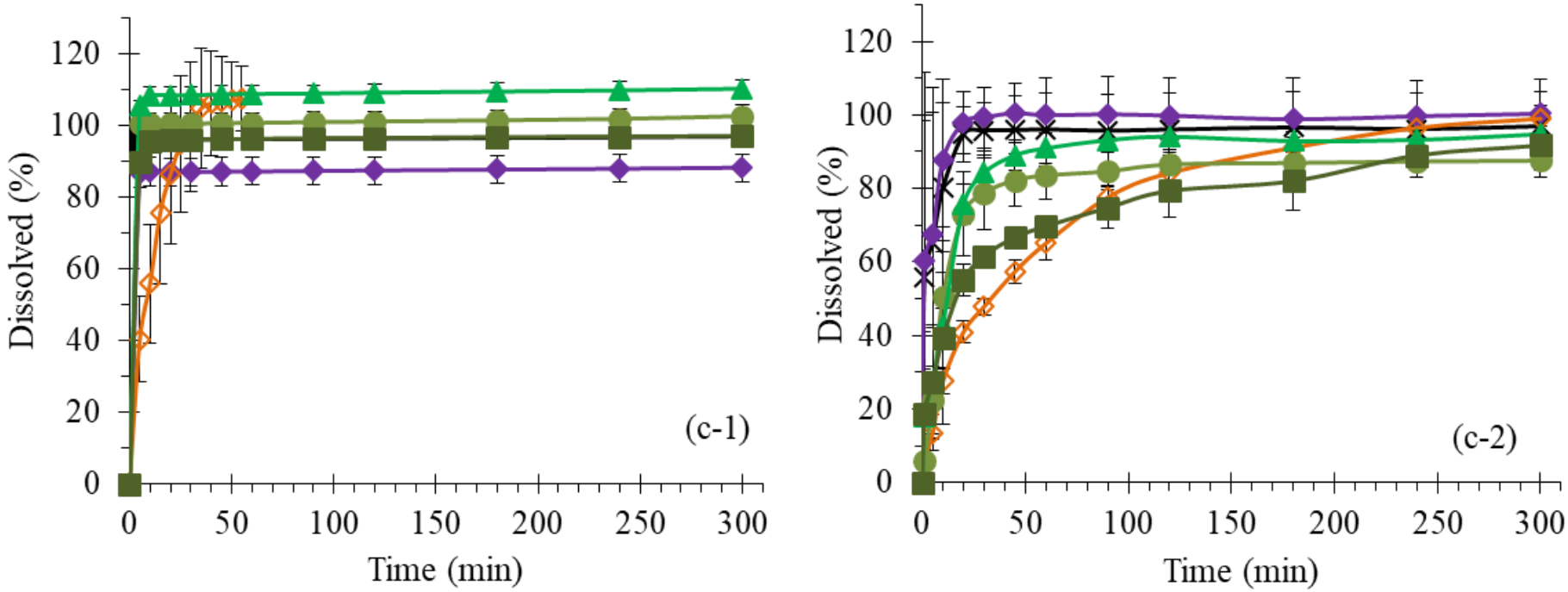

Figure 3.22. Effect of protein/polymer ratio on dissolution profiles for USP dissolution apparatus 1 (basket apparatus) (a-1, b-1, c-1) and USP dissolution apparatus 4 (flow-through cell) (a-2, b-2, and c-2). Dissolution profiles (presented as mean ± standard deviation [n=3]) of (a) 20%, (b) 50%, (c) 80% (w/w) CS-loaded microparticles with 4:1 (●), 1:1 (▲) and 1:4 (■) (w/w) protein/polymer ratios. Dissolution profiles of spray-dried CS (✕), 50% CS-loaded microparticles with 50% BSA (◆) and 50% PVA (◇) are also shown.

3.3.12 Mathematical models of dissolution profiles

The dissolution profiles of the formulations were fitted to linear plots of widely used mathematical models described in Section 2.8 and their coefficients of determination are shown in Table 3.6. Raw CS, spray-dried CS and CS/BSA-50/50-SD were highly water-soluble and had an almost instantaneous release and are difficult to describe accurately using the mathematical models. CS/PVA-50/50-SD could be accurately described by a few models including first order kinetics and the Baker-Lonsdale model.

Table 3.6. The Coefficients of Determination of Linear Plots of Widely Used Dissolution Profile Mathematical Models.

Formulation	Zero Order	First Order	Hixson-Crowell	Higuchi	Baker-Lonsdale	Korsmeyer-Peppas
0	0.293	0.566	0.441	0.536	-0.128	0.968 (3 points)
1	0.477	0.741	0.670	0.723	0.949	1.000 (2 points)
2	0.506	0.975	0.879	0.802	0.878	0.915
3	0.746	0.991	0.952	0.937	0.989	0.987
4	0.727	0.898	0.847	0.927	0.921	0.982
5	0.572	0.941	0.794	0.827	0.811	0.984
6	0.375	0.520	0.466	0.631	0.711	0.993 (3 points)
7	0.764	0.867	0.836	0.959	0.924	0.976
8	0.525	0.919	0.801	0.771	0.785	0.998 (3 points)
9	0.610	0.816	0.743	0.845	0.727	0.944 (3 points)
10	0.866	0.941	0.919	0.984	0.993	0.973
11	0.661	0.990	0.964	0.892	0.967	0.963
12	0.618	0.891	0.808	0.848	0.827	0.972

The spray-dried hybrid formulations were all well described by the Korsmeyer-Peppas model. The model is normally used when the release mechanism is not well known and when there may be more than one type of release mechanism involved, which perfectly fits the nature of the hybrid formulations with a slower dissolving polymer and a highly water-soluble protein. However, it has to be noted that due to the quick release nature of some of the formulations, only a few measurements were taken before 60% of the drug

was released, which is the degree to which the Korsmeyer-Peppas model is accurate to, and so may not fully reflect the closeness of the fit of the formulation to the model.

3.3.13 Optimised formulation

As described above, there are many interlinked factors in developing an effective controlled release pulmonary drug delivery system for a water-soluble active ingredient. It was found that the aerodynamic diameter of the particles provided a fair estimation into the FPF of the formulations. The factors that influence the aerodynamic diameter are the particles' specific density, size, and to an extent, microstructure. From the results above, it appeared that while the addition of PVA seemed to impart hollowness to the hybrid particles, its density was still higher than that of solid BSA particles and hence so was its aerodynamic diameter, resulting in a poorer aerosol performance.

However, PVA is an effective dissolution modulator so its detrimental effects on the aerosol performance have to be balanced with hydrophilic BSA. From our observations, we were able to utilise BSA to control the particle size of the formulation and also to improve the aerosolisation ability of powders, although one needs to be careful with the possibility that it could selectively bind to either the active ingredient or other excipients, affecting the release of the AI (Codrons *et al.*, (2003)). Based on the factorial study conducted, a formulator should be able to estimate with some certainty, the amount of excipients required for a desired dissolution and deposition profile. It is apparent that the addition of PVA is detrimental to the aerosol performance of the formulation while being able to sustain the release of CS. Formulation 4 perhaps provided the best balance of the formulations tested in attaining sustained release of CS and with an acceptable FPF. However, the release of CS was limited to about 80% over the time period tested. Taking things forward, one could test a formulation with a similar protein/polymer ratio but with an increased drug loading between 20% (w/w) and 50% (w/w) as the increased drug loading should increase the amount of CS released, albeit while reducing the FPF. It is this careful balance that needs to be maintained in considering formulations with excipients that appear to be both complementary and contradictory to each other. This could be useful in the design of formulations with specific purposes such as paediatric or geriatric formulations.

3.4 Conclusions

The physicochemical properties of a hybrid protein/polymer drug delivery system were studied and shown to be useful for modulating controlled release *in vitro*. PVA had already been shown to be effective in controlling the release of CS in the lung but suffered from poor *in vitro* deposition and a less than ideal particle size distribution. The addition of albumin was able to improve the formulation in other areas such as particle size distribution and *in vitro* deposition to create a better-balanced formulation. A formulator should be able to utilise BSA as an effective component in the excipient make up for a pulmonary drug delivery system as the addition of BSA to the carrier can help to modulate the sustained release of active ingredients from the carrier. Furthermore, the addition of BSA to the formulations also helped lower the density of the particles and hence their aerodynamic diameter for a better aerosol performance. The massive enhancement in the aerosol performance when only BSA was added to CS was lost with the addition of a small amount of PVA. The effect of PVA on BSA should be studied in further detail to understand the mechanism behind this action. These hybrid drug delivery systems show that, sometimes, a combination of complementary excipients may be needed to achieve the desired effect of certain pulmonary drug delivery systems and that the formulator may be able to find the optimal balance between the advantages and limitations of each excipient to develop an effective product.

4 PHYSICOCHEMICAL EVALUATION OF A POORLY WATER-SOLUBLE CORTICOSTEROID-AMPHIPHILIC POLYMER AMORPHOUS SOLID DISPERSION FOR PULMONARY DRUG DELIVERY

4.1 Introduction

There is a long history of delivering therapeutics by inhalation (Bryan, (1930)). Since then, respiratory ailments such as asthma, chronic obstructive pulmonary disease (COPD)

and infections can all be treated locally. This entails a reduction in the side effects of systemic delivery of active pharmaceutical ingredients (APIs) and the required dose may be reduced as hepatic first pass metabolism is avoided (Olsson *et al.*, (2011)). Systemic delivery of drugs to the lung is also an attractive prospect for pulmonary delivery due to the large surface area for absorption in the alveolar epithelium (Patton and Byron, (2007)). However, the poor solubility of APIs is one of the most challenging issues in the development of many pharmaceutical products and orally inhaled products are no exception. An estimated 40% of drugs listed in the US Pharmacopoeia is listed as poorly water-soluble, or insoluble (Williams *et al.*, (2013)). These drugs have poor bioavailability when administered because of poor solubility in biological fluids, and often fail to be commercialised. The dissolution rate is often the rate limiting step for Biopharmaceutical Classification System (BCS) Class II drugs, which have low solubility and high permeability, and there are several strategies which can be employed to mitigate this. These include particle size reduction (Jinno *et al.*, (2006)), co-crystallisation, the use of polymeric micelles (Liu *et al.*, (2008); Wais *et al.*, (2016)), inclusion in cyclodextrins (Uekama *et al.*, (1983); Vartiainen *et al.*, (2017)), nanocrystalline (De Smet *et al.*, (2014)) or amorphous forms (Chen *et al.*, (2016); Prasad *et al.*, (2014)) of the API.

An increased bioavailability will be beneficial for poorly water-soluble drugs adminstered by pulmonary delivery. While slowing the rate of release can be a strategy to prolong the retention of drugs in the lung and hence its effect, a release rate that is too slow will cause the drug to be more susceptible to clearance mechanisms (Mobley and Hochhaus, (2001)) and cause the drug concentration to dip below therapeutic levels. Insoluble particles will likely be engulfed by alveolar macrophages while a soluble particle will dissolve in lung fluid and exert its therapeutic action (Davies and Feddah, (2003)). Yet, not all the formulation strategies highlighted above can be applied to such systems. A combination of efficient lung clearance mechanisms and a limited pool of regulatory approved excipients for inhalation has been a major hurdle in developing viable pulmonary drug delivery systems (Smyth and Hickey, (2011)).

Amorphous solid dispersions have been a popular strategy in improving the dissolution behaviour of orally ingested drugs and it has also seen uptake for pulmonary delivery systems (Chen *et al.*, (2016); Giunchedi *et al.*, (2001); Wauthoz and Amighi, (2015)). Spray drying is one of the more common approaches to obtain amorphous solid dispersions (Seville *et al.*, (2007); Vehring, (2008)). The amorphous state is thermodynamically less stable than the crystalline state and that leads to an improvement

in the dissolution rate (Hancock *et al.*, (2002)). However, one of the foremost concerns regarding the amorphous state is its tendency to re-crystallise, which decreases the dissolution rate of the drug (Hancock *et al.*, (1995); Yoshioka *et al.*, (1994)). This is undesirable in the pharmaceutical field where active ingredients in their amorphous and crystalline form often have very different pharmacokinetic and pharmacodynamic profiles. This is especially pertinent for pulmonary delivery, where the surface characteristics of spray-dried powders have a sizeable influence on the FPF, which is an *in vitro* measurement of the amount of particles that will reach the lungs. Re-crystallisation of spray-dried particles during processing or storage could affect the particle surface and hence its FPF (Maa *et al.*, (1998)).

Soluplus® is a graft co-polymer (polyvinyl caprolactam-polyvinyl acetate-polyethylene glycol) introduced by BASF as a solubiliser. It has the ability to form solid solutions and its amphiphilic structure helps to solubilise poorly water-soluble drugs in aqueous media with the formation of micelles. Soluplus® has been used to formulate amorphous solid dispersions, especially with hot melt extrusion (Djuris *et al.*, (2013); Jing *et al.*, (2015); Lu *et al.*, (2015)), but also with spray-drying (Davis, Mark T., Potter, Catherine B., Mohammadpour and Maryam, Albadarin, Ahmad B., Walker, (2017); Lavra *et al.*, (2016)). Recently, Soluplus® was also investigated for the delivery of insulin *via* inhalation (Andrade *et al.*, (2015)) as well as a dry powder for nasal drug delivery (Pozzoli *et al.*, (2017)). It was found that lyophilised insulin-Soluplus® formulations did not have significant *in vitro* toxicity to respiratory cell lines, suggesting that it could be a viable candidate as an excipient in pulmonary drug delivery, especially given its unique bifunctional character in forming solid solutions, and micelles with a low critical micelle concentration (CMC).

Beclomethasone dipropionate (BDP) is a corticosteroid that is often prescribed for the treatment of asthma and chronic obstructive pulmonary disease to fight inflammation (Daley-Yates *et al.*, (2001); Sakagami *et al.*, (2002)). It is used as a form of prophylaxis treatment with long-acting bronchodilators to control asthma symptoms. However, its poor water solubility (0.16 μg/mL) may impact the bioavailability of drugs in the pulmonary tract.

Here, the spray-dried formulation of BDP and Soluplus® was investigated for its physicochemical properties such as dissolution and aerosolisation performance as well as physical stability. The purpose of the study was to determine if Soluplus® is a suitable excipient for the formulation of an amorphous solid dispersion of poorly water-soluble

drugs for pulmonary drug delivery.

4.2 Materials and methods

4.2.1 Materials

BDP was supplied from Junda Pharmaceutical Company Ltd. (Changzhou, China) and Soluplus® (M_r 90,000–140,000 g/mol) was kindly provided by BASF (Ludwigshafen, Germany). Polyvinylpyrrolidone (M_r 130,000 g/mol) (PVP K130) and sodium dodecyl sulphate (SDS) were procured from Sigma-Aldrich (St. Louis, MO, USA). HPLC grade methanol and acetonitrile were obtained from Duksan Pure Chemicals Co., Ltd (Gyeonggi-do, Republic of Korea). Ultrapure water was used in all the experiments.

4.2.2 Methods

4.2.2.1 Particle preparation

A set of formulations with a range of drug loadings (10, 15, 20, 30 and 40% w/w) were prepared. Pure BDP and 20% (w/w) drug loaded BDP-PVP K130 were also spray-dried for comparison. Typically, varying amounts of active ingredient were measured out and dissolved in methanol before the addition of polymer. The drug and polymer were allowed to dissolve fully overnight. Spray drying was performed on a laboratory scale spray dryer equipped with a high performance separating cyclone and 0.7 mm nozzle (B-290 Mini Spray Dryer, BÜCHI Labortechnik AG, Flawil, Switzerland). The mini spray dryer was operated in a 'closed loop' configuration with the Inert Loop B-295 accessory at the following conditions: inlet temperature 80 °C, outlet temperature ~50 °C, aspirator gas flow rate 35 m^3/h, atomising spray air flow rate 473 L/h and solution feed rate at 4 mL/min. All spray-dried powders were dried overnight in a vacuum desiccator filled with silica beads after collection.

BDP was cryogenically-milled as well, using a mixer mill (Mixer Mill MM 301, Retsch GmbH, Haan, Germany) equipped with a 50 mL stainless steel jar and a Ø50 mm grinding ball. Approximately 3 g of crystalline drug and the grinding ball were placed into the jar and pre-cooled in liquid nitrogen for ten minutes before being milled for 300 min at 20 Hz. Pre-cooling of the chamber was performed at two-minute intervals.

A physical mixture of cryo-milled (CM) BDP and Soluplus® was produced by

mixing 10% (w/w) cryo-milled BDP and 90% (w/w) raw Soluplus® in a bottle which was then capped and sealed tightly. The bottle was then placed into a multi-axis shaker-mixer (Alphie 3, Hexagon Product Development Pvt. Ltd, Gujarat, India) for three hours at 75 RPM to ensure complete mixing.

4.2.2.2 Thermal analysis

The thermal profiles of the powders were determined by differential scanning calorimetry (DSC). Experiments were conducted on a Mettler Toledo DSC 3 (Greifensee, Switzerland). Approximately 5 mg of powder was placed into an aluminium crucible. Measurements were taken at a heating rate of 10 °C/min.

4.2.2.3 *In vitro* dissolution studies

A United State Pharmacopoeia (USP) dissolution apparatus 4 (flow-through cell) (DFZ 720 flow-through-cell dissolution tester, Erweka GmbH, Heusenstamm, Germany) was used in the 'open-loop' configuration to conduct release studies of BDP. The temperature of the water baths surrounding the cells was maintained at 37 °C. 0.2% (w/v) sodium dodecyl sulphate solution was maintained at 37 °C before being pumped through the system using a peristaltic pump (IPC 8 microprocessor-controlled dispensing pump, Ismatec SA, IDEX Health & Science GmbH, Wertheim, Germany) at a constant flow rate of approximately 1.6 mL/min. A schematic of the dissolution apparatus setup is shown in Figure 4.1. Powders containing 20 mg of active ingredient, BDP, were weighed out and sandwiched between 1 mm glass beads (to promote laminar flow), which was bounded by 0.45 µm hydrophilic PTFE filters. The area exposed to vertical flow was 1.25 cm in diameter and dissolution medium exiting the flow-through cell was collected in beakers. At pre-determined time intervals, new collection beakers were put in place. The dissolution media collected in separate beakers were passed through 0.22 µm syringe filters and diluted with methanol (1:1 v/v) before being analysed for their concentrations using HPLC. Each formulation was tested in triplicate.

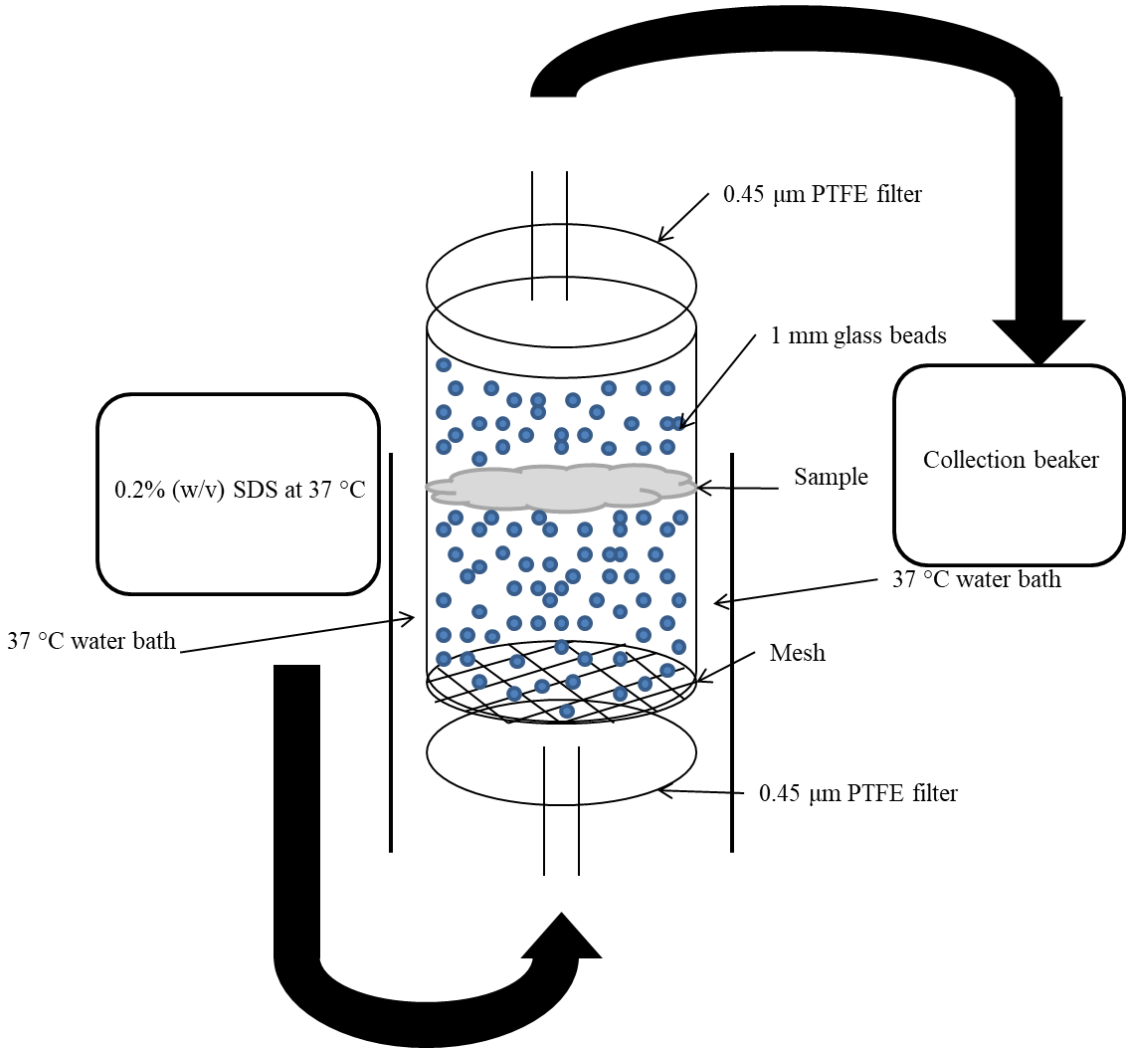

Figure 4.1. Schematic of Erweka DFZ 720 USP dissolution apparatus 4 (flow-through cell) in the 'open loop' configuration.

4.2.2.4 Drug assay

BDP content in the spray-dried powders was analysed *via* HPLC (1100 series; Agilent Technologies, Santa Clara, CA, USA) using a Zorbax Eclipse Plus C-18 column (4.6 mm x 250 mm, 5 µm) (Agilent, Technologies, Santa Clara, CA, USA) at a flow rate of 1 mL/min and an injection volume of 50 µL. Acetonitrile-water (65:35 v/v) was used as the mobile phase and the UV detection wavelength utilised was 254 nm. The retention time of BDP was approximately 11.8 min.

4.2.2.5 Stability testing

The co-spray dried powders were stored under accelerated stress test conditions recommended by the International Conference on Harmonisation (ICH) – ICH Q1A (R2)

of 40 °C/75% RH in open pans and were tested for their crystallinity with XRD at frequent time intervals.

4.3 Results and discussion

4.3.1 Yield, drug loading, and entrapment efficiency

The spray-drying yields, experimental drug loadings and entrapment efficiencies of the spray-dried formulations are shown in Table 4.1. The spray-drying yields were mostly high for BDP-Soluplus® formulations (> 70%) compared to the typical spray-drying yield of 50-70% achieved with the same spray-dryer for inhalable particles ("Laboratory scale spray drying Of inhalable drugs: A review," (2010)), with the exception of BDP-Soluplus®-30, due in part to the difficulty for even the high performance cyclone to separate small particles from the gas stream. Poor yields were also obtained for pure BDP and BDP-PVP K130. As will be seen in the moisture sorption data, BDP-PVP K130-20 was the most hygroscopic formulation and that may have been reflected in the increased difficulty to collect the particles in the spray-dryer. The experimental drug loadings were close to their theoretical ratios and the entrapment efficiency was close to 100% for all formulations, confirming spray-drying as a suitably efficacious method for preparing drug-loaded particles.

Table 4.1. Spray-drying Yield, Drug loading and Entrapment Efficiency of Spray-dried Formulations.

Sample	Spray-drying Yield (%)	Theoretical Drug Loading (%)	Experimental Drug Loading (%)	Entrapment Efficiency (%)
BDP-SD	48.5	-	-	-
BDP-Soluplus®-10	76.0	10	10.2	102.2
BDP-Soluplus®-15	81.3	15	14.4	95.7
BDP-Soluplus®-20	84.2	20	19.5	97.6
BDP-Soluplus®-30	40.4	30	28.5	95.1
BDP-Soluplus®-40	81.8	40	38.3	95.8
BDP-PVP K130-20	56.2	20	18.2	91.1

4.3.2 Powder crystallinity

As seen in Figure 4.2, all freshly prepared formulations displayed a broad diffuse peak, indicating X-ray amorphicity, except for BDP-SD which showed small crystalline peaks. It is, however, important to note that 30 cryo-milling cycles were required before an X-ray amorphous sample was obtained for cryo-milled BDP (BDP-CM), highlighting the difficulty in obtaining an amorphous form of BDP using either spray drying or cryo-milling. A physically mixed sample of cryo-milled BDP and raw Soluplus® (BDP-Soluplus®-PM) was X-ray amorphous after preparation.

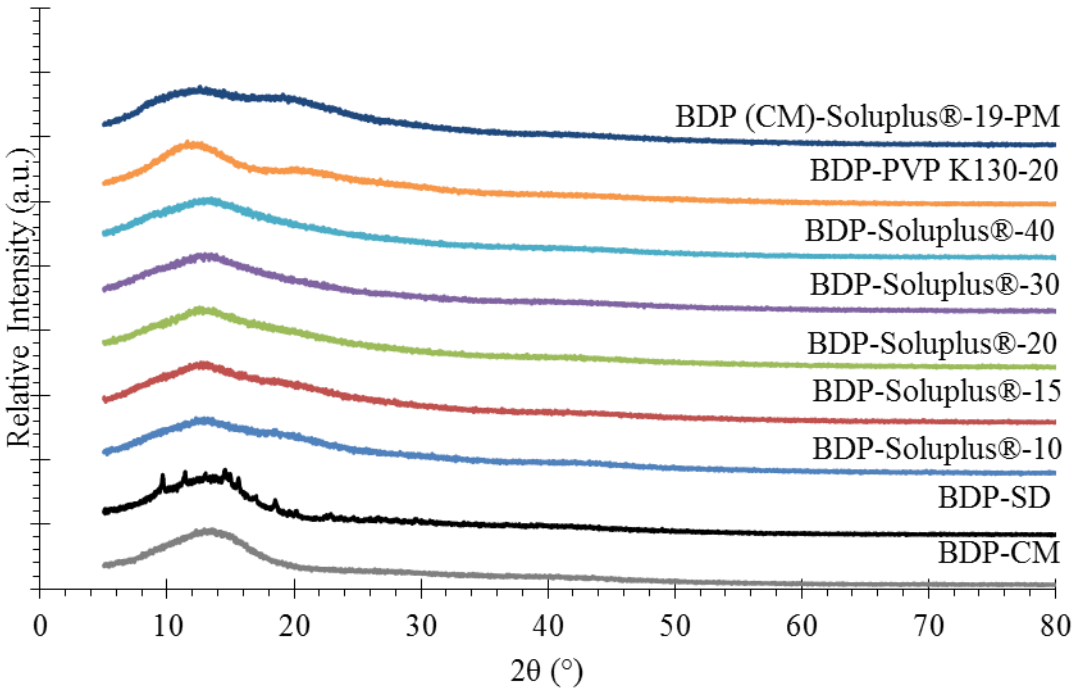

Figure 4.2. X-ray diffractograms of freshly prepared BDP samples.

4.3.3 Thermal analysis

The thermal profiles of the spray-dried powders are shown in Figure 4.3. BDP-SD showed a melting endotherm at 212 °C which agrees well with the melting point of the crystalline drug (Buttini *et al.*, (2014)). This endotherm was distinctly absent in all the other spray-dried formulations, which confirmed the amorphous form shown in the XRD measurements.

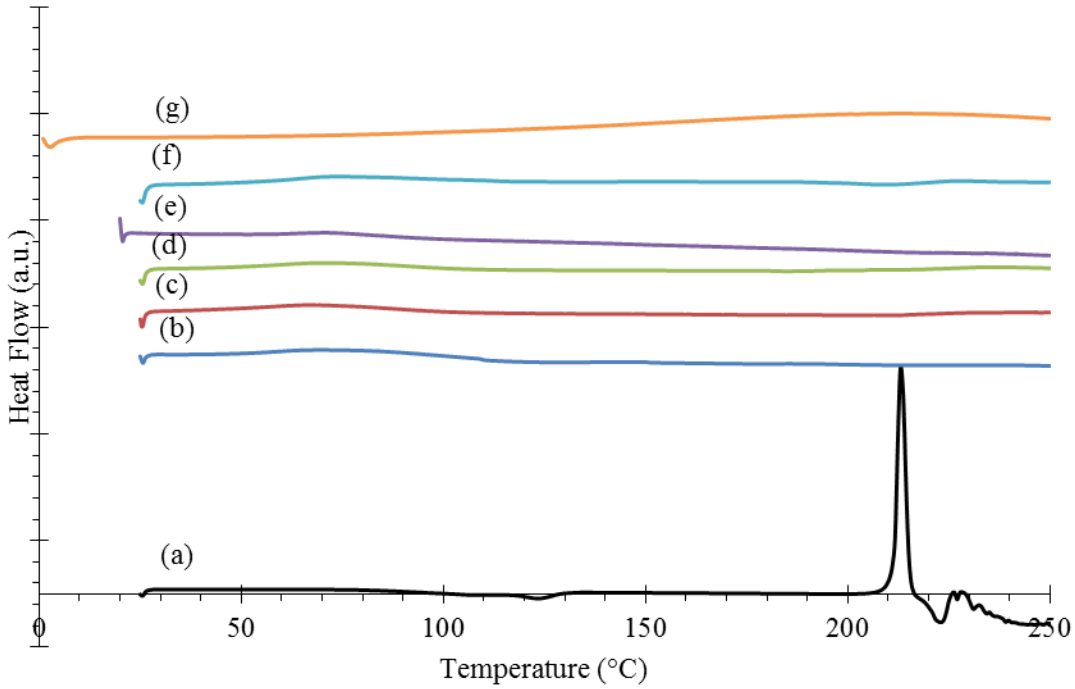

Figure 4.3. DSC thermogram of spray-dried formulations. a) BDP-SD, (b) BDP-Soluplus®-10, (c) BDP-Soluplus®-15, (d) BDP-Soluplus®-20, (e) BDP-Soluplus®-30, (f) BDP-Soluplus®-40, (g) BDP-PVP K130-20.

4.3.4 Moisture sorption

Moisture sorption isotherms of the spray-dried formulations are shown in Figure 4.4. As expected, the lipophilic BDP had a very low maximum mass change of only 2% (w/w) at 90% RH. There was no evidence of moisture-induced re-crystallisation and it was noted that BDP-PVP K130-20, which does not possess a hydrophobic group like amphiphilic Soluplus®, had a change in mass (33.17%) which was twice as much as BDP-Soluplus®-20 (16.32%) which also possessed 20% (w/w) of BDP as BDP-PVP K130-20. Due to the addition of amphiphilic Soluplus®, which has a hydrophilic group, the relative moisture sorption of the spray-dried formulation increased with increasing amount of Soluplus® added. Upon closer examination, this relationship was found to be a linear one from 10-40% (w/w) of Soluplus® (Figure 4.5), although not from 0-10% (w/w) Soluplus®.

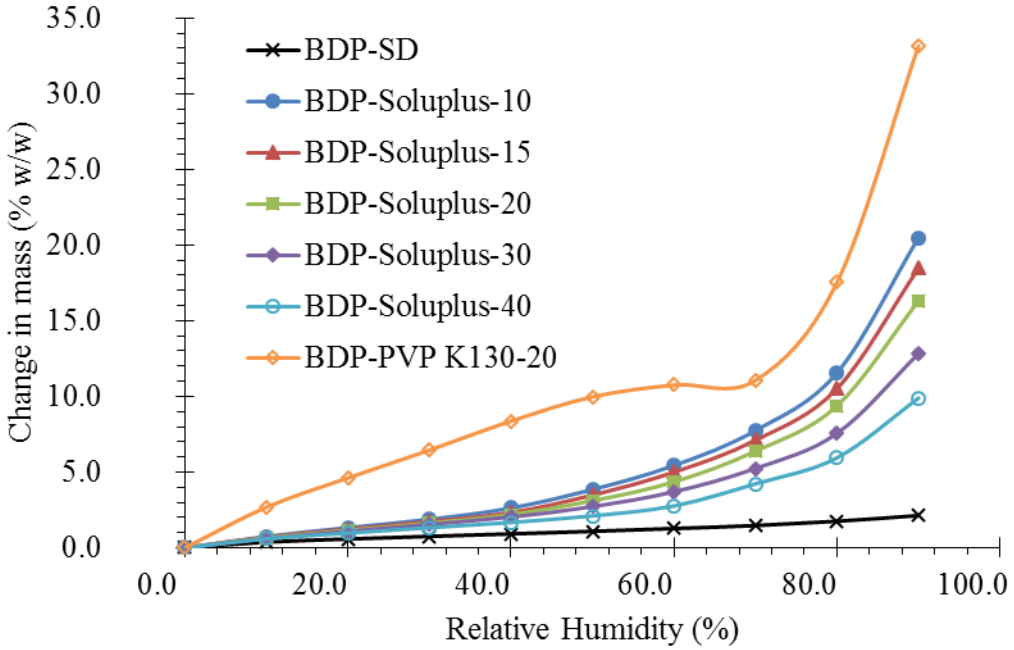

Figure 4.4. DVS sorption isotherms of spray-dried formulations.

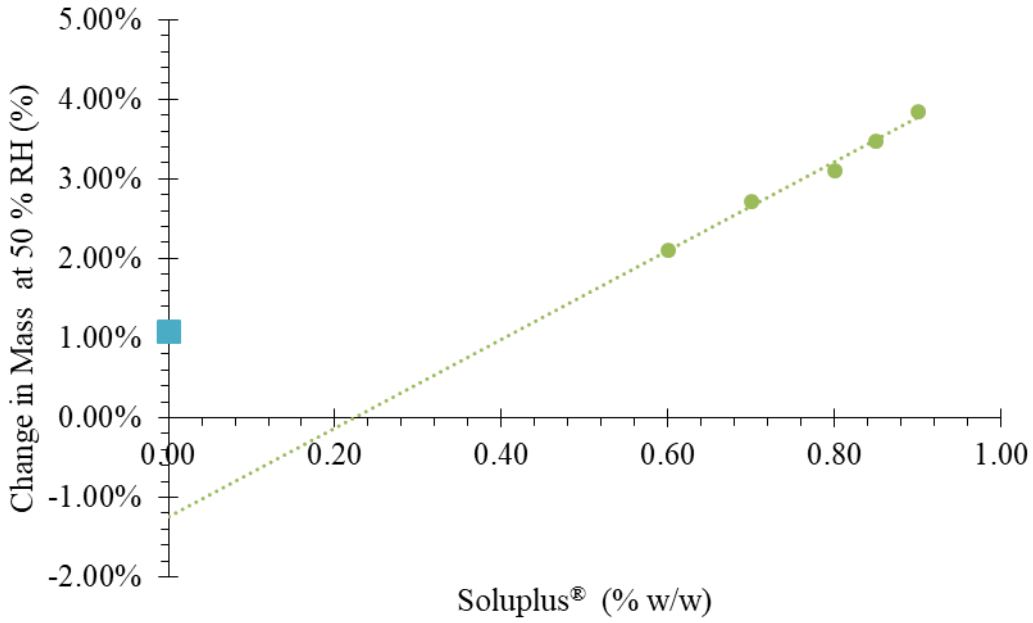

Figure 4.5. Moisture sorption at 50% RH plotted as a function of Soluplus® percentage in formulation. Spray-dried BDP is shown as (■).

4.3.5 Surface composition estimation

The surface composition of the raw, as well as spray-dried drug and polymers, were estimated from XPS peaks and shown in Table 4.2. The surface composition of BDP compared well with both the calculated theoretical atomic percentage as well as other

experimentally-derived measurements (Bouhroum *et al.*, (2010)) reported in literature. While the experimentally-derived surface compositions were similar for that of the raw and spray-dried forms of BDP and PVP K130, there was a noticeable difference between that of raw Soluplus® and spray-dried Soluplus®. A greater percentage of carbon and nitrogen was found on the surface for spray-dried Soluplus® which suggests that a certain degree of surface alteration by the spray-drying process was present.

Table 4.2. Surface Composition (Atomic %) of Raw and Spray-dried Drug and Polymer Components.

Sample	Carbon (%)	Oxygen (%)	Chlorine (%)	Nitrogen (%)
BDP-raw	81.7	15.6	2.7	-
BDP-SD	81.5	16.3	2.2	-
Soluplus®-raw	72.7	27.1	-	0.3
Soluplus®-SD	79.1	15.6	-	5.2
PVP K130-raw	79.5	10.8	-	9.6
PVP K130-SD	79.2	11.7	-	9.2

In Table 4.3, the estimated surface coverage of the spray-dried formulations of drug and polymer can be seen. As can immediately be noted, both polymers dominated the surface coverage, with only minuscule amounts of BDP found on the surface of the particles. Increasing the drug loading only made a small difference in the amount of BDP on the surface of the particles. This surface coverage may explain the increased physical stability of the spray-dried formulations with lower drug loadings, by inhibiting nucleation and re-crystallisation through mechanical obstruction (Priemel *et al.*, (2013)).

Table 4.3. Estimated Surface Coverage (Wt %) of Spray-dried Formulations.

Sample	BDP-SD (%)	Soluplus®-SD (%)	PVP K130-SD (%)
BDP-Soluplus®-10	0.03	99.97	-
BDP-Soluplus®-15	0.14	99.86	-
BDP-Soluplus®-20	0.17	99.83	-
BDP-Soluplus®-30	0.16	99.84	-
BDP-Soluplus®-40	0.41	99.59	-
BDP-PVP K130-20	0.24	-	99.76

4.3.6 Particle morphology and size distribution

The particle size distribution of the spray-dried formulations can be found in Table 4.4. The particle size and span of the spray-dried BDP-Soluplus® formulations were found to be largely similar, due in part that they were all spray-dried with the same conditions. The spray-dried particles were in the respirable range, with the exception of BDP-PVP K130-20, which was found to have a much larger span, with d_{90} of 64.74 µm.

Table 4.4. Volume Particle Size Distribution of Spray-dried Formulations.

Sample	d_{10} (µm)	d_{50} (µm)	d_{90} (µm)	Span (µm)
BDP-SD	1.20 ± 0.07	2.35 ± 0.05	4.62 ± 0.34	1.45
BDP-Soluplus®-10	1.52 ± 0.01	3.00 ± 0.02	5.73 ± 0.05	1.40
BDP-Soluplus®-15	1.38 ± 0.07	2.76 ± 0.06	5.47 ± 0.30	1.48
BDP-Soluplus®-20	1.26 ± 0.11	2.84 ± 0.08	6.11 ± 0.19	1.71
BDP-Soluplus®-30	0.76 ± 0.02	1.47 ± 0.05	2.79 ± 0.19	1.38
BDP-Soluplus®-40	1.09 ± 0.05	2.27 ± 0.04	4.69 ± 0.29	1.59
BDP-PVP K130-20	1.40 ± 0.01	5.80 ± 0.11	64.74 ± 4.39	10.92

The particle morphologies of spray-dried Soluplus®, spray-dried BDP, spray-dried BDP-Soluplus®, spray-dried PVP K130, and spray-dried BDP-PVP K130 formulations can be seen in Figure 4.6. All the spray-dried particles were generally spherical in shape. Spray-dried Soluplus® (Figure 4.6a) had a dimpled and corrugated surface while spray-dried BDP was more spherical, although plate-shaped crystals could be made out on some particles. This is in good agreement with the XRD results where it was observed that

spray-dried BDP was unable to form fully amorphous BDP. The spray-dried BDP-Soluplus® formulations had a similar surface morphology to that of Soluplus®-SD. Some fibres were seen for BDP-PVP K130-20 (Figure 4.6i). These fibres do not appear in all the other formulations and hence can be assumed to be ascribed to PVP K130. Traces of these fibres can also be seen near the top of the left column image for spray-dried PVP K130 (Figure 4.6g). The particles seen in Figure 4.6h were also smaller than the rest with concave saucer-like surfaces. These small particles (< 1 μm) would probably be very cohesive and may aggregate together to account for the large d_{90} values seen for BDP-PVP K130-20.

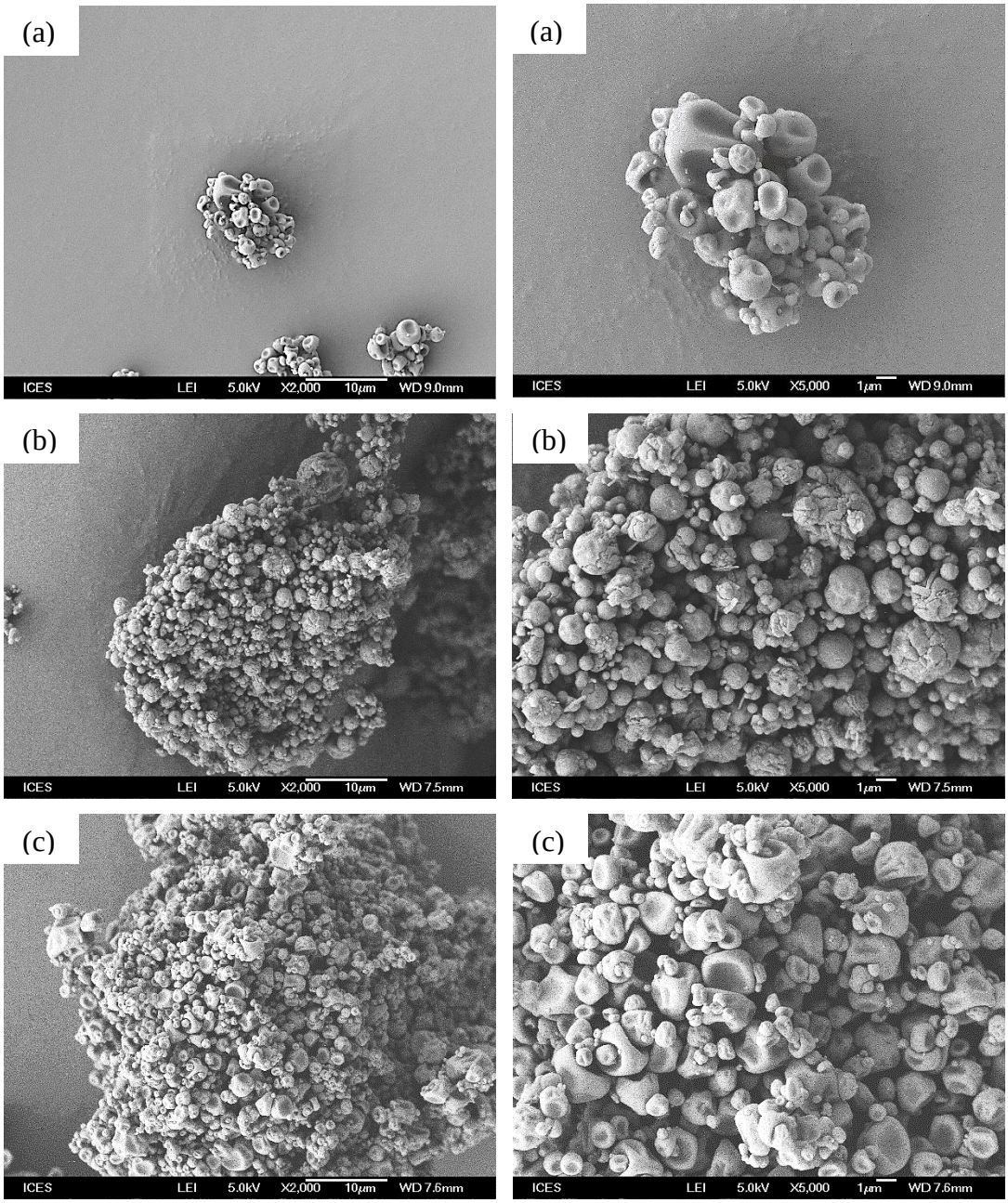

Figure 4.6. Field emission scanning electron micrographs of spray-dried (a) Soluplus®, (b) BDP, (c) BDP-Soluplus®-10, (d) BDP-Soluplus®-15, (e) BDP-Soluplus®-20, (f) BDP-Soluplus®-30, (g) BDP-Soluplus®-40, (h) PVP K130-SD, and (i) BDP-PVP K130-20. Images in the right column are magnifications of those in the corresponding left column. Scale bars of the images in the left column indicate 10 µm and the scale bars of the images in the right column indicate 1 µm.

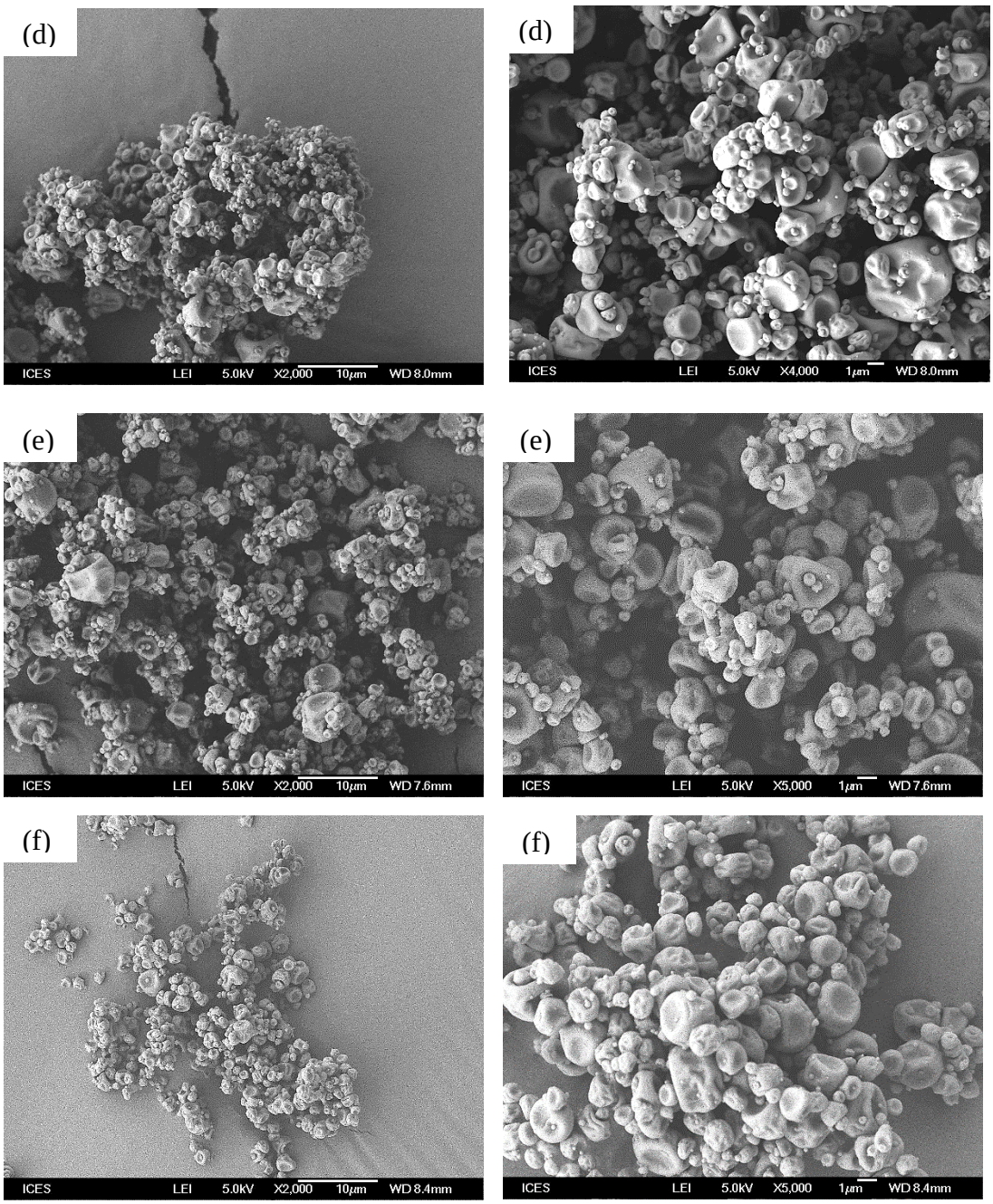

Figure 4.6. Field emission scanning electron micrographs of spray-dried (a) Soluplus®, (b) BDP, (c) BDP-Soluplus®-10, (d) BDP-Soluplus®-15, (e) BDP-Soluplus®-20, (f) BDP-Soluplus®-30, (g) BDP-Soluplus®-40, (h) PVP K130-SD, and (i) BDP-PVP K130-20. Images in the right column are magnifications of those in the corresponding left column. Scale bars of the images in the left column indicate 10 μm and the scale bars of the images in the right column indicate 1 μm.

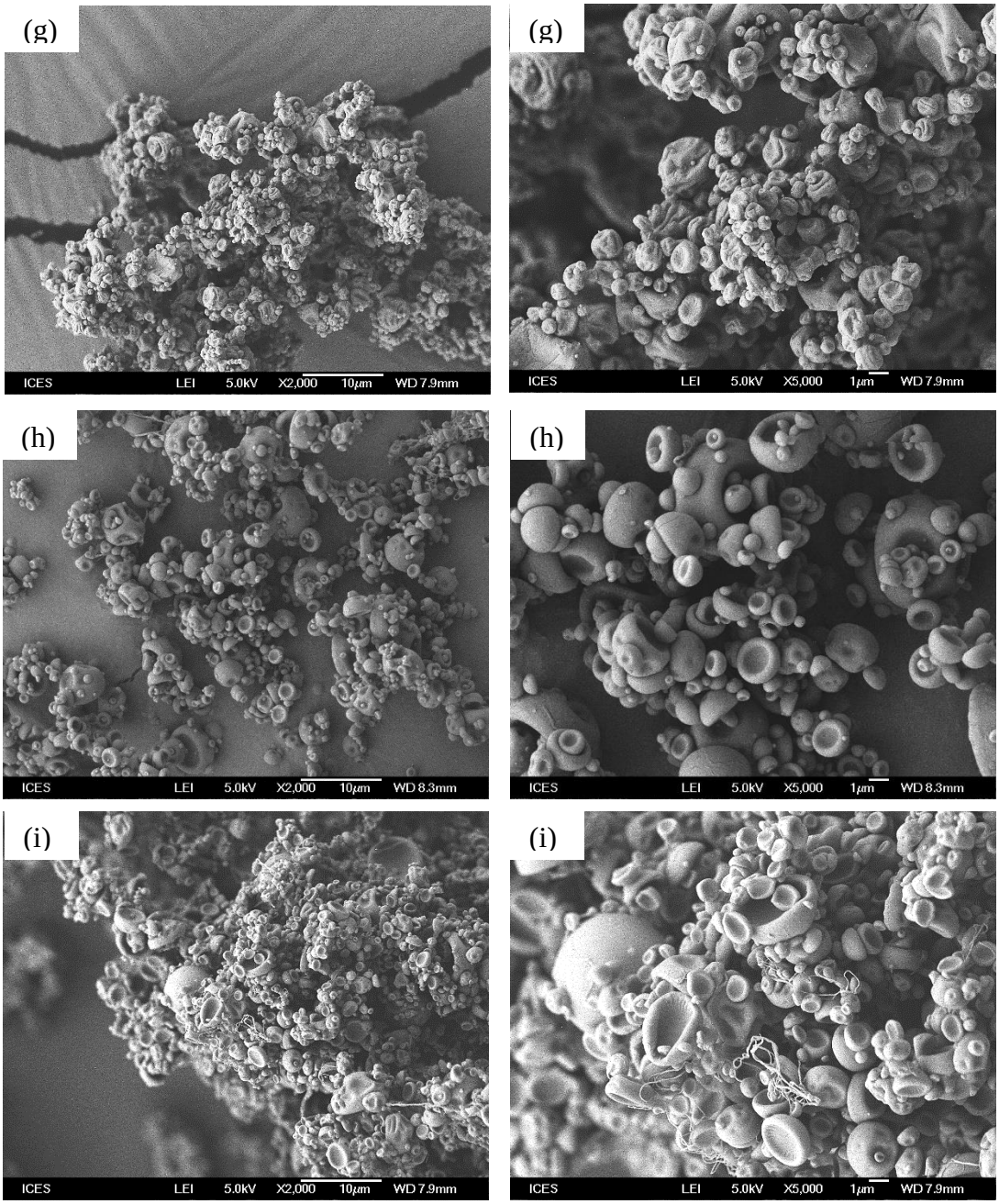

Figure 4.6. Field emission scanning electron micrographs of spray-dried (a) Soluplus®, (b) BDP, (c) BDP-Soluplus®-10, (d) BDP-Soluplus®-15, (e) BDP-Soluplus®-20, (f) BDP-Soluplus®-30, (g) BDP-Soluplus®-40, (h) PVP K130-SD, and (i) BDP-PVP K130-20. Images in the right column are magnifications of those in the corresponding left column. Scale bars of the images in the left column indicate 10 μm and the scale bars of the images in the right column indicate 1 μm.

4.3.7 *In vitro* aerosol performance

The aerosol performance of the spray-dried formulations is shown in Figure 4.7, and

Table 4.5. Spray-dried BDP and spray-dried BDP-Soluplus® formulations all had an FPF of approximately 40%, with a large percentage of particles found in stages 3 and 4, indicating greater deposition in the lower airways. The amount of particles trapped in the device increased for BDP-Soluplus®-30 and BDP-Soluplus®-40, due to the increased cohesive nature of the particles resulting from their smaller particle size, heightening the gap between the FPF and FPF (emitted) for those formulations. It is also worth noting that the FPFs of BDP-Soluplus®-15 and BDP-Soluplus®-20 were higher than that of BDP-SD despite having larger mean particle sizes, suggesting that the collapsed, dimpled surface morphology of the particles seen in Figure 4.6d and Figure 4.6e, may have contributed to an increased aerosolisation ability of the particles, in the same way wrinkled surfaces do (Healy *et al.*, (2014)).

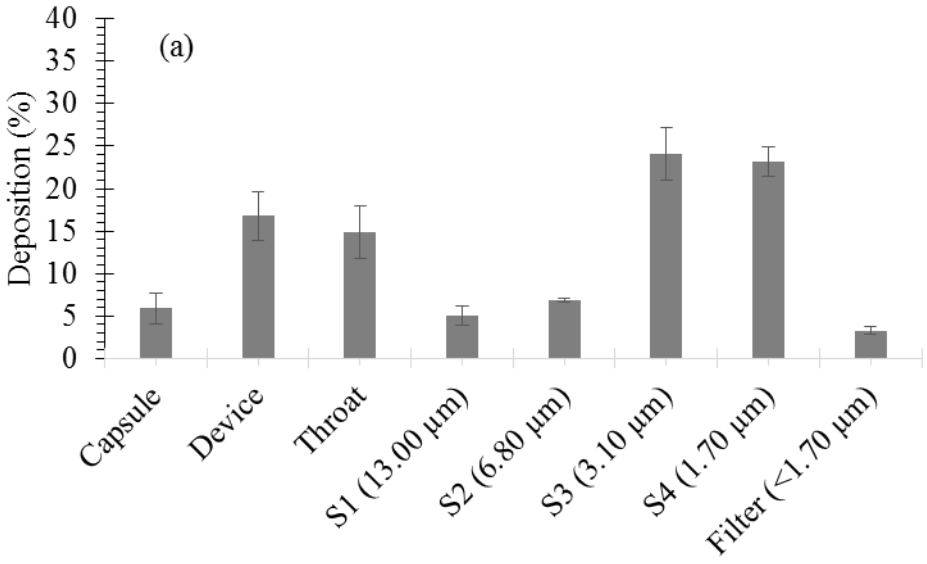

Figure 4.7. *In vitro* deposition of (a) BDP-SD, (b) BDP-Soluplus®-10, (c) BDP-Soluplus®-15, (d) BDP-Soluplus®-20, (e) BDP-Soluplus®-30, (f) BDP-Soluplus®-40, (g) BDP-PVP K130-20. Data presented as mean ± SD (n=3). S1-S4 denote impactor stages, followed by their corresponding lower aerodynamic cutoff diameter in parentheses.

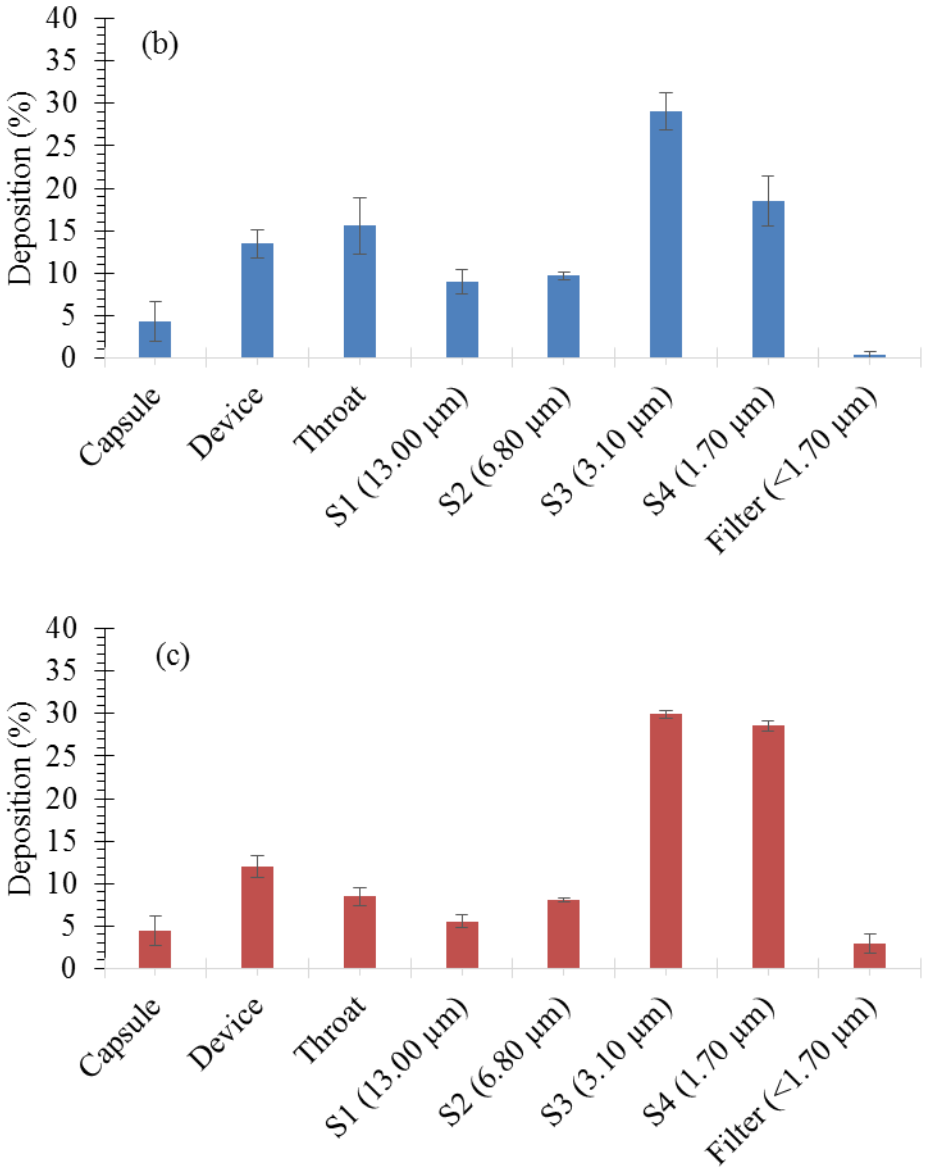

Figure 4.7. *In vitro* deposition of (a) BDP-SD, (b) BDP-Soluplus®-10, (c) BDP-Soluplus®-15, (d) BDP-Soluplus®-20, (e) BDP-Soluplus®-30, (f) BDP-Soluplus®-40, (g) BDP-PVP K130-20. Data presented as mean ± SD (n=3). S1-S4 denote impactor stages, followed by their corresponding lower aerodynamic cutoff diameter in parentheses.

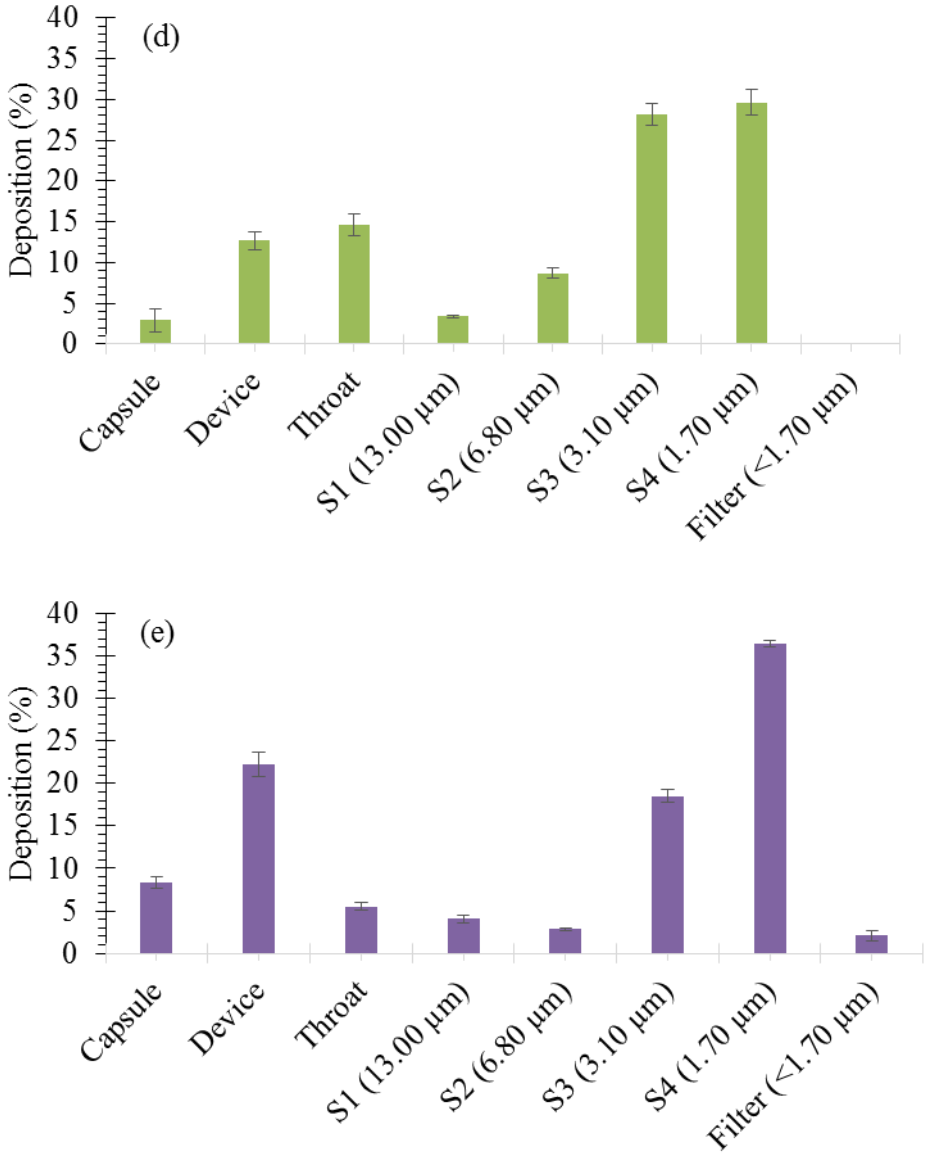

Figure 4.7. *In vitro* deposition of (a) BDP-SD, (b) BDP-Soluplus®-10, (c) BDP-Soluplus®-15, (d) BDP-Soluplus®-20, (e) BDP-Soluplus®-30, (f) BDP-Soluplus®-40, (g) BDP-PVP K130-20. Data presented as mean ± SD (n=3). S1-S4 denote impactor stages, followed by their corresponding lower aerodynamic cutoff diameter in parentheses.

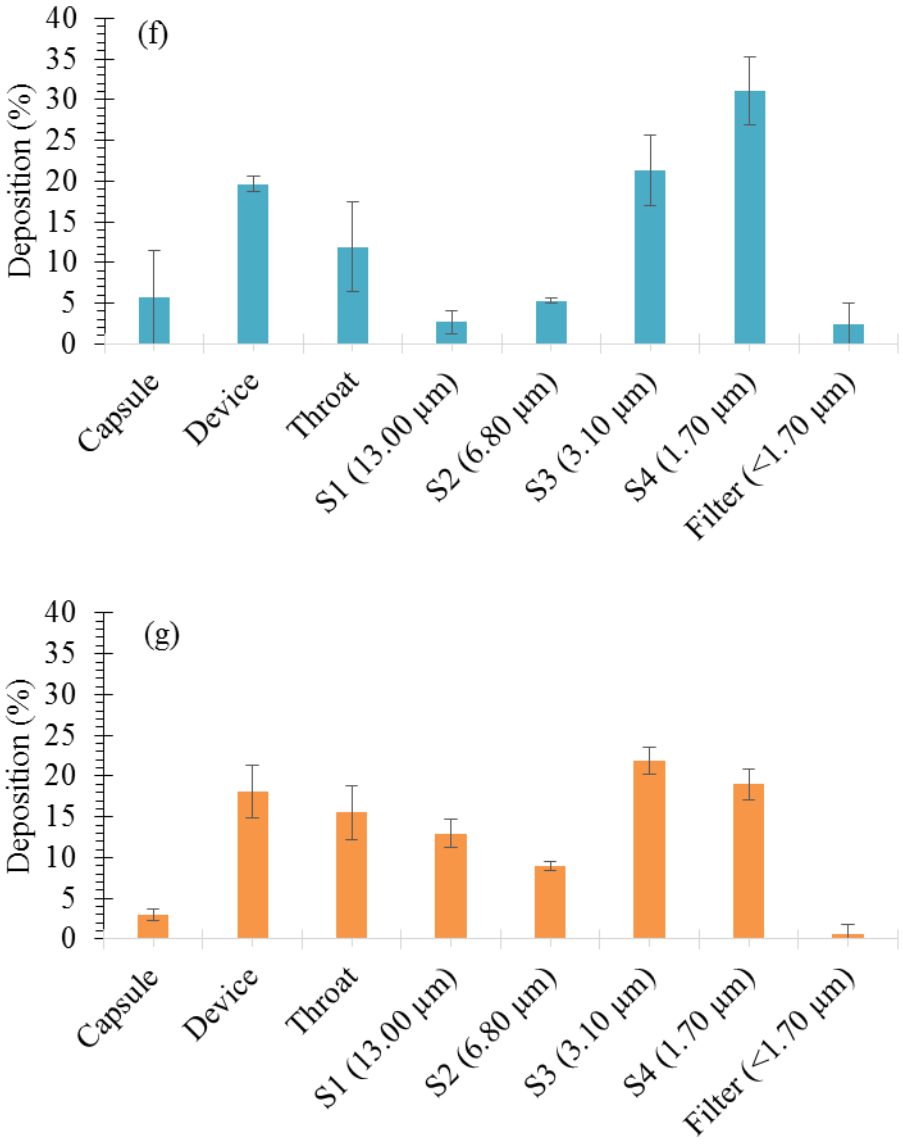

Figure 4.7. *In vitro* deposition of (a) BDP-SD, (b) BDP-Soluplus®-10, (c) BDP-Soluplus®-15, (d) BDP-Soluplus®-20, (e) BDP-Soluplus®-30, (f) BDP-Soluplus®-40, (g) BDP-PVP K130-20. Data presented as mean ± SD (n=3). S1-S4 denote impactor stages, followed by their corresponding lower aerodynamic cutoff diameter in parentheses.

Table 4.5. Deposition Parameters (Mean ± SD, n=3) of Different Formulations Measured

by MSLI.

Sample	FPF (%)	FPF (emitted) (%)
BDP-SD	38.8 ± 3.0	50.2 ± 3.6
BDP-Soluplus®-10	33.8 ± 3.6	41.1 ± 3.6
BDP-Soluplus®-15	46.9 ± 1.2	56.2 ± 0.9
BDP-Soluplus®-20	44.1 ± 1.1	52.2 ± 1.3
BDP-Soluplus®-30	48.0 ± 1.3	70.4 ± 2.8
BDP-Soluplus®-40	44.4 ± 6.2	59.5 ± 5.8
BDP-PVP K130-20	30.8 ± 2.5	39.1 ± 3.6

In Figure 4.8, the relationship between the mean particle size of the spray-dried formulations and their FPF and FPF (emitted) can be studied. There was a very clear relationship between the particle size and the FPF. This suggests that the particles were not likely to be porous or hollow. Porous or hollow particles may have a large geometric diameter measured by laser scattering, but due to their low density, a low MMAD and hence a higher than expected FPF (Edwards *et al.*, (1997)). BDP-PVP K130-20 had poor aerosolisation ability which will doubtless be due, in part, to its large d_{90} values, possibly from agglomerated particles.

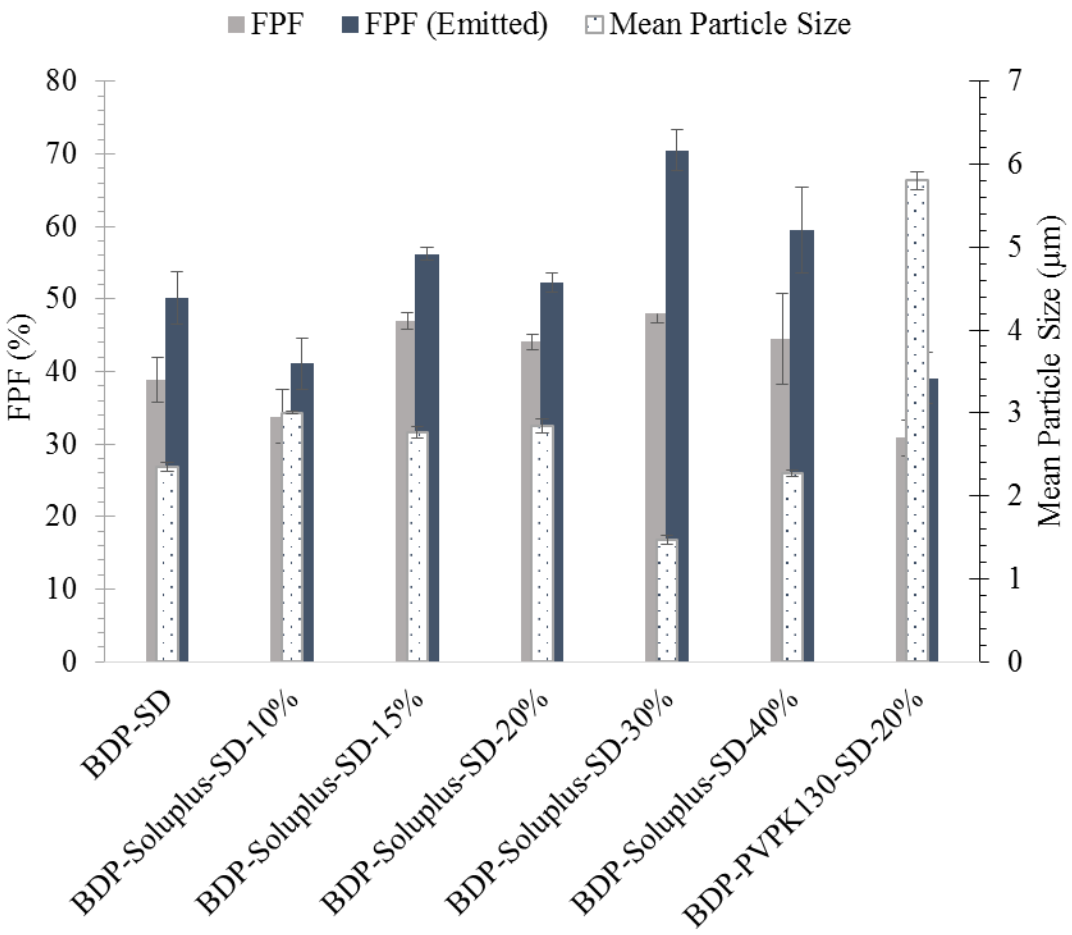

Figure 4.8. FPF and FPF (emitted) of spray-dried formulations overlaid with the mean particle size (secondary axis) of each formulation.

4.3.8 *In vitro* dissolution studies

BDP is a Biopharmaceutical Classification System (BCS) Class II drug with low solubility and high permeability. It is limited by dissolution rate kinetics (Daley-Yates *et al.*, (2001)) and would hence benefit from an increase in solubility for absorption in the lungs.

The dissolution rate profiles of spray-dried BDP-Soluplus® formulations alongside raw BDP, spray-dried BDP and spray-dried BDP-PVP K130 are shown in Figure 4.9. According to the Noyes-Whitney equation (Chapter 1.4, Equation 3 and 4), the rate of dissolution is proportional to the surface area of the solid (Noyes and Whitney, (1897)). As spray-dried BDP had a far lower mean particle size than raw BDP, it should be expected to have a faster dissolution rate than the crystalline drug. However, this cannot be seen in Figure 4.9, with both raw and spray-dried drug having a similarly limited and slow release. With greater Soluplus® content, the dissolution rate and amount dissolved

both increased. This effect is especially marked for BDP-Soluplus®-10 and BDP-Soluplus®-15, while BDP-Soluplus®-20, BDP-Soluplus®-30 and BDP-Soluplus®-40 all had very similar dissolution profiles. BDP-PVP K130-20 had an initial burst release of drug which plateaued after an hour, finally releasing a similarly low amount of BDP as spray-dried and raw BDP. Soluplus® has a low critical micelle concentration (CMC) of 7.6 mg/mL. However, the spray-dried formuliatons were likely unable to form micelles in the USP dissolution apparatus 4 (flow-through cell) cell due to the slow flow rate. Visually, the distinct hue of turbidity apparent after micelle formation was absent. Further tests could be conducted on the aliquots to determine the formation of micelles (using dynamic light scattering) and further, the ability of the micelles to solubilise the drug by testing its crystallinity with small angle x-ray spectroscopy (SAXS).

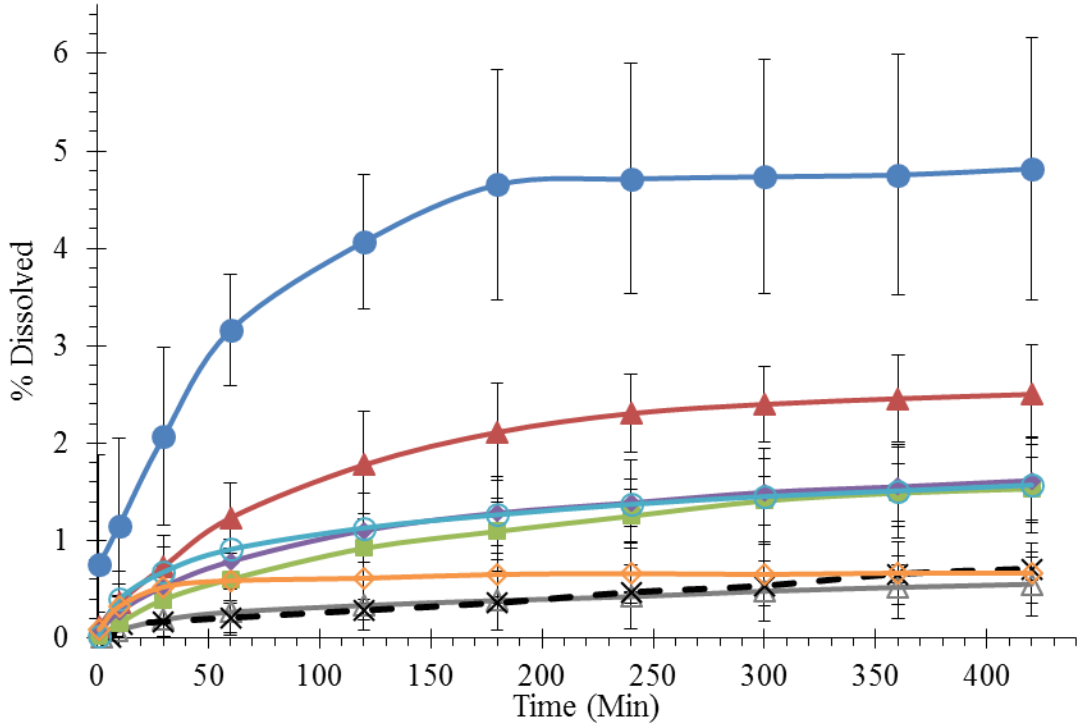

Figure 4.9. *In vitro* dissolution profiles of raw-BDP (△), BDP-SD (✕), spray-dried BDP-Soluplus®-10 (●), BDP-Soluplus®-15 (▲), BDP-Soluplus®-20 (■), BDP-Soluplus®-30 (◆), BDP-Soluplus®-40 (○), BDP-PVP K130-20 (◇).

Although there is still no regulatory approved dissolution test for orally inhaled products, the bioavailability and therapeutic action of inhaled particles are based on the amount of particles that dissolve in the fluid in the respiratory tract (Riley *et al.*, (2012)). Yet, due to the complexity of the human respiratory system, there still does not exist a suitable dissolution testing apparatus to satisfactorily measure the dissolution profile of inhaled products. The USP dissolution apparatus 4 (flow-through cell) is one such apparatus that

has been mooted as a possible candidate for measuring dissolution in the lung. First introduced in 1957 by the FDA (Langenbucher *et al.*, (1989)), the flow-through cell is the preferred dissolution apparatus for measuring the dissolution profile of poorly water-soluble drugs due to its ability to maintain sink conditions in the 'open-loop' configuration, where fresh medium flows over the sample continuously (Fotaki, (2011)). When used in this study, the samples were placed in the middle of the USP dissolution apparatus 4 (flow-through cell) cell, surrounded by 1 mm diamater glass beads. The tight packing of the powder in the cell may have contributed to the formation of an observed viscous gel layer, in which sink conditions may not be present locally. One can conclude that the USP dissolution apparatus 4 (flow-through cell) in this setup is not a good analogue for the lung, nor does it claim or attempt to be. The *in vitro* drug release profiles obtained from the USP dissolution apparatus 4 (flow-through cell) dissolution test give an indication of what the release could be like in the lung, but should not be used to correlate what happens *in vivo*. The lung has a far larger surface area than the USP dissolution apparatus 4 (flow-through cell) cell so the inhaled dose is expected to be much more dispersed and the formation of a gel cake far less likely.

The presence of the viscous gel layer is probably a key reason why so little of the sample is released even after seven hours. This was referred to for a Soluplus®-Budesonide physical mixture in work conducted by Pozzoli *et al.*, (2017). Analysis of the inherent properties of Soluplus® (Shi *et al.*, (2016)) showed that its viscosity increased with temperature in media such as water and PBS, with dramatic increases from 37 °C to 42 °C. The possibility of the formation of strong gel networks at the dissolution test conditions could explain the slow and incomplete release of the loaded drugs, especially at a low flow rate like the one used in this test. Further analysis of the formation of the gel will give a better idea of its effect on drug release. The formation of such a gel network could also give rise to possibilities in forming sustained release formulations (Miyazaki *et al.*, (2009)), once its formation is better understood.

4.3.9 Mathematical models for dissolution profiles

The dissolution profiles of the formulations described in Section 4.3.8 were fitted to commonly used mathematical models and their coefficients of determination are shown in Table 4.6. The spray-dried BDP-Soluplus® formulations were found to fit the Higuchi, Korsmeyer-Peppas and Baker-Lonsdale models well. This suggests that the dissolution process was largely diffusion based from microspheres and with possibly more than one

mode of release mechanism, which describes the system well. BDP-PVP K130-20 did not fit any model particularly well and was best described by the Korsmeyer-Peppas model. It has to be taken in mind that, as mentioned above, the dissolution profiles were not fully resolved by the USP dissolution apparatus 4 (flow-though cell) and while it provided a basis for comparison between formulations, it would not be at all indicative of the actual dissolution process of the powders.

Table 4.6. The Coefficient of Determination of Linear Plots of Most Widely Used Dissolution Profile Mathematical Models.

Sample	Zero Order	First Order	Hixson-Crowell	Higuchi	Baker-Lonsdale	Korsmeyer-Peppas
BDP-raw	0.999	0.999	0.999	0.954	0.911	0.999
BDP-SD	0.968	0.968	0.968	0.970	0.957	0.758
BDP-Soluplus®-10	0.726	0.729	0.728	0.911	0.743	0.961
BDP-Soluplus®-15	0.836	0.838	0.837	0.968	0.919	0.988
BDP-Soluplus®-20	0.907	0.908	0.908	0.993	0.988	0.975
BDP-Soluplus®-30	0.851	0.853	0.852	0.979	0.951	0.983
BDP-Soluplus®-40	0.794	0.795	0.795	0.952	0.905	0.900
BDP-PVP K130-20	0.511	0.512	0.512	0.743	0.240	0.866

4.3.10 Stability studies

One of the foremost concerns regarding spray-dried formulations is that the product is usually amorphous. This constitutes a challenge to the physical stability of the formulations as the amorphous state will tend to the more thermodynamically stable crystalline state with time. This is undesirable in the pharmaceutical field where active ingredients in the amorphous and crystalline form often have very different pharmacokinetic and pharmacodynamic profiles. Especially pertinent for pulmonary delivery, the surface characteristics of spray-dried powders have a sizeable influence on the FPF. Re-crystallisation of spray-dried particles could affect the particle surface and hence its FPF (Maa *et al.*, (1998)).

The stability tests for the spray-dried formulations as well as cryo-milled BDP and physically mixed BDP-Soluplus® at accelerated storage conditions of 40 °C and 75% RH

are shown in Figure 4.10. As noted earlier, most formulations were amorphous immediately after formulation with the exception of BDP-SD (Figure 4.10a). The micro-peaks present in the fresh BDP-SD sample developed into peaks with greater intensity and definition within a day of storage at the accelerated stress test conditions. Similarly, for BDP-CM (Figure 4.10h), well-defined crystalline peaks developed within just two days of storage at accelerated stress test conditions.

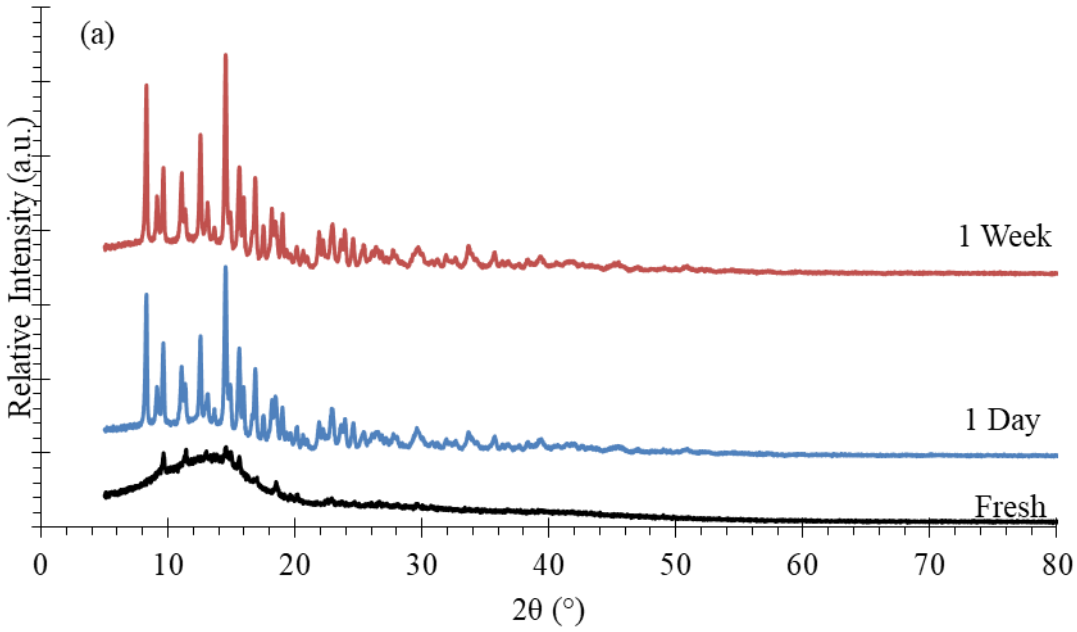

Figure 4.10. X-ray diffractograms of spray-dried BDP formulations after storage at accelerated stress test conditions of 40 °C/75% RH for up to nine months. (a) BDP-SD, (b) BDP-Soluplus®-10, (c) BDP-Soluplus®-15, (d) BDP-Soluplus®-20, (e) BDP-Soluplus®-30, (f) BDP-Soluplus®-40, (g) BDP-PVP K130-20, (h) Cryo-milled BDP, (i) Physically mixed 20% (w/w) BDP-CM and 80% (w/w) Soluplus®.

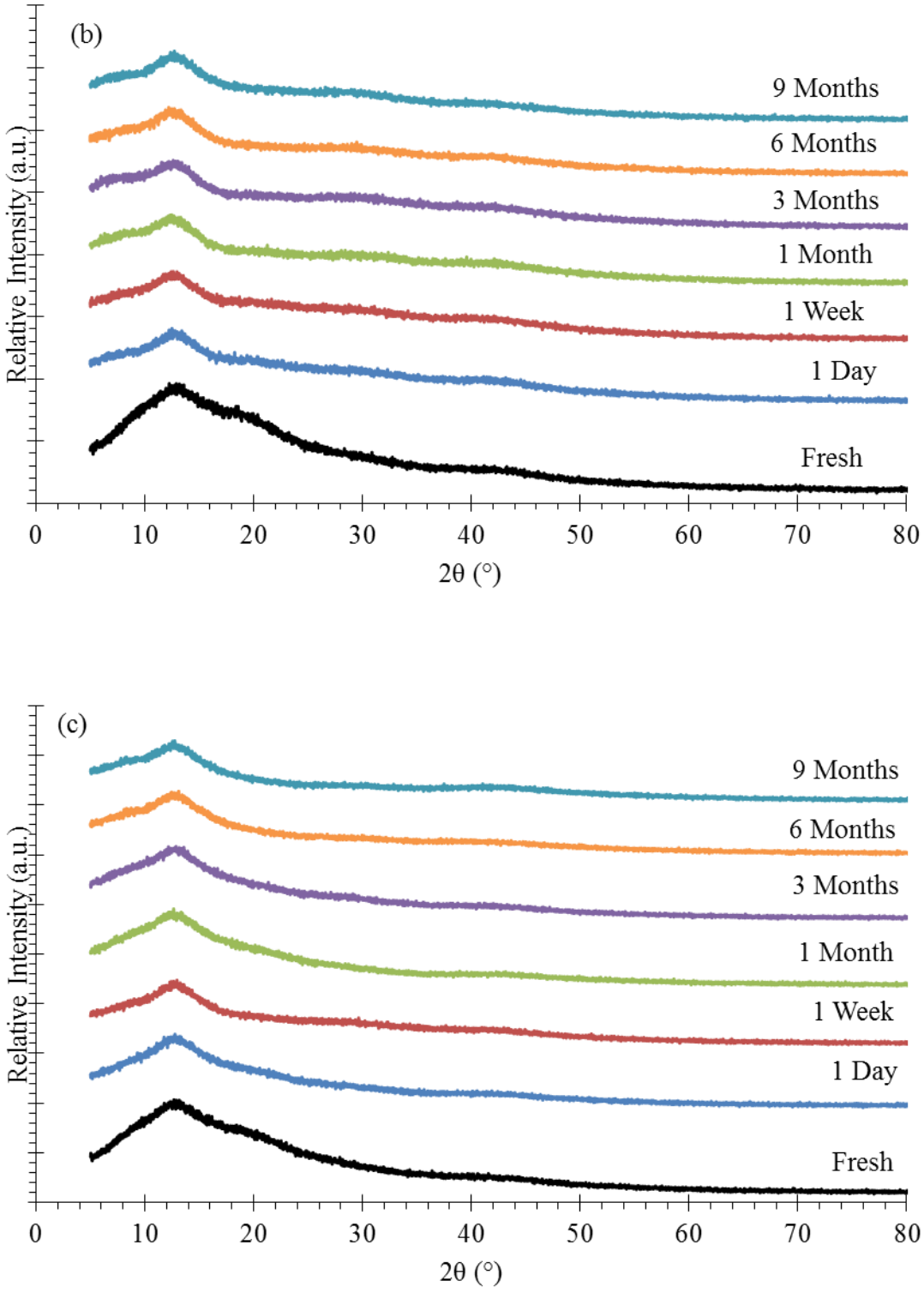

Figure 4.10. X-ray diffractograms of spray-dried BDP formulations after storage at accelerated stress test conditions of 40 °C/75% RH for up to nine months. (a) BDP-SD, (b) BDP-Soluplus®-10, (c) BDP-Soluplus®-15, (d) BDP-Soluplus®-20, (e) BDP-Soluplus®-30, (f) BDP-Soluplus®-40, (g) BDP-PVP K130-20, (h) Cryo-milled BDP, (i) Physically mixed 20% (w/w) BDP-CM and 80% (w/w) Soluplus®.

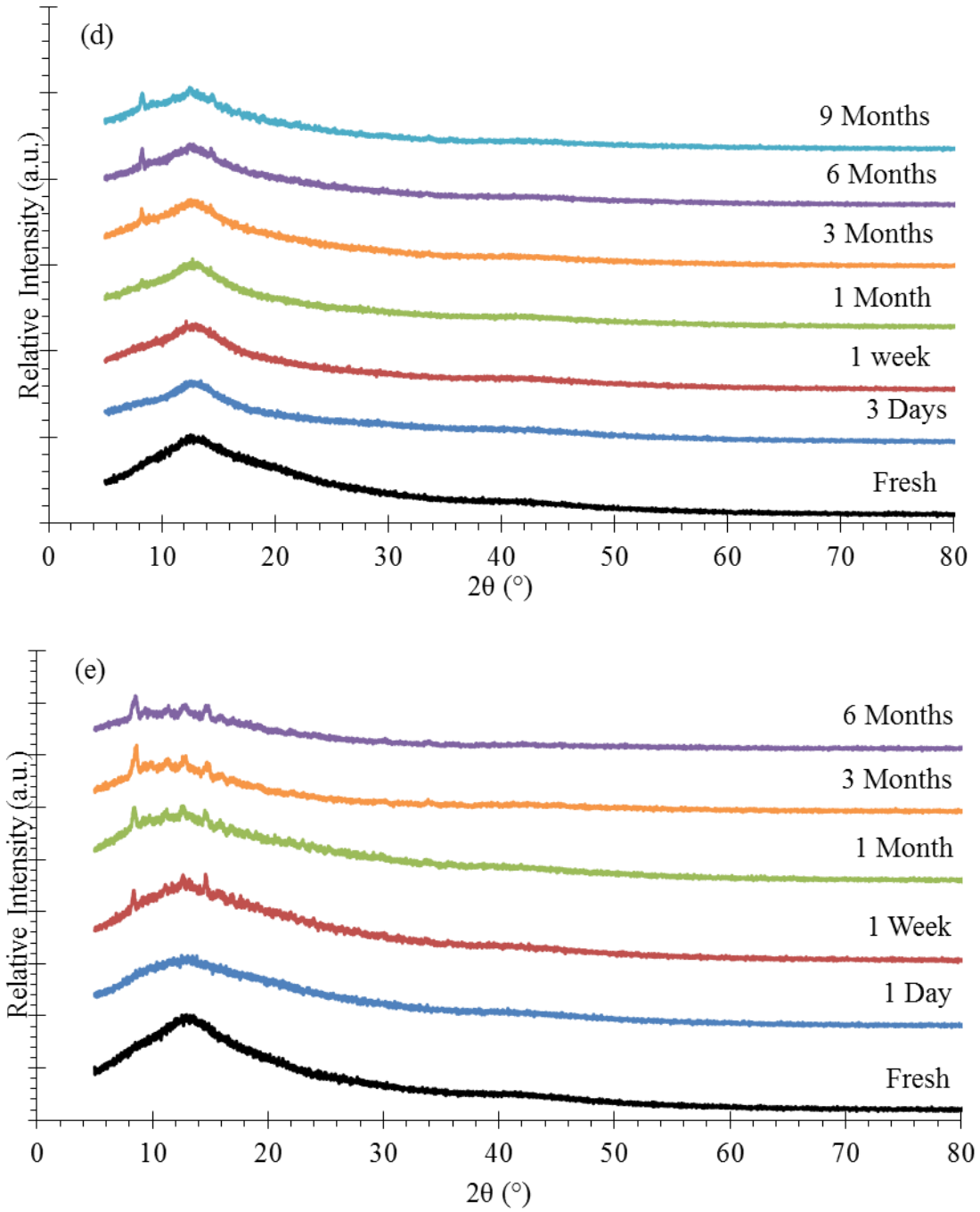

Figure 4.10. X-ray diffractograms of spray-dried BDP formulations after storage at accelerated stress test conditions of 40 °C/75% RH for up to nine months. (a) BDP-SD, (b) BDP-Soluplus®-10, (c) BDP-Soluplus®-15, (d) BDP-Soluplus®-20, (e) BDP-Soluplus®-30, (f) BDP-Soluplus®-40, (g) BDP-PVP K130-20, (h) Cryo-milled BDP, (i) Physically mixed 20% (w/w) BDP-CM and 80% (w/w) Soluplus®.

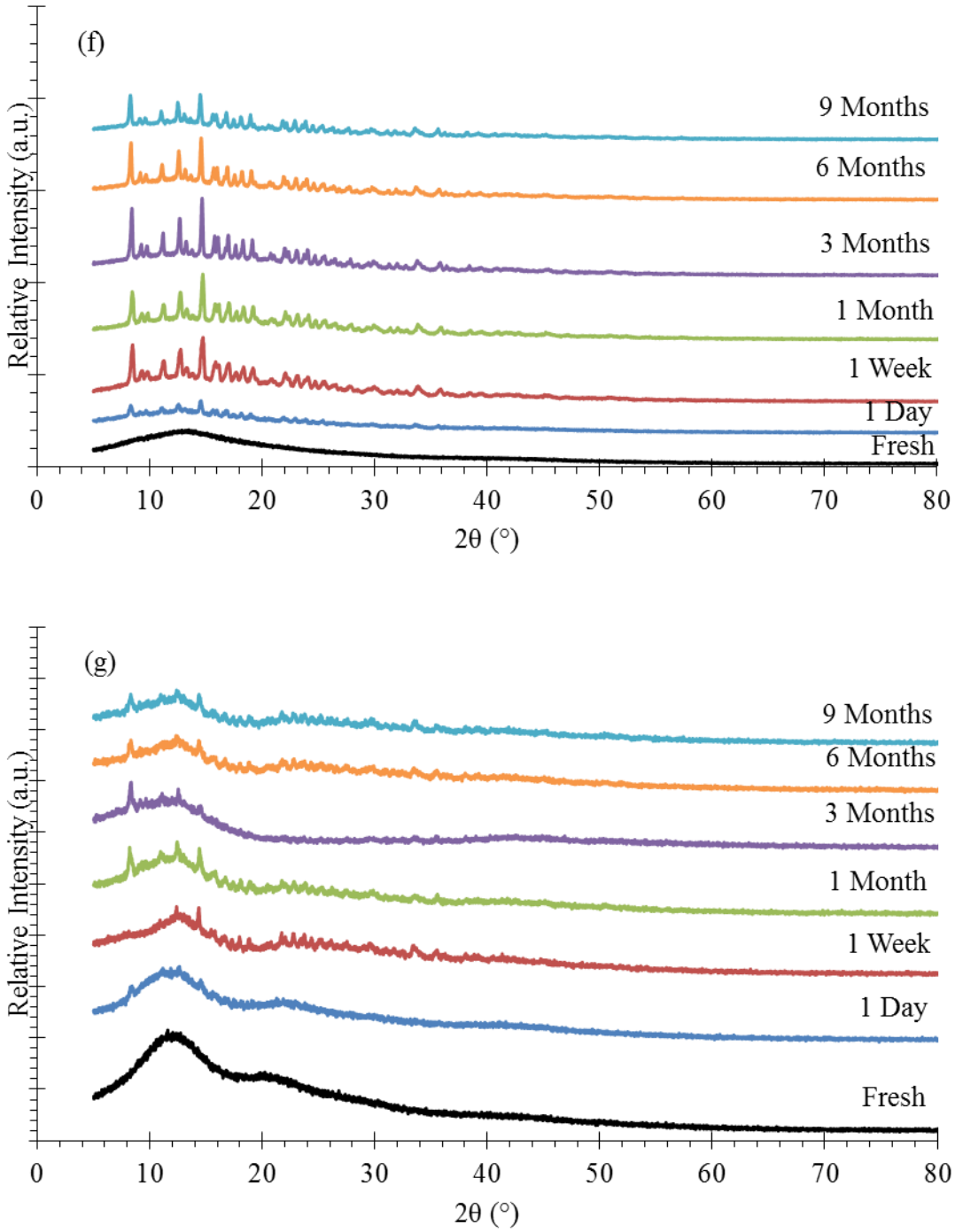

Figure 4.10. X-ray diffractograms of spray-dried BDP formulations after storage at accelerated stress test conditions of 40 °C/75% RH for up to nine months. (a) BDP-SD, (b) BDP-Soluplus®-10, (c) BDP-Soluplus®-15, (d) BDP-Soluplus®-20, (e) BDP-Soluplus®-30, (f) BDP-Soluplus®-40, (g) BDP-PVP K130-20, (h) Cryo-milled BDP, (i) Physically mixed 20% (w/w) BDP-CM and 80% (w/w) Soluplus®.

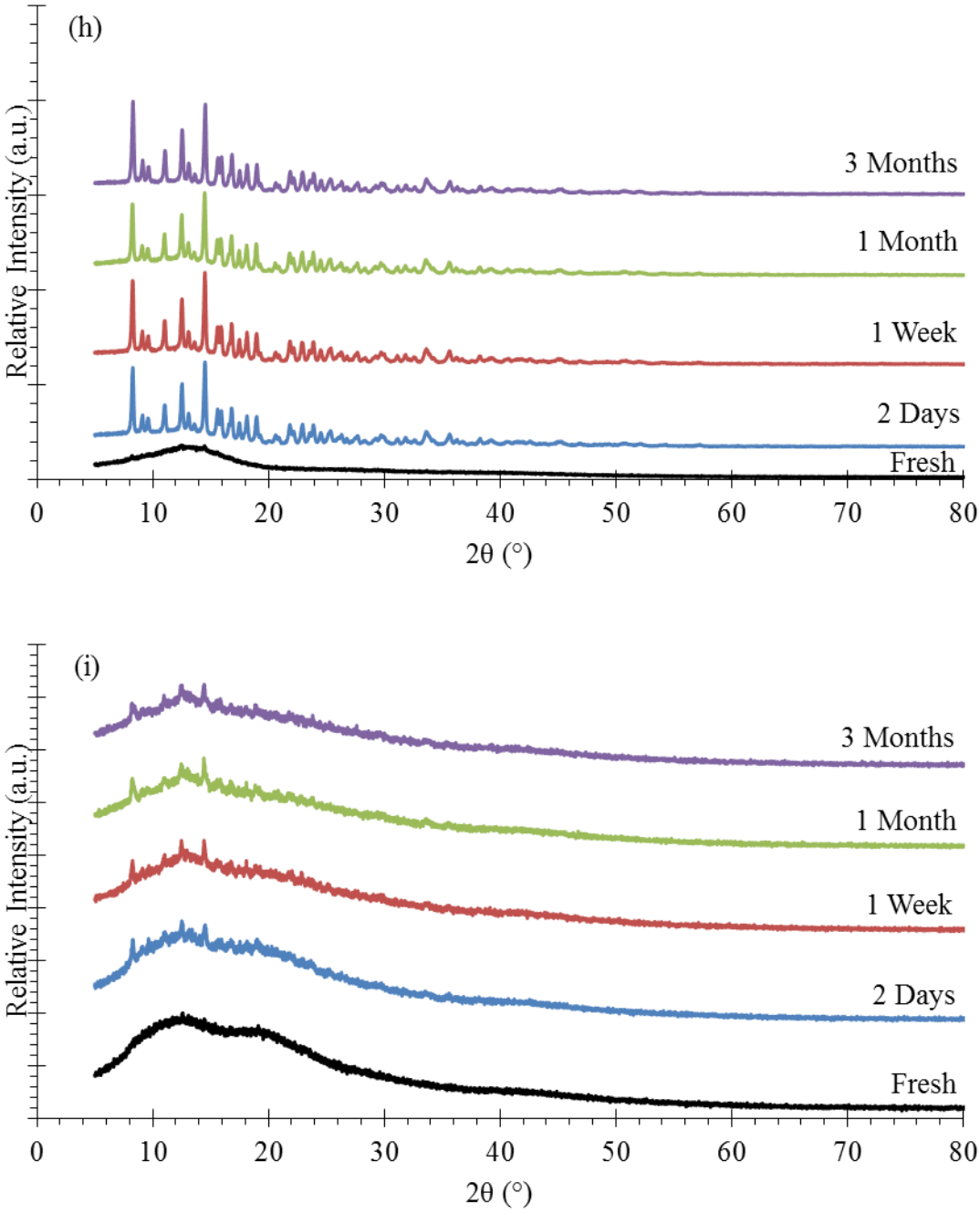

Figure 4.10. X-ray diffractograms of spray-dried BDP formulations after storage at accelerated stress test conditions of 40 °C/75% RH for up to nine months. (a) BDP-SD, (b) BDP-Soluplus®-10, (c) BDP-Soluplus®-15, (d) BDP-Soluplus®-20, (e) BDP-Soluplus®-30, (f) BDP-Soluplus®-40, (g) BDP-PVP K130-20, (h) Cryo-milled BDP, (i) Physically mixed 20% (w/w) BDP-CM and 80% (w/w) Soluplus®.

For the co-spray dried BDP-Soluplus® samples, physical stability decreased with increasing drug loading. At 40% (w/w) drug loading (BDP-Soluplus®-40, Figure 4.10f), small peaks started appearing in the X-ray diffractogram after one day, which developed into well-defined crystalline peaks by one week. Peaks appeared for BDP-Soluplus®-30

(Figure 4.10e) after a week and a single peak at ~ 8° started manifesting for BDP-Soluplus®-20 after a month. BDP-Soluplus®-10 and BDP-Soluplus®-15 remained X-ray amorphous for the entire six-month duration of the accelerated stability study. By contrast, the physically mixed sample of amorphous cryo-milled BDP and raw Soluplus® started re-crystallising after just one day at accelerated storage conditions.

BDP-PVP K130-20 started re-crystallising after just one day, compared to a month for BDP-Soluplus®-20. Small peaks appeared after a day at accelerated stress test conditions and developed over a month into a series of peaks compared to the single peak at ~8° for BDP-Soluplus®-20, suggesting that PVP K130 is unable to stabilise amorphous BDP to the degree that Soluplus® can.

As mentioned earlier, re-crystallisation brings about changes in the morphology and particle surface which could be detrimental to its aerosolisation ability, as well as removing the dissolution rate enhancement that the amorphous form brings. The results show that high temperature and humidity affect the physical stability of the formulations. However, this could be mitigated using moisture-protective blister packaging.

4.4 Conclusions

The viability of Soluplus® as an excipient for formulating poorly water-soluble BDP for pulmonary delivery was investigated. While amorphous BDP was difficult to obtain through spray-drying or cryo-milling, co-spray dried BDP-Soluplus® were able to form amorphous powders easily. These co-spray dried formulations were able to achieve high entrapment efficiencies and yields and were also X-ray amorphous at accelerated stress test conditions up to a drug loading of 15% (w/w). The co-spray dried formulations were of a respirable size (d_{50} ~ 2.5 µm) and achieved FPFs of up to 48%. The amorphous, co-spray dried BDP-Soluplus® powders were able to achieve up to 2X faster dissolution rate with 7X more BDP released although the USP dissolution apparatus 4 (flow-through cell) was not able to fully investigate the dissolution behaviour of the powders. It was hypothesised that a gel was formed due the high hydrophilicity of Soluplus, and diffusion through the gel layer competed with the dissolution rate enhancement that the amorphous form of BDP embodies. The co-spray dried BDP-Soluplus® powders were compared with another commonly used hydrophilic excipient for stabilising amorphous substances, PVP. The co-spray dried BDP-PVP powder was unable to display the same narrow particle size distribution, FPF, dissolution rate enhancement and physical stability as the similarly

loaded co-spray dried BDP-Soluplus®. Co-spray dried BDP-Soluplus® has shown potential to be a possible viable formulation for poorly water-soluble drugs for pulmonary delivery, however, further studies should be conducted about the gel-forming behaviour of Soluplus® and its suitability for use as a sustained release excipient instead.

Small angle X-ray scattering (SAXS) could be used to study the formation of this gel and help in the identification of steps to minimise its formation and also to confirm that the gel is indeed responsible for the limited release of active ingredient for the dissolution test. A flow-through sample holder could be a suitable setup, albeit one that is only able to perform at room temperature.

5 PRELIMINARY TERAHERTZ TIME-DOMAIN SPECTROSCOPY ON PREDICTING THE CRYSTALLISATION OF AMORPHOUS FORMULATIONS

5.1 Predicting crystallisation of amorphous formulations

5.1.1 Introduction

It is clear that particle engineering has a large part to play in the formulation of dry powder particles for inhalation. As a facile, one-step process suitable for drying solutions and suspensions into dry particles, spray drying is an invaluable technique for formulating dry powder particles for inhalation (Seville *et al.*, (2007); Vehring, (2008)). One of the main attractions of spray drying as a manufacturing technique is that it is a scalable process

which provides the user control over the particle size, size distribution, morphology, moisture content and surface properties of the powders by tuning the spray drying temperature, aspirator flow rate, atomising gas flow rate and the feed flow rate of the stock solution into the spray dryer. Indeed, spray-drying is used for many other diverse applications such as food production (milk powders, instant coffee), catalyst supports and paint pigment production.

One of the foremost concerns regarding spray-dried formulations is that the product is usually amorphous. This constitutes a challenge to the physical stability of the formulations as the amorphous state will tend to the more thermodynamically stable crystalline state with time. This is undesirable in the pharmaceutical field where active ingredients in the amorphous and crystalline form often have very different pharmacokinetic and pharmacodynamic profiles. Amorphisation is a key strategy in the formulation of poorly water-soluble drugs, with the bioavailability enhancement that the metastable amorphous form brings. Especially pertinent for pulmonary delivery, the surface characteristics of spray-dried powders have a sizeable influence on the FPF. Re-crystallisation of spray-dried particles could affect the particle surface and hence its FPF (Maa *et al.*, (1998)).

According to the World Health Organization (WHO)'s guidelines for the "Stability testing of active pharmaceutical ingredients and finished pharmaceutical products" (*WHO Stability Guide Annex 2 Stability testing of active pharmaceutical ingredients and finished pharmaceutical products*, (2009)), stability testing at stress test conditions usually involves storing the pharmaceutical product at storage conditions that test its thermal stability and (if necessary) its moisture sensitivity. At regular intervals up to six months in duration, the samples have to be tested to determine if "significant change" has occurred in the key attributes of the product that may "affect its quality, safety and/or efficacy". These tests can take up to a year to conduct and constitute a large part of the characterisation of a new pharmaceutical product formulation.

Molecular motions are one of the mechanisms in the crystallisation of amorphous solids. Primary (α) and secondary (β) relaxations both take place for amorphous compounds and of particular interest are the Johari-Goldstein (JG) β-relaxations, which are a peak in mechanical or dielectric loss at a particular frequency. These relaxations are typically observed using dielectric spectroscopy, although recent studies have shown that neutron and light scattering (Ngai, (2004); Sokolov *et al.*, (2001)), as well as terahertz time-domain spectroscopy (THz-TDS), are also sensitive to changes in molecular dynamics.

In their study of amorphous polyalcohols, Sibik *et al.* found three features in the dielectric losses shown in Figure 5.1. The vibrational density of states (VDOS) peak is noted at temperatures below T_g and is independent of temperature. The origins of this peak are due to libration-vibration (rotating slightly back and forth) motions which can be found in disordered solids but not in crystals. When T was between ~0.67 T_g and T_g, a temperature-dependent β-relaxation could be observed. This was mainly ascribed to JG β-relaxation. α-relaxation processes were found above T_g. The paper also described that changes in the hydrogen-bonding of the samples played a role in the thermal related changes of the α and β-relaxations. Recently, Sibik *et al.*, 2015 were able to demonstrate that the three temperature regimes displayed for amorphous polyalcohols were also present in amorphous drug molecules.

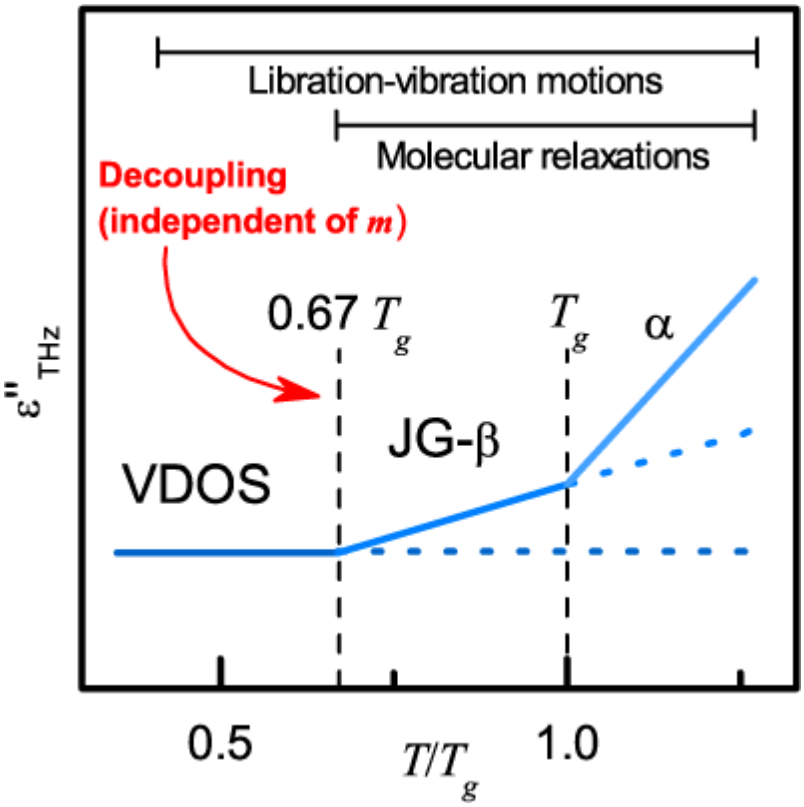

Figure 5.1. Schematic of the thermal decoupling of the molecular relaxation processes from the VDOS or microscopic peak, in supercooled hydrogen-bonded liquids (Used with permission from Sibik *et al.*, 2014).

It is traditionally believed that storing amorphous systems at temperatures below their T_g, and at low humidty will reduce the risk of recrystallisation. The Kauzmann temperature, roughly estimated as T_g – 50 °C (Hancock *et al.*, (1995); Hancock and Zografi, (1997); Zhou *et al.*, (2002)), was assumed to be a temperature below which amorphous systems would be stable (Kauzmann, (1948)). However, it is now known that, even at those

temperatures, there may be sufficient molecular mobility, which results from JG-*β* relaxation (Bhattacharya and Suryanarayanan, (2009); Grzybowska *et al.*, (2010); Hikima *et al.*, (1999); Okamoto and Oguni, (1996)), for the systems to crystallise.

While these relaxations are typically observed using methods such as dielectric spectroscopy, recently, Sibik *et al.*, 2015 described using THz-TDS as a technique to predict crystallisation of amorphous drugs, given its ability to accurately measure the onset of local mobility in an amorphous system. When comparing between different amorphous systems, the study established a correlation between the thermal gradient of terahertz absorption and the physical stability of the samples (Figure 5.2). It was found that the greater the thermal gradient between the temperature range of $T_{g\beta}$ and $T_{g\alpha}$, the greater the contribution of local mobility which may facilitate crystallisation, and hence, the poorer the physical stability of the system.

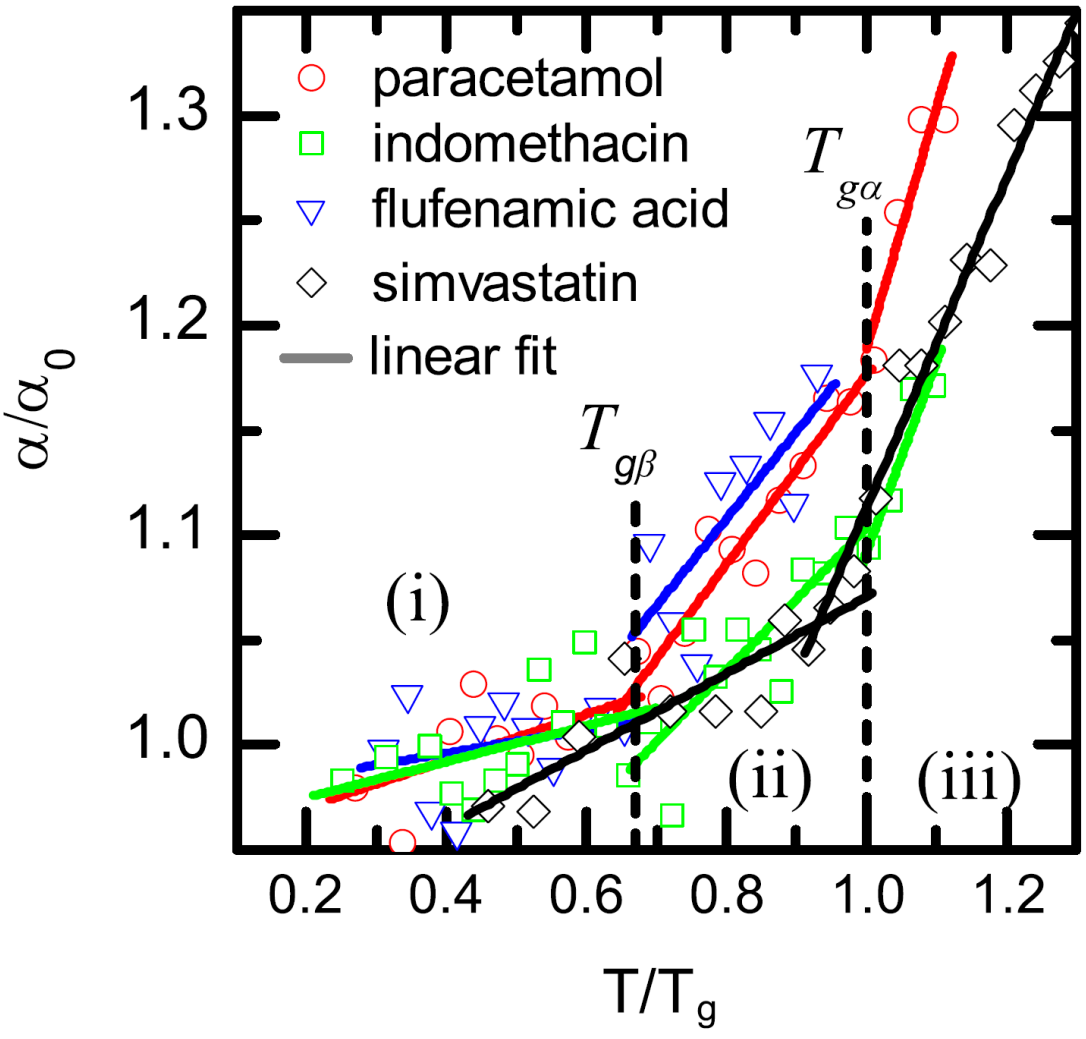

Figure 5.2. Absorption of amorphous paracetamol, flufenamic acid, indomethacin and simvastatin at 1.0 THz. For each sample the absorption coefficient, α, is rescaled by its low temperature average α_0. The temperature is rescaled by T_g (=$T_{g\alpha}$) and the solid lines represent linear fits. Paracetamol and flufenamic acid both exhibit a large increase in absorption upon heating between $T_{g\beta}$ and $T_{g\alpha}$. They are highly unstable and recrystallise within a few minutes at ambient conditions. In contrast, simvastatin shows only a small increase in terahertz absorption upon heating between $T_{g\beta}$ and $T_{g\alpha}$ and remains amorphous for over 220 days under ambient conditions. Indomethacin represents an intermediate case, staying stable for about 7 days before recrystallisation (Used with permission from (Sibik and Zeitler, (2016)).

This method offers a useful complementary technique, which is also more cost effective and easier to use than methods such as neutron and light scattering (Sibik and Zeitler, (2016)), to predict the physical stability of APIs, giving an insight into the molecular dynamics that underpin this. It could be utilised as a "first-pass" test to screen drugs for their physical stability before expanding research on the more promising candidates. However, the study only performed studies on pure drug particles whereas a typical commercial product will contain several other excipients together with the active ingredient.

Here, we tried to build on that work by testing the spray-dried hybrid formulations of CS, BSA and PVA examined in Chapter 2.8.1 with the THz-TDS system. This pulmonary drug delivery system, with two different excipients, is a more accurate analogue for a commercially available pharmaceutical product. In this study, THz-TDS was used to predict the stability of these pulmonary delivery systems to investigate its applicability as a part of the stability testing regime for pharmaceutical products.

5.1.2 Materials and Methods

5.1.2.1 Materials

CS was supplied by Sanofi-Aventis (Paris, France) while PVA (MW 88,000) was supplied by Tokyo Chemical Industry Co. Ltd (Tokyo, Japan). BSA was procured from Sigma-Aldrich (St. Louis, MO, USA). Potassium dihydrogen phosphate (Alfa-Aesar, Ward Hill, MA, USA) and sodium hydroxide (Merck KGaA, Darmstadt, Germany) were used to make pH 7.4 phosphate buffer solution (PBS). All water used throughout was

purified *via* reverse osmosis by an ELGA PURELAB Option-Q (Veolia Water, Paris, France) purification system.

5.1.2.2 Methods

5.1.2.2.1 Preparation of amorphous pulmonary drug delivery systems

Formulation 1 (CS-SD), Formulation 2 (CS/BSA-50/50-SD), Formulation 3 (CS/PVA-50/50-SD), Formulation 4 (CS/BSA/PVA-20/64/16-SD), Formulation 8 (CS/BSA/PVA-50/25/25-SD), Formulation 9 (CS/BSA/PVA-80/10/10-SD) from Chapter 2.8.1 were analysed in this study. Details of their preparation were shown in Section 3.2.2.1.

5.1.2.2.2 Powder X-ray diffraction (XRD)

Powder X-ray diffractograms were obtained for the co-spray dried particles prior to THz-TDS analysis using an X-ray diffractometer (D8 ADVANCE, Bruker Corporation, Madison, WI, USA) in steps of 0.05° using Cu Kα radiation as the X-ray source. The measurement conditions were as follows: target, Cu; filter, Ni; voltage, 40 kV; current, 40 mA; scanning speed, 7.5°/min

5.1.2.2.3 Stability testing

The co-spray dried powders were stored under the same conditions as for the BDP samples detailed in Section 4.2.2.5.

5.1.2.2.4 Determination of glass transition temperature

The thermal profile of the powders was determined by DSC and MDSC. Experiments were conducted on a TA Instruments Q2000 Differential Scanning Calorimeter (New Castle, DE, USA). Approximately 3-5 mg of powder was placed into a Tzero® aluminium pan and a lid was crimped on. An empty pan was used as reference. Measurements were taken in DSC mode with a heating rate of 10 °C/min, and in modulation mode with a heating rate of 5 °C/min, and modulation of ± 0.5 °C every 100s. T_g was determined by analysing the reversing heat flow signal.

5.1.2.2.5 Temperature controlled terahertz time-domain spectroscopy (THz-TDS)

The THz-TDS setup used is a standard transmission spectrometer that makes use of a

wide gap photoconductive antenna to generate THz pulses and a ZnTe crystal for electro-optic detection (Figure 5.3).

(a)

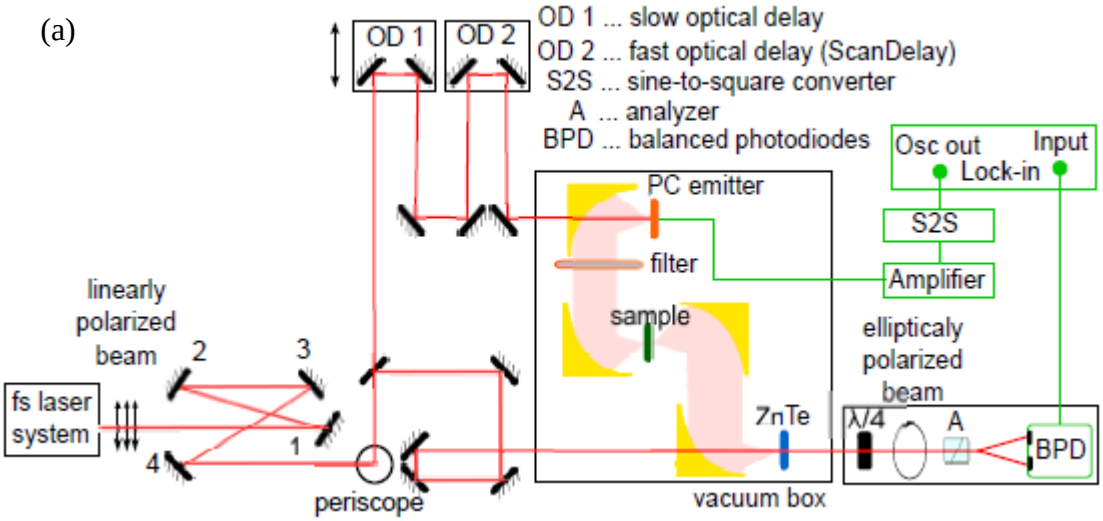

(b)

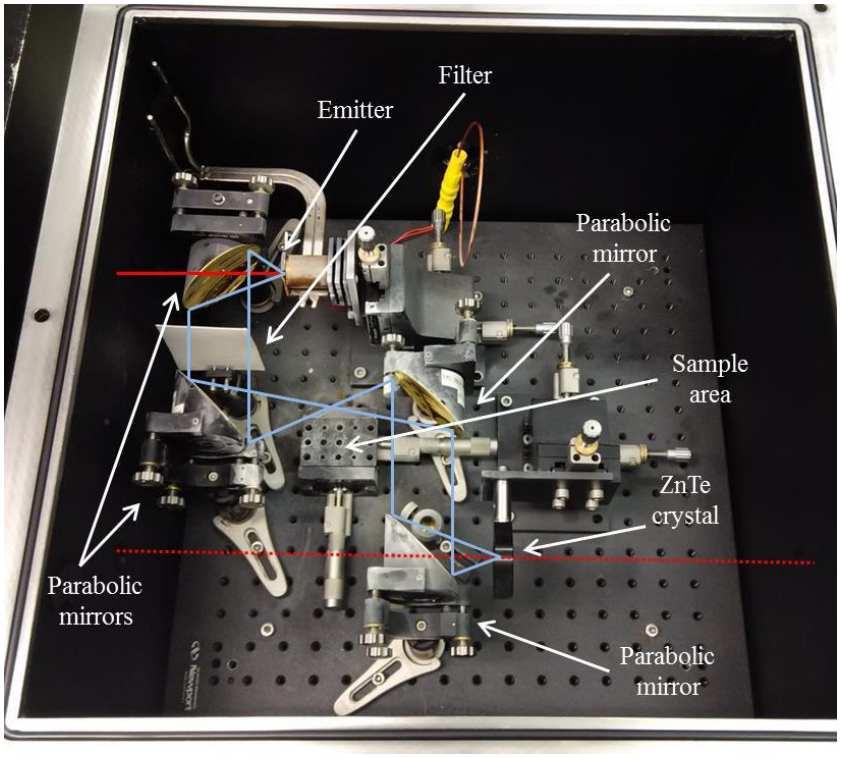

Figure 5.3. (a) Schematic and (b) image of the THz-TDS setup used. Solid and dashed red lines represent optical pump and probe laser beams respectively. Blue lines represent terahertz beam.

The variable temperature measurements were carried out using a modified Janis ST-100 FTIR cryostat (Janis, Wilmington, USA; Figure 5.4). The cryostat was secured through an opening in the lid of the sample chamber and was cooled with a continuous flow of liquid nitrogen. Before cooling the cryostat, the sample chamber was evacuated with a

vacuum pump to 2 mbar. The temperature was monitored by a Lakeshore 331 temperature controller (Lakeshore, Westerville, USA) and was measured with a thermocouple and a silicon diode which was attached to the end of the cold finger of the cryostat. Heating was also achieved using the temperature controller which was attached to cartridge heaters on the cryostat.

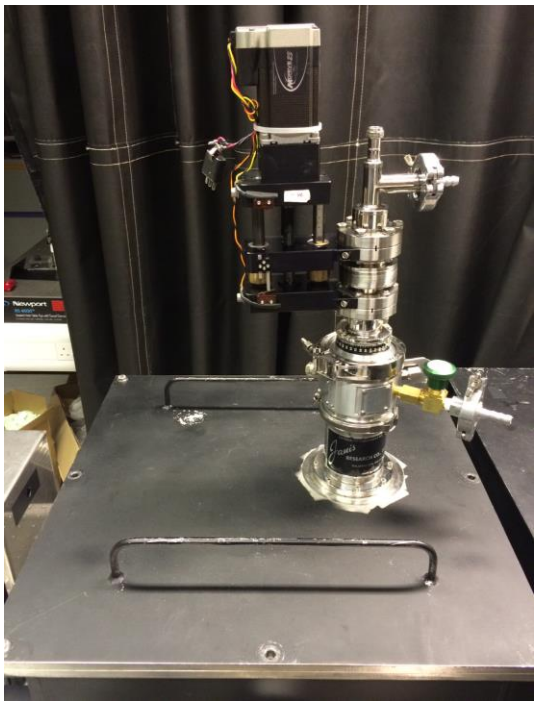

Figure 5.4. Image of cryostat used for THz-TDS measurements.

The hybrid formulation powders were pressed into 13 mm pellets using a hydraulic pellet press (Specac Ltd, Kent, UK) and a 13 mm die. The powders were subjected to 2-3 tonnes of force for 3-5 minutes in order to form well-compacted pellets which were then mounted onto an oxygen-free copper sample mount at the end of the cryostat with individual copper sample holders (Figure 5.5). These sample holders consisted of two separate copper pieces with 13 mm holes to hold the pellets, and can be directly screwed onto the sample mount. The pellets were sandwiched between two z-cut quartz windows onto the sample holders which were then screwed to the sample mount. A sample holder bearing a pair of quartz windows was used as a reference. Further details can be found in (Parrott *et al.*, (2009); Sibik, (2014); Tan, (2015)).

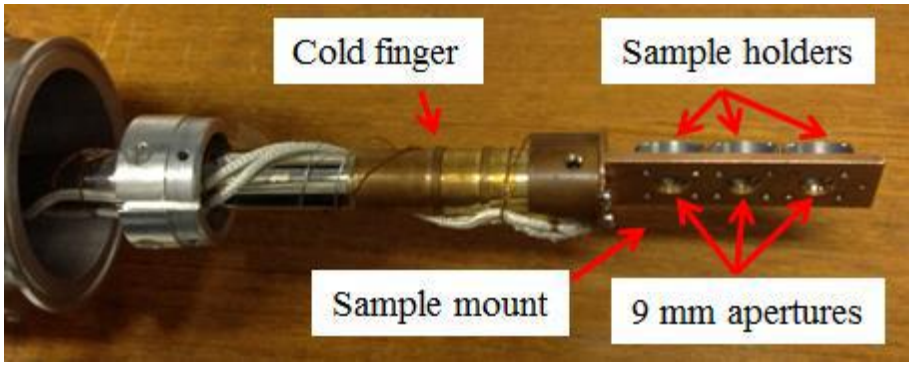

Figure 5.5. Image of copper sample mount with sample holders.

Terahertz spectra were acquired in the frequency range of 0.2-2.5 THz over a temperature range of 80 K to 430 K. Terahertz frequency data was extracted from the time-domain data (Duvillaret *et al.*, (1996)) and the spectral absorption coefficient, α, at 1 THz was analysed as a function of temperature.

5.1.3 Results and Discussion

5.1.3.1 Crystallinity of Formulations

All the tested formulations were examined for their crystalline content before THz-TDS studies and found to be X-ray amorphous as shown in Figure 5.6.

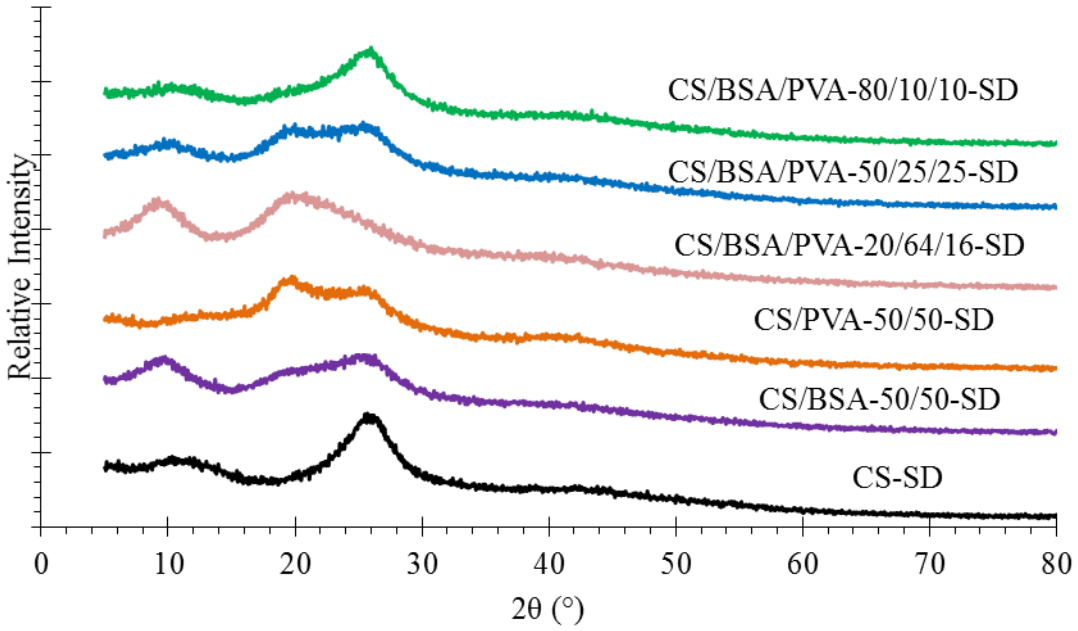

Figure 5.6. X-ray diffractograms of amorphous spray-dried formulations.

Thereafter, the formulations were stored at accelerated stress conditions of 40 °C/75%

RH as recommended by the ICH Q1A (R2) guidelines. After storage for 14 days, their X-ray diffractograms can be seen in Figure 5.7. As can be seen, the initially amorphous formulations had all crystallised.

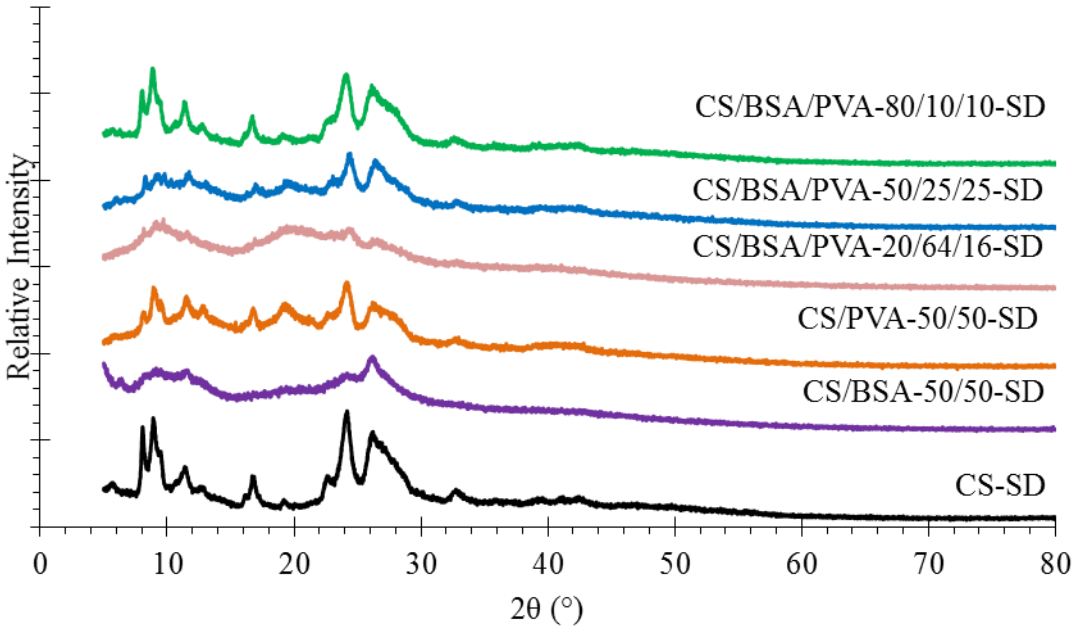

Figure 5.7. X-ray diffractograms of co-spray dried formulations after storage at accelerated stress test conditions of 40 °C/75% RH for 14 days.

5.1.3.2 Determination of glass transition temperature

As previously discussed in Section 3.3.3, the T_g of CS had not been previously reported due to the large evaporation endotherm overlapping with the glass transition. Using MDSC, we were able to determine the T_g of amorphous spray-dried CS as well as the co-spray dried hybrid formulations. The T_g was determined from the reversing heat flow signal (which contains heat capacity related events such as the glass transition) of the MDSC thermograms and shown in Figure 5.8. The glass transition of amorphous spray-dried CS was previously discussed and can be referred to in Section 3.3.3.

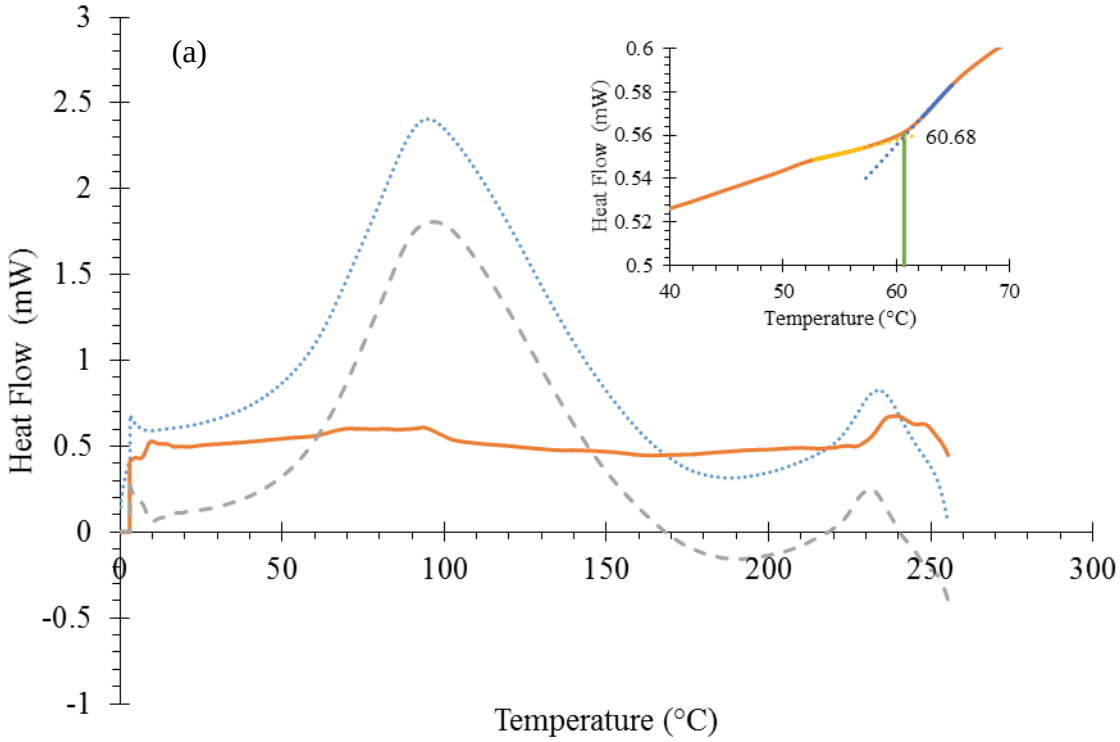

Figure 5.8. MDSC thermograms of (a) CS/BSA-50/50-SD, (b) CS/PVA-50/50-SD, (c) CS/BSA/PVA-20/64/16-SD, (d) CS/BSA/PVA-50/25/25-SD, and (e) CS/BSA/PVA-80/10/10-SD with inset of glass transition. Total heat flow represented with (• • • •), non-reversing heat flow with (— —), and reversing heat flow with (——).

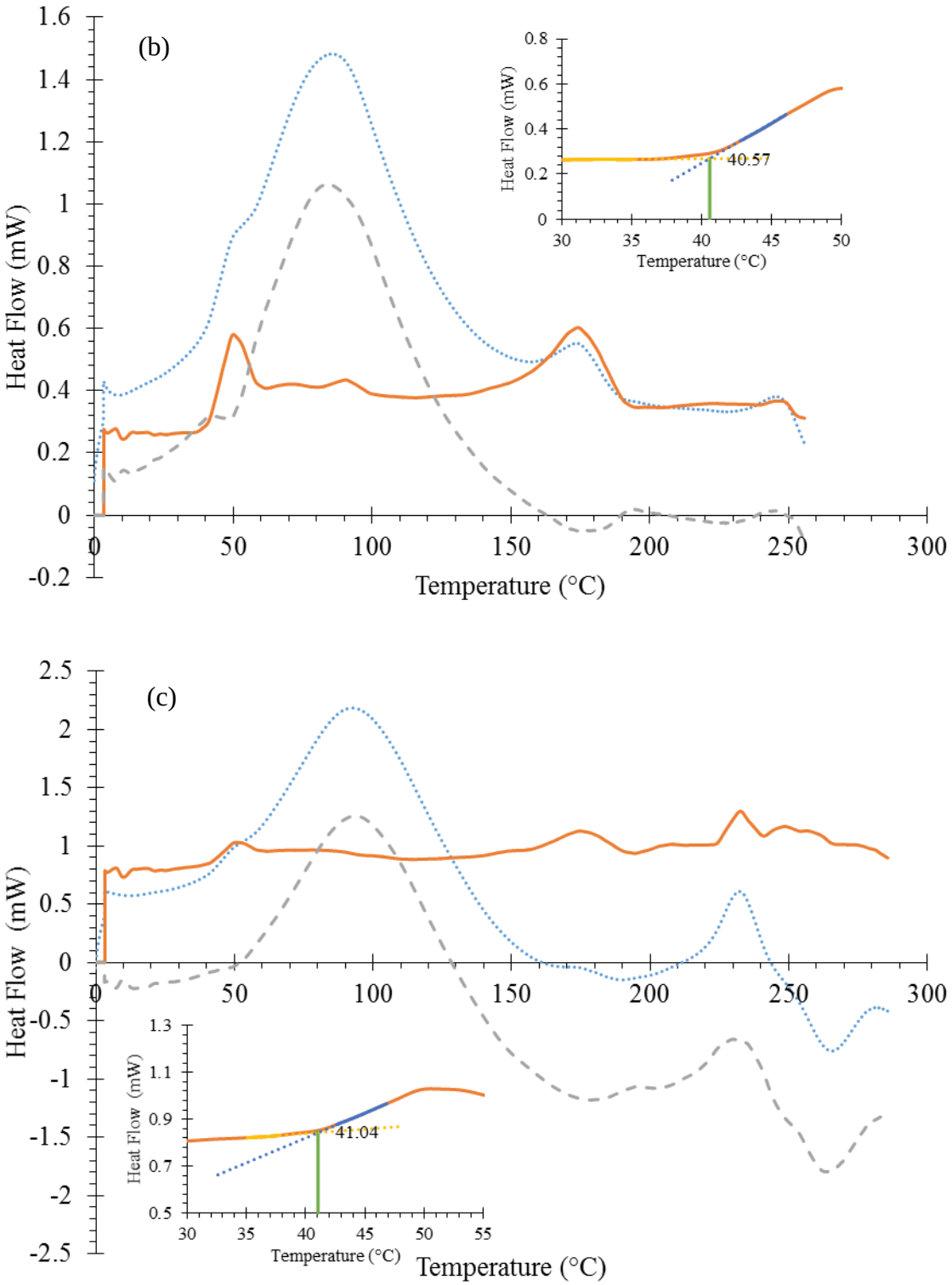

Figure 5.8. MDSC thermograms of (a) CS/BSA-50/50-SD, (b) CS/PVA-50/50-SD, (c) CS/BSA/PVA-20/64/16-SD, (d) CS/BSA/PVA-50/25/25-SD, and (e) CS/BSA/PVA-80/10/10-SD with inset of glass transition. Total heat flow represented with (• • • •), non-reversing heat flow with (— —), and reversing heat flow with (——).

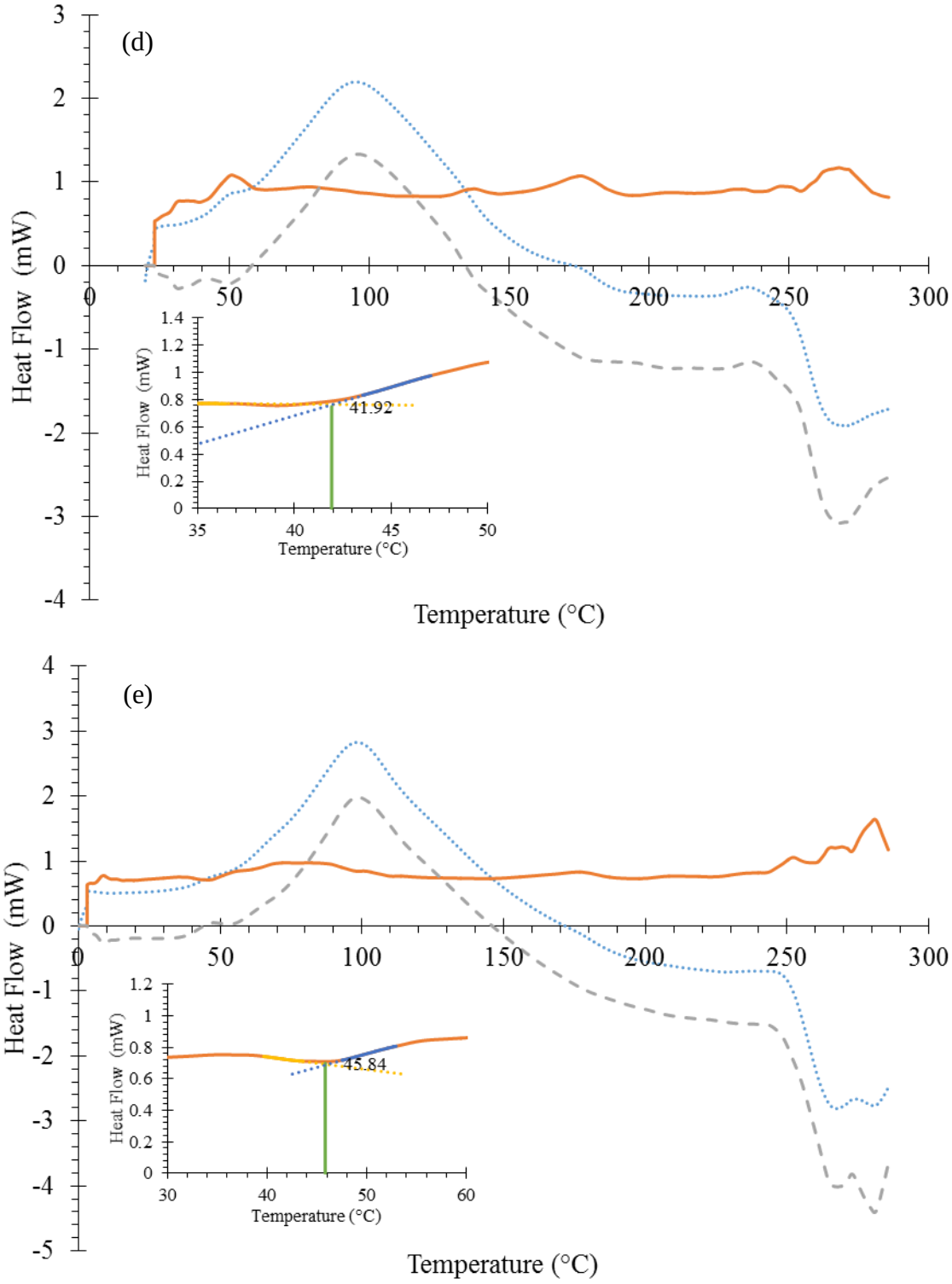

Figure 5.8. MDSC thermograms of (a) CS/BSA-50/50-SD, (b) CS/PVA-50/50-SD, (c) CS/BSA/PVA-20/64/16-SD, (d) CS/BSA/PVA-50/25/25-SD, and (e) CS/BSA/PVA-80/10/10-SD with inset of glass transition. Total heat flow represented with (• • • •), non-reversing heat flow with (— —), and reversing heat flow with (——).

As can be noted, the T_g of CS/BSA-50/50-SD (60.7 °C) was similar to that of CS-SD (57.9 °C), but the addition of PVA to CS caused the T_g to drop to ~40 °C, where it

remained for the hybrid formulations, despite the addition of BSA.

5.1.3.3 THz-TDS Spectroscopy

The terahertz absorption spectra of the amorphous spray-dried formulations at 1.0 THz can be seen in Figure 5.9. Here, the absence of the distinct temperature regimes as noted by Sibik *et al.* is prominent. In fact, the THz absorption even drops where it was expected to rise relatively strongly with increasing temperature above T_g. This effect was determined to be related to the water content in the formulations and was resolved by drying the highly hygroscopic formulations over phosphorus pentoxide (P_2O_5) prior to analysis as seen in Figure 5.10. The decrease in terahertz absorption is no longer present. Similar behaviour was found when the experiment was repeated for CS/BSA-50/50-SD, CS/PVA-50/50-SD and CS/BSA/PVA-50/25/25-SD (not shown).

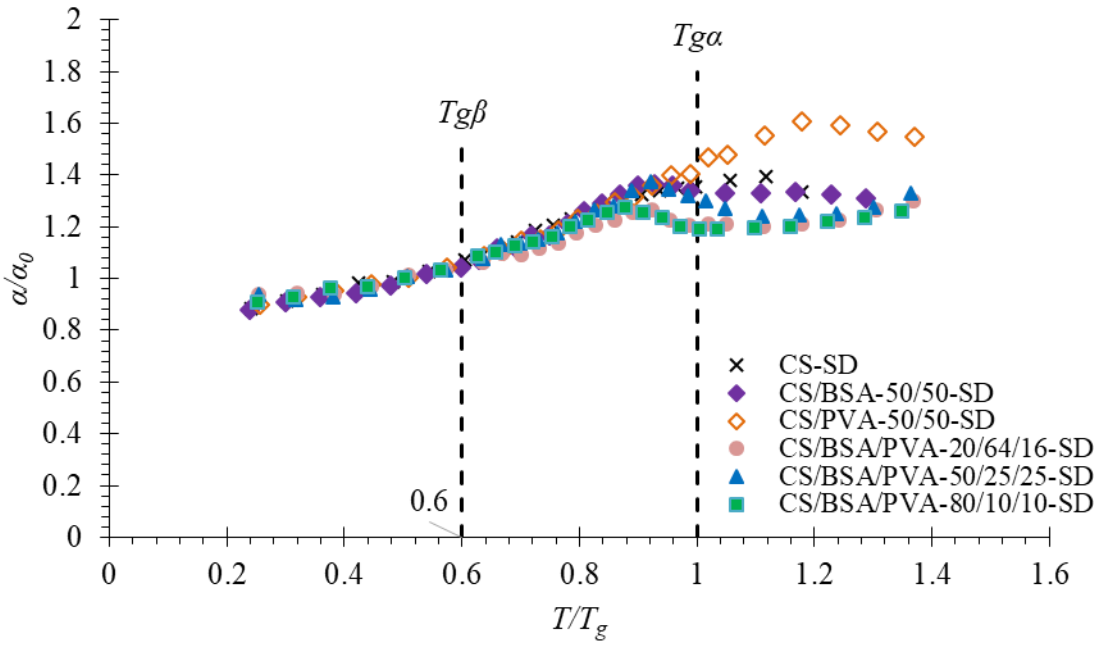

Figure 5.9. The change in absorption coefficient, α, at 1.0 THz as a function of temperature for a range of formulations. Samples were measured without any prior drying of the sample pellets. The absorption coefficient is rescaled by the low-temperature average α_0; the temperature is rescaled by T_g.

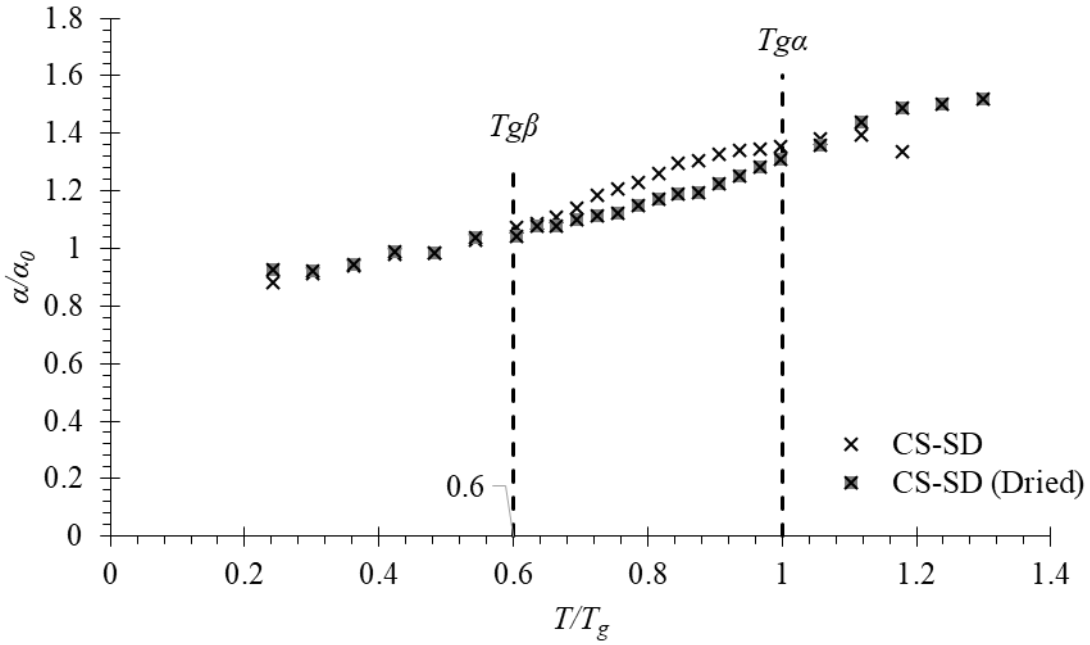

Figure 5.10. Terahertz absorption spectra of CS-SD at 1.0 THz. Filled crosses indicate when the sample was dried with P_2O_5 prior to analysis.

The temperature regime identified by Sibik *et al.* as that of importance when comparing between different amorphous drugs was between $T_{g\beta}$ and $T_{g\alpha}$, and was described to be between 0.67 $T_{g\alpha}$ and $T_{g\alpha}$. Since then, it has been determined that $T_{g\beta}$ can be determined by dielectric spectroscopy to be when the JG β-relaxation time, τ_{JG}, reaches 100 s (Capaccioli *et al.*, (2015)). From Figure 5.9, the range appeared to be between 0.6 $T_{g\alpha}$ and $T_{g\alpha}$ for the systems studied. That said, there was no significant difference in the terahertz absorption in this region for the different spray-dried formulations tested. This result is in keeping with the accelerated stress test XRD results seen in Figure 5.7, where all the formulations crystallised at the accelerated stress test storage conditions after just two weeks.

However, the DSC thermograms seen in Figure 5.8 have a distinct lack of a crystallisation trough, which suggests that the amorphous solid does not crystallise with temperature in a dry environment, such as the N_2 atmosphere in the DSC, and the vacuum of the THz-TDS setup. Water has been shown to have an effect on the molecular mobility and physical stability of amorphous drugs (Mehta *et al.*, (2016)) and as both the drug and excipients in the system studied are highly hygroscopic, the first stage of crystallisation may be water absorption and that with the plasticising effect of water, differences in the hydrogen-bonding and molecular mobility would be more pronounced if the conditions of the THz-TDS setup followed that of the accelerated stress test RH of 75% in a similar

way that McIntosh *et al.* performed with amorphous lactose. Thus, in the same way Sibik *et al.* used THz-TDS to predict the crystallisation of amorphous drugs by testing at a range of temperatures, one could modify the setup to test the molecular mobility of a formulation at different relative humidities to determine the conditions at which amorphous drug formulations should be packaged at in order to preserve their physical stability as well as the upper limit of RH that the formulation can be exposed to before crystallisation occurs. This could be a useful tool in the development of amorphous dispersions as increasing numbers of new drug entities display poor aqueous solubility and turn to amorphous formulations to increase their bioavailability.

5.1.4 Conclusions

As the formulation of drugs become increasingly complex, having to work around the unfavourable nature of new drug entities, one has to be careful to ensure that the efficacy of the new formulation is preserved over time. As a relatively simple technique to increase solubility and dissolution rate, amorphisation of crystalline drugs is widely utilised to formulate poorly aqueous soluble drugs. Their inherent physical instability is a huge drawback as the metastable drugs tend to the lower energy and stable crystalline form. Accelerated stress tests have been devised to reduce the amount of time needed to probe a formulation's stability over time to determine its packaging and handling requirements, but this test still requires six months of testing. A rapid and simple method to predict a formulation's crystallisation tendency would be very useful for formulators to eliminate formulations with poor stability without having to undergo six months of testing. THz-TDS is a novel technique which could fulfil that role and although the initial testing conditions for the spray-dried CS formulations can be improved further, promising data was obtained in which drug formulations with several components were analysed, showing that the technique could be applied to formulations as well as pure drugs. Although it must be emphasised that terahertz analysis will not provide a complete picture of all the factors governing crystallisation, it is hypothesised that a redesigned setup could be used to study the changes in the molecular dynamics of the formulations and how it may facilitate the crystallisation of amorphous formulations, and thus be a very useful complementary technique in the characterisation of amorphous formulations.

6 CONCLUDING REMARKS

Pulmonary drug delivery has been championed for various reasons: circumvention of hepatic first pass metabolism, localised treatment of respiratory diseases which reduces systemic exposure and thus side effects, a large absorptive surface with a thin diffusion path for systemic circulation, and a non-invasive route to deliver drugs.

However, pulmonary drug delivery is limited by robust clearance mechanisms in the lungs, such as mucociliary clearance in the upper airways and phagocytosis by alveolar macrophages in the alveoli. An optimal release of active ingredients in the lung – where the rate of absorption is not too fast to induce an adverse reaction from excessive drug concentrations, or too slow to not reach therapeutic levels – can help to improve the therapeutic outcome of pulmonary drug delivery as well as improve patient convenience and compliance by requiring less frequent dosing. It is also imperative to develop cost-effective inhaled therapy for the unmet needs of developing nations, where the bulk of respiratory-related deaths from asthma and COPD occur. Controlled pulmonary delivery in those countries could bring about benefits of not requiring a trained medical professional to administer medication, in addition to the aforementioned benefits.

In this study, two controlled pulmonary delivery systems were developed and characterised for their efficacy in delivering drugs of two different natures – water-soluble and poorly water-soluble – in a controlled manner.

6.1 Modulation of drug release from a water-soluble drug

For the control of a water-soluble drug, a commonly used pharmaceutical excipient, PVA, was utilised to modulate the release of an anti-asthma drug, cromolyn sodium. A protein,

BSA, was also incorporated into the formulation to impart superior aerosolisation properties. The two excipients and the drug were mixed and spray-dried in varying quantities to produce aerosol powders. The effect that each component had on the overall performance of the controlled pulmonary delivery system was then determined, especially for aerosol performance and dissolution rate.

It was found that there is a complex interplay between the two excipients, who although have complementary features such as dissolution rate modulation and increased aerosolisation ability, have other characteristics which affect the desired attribute of the other excipient. The drug itself has an influence on the performance of the overall system, and finding an optimal balance between the merits and demerits of each component in the system is a complex task.

6.2 Dissolution rate and solubility enhancement of a poorly water-soluble drug

A poorly water-soluble drug, beclomethasone dipropionate (BDP), was formulated with a commercially available graft co-polymer, Soluplus®. Soluplus® is an amphiphilic polymer with a bifunctional character, capable of forming solid solutions and solubilising poorly water-soluble drugs in an aqueous environment through the formation of micelles. Soluplus® has been found to be suitable for the delivery drugs to the lung in low concentrations, as corticosteroids usually are (Andrade *et al.*, (2015)). The drug and polymer were spray-dried to produce aerosol powders which were then evaluated for aerosol performance properties as well as dissolution and solubility enhancement.

It was found that the Soluplus® has the ability to increase the solubility and dissolution rate of BDP to a certain extent, but due to limitations in the USP dissolution apparatus 4 (flow-through cell) to accurately mimic the physiological conditions in the lung, and also the inherent properties of Soluplus®, the solubility and dissolution rate enhancements were less than expected. It was found that Soluplus® may form gels at physiological temperature, and in low amounts of dissolution medium. While this property is not beneficial for dissolution rate enhancement, it could find use in modulating the release of drug through the gel structure.

The physical stability of the spray-dried formulations was also probed. As the amorphous spray-dried powders would be expected to achieve a faster dissolution rate and higher apparent solubility due to the metastable amorphous state, it is imperative that the state is preserved for the formulation to work effectively over a period of transport and storage.

It was found that the amorphous powders were able to retain its amorphous character up to 9 months at accelerated stress test conditions, with a drug loading of up to 15% (w/w), displaying the formulations' potential as a controlled pulmonary delivery system.

6.3 Probing the physical stability of amorphous aerosol powders

Spray drying is an industrially viable, facile manufacturing process capable of forming dry powders from a solution or suspension in a single step. Due to the quick drying time of the feed, the powders formed are usually in the amorphous form. While the amorphous form brings about benefits such as dissolution rate enhancement and increased solubility, it is inherently unstable and tends to revert to its more thermodynamically stable crystalline form over time. This crystallisation may bring about undesired properties to the dry powders, affecting the morphology and surface characteristics, which in turn affect the powders' aerosol performance.

The importance of the physical stability of the formulations cannot be understated and amorphous formulations are typically subjected to stability tests to determine its physical stability. These tests last for a minimum of six months under accelerated stress test conditions. The ability to predict the physical stability of amorphous formulations would be hugely beneficial to a formulation scientist, not especially given that a majority of drugs in the pharmacopoeia are poorly water-soluble and amorphisation is one of the leading strategies to formulate such drugs.

A novel method using terahertz time-domain spectroscopy (THz-TDS) to predict the physical stability of amorphous drugs was developed by Sibik *et al.*, (2015). However, the method was only applied to pure, amorphous drugs, and not to multi-component formulations. This novel system was tested on the amorphous spray-dried hybrid formulations of CS, BSA and PVA. The formulations all displayed a similar absorption of THz, indicating a similar physical stability. The accelerated stability tests confirmed that all the initially amorphous spray-dried hybrid formulations all crystallised over a period of 12 months, agreeing with the THz-TDS data. However, a potentially useful modification could be made to the apparatus to investigate the terahertz absorption over a range of relative humidities instead to better analyse hygroscopic formulations such as the ones tested. Nonetheless, the technique shows the ability to analyse formulations as well as pure drugs, and much promise as a complementary tool in a formulation scientists' tool box, possibly as an initial screening test for amorphous formulations.

6.4 Future work

For the hybrid protein-polymer particles investigated in Chapter 3, a formulation with a similar protein/polymer ratio but with an increased drug loading between 20% (w/w) and 50% (w/w) could be tested as the increased drug loading should increase the amount of CS released, albeit while reducing the FPF. It is this careful balance that needs to be maintained in considering formulations with excipients that appear to be both complementary and contradictory to each other.

It is clear that the inability to comprehensively probe the dissolution profile of the BDP-Soluplus® system in Chapter 4 clouded the study of what may be a promising system to improve the dissolution rate of a poorly water-soluble drug for pulmonary delivery. To gain a better understanding of the unexpected low amount of drug dissolved during the dissolution test, the aliquots could be examined to determine the formation of micelles (using dynamic light scattering) and further, the ability of the micelles to solubilise the drug by testing its crystallinity with small angle x-ray spectroscopy (SAXS). SAXS could also be used to study the formation of gel formed within the cells of the dissolution apparatus. This could help in the identification of steps to minimise its formation and also to confirm that the gel is indeed responsible for the limited release of active ingredient for the dissolution test, hence improving the conduct and accuracy of the dissolution test.

6.5 Final comments

Developing controlled pulmonary drug delivery systems is a complex process with many different factors to consider. The studies performed here have gone some way to better understanding the mechanisms and properties governing each formulation. As no perfect formulation exists, the difficulty is in developing an optimal blend of beneficial characteristics for a suitable pulmonary drug delivery system, which will doubtless bring many benefits to any sufferer of respiratory disease, with promise for the systemic delivery of drugs and vaccines.

7 REFERENCES

Adi, H., Traini, D., Chan, H.K., Young, P.M. (2008). The influence of drug morphology on the aerosolisation efficiency of dry powder inhaler formulations. *Journal of Pharmaceutical Sciences* 97(7):2780–2788.

Andrade, F., Neves, J., Gener, P., Schwartz Jr, S., Ferreira, D., Oliva, M., Sarmento, B. (2015). Biological assessment of self-assembled polymeric micelles for pulmonary administration of insulin. *Nanomedicine: Nanotechnology, Biology, and Medicine* 11(7):1621–1631.

Anhøj, J., Bisgaard, H., Lipworth, B.J. (1999). Effect of electrostatic charge in plastic spacers on the lung delivery of HFA-salbutamol in children. *British Journal of Clinical Pharmacology* 47(3):333–336.

Baker, R.W., Lonsdale, H.S. (1974). Controlled Release-Mechanisms and Rates, in: Taquary, A.C., Lacey, R.E. (Eds.), Controlled Release of Biologically Active Agents. Plenum Press, New York, pp. 15–71.

Batycky, R.P., Hanes, J., Langer, R., Edwards, D.A. (1997). A theoretical model of erosion and macromolecular drug release from biodegrading microspheres. *Journal of Pharmaceutical Sciences* 86(12):1464–1477.

Beck-Broichsitter, M., Rieger, M., Reul, R., Gessler, T., Seeger, W., Schmehl, T. (2013). Correlation of drug release with pulmonary drug absorption profiles for nebulizable liposomal formulations. *European Journal of Pharmaceutics and Biopharmaceutics* 84(1):106–114.

Beck-Broichsitter, M., Schweiger, C., Schmehl, T., Gessler, T., Seeger, W., Kissel, T.

(2012). Characterization of novel spray-dried polymeric particles for controlled pulmonary drug delivery. *Journal of Controlled Release* 158(2):329–335.

Beloqui, A., Solins, M. ngeles, Gascn, A.R., del Pozo-Rodrguez, A., des Rieux, A., Prat, V. (2013). Mechanism of transport of saquinavir-loaded nanostructured lipid carriers across the intestinal barrier. *Journal of Controlled Release* 166(2):115–123.

Berkenfeld, K., Lamprecht, A., McConville, J.T. (2015). Devices for dry powder drug delivery to the lung. *AAPS PharmSciTech* 16(3):479–490.

Bhattacharya, S., Suryanarayanan, R. (2009). Local mobility in amorphous pharmaceuticals-Characterization and implications on stability. *Journal of Pharmaceutical Sciences* 98(9):2935–53.

Bi, R., Shao, W., Wang, Q., Zhang, N. (2008). Spray-freeze-dried dry powder inhalation of insulin-loaded liposomes for enhanced pulmonary delivery. *Journal of Drug Targeting* 16(9):639–648.

Bitounis, D., Fanciullino, R., Iliadis, A., Ciccolini, J. (2012). Optimizing druggability through liposomal formulations: New approaches to an old Concept. *ISRN Pharmaceutics* 2012:1–11.

Bonini, M., Usmani, O.S. (2015). The importance of inhaler devices in the treatment of COPD. *COPD Research and Practice* 1(1):9.

Bosquillon, C., Lombry, C., Préat, V., Vanbever, R. (2001). Influence of formulation excipients and physical characteristics of inhalation dry powders on their aerosolization performance. *Journal of Controlled Release* 70(3):329–339.

Bouhroum, A., Burley, J.C., Champness, N.R., Toon, R.C., Jinks, P.A., Williams, P.M., Roberts, C.J. (2010). An assessment of beclomethasone dipropionate clathrate formation in a model suspension metered dose inhaler. *International Journal of Pharmaceutics* 391(1–2):98–106.

Brannon-Peppas, L., Vert, M. (2000). Polylactic and polyglycolic acids as drug carriers, in: Wise, D.L. (Ed.), Handbook of Pharmaceutical Controlled Release Technology. Marcel Dekker, New York, pp. 99–130.

Brocklebank, D., Ram, F., Wright, J., Barry, P.W., Cates, C., Davies, L., Douglas, G., Muers, M., Smith, D., White, J. (2001). Comparison of the effectiveness of inhaler devices in asthma and chronic obstructive airways disease: a systematic review of the literature. *Health Technology Assessment* 5(26):1–149.

Bryan, C.P. (1930). The Papyrus Ebers. Geoffrey Bles, London.

Buddiga, P. (2015). No Title [WWW Document]. *Medscape*.

Buttini, F., Miozzi, M., Giulia, A., Royall, P.G., Brambilla, G., Colombo, P., Bettini, R., Forbes, B. (2014). Differences in physical chemistry and dissolution rate of solid particle aerosols from solution pressurised inhalers. *International Journal of Pharmaceutics* 465(1–2):42–51.

Byron, P.R. (1986). Prediction of drug residence times in regions of the human respiratory tract following aerosol inhalation. *Journal of Pharmaceutical Sciences* 75(5):433–438.

Capaccioli, S., Ngai, K.L., Shahin Thayyil, M., Prevosto, D. (2015). Coupling of caged molecule dynamics to JG β-relaxation: I. *Journal of Physical Chemistry B* 119(28):8800–8808.

Carvalho, S.R., Watts, A.B., Peters, J.I., Iii, R.O.W. (2015). Dry Powder Inhalation for Pulmonary Delivery : Recent Advances and Continuing Challenges, in: Nokhodchi, A., Martin, G.P. (Eds.), Pulmonary Drug Delivery: Advances and Challenges. John Wiley & Sons, Ltd, Hoboken, pp. 35–62.

Carvalho, T.C., Peters, J.I., Williams, R.O. (2011). Influence of particle size on regional lung deposition--what evidence is there? *International journal of pharmaceutics* 406(1–2):1–10.

Chan, H.-K. (2008). What is the role of particle morphology in pharmaceutical powder aerosols? *Expert Opinion on Drug Delivery* 5(8):909–914.

Chen, L., Okuda, T., Lu, X.-Y., Chan, H.-K. (2016). Amorphous powders for inhalation drug delivery. *Advanced Drug Delivery Reviews* 100:102–115.

Chew, N.Y.K., Chan, H.-K. (2002). Effect of powder polydispersity on aerosol generation. *Journal of Pharmacy and Pharmaceutical Sciences* 5(2):162–168.

Chew, N.Y.K., Chan, H.-K. (2001). Use of solid corrugated particles to enhance powder aerosol performance. *Pharmaceutical Research* 18(11):1570–1577.

Chew, N.Y.K., Chan, H.-K. (2000). The effect of spacers on the delivery of metered dose aerosols of nedocromil sodium and disodium cromoglycate. *International Journal of Pharmaceutics* 200(1):87–91.

Chew, N.Y.K., Chan, H.-K. (1999). Influence of particle size, air flow, and inhaler device on the dispersion of mannitol powders as aerosols. *Pharmaceutical Research* 16(7):1098–1103.

Chew, N.Y.K., Tang, P., Chan, H.-K., Raper, J.A. (2005). How much particle surface corrugation is sufficient to improve aerosol performance of powders? *Pharmaceutical Research* 22(1):148–152.

Chow, A.H.L., Tong, H.H.Y., Chattopadhyay, P., Shekunov, B.Y. (2007). Particle

engineering for pulmonary drug delivery. *Pharmaceutical Research* 24(3):411–437.

Chow, K.T., Zhu, K., Tan, R.B.H., Heng, P.W.S. (2008). Investigation of electrostatic behavior of a lactose carrier for dry powder inhalers. *Pharmaceutical Research* 25(12):2822–34.

Codrons, V., Vanderbist, F., Verbeeck, R.K., Arras, M., Lison, D., Préat, V., Vanbever, R. (2003). Systemic delivery of parathyroid hormone (1-34) using inhalation dry powders in rats. *Journal of Pharmaceutical Sciences* 92(5):938–950.

Cook, R.O., Pannu, R.K., Kellaway, I.W. (2005). Novel sustained release microspheres for pulmonary drug delivery. *Journal of Controlled Release* 104(1):79–90.

Costa, P., Sousa Lobo, J.M. (2001). Modeling and comparison of dissolution profiles. *European Journal of Pharmaceutical Sciences* 13(2):123–133.

Courrier, H.M., Butz, N., Vandamme, T.F. (2002). Pulmonary drug delivery systems: recent developments and prospects. *Critical Reviews™ in Therapeutic Drug Carrier Systems* 19(4–5):425–498.

Cox, J.S.G., Woodward, G.D., McCrone, W.C. (1971). Solid-state chemistry of cromolyn sodium (disodium cromoglycate). *Journal of Pharmaceutical Sciences* 60(10):1458–1465.

Crompton, G. (2006). A brief history of inhaled asthma therapy over the last fifty years. *Primary Care Respiratory Journal* 15(6):326–331.

Cryan, S.-A., Sivadas, N., Garcia-Contreras, L. (2007). In vivo animal models for drug delivery across the lung mucosal barrier. *Advanced Drug Delivery Reviewsrug delivery reviews* 59(11):1133–51.

D'Addio, S.M., Chan, J.G.Y., Kwok, P.C.L., Prud'Homme, R.K., Chan, H.-K. (2012). Constant size, variable density aerosol particles by ultrasonic spray freeze drying. *International Journal of Pharmaceutics* 427(2):185–191.

Daley-Yates, P.T., Price, A.C., Sisson, J.R., Pereira, A., Dallow, N. (2001). Beclomethasone dipropionate: Absolute bioavailability, pharmacokinetics and metabolism following intravenous, oral, intranasal and inhaled administration in man. *British Journal of Clinical Pharmacology* 51(5):400–409.

Davies, N.M., Feddah, M.R. (2003). A novel method for assessing dissolution of aerosol inhaler products. *International Journal of Pharmaceutics* 255(1–2):175–187.

Davis, Mark T., Potter, Catherine B., Mohammadpour, Maryam, Albadarin, Ahmad B., Walker, G.M. (2017). Design of spray dried ternary solid dispersions comprising itraconazole, soluplus and HPMCP: Effect of constituent compositions. *International*

Journal of Pharmaceutics 519(1–2):365–372.

de Boer, A.H., Hagedoorn, P., Hoppentocht, M., Buttini, F., Grasmeijer, F., Frijlink, H.W. (2017). Dry powder inhalation: past, present and future. *Expert Opinion on Drug Delivery* 14(4):499–512.

De Smet, L., Saerens, L., De Beer, T., Carleer, R., Adriaensens, P., Bocxlaer, J. Van, Vervaet, C., Paul, J. (2014). Formulation of itraconazole nanococrystals and evaluation of their bioavailability in dogs. *European Journal of Pharmaceutics and Biopharmaceutics* 87(1):107–113.

Djuris, J., Nikolakakis, I., Ibric, S., Djuric, Z., Kachrimanis, K. (2013). Preparation of carbamazepine–Soluplus® solid dispersions by hot-melt extrusion, and prediction of drug–polymer miscibility by thermodynamic model fitting. *European Journal of Pharmaceutics and Biopharmaceutics* 84(1):228–237.

Doan, T.V.P., Couet, W., Olivier, J.C. (2011). Formulation and in vitro characterization of inhalable rifampicin-loaded PLGA microspheres for sustained lung delivery. *International Journal of Pharmaceutics* 414(1–2):112–117.

Dunbar, C., Hickey, A., Holzer, P. (1998). Dispersion and characterisation of phamaceutical dry powder aerosols. *Kona* 16(16):7–45.

Duvillaret, L., Garet, F., Coutaz, J.-L. (1996). A reliable method for extraction of material parameters in terahertz time-domain spectroscopy. *IEEE Journal of Selected Topics in Quantum Electronics* 2(3).

Edwards, D.A., Hanes, J., Caponetti, G., Hrkach, J., Ben-Jebria, A., Eskew, M. Lou, Mintzes, J., Deaver, D., Lotan, N., Langer, R. (1997). Large porous particles for pulmonary drug delivery. *Science* 276(5320):1868–1871.

Ehsan, Z., Clancy, J.P. (2015). Management of Pseudomonas aeruginosa infection in cystic fibrosis patients using inhaled antibiotics with a focus on nebulized liposomal amikacin. *Future Microbiology* 10(12):1901–1912.

Ei-Arini, S.K., Leuenberger, H. (1995). Modelling of drug release from polymer matrices: Effect of drug loading. *International Journal of Pharmaceutics* 121(2):141–148.

El-Sherbiny, I.M., McGill, S., Smyth, H.D.C. (2010). Swellable microparticles as carriers for sustained pulmonary drug delivery. *Journal of pharmaceutical sciences* 99(5):2343–2356.

El-Sherbiny, I.M., Smyth, H.D.C. (2012). Controlled release pulmonary administration of curcumin using swellable biocompatible microparticles. *Molecular Pharmaceutics* 9(2):269–80.

El-Sherbiny, I.M., Smyth, H.D.C. (2010). Novel cryomilled physically cross-linked biodegradable hydrogel microparticles as carriers for inhalation therapy. *Journal of Microencapsulation* 27(8):657–668.

El-Sherbiny, I.M., Smyth, H.D.C. (2010). Biodegradable nano-micro carrier systems for sustained pulmonary drug delivery: (I) Self-assembled nanoparticles encapsulated in respirable/swellable semi-IPN microspheres. *International Journal of Pharmaceutics* 395(1–2):132–141.

El-Sherbiny, I.M., Villanueva, D.G., Herrera, D., Smyth, H.D.C. (2011). Overcoming lung clearance mechanisms for controlled release drug delivery, in: Smyth, H.D.C., Hickey, A.J. (Eds.), Controlled Pulmonary Delivery. Springer, New York, pp. 101–126.

Elsadek, B., Kratz, F. (2012). Impact of albumin on drug delivery - New applications on the horizon. *Journal of Controlled Release* 157(1):4–28.

Elversson, J., Millqvist-Fureby, A. (2005). Aqueous two-phase systems as a formulation concept for spray-dried protein. *International Journal of Pharmaceutics* 294(1–2):73–87.

Fäldt, P., Bergenståhl, B., Carlsson, G. (1993). The surface coverage of fat on food powders analyzed by ESCA (electron spectroscopy for chemical analysis). *Food structure* 12(2):225–234.

Fanta, C.H. (2009). Asthma. *The New England Journal of Medicine* 360(10):1002–14.

Fotaki, N. (2011). Flow-through cell apparatus (USP Apparatus 4): Operation and features. *Dissolution Technologies* 18(4):46–49.

Friebel, C., Steckel, H. (2010). Single-use disposable dry powder inhalers for pulmonary drug delivery. *Expert Opinion on Drug Delivery* 7(12):1359–1372.

Gibbons, A., McElvaney, N.G., Cryan, S.-A. (2010). A dry powder formulation of liposome-encapsulated recombinant secretory leukocyte protease inhibitor (rSLPI) for inhalation: Preparation and characterisation. *AAPS PharmSciTech* 11(3):1411–1421.

Giunchedi, P., Conti, B., Genta, I., Conte, U., Puglisi, G. (2001). Emulsion spray-drying for the preparation of albumin-loaded PLGA microspheres. *Drug Development and Industrial Pharmacy* 27(7):745–750.

Green, M.R., Manikhas, G.M., Orlov, S., Afanasyev, B., Makhson, A.M., Bhar, P., Hawkins, M.J. (2006). Abraxane, a novel Cremophor-free, albumin-bound particle form of paclitaxel for the treatment of advanced non-small-cell lung cancer. *Annals of Oncology* 17(8):1263–8.

Grenha, A., Grainger, C.I., Dailey, L.A., Seijo, B., Martin, G.P., Remuñán-López, C., Forbes, B. (2007). Chitosan nanoparticles are compatible with respiratory epithelial cells

in vitro. *European Journal of Pharmaceutical Sciences* 31(2):73–84.

Grzybowska, K., Paluch, M., Grzybowski, A., Wojnarowska, Z., Hawelek, L., Kolodziejczyk, K., Ngai, K.L. (2010). Molecular dynamics and physical stability of amorphous anti-inflammatory drug: celecoxib. *The Journal of Physical Chemistry. B* 114(40):12792–12801.

Gul, M.O., Jones, S.A., Dailey, L.A., Nacer, H., Ma, Y., Sadouki, F., Hider, R., Araman, A., Forbes, B. (2009). A poly(vinyl alcohol) nanoparticle platform for kinetic studies of inhaled particles. *Inhalation Toxicology* 21(7):631–40.

Haghi, M., Salama, R., Traini, D., Bebawy, M., Young, P.M. (2012). Modification of disodium cromoglycate passage across lung epithelium in vitro via incorporation into polymeric microparticles. *The AAPS Journal* 14(1):79–86.

Hamishehkar, H., Emami, J., Najafabadi, A.R., Gilani, K., Minaiyan, M., Mahdavi, H., Nokhodchi, A. (2010). Effect of carrier morphology and surface characteristics on the development of respirable PLGA microcapsules for sustained-release pulmonary delivery of insulin. *International Journal of Pharmaceutics* 389(1–2):74–85.

Hancock, B.C., Carlson, G.T., Ladipo, D.D., Langdon, B.A., Mullarney, M.P. (2002). Comparison of the mechanical properties of the crystalline and amorphous forms of a drug substance. *International Journal of Pharmaceutics* 241(1):73–85.

Hancock, B.C., Shamblin, S.L., Zografi, G. (1995). Molecular mobility of amorphous pharmaceutical solids below their glass transition temperatures. *Pharmaceutical Research* 12(6):799–806.

Hancock, B.C., Zografi, G. (1997). Characteristics and significance of the amorphous state in pharmaceutical systems. *Journal of Pharmaceutical Sciences* 86(1):1–12.

Handbook for the Montreal Protocol on Substances that Deplete the Ozone Layer, 11th ed. (2017). . United Nations Environment Programme, Nairobi.

Haughney, J., Price, D., Barnes, N.C., Virchow, J.C., Roche, N., Chrystyn, H. (2010). Choosing inhaler devices for people with asthma: Current knowledge and outstanding research needs. *Respiratory Medicine CME* 3(3):125–131.

He, C., Hu, Y., Yin, L., Tang, C., Yin, C. (2010). Effects of particle size and surface charge on cellular uptake and biodistribution of polymeric nanoparticles. *Biomaterials* 31(13):3657–3666.

Healy, A.M., Amaro, M.I., Paluch, K.J., Tajber, L. (2014). Dry powders for oral inhalation free of lactose carrier particles. *Advanced Drug Delivery Reviews* 75:32–52.

Heng, D., Lee, S.H., Ng, W.K., Tan, R.B.H. (2011). The nano spray dryer B-90. *Expert*

opinion on drug delivery 8(7):965–972.

Heng, D., Tang, P., Cairney, J.M., Chan, H.-K., Cutler, D.J., Salama, R., Yun, J. (2007). Focused-ion-beam milling: a novel approach to probing the interior of particles used for inhalation aerosols. *Pharmaceutical Research* 24(9):1608–1617.

Heyder, J. (2004). Deposition of Inhaled Particles in the Human Respiratory Tract and Consequences for Regional Targeting in Respiratory Drug Delivery. *Proceedings of the American Thoracic Society* 1(4):315–320.

Heyder, J., Gebhart, J., Rudolf, G., Schiller, C.F., Stahlhofen, W. (1986). Deposition of particles in the human respiratory tract in the size range 0.005-15 μm. *Journal of Aerosol Science* 17(5):811–825.

Hickey, A., Mansour, H. (2008). Formulation challenges of powders for the delivery of small- molecular-weight molecules as aerosols, in: Rathbone, M.J., Hadgraft, J., Roberts, M.S., Lane, M.E. (Eds.), Modified-Release Drug Delivery Technology. CRC Press, Boca Raton, pp. 835–848.

Higuchi, T. (1963). Mechanism of sustained-action medication. Theoretical anaylsis of rate of release of solid drugs dispersed in solid matrices. *Journal of Pharmaceutical Sciences* 52(12):1145–1149.

Higuchi, T. (1961). Rate of release of medicaments from ointment bases containing drugs in suspension. *Journal of pharmaceutical sciences* 50:874–875.

Hikima, T., Hanaya, M., Oguni, M. (1999). Microscopic observation of a peculiar crystallization in the glass transition region and β-process as potentially controlling the growth rate in triphenylethylene. *Journal of Molecular Structure* 479(2–3):245–250.

Hixson, A.W., Crowell, J.H. (1931). Dependence of Reaction Velocity upon Surface and Agitation: III—Experimental Procedure in Study of Agitation. *Industrial and Engineering Chemistry* 23(10):1160–1168.

How to Use Your Inhaler [WWW Document]. n.d. . *Asthma Society of Canada*.

Hu, J., Johnston, K.P., Williams, R.O. (2003). Spray freezing into liquid (SFL) particle engineering technology to enhance dissolution of poorly water soluble drugs: Organic solvent versus organic/aqueous co-solvent systems. *European Journal of Pharmaceutical Sciences* 20(3):295–303.

Hu, J., Rogers, T.L., Brown, J., Young, T., Johnston, K.P., Williams III, R.O. (2002). Improvement of dissolution rates of poorly water soluble APIs using novel spray freezing into liquid technology. *Pharmaceutical Research* 19(9):1278–1284.

Issar, M., Mobley, C., Khan, P., Hochhaus, G. (2003). Pharmacokinetics and

pharmacodynamics of drugs delivered to the lungs, in: Hickey, A.J. (Ed.), Pharmaceutical Inhalation Aerosol Technology. CRC Press, Boca Raton.

Jeong, S.H., Park, J.H., Park, K. (2006). Formulation issues around lipid-based oral and parenteral delivery systems, in: Role of Lipid Excipients in Modifying Oral and Parenteral Drug Delivery: Basic Principles and Biological Examples. Wiley-Interscience, Hoboken, pp. 32–47.

Jing, G., Zhong, Y., Zhang, L., Gou, J., Ji, X., Huang, H., Zhang, Y., Wang, Y., He, H., Tang, X. (2015). Increased dissolution of disulfiram by dry milling with silica nanoparticles. *Drug Development and Industrial Pharmacy* 41(8):1328–1337.

Jinno, J.I., Kamada, N., Miyake, M., Yamada, K., Mukai, T., Odomi, M., Toguchi, H., Liversidge, G.G., Higaki, K., Kimura, T. (2006). Effect of particle size reduction on dissolution and oral absorption of a poorly water-soluble drug, cilostazol, in beagle dogs. *Journal of Controlled Release* 111(1–2):56–64.

Kang, B.K., Chon, S.K., Kim, S.H., Jeong, S.Y., Kim, M.S., Cho, S.H., Lee, H.B., Khang, G. (2004). Controlled release of paclitaxel from microemulsion containing PLGA and evaluation of anti-tumor activity in vitro and in vivo. *International Journal of Pharmaceutics* 286(1–2):147–156.

Kauzmann, W. (1948). The nature of the glassy state and the behavior of liquids at low temperatures. *Chemical Reviews* 43(2):219–256.

Kim, C.S., Jaques, P.A. (2004). Analysis of total respiratory deposition of inhaled ultrafine particles in adult subjects at various breathing patterns. *Aerosol Science and Technology* 38(6):525–540.

Kim, I., Byeon, H.J., Kim, T.H., Lee, E.S., Oh, K.T., Shin, B.S., Lee, K.C., Youn, Y.S. (2012). Doxorubicin-loaded highly porous large PLGA microparticles as a sustained-release inhalation system for the treatment of metastatic lung cancer. *Biomaterials* 33(22):5574–5583.

Korsmeyer, R.W., Gurny, R., Doelker, E., Buri, P., Peppas, N.A. (1983). Mechanisms of solute release from porous hydrophilic polymers. *International Journal of Pharmaceutics* 15(1):25–35.

Koushik, K., Kompella, U. (2004). Particle & device engineering for inhalation drug delivery. *Drug Development & Delivery* 4(2):1–10.

Kramer, P. (1974). Albumin microspheres as vehicles for achieving specificity in drug delivery. *Journal of Pharmaceutical Sciences* (2):13–14.

Kratz, F. (2008). Albumin as a drug carrier: design of prodrugs, drug conjugates and

nanoparticles. *Journal of Controlled Release* 132(3):171–83.

Kreyling, W.G., Semmler-Behnke, M., Möller, W. (2006). Ultrafine particle–lung interactions: Does size matter? *Journal of Aerosol Medicine* 19(1):74–83.

Kunda, N.K., Alfagih, I.M., Saleem, I.Y., Hutcheon, G.A. (2015). Polymer-based delivery systems for the pulmonary delivery of biopharmaceuticals, in: Nokhodchi, A., Martin, G.P. (Eds.), Pulmonary Drug Delivery: Advances and Challenges. Wiley, Chichester, United Kingdom, pp. 301–320.

Kwek, J.W., Heng, D., Lee, S.H., Ng, W.K., Chan, H.K., Adi, S., Heng, J., Tan, R.B.H. (2013). High speed imaging with electrostatic charge monitoring to track powder deagglomeration upon impact. *Journal of Aerosol Science* 65:77–87.

Labiris, N.R., Dolovich, M.B. (2003). Pulmonary drug delivery. Part I: physiological factors affecting therapeutic effectiveness of aerosolized medications. *British Journal of Clinical Pharmacology* 56(6):588–599.

Laboratory scale spray drying Of inhalable drugs: A review. (2010). . *Best@Buchi* (59).

Lamprecht, A., Saumet, J.-L., Roux, J., Benoit, J.-P. (2004). Lipid nanocarriers as drug delivery system for ibuprofen in pain treatment. *International Journal of Pharmaceutics* 278(2):407–414.

Langenbucher, F., Benz, D., Kurth, W., Moller, H., Otz, M. (1989). Standardized flow-cell method as an alternative to existing pharmacopeial dissolution testing. *Pharmazeutische Industrie* 51(11):1276–1281.

Lansley, A.B. (1993). Mucociliary clearance and drug delivery via the respiratory tract. *Advanced Drug Delivery Reviews*.

Lavorini, F. (2013). The Challenge of Delivering Therapeutic Aerosols to Asthma Patients. *ISRN Allergy* 2013:102418.

Lavra, Z.M.M., Pereira de Santana, D., Ré, M.I. (2016). Solubility and dissolution performances of spray-dried solid dispersion of Efavirenz in Soluplus. *Drug Development and Industrial Pharmacy* 9045(June):1–13.

Learoyd, T.P., Burrows, J.L., French, E., Seville, P.C. (2008). Chitosan-based spray-dried respirable powders for sustained delivery of terbutaline sulfate. *European Journal of Pharmaceutics and Biopharmaceutics* 68(2):224–234.

Lee, J., Oh, Y.J., Lee, S.K., Lee, K.Y. (2010). Facile control of porous structures of polymer microspheres using an osmotic agent for pulmonary delivery. *Journal of Controlled Release* 146(1):61–67.

Lee, S.H., Heng, D., Ng, W.K., Chan, H.K., Tan, R.B.H. (2011). Nano spray drying: A

novel method for preparing protein nanoparticles for protein therapy. *International Journal of Pharmaceutics* 403(1–2):192–200.

Lehnert, B.E. (1992). Pulmonary and thoracic macrophage subpopulations and clearance of particles from the lung, in: Environmental Health Perspectives. pp. 17–46.

Lenney, J., Innes, J.A., Crompton, G.K. (2000). Inappropriate inhaler use: assessment of use and patient preference of seven inhalation devices. *Respiratory Medicine* 94(5):496–500.

Li, F.Q., Hu, J.H., Lu, B., Yao, H., Zhang, W.G. (2001). Ciprofloxacin-loaded bovine serum albumin microspheres: preparation and drug-release in vitro. *Journal of Microencapsulation* 18(6):825–9.

Li, L., Sun, S., Parumasivam, T., Denman, J.A., Gengenbach, T., Tang, P., Mao, S., Chan, H. (2016). L-Leucine as an excipient against moisture on in vitro aerosolization performances of highly hygroscopic spray-dried powders. *European Journal of Pharmaceutics and Biopharmaceutics* 102(March):132–141.

Liang, Z., Ni, R., Zhou, J., Mao, S. (2015). Recent advances in controlled pulmonary drug delivery. *Drug Discovery Today* 20(3):380–389.

Lin, C.-H., Chen, C.-H., Lin, Z.-C., Fang, J.-Y. (2017). Recent advances in oral delivery of drugs and bioactive natural products using solid lipid nanoparticles as the carriers. *Journal of Food and Drug Analysis* 25(2):219–234.

Liu, R.R., Forrest, M.L., Kwon, G.S. (2008). Micellization and Drug Solubility Enhancement Part II : Polymeric Micelles, in: Liu, R. (Ed.), Water-Insoluble Drug Formulation. CRC Press, Boca Raton, pp. 307–374.

Loira-Pastoriza, C., Todoroff, J., Vanbever, R. (2014). Delivery strategies for sustained drug release in the lungs. *Advanced Drug Delivery Reviews* 75:81–91.

Lombry, C. (2003). Alveolar macrophages are a primary barrier to pulmonary absorption of macromolecules. *American Journal of Physiology: Lung Cellular and Molecular Physiology* 286(5):L1002–L1008.

Lu, J., Cuellar, K., Hammer, N.I., Jo, S., Gryczke, A., Kolter, K., Langley, N., Repka, M.A. (2015). Solid-state characterization of Felodipine–Soluplus amorphous solid dispersions. *Drug Development and Industrial Pharmacy* 9045(November):1–12.

Maa, Y.F., Nguyen, P.A., Andya, J.D., Dasovich, N., Sweeney, T.D., Shire, S.J., Hsu, C.C. (1998). Effect of spray drying and subsequent processing conditions on residual moisture content and physical/biochemical stability of protein inhalation powders. *Pharmaceutical Research* 15(5):768–775.

Mallapragada, S.K., McCarthy-Schroeder, S. (2000). Poly(vinyl alcohol) as a drug delivery carrier, in: Wise, D.L. (Ed.), Handbook of Pharmaceutical Controlled Release Technology. CRC Press, New York, pp. 31–46.

Mallapragada, S.K., Peppas, N.A., Colombo, P. (1996). Crystal dissolution-controlled release systems . II . Metronidazole release from semicrystalline poly (vinyl alcohol) systems.

Martonen, T.B., Smyth, H.D., Isaacs, K.K., Burton, R.T. (2005). Issues in drug delivery: concepts and practice. *Respiratory Care* 50(9):1228–1252.

Maury, M., Murphy, K., Kumar, S., Shi, L., Lee, G. (2005). Effects of process variables on the powder yield of spray-dried trehalose on a laboratory spray-dryer. *European Journal of Pharmaceutics and Biopharmaceutics* 59(3):565–573.

McCalden, T.A. (1990). Particulate systems for drug delivery to the lung. *Advanced Drug Delivery Reviews* 5(3):253–263.

McDonald, K.J., Martin, G.P. (2000). Transition to CFC-free metered dose inhalers - Into the new millennium. *International Journal of Pharmaceutics* 201(1):89–107.

McIntosh, A.I., Yang, B., Goldup, S.M., Watkinson, M., Donnan, R.S. (2013). Crystallization of amorphous lactose at high humidity studied by terahertz time domain spectroscopy. *Chemical Physics Letters* 558:104–108.

Mehta, M., Kothari, K., Ragoonanan, V., Suryanarayanan, R. (2016). Effect of water on molecular mobility and physical stability of amorphous pharmaceuticals. *Molecular Pharmaceutics* 13(4):1339–1346.

Misra, A., Jinturkar, K., Patel, D., Lalani, J., Chougule, M. (2009). Recent advances in liposomal dry powder formulations: preparation and evaluation. *Expert Opinion on Drug Delivery* 6(1):71–89.

Miyazaki, S., Takahashi, A., Itoh, K., Ishitani, M., Dairaku, M., Togashi, M., Mikami, R., Attwood, D. (2009). Preparation and evaluation of gel formulations for oral sustained delivery to dysphagic patients. *Drug Development and Industrial Pharmacy* 35(7):780–787.

Mizuno, M., Pikal, M.J. (2013). Is the pre-Tg DSC endotherm observed with solid state proteins associated with the protein internal dynamics? Investigation of bovine serum albumin by solid state hydrogen/deuterium exchange. *European Journal of Pharmaceutics and Biopharmaceutics* 85(2):170–6.

Mobley, C., Hochhaus, G. (2001). Methods used to assess pulmonary deposition and absorption of drugs. *Drug Discovery Today* 6(7):367–375.

Möbus, K., Siepmann, J., Bodmeier, R. (2012). Zinc-alginate microparticles for controlled pulmonary delivery of proteins prepared by spray-drying. *European Journal of Pharmaceutics and Biopharmaceutics* 81(1):121–130.

Moghaddam, P.H., Ramezani, V., Esfandi, E., Vatanara, A., Nabi-Meibodi, M., Darabi, M., Gilani, K., Najafabadi, A.R. (2013). Development of a nano-micro carrier system for sustained pulmonary delivery of clarithromycin. *Powder Technology* 239:478–483.

Molina, M.J., Rowland, F.S. (1974). Stratospheric sink for chlorofluoromethanes: chlorine atomc-atalysed destruction of ozone. *Nature* 249(5460):810–812.

Mudge, J. (1778). A radical and expeditious cure for a recent catarrhous cough. E. Allen, London.

Müller, R., Mäder, K., Gohla, S. (2000). Solid lipid nanoparticles (SLN) for controlled drug delivery: a review of the state of the art. *European Journal of Pharmaceutics and Biopharmaceutics* 50(1):161–177.

Myrdal, P.B., Sheth, P., Stein, S.W. (2014). Advances in metered dose inhaler technology: Formulation development. *AAPS PharmSciTech* 15(2):434–455.

Najafabadi, A.R., Gilani, K., Barghi, M., Rafiee-Tehrani, M. (2004). The effect of vehicle on physical properties and aerosolisation behaviour of disodium cromoglycate microparticles spray dried alone or with L-leucine. *International Journal of Pharmaceutics* 285(1–2):97–108.

Nakamura, T., Ueda, H., Tsuda, T., Li, Y.H., Kiyotani, T., Inoue, M., Matsumoto, K., Sekine, T., Yu, L., Hyon, S.H., Shimizu, Y. (2001). Long-term implantation test and tumorigenicity of polyvinyl alcohol hydrogel plates. *Journal of Biomedical Materials Research* 56(2):289–296.

Nernst, W. (1904). Theorie der Reaktionsgeschwindigkeit in heterogenen Systemen. *Zeitschrift für physikalische Chemie* 47:52–55.

Newman, S.P. (2005). Principles of metered-dose inhaler design. *Respiratory Care* 50(9):1177–1190.

Ngai, K.L. (2004). Why the fast relaxation in the picosecond to nanosecond time range can sense the glass transition. *Philosophical Magazine* 84(13–16):1341–1353.

Ni, R., Zhao, J., Liu, Q., Liang, Z., Muenster, U., Mao, S. (2017). Nanocrystals embedded in chitosan-based respirable swellable microparticles as dry powder for sustained pulmonary drug delivery. *European Journal of Pharmaceutical Sciences* 99:137–146.

Nolan, L.M., Li, J., Tajber, L., Corrigan, O.I., Healy, A.M. (2011). Particle engineering of materials for oral inhalation by dry powder inhalers. II - Sodium cromoglicate.

International Journal of Pharmaceutics 405(1–2):36–46.

Noyes, A.A., Whitney, W.R. (1897). The rate of solution of solid substances in their own solutions. *Journal of the American Chemical Society* 19(12):930–934.

O'Connor, B.J. (2004). The ideal inhaler: Design and characteristics to improve outcomes. *Respiratory Medicine* 98(SUPPL. A).

Oberdörster, G. (1988). Lung clearance of inhaled insoluble and soluble particles. *Journal of Aerosol Medicine* 1(4):289–330.

Oberdörster, G., Ferin, J., Lehnert, B.E. (1994). Correlation between particle size, in vivo particle persistence, and lung injury, in: Environmental Health Perspectives. pp. 173–179.

Oenbrink, R.J. (1993). Unexpected adverse effects of Freon 11 and Freon 12 as medication propellants. *Journal of the American Osteopathic Association* 93(6):714–718.

Okamoto, N., Oguni, M. (1996). Discovery of crystal nucleation proceeding much below the glass transition temperature in a supercooled liquid. *Solid State Communications* 99(1):53–56.

Olsson, B., Bondesson, E., Borgström, L., Edsbäcker, S., Ekelund, K., Gustavsson, L., Hegelund-myrbäck, T. (2011). Pulmonary Drug Metabolism, Clearance and Absorption, in: Smyth, H.D.C., Hickey, A.J. (Eds.), Controlled Pulmonary Drug Delivery. Springer, New York, pp. 21–50.

Park, K. (2014). Controlled drug delivery systems: Past forward and future back. *Journal of Controlled Release* 190:3–8.

Park, K. (2012). Albumin: a versatile carrier for drug delivery. *Journal of Controlled Release* 157(1):3.

Park, K. (Ed.). (1997). Controlled Drug Delivery: Challenges and Strategies, 1st ed. American Chemical Society, Washington D.C.

Parrott, E., Zeitler, J., Friščić, T., Pepper, M., Jones, W., Day, G., Gladden, L. (2009). Testing the sensitivity of terahertz spectroscopy to changes in molecular and supramolecular structure: A study of structurally similar cocrystals. *Crystal Growth & Design* 9(3):1452–1460.

Patton, J.S. (1996). Mechanisms of macromolecule absorption by the lungs. *Advanced Drug Delivery Reviews*.

Patton, J.S., Brain, J.D., Davies, L.A., Fiegel, J., Gumbleton, M., Kim, K.-J., Sakagami, M., Vanbever, R., Ehrhardt, C. (2010). The particle has landed-characterizing the fate of inhaled pharmaceuticals. *Journal of Aerosol Medicine and Pulmonary Drug Delivery* 23(Supplement 2):S71–S87.

Patton, J.S., Byron, P.R. (2007). Inhaling medicines: delivering drugs to the body through the lungs. *Nature Reviews Drug Discovery* 6(1):67–74.

Pérez-Gil, J. (2008). Structure of pulmonary surfactant membranes and films: The role of proteins and lipid-protein interactions. *Biochimica et Biophysica Acta - Biomembranes*.

Pham, D.D., Fattal, E., Ghermani, N., Guiblin, N., Tsapis, N. (2013). Formulation of pyrazinamide-loaded large porous particles for the pulmonary route: Avoiding crystal growth using excipients. *International Journal of Pharmaceutics* 454(2):668–677.

Phillips, E.M., Byron, P.R. (1994). Surfactant promoted crystal growth of micronized methylprednisolone in trichloromonofluoromethane. *International Journal of Pharmaceutics* 110(1):9–19.

Pilcer, G., Amighi, K. (2010). Formulation strategy and use of excipients in pulmonary drug delivery. *International Journal of Pharmaceutics* 392(1–2):1–19.

Pipeline [WWW Document]. n.d.

Porush, I., Maison, G.L. (1959). Self-propelling compositions for inhalation therapy containing a salt of isoproterenol or epinephrine. 2,868,691.

Pozzoli, M., Traini, D., Young, P.M., Sukkar, M.B., Sonvico, F. (2017). Development of a Soluplus® Budesonide Freeze-Dried Powder for Nasal Drug Delivery. *Drug Development and Industrial Pharmacy* 0(0):1–31.

Prankerd, R.J., Nguyen, T.H., Ibrahim, J.P., Bischof, R.J., Nassta, G.C., Olerile, L.D., Russell, A.S., Meiser, F., Parkington, H.C., Coleman, H.A., Morton, D.A. V, McIntosh, M.P. (2013). Pulmonary delivery of an ultra-fine oxytocin dry powder formulation: Potential for treatment of postpartum haemorrhage in developing countries. *PLoS ONE* 8(12):1–9.

Prasad, D.E. V, Chauhan, H., Atef, E. (2014). Amorphous stabilization and dissolution enhancement of amorphous ternary solid dispersions: Combination of polymers showing drug–polymer interaction for synergistic effects. *Journal of Pharmaceutical Sciences* 103:3511–3523.

Priemel, P.A., Laitinen, R., Barthold, S., Grohganz, H., Lehto, V.P., Rades, T., Strachan, C.J. (2013). Inhibition of surface crystallisation of amorphous indomethacin particles in physical drug-polymer mixtures. *International Journal of Pharmaceutics* 456(2):301–306.

Purewal, T.S., Grant, D.J. (Eds.). (1997). Metered Dose Inhaler Technology. CRC Press, Boca Raton.

Raabe, O.G. (1976). Aerosol aerodynamic size conventions for inertial sampler

calibration. *Journal of the Air Pollution Control Association* 26(9):856–860.

Ravi Kumar, M.N.. (2000). A review of chitin and chitosan applications. *Reactive and Functional Polymers* 46(1):1–27.

Respiratory System [WWW Document]. n.d.

Riley, T., Christopher, D., Arp, J., Casazza, A., Colombani, A., Cooper, A., Dey, M., Maas, J., Mitchell, J., Reiners, M., Sigari, N., Tougas, T., Lyapustina, S. (2012). Challenges with developing in vitro dissolution tests for orally inhaled products (OIPs). *AAPS PharmSciTech* 13(3):978–989.

Rogers, T.L., Nelsen, A.C., Hu, J., Brown, J.N., Sarkari, M., Young, T.J., Johnston, K.P., Williams, R.O. (2002). A novel particle engineering technology to enhance dissolution of poorly water soluble drugs: Spray-freezing into liquid. *European Journal of Pharmaceutics and Biopharmaceutics* 54(3):271–280.

Rouse, J.J., Whateley, T.L., Thomas, M., Eccleston, G.M. (2007). Controlled drug delivery to the lung: Influence of hyaluronic acid solution conformation on its adsorption to hydrophobic drug particles. *International Journal of Pharmaceutics* 330(1–2):175–182.

Sahin, S., Selek, H., Ponchel, G., Ercan, M.T. (2002). Preparation , characterization and in vivo distribution of terbutaline sulfate loaded albumin microspheres. *Journal of Controlled Release* 82:345–358.

Saigal, A., Ng, W.K., Tan, R.B.H., Chan, S.Y. (2013). Development of controlled release inhalable polymeric microspheres for treatment of pulmonary hypertension. *International Journal of Pharmaceutics* 450(1–2):114–122.

Sakagami, M. (2006). In vivo, in vitro and ex vivo models to assess pulmonary absorption and disposition of inhaled therapeutics for systemic delivery. *Advanced Drug Delivery Reviews* 58(9–10):1030–1060.

Sakagami, M., Kinoshita, W., Sakon, K., Sato, J., Makino, Y. (2002). Mucoadhesive beclomethasone microspheres for powder inhalation: Their pharmacokinetics and pharmacodynamics evaluation. *Journal of Controlled Release* 80(1–3):207–218.

Salama, R., Hoe, S., Chan, H.K., Traini, D., Young, P.M. (2008). Preparation and characterisation of controlled release co-spray dried drug-polymer microparticles for inhalation 1: Influence of polymer concentration on physical and in vitro characteristics. *European Journal of Pharmaceutics and Biopharmaceutics* 69(2):486–495.

Salama, R., Traini, D., Chan, H.-K., Young, P.M. (2009). Recent advances in controlled release pulmonary therapy. *Current Drug Delivery* 6(4):404–14.

Salama, R.O., Ladd, L., Chan, H.-K., Traini, D., Young, P.M. (2009a). Development of an in vivo ovine dry powder inhalation model for the evaluation of conventional and controlled release microparticles. *The AAPS Journal* 11(3):465–8.

Salama, R.O., Traini, D., Chan, H.-K., Sung, A., Ammit, A.J., Young, P.M. (2009b). Preparation and evaluation of controlled release microparticles for respiratory protein therapy. *Journal of Pharmaceutical Sciences* 98(8):2709–2717.

Salama, R.O., Traini, D., Chan, H.K., Young, P.M. (2008). Preparation and characterisation of controlled release co-spray dried drug-polymer microparticles for inhalation 2: Evaluation of in vitro release profiling methodologies for controlled release respiratory aerosols. *European Journal of Pharmaceutics and Biopharmaceutics* 70(1):145–152.

Schiller, C.H.F., Gebhart, J., Heyder, J., Rudolf, G., Stahlhofen, W. (1988). Deposition of monodisperse insoluble aerosol particles in the 0.005 to 0.2 µm size range within the human respiratory tract. *Annals of Occupational Hygiene* 32(inhaled_particles_VI):41–49.

Selvam, P., El-Sherbiny, I.M., Smyth, H.D.C. (2011). Swellable hydrogel particles for controlled release pulmonary administration using propellant-driven metered dose inhalers. *Journal of Aerosol Medicine and Pulmonary Drug Delivery* 24(1):25–34.

Seville, P.C., Li, H., Learoyd, T.P. (2007). Spray-dried powders for pulmonary drug delivery. *Critical Reviews^{TM} in Therapeutic Drug Carrier Systems* 24(4):307–360.

Shen, S.-C., Ng, W.K., Shi, Z., Chia, L., Neoh, K.G., Tan, R.B.H. (2011). Mesoporous silica nanoparticle-functionalized poly(methyl methacrylate)-based bone cement for effective antibiotics delivery. *Journal of Materials Science: Materials in Medicine* 22(10):2283–2292.

Sheth, P., Myrdal, P.B. (2011a). Excipients Utilized for Modifying Pulmonary Drug Release, in: Smyth, H.D.C., Hickey, A.J. (Eds.), Controlled Pulmonary Drug Delivery. Springer New York, New York, NY, pp. 237–263.

Sheth, P., Myrdal, P.B. (2011b). Polymers for Pulmonary Drug Delivery, in: Smyth, H.D.C., Hickey, A.J. (Eds.), Controlled Pulmonary Drug Delivery. Springer, New York, pp. 265–283.

Shi, N.-Q., Lai, H.-W., Zhang, Y., Feng, B., Xiao, X., Zhang, H.-M., Li, Z.-Q., Qi, X.-R. (2016). On the inherent properties of Soluplus and its application in ibuprofen solid dispersions generated by microwave-quench cooling technology. *Pharmaceutical Development and Technology* 0(0):1–14.

Sibik, J. (2014). Terahertz Spectroscopy of Glasses and Supercooled Liquids. University of Cambridge.

Sibik, J., Elliott, S.R., Zeitler, J.A. (2014). Thermal decoupling of molecular-relaxation processes from the vibrational density of states at terahertz frequencies in supercooled hydrogen-bonded liquids. *The Journal of Physical Chemistry Letters* 5(11):1968–1972.

Sibik, J., Löbmann, K., Rades, T., Zeitler, J.A. (2015). Predicting crystallization of amorphous drugs with terahertz spectroscopy. *Molecular Pharmaceutics* 12(8):3062–3068.

Sibik, J., Zeitler, J.A. (2016). Direct measurement of molecular mobility and crystallisation of amorphous pharmaceuticals using terahertz spectroscopy. *Advanced Drug Delivery Reviews* 100:147–157.

Silva, A.S., Sousa, A.M., Cabral, R.P., Silva, M.C., Costa, C., Miguel, S.P., Bonif??cio, V.D.B., Casimiro, T., Correia, I.J., Aguiar-Ricardo, A. (2017). Aerosolizable gold nano-in-micro dry powder formulations for theragnosis and lung delivery. *International Journal of Pharmaceutics* 519(1–2):240–249.

Sleigh, M.A., Blake, J.R., Llron, N. (1988). The propulsion of mucus by cilia. *The American Review of Respiratory Disease* 137(3):726–41.

Smyth, H.D.C. (2003). The influence of formulation variables on the performance of alternative propellant-driven metered dose inhalers, in: Advanced Drug Delivery Reviews. pp. 807–828.

Smyth, H.D.C., Hickey, A.J. (Eds.). (2011). Controlled Pulmonary Drug Delivery, 1st ed. Springer, New York.

Sokolov, A.P., Kisliuk, A., Novikov, V., Ngai, K.L. (2001). Observation of constant loss in fast relaxation spectra of polymers. *Physical Review B* 63(17):172204.

Son, Y.-J., McConville, J.T. (2012). Preparation of sustained release rifampicin microparticles for inhalation. *The Journal of Pharmacy and Pharmacology* 64(9):1291–302.

Stahlhofen, W., Koebrich, R., Rudolf, G., Scheuch, G. (1990). Short-term and long-term clearance of particles from the upper human respiratory tract as function of particle size. *Journal of Aerosol Science* 21:S407–S410.

Stein, S.W., Sheth, P., Hodson, P.D., Myrdal, P.B. (2014). Advances in metered dose inhaler technology: Hardware development. *AAPS PharmSciTech* 15(2):326–338.

Stocks, J., Hislop, A.A. (2001). Structure and Function of the Respiratory System, in: Bisgaard, H., O'Callaghan, C., Smaldone, G.C. (Eds.), Drug Delivery to the Lung, Lung

Biology in Health and Disease. CRC Press, New York, pp. 47–104.

Sun, L., Zhou, S., Wang, W., Li, X., Wang, J., Weng, J. (2009). Preparation and characterization of porous biodegradable microspheres used for controlled protein delivery. *Colloids and Surfaces A: Physicochemical and Engineering Aspects* 345(1–3):173–181.

Surendrakumar, K., Martyn, G.P., Hodgers, E.C.M., Jansen, M., Blair, J.A. (2003). Sustained release of insulin from sodium hyaluronate based dry powder formulations after pulmonary delivery to beagle dogs. *Journal of Controlled Release* 91(3):385–394.

Swaminathan, J., Ehrhardt, C. (2011). Liposomes for Pulmonary Drug Delivery, in: Smyth, H.D.C., Hickey, A.J. (Eds.), Controlled Pulmonary Drug Delivery. Springer, New York, pp. 313–334.

Tan, N.Y. (2015). Terahertz Spectroscopy of Organic Systems with Bulk Structural Order and Disorder. University of Cambridge.

Tang, Y., Zhang, H., Lu, X., Jiang, L., Xi, X., Liu, J., Zhu, J. (2015). Development and evaluation of a dry powder formulation of liposome-encapsulated oseltamivir phosphate for inhalation. *Drug Delivery* 22(5):608–618.

Technology Solutions for Global Health - Intranasal and Pulmonary Delivery Devices. (2013). . Seattle.

Telko, M.J., Hickey, A.J. (2005). Dry Powder Inhaler Formulation. *Respiratory Care* 50(9):1209–1227.

Thalberg, K., Berg, E., Fransson, M. (2012). Modeling dispersion of dry powders for inhalation. The concepts of total fines, cohesive energy and interaction parameters. *International Journal of Pharmaceutics* 427(2):224–233.

The Global Impact of Respiratory Disease - Second Edition. (2017). . Sheffield.

Thiel, C.G. (1996). From Susie's question to CFC free: An inventor's perspective on forty years of MDI development and regulation, in: Dalby, R.N., Byron, P.R., Farr, S. (Eds.), Respiratory Drug Delivery V. Interpharm Press, Buffalo Grove, IL, pp. 115–124.

Ting, T.Y., Gonda, I., Gipps, E.M. (1992). Microparticles of polyvinyl alcohol for nasal delivery. I. Generation by spray-drying and spray-desolvation. *Pharmaceutical Research*.

Todoroff, J., Vanbever, R. (2011). Fate of nanomedicines in the lungs. *Current Opinion in Colloid and Interface Science* 16(3):246–254.

Traini, D., Young, P.M. (2013). Inhalation and Nasal Products, in: Inhalation Drug Delivery. John Wiley & Sons, Ltd, Chichester, United Kingdom, pp. 15–30.

Tsapis, N., Bennett, D., Jackson, B., Weitz, D.A., Edwards, D.A. (2002). Trojan particles:

Large porous carriers of nanoparticles for drug delivery. *Proceedings of the National Academy of Sciences* 99(19):12001–12005.

Uekama, K., Fujinaga, T., Hirayama, F., Otagiri, M., Yamasaki, M., Seo, H., Hashimoto, T., Tsuruoka, M. (1983). Improvement of the oral bioavailability of digitalis glycosides by cyclodextrin complexation. *Journal of Pharmaceutical Sciences* 72(11):1338–1341.

Uhrich, K.E., Cannizzaro, S.M., Langer, R.S., Shakesheff, K.M. (1999). Polymeric systems for controlled drug release. *Chemical Reviews* 99(11):3181–3198.

Ungaro, F., D'Angelo, I., Coletta, C., D'Emmanuele Di Villa Bianca, R., Sorrentino, R., Perfetto, B., Tufano, M.A., Miro, A., La Rotonda, M.I., Quaglia, F. (2012a). Dry powders based on PLGA nanoparticles for pulmonary delivery of antibiotics: Modulation of encapsulation efficiency, release rate and lung deposition pattern by hydrophilic polymers. *Journal of Controlled Release* 157(1):149–159.

Ungaro, F., D'Angelo, I., Miro, A., La Rotonda, M.I., Quaglia, F. (2012b). Engineered PLGA nano- and micro-carriers for pulmonary delivery: challenges and promises. *The Journal of Pharmacy and Pharmacology* 64(9):1217–35.

Valdes, J., Shipley, T., Rey, J. a. (2014). Loxapine inhalation powder (adasuve): a new and innovative formulation of an antipsychotic treatment for agitation. *Pharmacy & Therapeutics* 39(9):621–3, 648.

Vanbever, R., Ben-Jebria, A., Mintzes, J.D., Langer, R., Edwards, D.A. (1999). Sustained release of insulin from insoluble inhaled particles. *Drug Development Research* 48(4):178–185.

Vartiainen, V., Bimbo, L.M., Hirvonen, J., Kauppinen, E.I., Raula, J. (2017). Aerosolization, drug permeation and cellular interaction of dry powder pulmonary formulations of corticosteroids with hydroxypropyl-β-cyclodextrin as a solubilizer. *Pharmaceutical Research* 34:25–35.

Vehring, R. (2008). Pharmaceutical particle engineering via spray drying. *Pharmaceutical Research* 25(5):999–1022.

Vidgrén, M., Vidgrén, P., Paronen, T. (1987). Comparison of physical and inhalation properties of spray-dried and mechanically micronized disodium cromoglycate. *International Journal of Pharmaceutics* 35:139–144.

Wais, U., Jackson, A.W., He, T., Zhang, H. (2016). Nanoformulation and encapsulation approaches for poorly water-soluble drug nanoparticles. *Nanoscale* 8:1746–1769.

Wauthoz, N., Amighi, K. (2015). Formulation Strategies for Pulmonary Delivery of Poorly Soluble Drugs, in: Nokhodchi, A., Martin, G.P. (Eds.), Pulmonary Drug Delivery:

Advances and Challenges. John Wiley & Sons, Ltd., Hoboken.

Webb, S.D., Golledge, S.L., Cleland, J.L., Carpenter, J.F., Randolph, T.W. (2002). Surface adsorption of recombinant human interferon-γ in lyophilized and spray-lyophilized formulations. *Journal of Pharmaceutical Sciences* 91(6):1474–1487.

Weibel, E.R. (1963). Morphometry of the human lung, 1st ed. Academic Press, Cambridge.

Weibel, E.R., Sapoval, B., Filoche, M. (2005). Design of peripheral airways for efficient gas exchange, in: Respiratory Physiology and Neurobiology. pp. 3–21.

Whitsett, J.A., Weaver, T.E. (1991). Structure, Function, and Regulation of Pulmonary Surfactant Proteins, in: Bourbon, J.R. (Ed.), Pulmonary Surfactant: Biochemical, Functional, Regulatory, and Clinical Concepts. CRC Press, pp. 77–104.

WHO | Asthma [WWW Document]. (2017). . *WHO*.

WHO | Chronic obstructive pulmonary disease (COPD) [WWW Document]. (2016). . *WHO*.

WHO Stability Guide Annex 2 Stability testing of active pharmaceutical ingredients and finished pharmaceutical products. (2009). . Geneva.

Widmaier, E.P., Raff, H., Strang, K.T. (2008). Vander's Human Physiology. McGraw-Hill Higher Education, Boston.

Williams, H., Trevaskis, N., Charman, S., Shanker, R., Charman, W., Pouton, C., Porter, C. (2013). Strategies to address low drug solubility in discovery and development. *Pharmacological Reviews* 65(1):315–499.

Willis, L., Hayes, D., Mansour, H.M. (2012). Therapeutic liposomal dry powder inhalation aerosols for targeted lung delivery. *Lung* 190(3):251–262.

Woods, A., Bicer, E.M., Apfelthaler, C., Bruce, K., Dailey, L.A., Forbes, B. (2014). Albumin nanoparticles for drug delivery to the lungs - In vitro investigation of biodegradation as a mechanism of clearance. *Journal of Aerosol Medicine and Pulmonary Delivery* 27(4):A-15-A-15.

Woods, A., de Rosales, R.T.M., Spina, D., Vasquez, Y.R., Patel, A., Bruce, K., Dailey, L.A., Forbes, B. (2013). In vivo clearance kinetics of In-111 labelled albumin nanoparticles delivered to the mouse lung. *Journal of Aerosol Medicine and Pulmonary Drug Delivery* 26(5):A-22-A-22.

Woods, A., Patel, A., Spina, D., Riffo-Vasquez, Y., Babin-Morgan, A., de Rosales, R.T.M., Sunassee, K., Clark, S., Collins, H., Bruce, K., Dailey, L. a., Forbes, B. (2015). In vivo biocompatibility, clearance, and biodistribution of albumin vehicles for

pulmonary drug delivery. *Journal of Controlled Release* 210:1–9.

Wu, C., Ji, P., Yu, T., Liu, Y., Jiang, J., Xu, J., Zhao, Y., Hao, Y., Qiu, Y., Zhao, W. (2016). Naringenin-loaded solid lipid nanoparticles: preparation, controlled delivery, cellular uptake, and pulmonary pharmacokinetics. *Drug Design, Development and Therapy* 10:911.

Wu, Z.-Z., Thatcher, M.L., Lungberg, J.K., Ogawa, M.K., Jacoby, C.B., Battiste, J.L., Ledoux, K.A. (2012). Forced degradation studies of corticosteroids with an alumina-steroid-ethanol model for predicting chemical stability and degradation products of pressurized metered-dose inhaler formulations. *Journal of Pharmaceutical Sciences* 101(6):2109–2122.

Yamamoto, A., Yamada, K., Muramatsu, H., Nishinaka, A., Okumura, S., Okada, N., Fujita, T., Muranishi, S. (2004). Control of pulmonary absorption of water-soluble compounds by various viscous vehicles. *International Journal of Pharmaceutics* 282(1–2):141–149.

Yang, Y., Bajaj, N., Xu, P., Ohn, K., Tsifansky, M.D., Yeo, Y. (2009). Development of highly porous large PLGA microparticles for pulmonary drug delivery. *Biomaterials* 30(10):1947–1953.

Yeh, T.H., Hsu, L.W., Tseng, M.T., Lee, P.L., Sonjae, K., Ho, Y.C., Sung, H.W. (2011). Mechanism and consequence of chitosan-mediated reversible epithelial tight junction opening. *Biomaterials* 32(26):6164–6173.

Yildiz, A., John, E., Özsoy, Y., Araman, A., Birchall, J.C., Broadley, K.J., Gumbleton, M. (2012). Inhaled extended-release microparticles of heparin elicit improved pulmonary pharmacodynamics against antigen-mediated airway hyper-reactivity and inflammation. *Journal of Controlled Release* 162(2):456–463.

Yoshioka, M., Hancock, B.C., Zografi, G. (1994). Crystallization of indomethacin from the amorphous state below and above its glass transition temperature. *Journal of Pharmaceutical Sciences* 83(12):1700–1705.

Yu, Z., Johnston, K.P., Williams, R.O. (2006). Spray freezing into liquid versus spray-freeze drying: Influence of atomization on protein aggregation and biological activity. *European Journal of Pharmaceutical Sciences* 27(1):9–18.

Zeng, X.M., Martin, G.P., Marriott, C. (1995). The controlled delivery of drugs to the lung. *International Journal of Pharmaceutics* 124:149–164.

Zeng, X.M., Martin, G.P., Marriott, C., Pritchard, J. (2000). The effects of carrier size and morphology on the dispersion of salbutamol sulphate after aerosolization at different

flow rates. *The Journal of Pharmacy and Pharmacology* 52(10):1211–1221.

Zhao, Y., Chang, Y.-X., Hu, X., Liu, C.-Y., Quan, L.-H., Liao, Y.-H. (2017). Solid lipid nanoparticles for sustained pulmonary delivery of Yuxingcao essential oil: Preparation, characterization and in vivo evaluation. *International Journal of Pharmaceutics* 516(1–2):364–371.

Zhou, D., Zhang, G.G.Z., Law, D., Grant, D.J.W., Schmitt, E.A. (2002). Physical stability of amorphous pharmaceuticals: Importance of configurational thermodynamic quantities and molecular mobility. *Journal of Pharmaceutical Sciences* 91(8):1863–1872.

Zhu, K., Ng, W.K., Shen, S., Tan, R.B.H., Heng, P.W.S. (2008). Design of a device for simultaneous particle size and electrostatic charge measurement of inhalation drugs. *Pharmaceutical Research* 25(11):2488–96.

Zhu, K., Tan, R.B.H., Chen, F., Ong, K.H., Heng, P.W.S. (2007). Influence of particle wall adhesion on particle electrification in mixers. *International Journal of Pharmaceutics* 328(1):22–34.